A segregated finite element method for cardiac elastodynamics in a fully coupled human heart model

Zur Erlangung des akademischen Grades eines

Doktors der Naturwissenschaften

von der KIT-Fakultät für Mathematik des
Karlsruher Instituts für Technologie (KIT)
genehmigte

Dissertation

von

M.Sc. Jonathan Samuel Fröhlich

Tag der mündlichen Prüfung: 16.03.2022

Referent:	Prof. Dr. rer. nat. Christian Wieners
Koreferent:	Prof. Dr. rer. nat. Olaf Dössel
Koreferent:	PD Dr.-Ing. Axel Loewe

ABSTRACT

One key characterstic of the cardiac function is its complexity, i.e., the multitude of different phenomena acting on various temporal and spatial scales interacting with each other. Over the past decades, many models varying in complexity describing these interactions were presented and are used in current research. Despite the incredible progress made in describing and simulating cardiac function, most of the more detailed models are not properly embedded within mathematical theory.

This work aims to give a precise and comprehensive mathematical formulation of coupled cardiac elastodynamics, including electrophysiology, elasticity and physiological boundary conditions developed in recent years. Focussing on the analysis of dynamic elasticity, the concept of anisotropy is applied to common cardiac tissue models, such as the models of Guccione et al. and Holzapfel and Ogden. Frequently used modeling approaches, such as incompressibility and the active strain decomposition, are integrated in one overarching framework, allowing for propositions on polyconvexity of the materials and solvability of the elastic system. The equations of elastodynamics are then complemented by the monodomain equations, describing the propagation of the excitation potential in cardiac tissue, and a surrogate model to simulate cardiovascular blood pressure. The full mathematical description of this coupled model allows a detailed formulation of a discretization scheme in space and time for the electro-elastodynamical system.

The classification of the coupled model within the context of weak solutions is presented and a time-segregated numerical approximation method for the full system is derived. The formulated numerical method is then examined by application on coupled test cases, providing first convergence results in space for the displacement in coupled cardiac problems.

Keywords:

cardiac modeling, cardiac coupling, computational modeling, elasto-dynamics, finite element methods

ZUSAMMENFASSUNG

Ein zentrales Merkmal der Funktionalität des Herzens ist dessen Komplexität, d.h. die Vielzahl verschieder Phänomene, die auf unterschiedlichen Zeit- und Raumskalen stattfinden und miteinander interagieren. In den letzten Jahrzehnten wurden viele unterschiedlich komplexe Modelle, die solche Interaktionen beschreiben, vorgestellt und in Forschung und Praxis verwendet. Trotz der erstaunlichen Fortschritte in der Beschreibung und Simulation der Herzfunktion existiert für die meisten der detaillierteren Modelle jedoch keine zugehörige mathematische Theorie.

Ziel dieser Arbeit ist es, eine präzise und vollständige mathematische Formulierung gekoppelter elastodynamischer Herzphänomene vorzustellen, welche Elektrophysiologie, Elastizität sowie physiologische Randbedingungen umfasst. Der Fokus liegt hierbei auf der Analysis der dynamischen Elastizität. Die Theorie der Anisotropie wird aufbereitet und auf gängige Materialmodelle von Herzmuskelgewebe, wie die Modelle von Guccione et al. und Holzapfel und Ogden, angewandt. Häufig genutzte Modellierungsansätze, wie Inkompressibilität und die Active Strain Zerlegung, werden in ein übergreifendes System integriert, sodass Aussagen über die Polykonvexität der Materialien und der Lösbarkeit des Systems möglich werden. Die dynamischen Bewegungsgleichungen werden durch die Monodomain-Gleichungen, welche die elektrische Reizübertragung in Herzgewebe bescheiben, sowie ein Ersatzmodell für den Blutkreislauf ergänzt. Die vollständige mathematische Darstellung dieses gekoppelten Systems erlaubt eine detaillierte Formulierung eines in Raum und Zeit diskreten Verfahrens zur Lösung des elektro-elastodynamischen Systems.

Die Einordnung des gekoppelten Modells in den Kontext schwacher Lösungen wird vorgestellt und ein in der Zeit gestaffeltes Verfahren zur numerischen Approximation des vollständigen Systems wird hergeleitet. Das formulierte numerische Verfahren wird anhand ausgewählter Versuche untersucht sowie erste Konvergenzergebnisse im Ort für die Verschiebung bei gekoppelten Problemen präsentiert.

DANKSAGUNG

An dieser Stelle möchte ich mich sehr herzlich bei all den Menschen bedanken, ohne die diese Arbeit nicht möglich gewesen wäre.

Mein tiefster Dank gilt zunächst meinem Doktorvater Herrn Prof. Dr. Wieners für das entgegengebrachte Vertrauen und die tatkräftige Unterstüzung – vielen Dank, dass Sie mir die Freiheit gegeben haben, meinen Weg durch dieses facettenreiche Thema selbst zu wählen. Ihre Tür stand mir immer offen, egal ob für fachliche Diskussionen oder zum Debugging. Sie sagen immer, Sie *„bilden Ihre Doktoranden für die Industrie"* aus, das ist Ihnen meines Erachtens auch gut gelungen. Des Weiteren bedanke bei meinen Koreferenten Prof. Dr. Olaf Dössel und PD Dr.-Ing. Axel Loewe – insbesondere für Ihre Kooperationsbereitschaft, durch die das ursprüngliche gemeinsame Projekt entstanden ist. Ohne Sie hätte ich nicht die Möglichkeit gehabt, über ein Thema zu schreiben, welches mir selbst sehr wichtig ist.

Außerdem bedanke ich mich bei allen Kollegen des IANM 3 und IBT, die die letzten fünf Jahre zu etwas ganz Besonderem gemacht haben: Laura Lindner, die mich durch viele fachliche und persönliche Gespräche immer wieder auf neue Ideen gebracht hat – du konntest meine Probleme aus persönlicher Erfahrung gut nachvollziehen. Danke, dass du dir dafür immer Zeit genommen hast. Tobias Gerach und Ekaterina Kovacheva, ohne deren Geometrien, Modelle und fachlichen Input ich nie so viel über die Modellierung des menschlichen Herzens gelernt hätte. Gerne erinnere ich mich an unsere gemeinsamen Workshops in Italien zurück. Dr. Daniel Weiß, der für alles und jeden ein offenes Ohr hat und dessen Energie und Motivation, insbesondere für die Lehre, geradezu ansteckend sind. Niklas Baumgarten, ohne dessen Beharrlichkeit unser Quellcode wahrscheinlich immer noch nur auf der lokalen Festplatte liegen würde – vielen Dank, dass du unsere Bequemlichkeit nie der *continuous integration* im Weg stehen lässt. Jonathan Wunderlich, dessen Tatkraft für die Umstrukturierung der Codebasis auch mir Ansporn gegeben hat, mehr als nur das Nötigste zu tun. Daniele Corallo, mit dem ich oft über die Bugs im Code diskutiert habe und der sehr spontan den gesamten Text, teilweise sogar zweimal, korrekturgelesen hat. Euch und all den nicht namentlich erwähnten Kollegen des IANM3 danke ich vor allem auch für eure Menschlichkeit, die vielen spannenden Diskussionen in den Pausen, die kassierten Tore beim Tischkicker, die leckeren Back- und Eiswaren jeglicher Art und die lustigen Arbeitsgruppenfeste.

Besonders hervorheben möchte ich noch meinen Kollegen, Freund und Leidensgenossen Benny Stein – gerade in der stressigen Endphase habe ich mich immer gefreut, wenn auch du zu später Stunde noch im Büro warst. So blieben mir viele einsame Mahlzeiten erspart und wir konnten uns gegenseitig unser Leid klagen. Du hast die abschließenden Monate erträglich gemacht und dafür danke ich dir vielmals.

Ebenso danke ich meinem Freund und Ex-Kollegen Felix Hagemann – die unzähligen lustigen Stunden zusammen mit dir und Benny haben viele Abende in Karlsruhe unvergesslich gemacht.

Nicht genügend bedanken kann ich mich bei meiner wundervollen Frau Claudia – danke, dass du mir stets den Rücken freigehalten hast und du so viel Organisation, Planung und Aufwand in allen Lebensbereichen für uns beide auf dich genommen hast.

Natürlich gilt meine Dankbarkeit auch all meinen Freunden und meiner (erweiterten) Familie – eure stetige Unterstützung und Interesse, trotz meiner oft wirren Erklärungsversuche, haben mich in meiner Arbeit stets bestärkt.

CONTENTS

LIST OF SYMBOLS

Symbol	Descripion
$\mathbb{R}$	Real numbers
$\mathbb{R}^3$	Real-valued three-dimensional vectors
$\mathbb{R}^{3\times 3}$	Real-valued 3×3 matrices
$\mathbb{R}^{3\times 3}_{\text{sym}}$	Symmetric real-valued 3×3 matrices
$\mathbb{O}^{3\times 3}$	Orthogonal matrices in $\mathbb{R}^{3\times 3}$
$\mathbb{SO}(3)$	Orthogonal matrices $\mathbf{Q}$ with $\det(\mathbf{Q}) = 1$
$\mathbb{O}^{3\times 3}_{\text{orth}} \subset \mathbb{O}^{3\times 3}$	Orthotropic symmetry group

Functions and function spaces

$\mathcal{M}ap(\mathcal{X};\mathcal{Y})$	Mappings from $\mathcal{X}$ to $\mathcal{Y}$
$\mathcal{L}in(\mathcal{X};\mathcal{Y})$	Linear mappings from $\mathcal{X}$ to $\mathcal{Y}$
$\mathcal{C}(\mathcal{X};\mathcal{Y})$	Continuous mappings from $\mathcal{X}$ to $\mathcal{Y}$
$\mathcal{C}^k(\mathcal{X};\mathcal{Y})$	k-times continuously differentiable mappings from $\mathcal{X}$ to $\mathcal{Y}$
$\mathcal{L}^p(\mathcal{X};\mathcal{Y})$	Measurable and p-integrable functions from $\mathcal{X}$ to $\mathcal{Y}$
$\mathcal{W}^{k,p}(\mathcal{X};\mathcal{Y})$	Sobolev space of mappings from $\mathcal{X}$ to $\mathcal{Y}$
$\mathcal{W}^{k,p}([0,T];\mathcal{V})$	Bochner space of mappings from $[0,T]$ to $\mathcal{V}$

Differential geometry

$\mathcal{M}$	Smooth n-manifold, $\mathbf{n} \in \mathbb{N}$
$T_{\mathbf{x}}\mathcal{M}$	Tangent space of $\mathcal{M}$ in $\mathbf{x} \in \mathcal{M}$
$T\mathcal{M}$	Tangent bundle of $\mathcal{M}$
$\boldsymbol{\phi}_*\mathbf{v}$	Push-forward of a vectorfield $\mathbf{v}$ by $\boldsymbol{\phi}$
$\boldsymbol{\phi}^*\mathbf{v}^{\phi}$	Pull-back of a vectorfield $\mathbf{v}^{\phi}$ by $\boldsymbol{\phi}$

Kinematics

$\Omega \subset \mathbb{R}^3$	Continuum body

$\Gamma = \partial\Omega$	Boundary of Ω
$\boldsymbol{\phi}\colon \Omega \to \mathbb{R}^3$	Configuration of Ω
$\boldsymbol{\Phi}(\Omega)$	Set of all configurations of Ω
$\boldsymbol{\varphi}\colon [0,T] \times \Omega \to \mathbb{R}^3$	Motion of Ω
$\mathbf{u}\colon [0,T] \times \Omega \to \mathbb{R}^3$	Displacement part of a motion of Ω, $\mathbf{u}(t,\mathbf{x}) = \boldsymbol{\varphi}(t,\mathbf{x}) - \mathbf{x}$
$\mathbf{v}\colon [0,T] \times \Omega \to \mathbb{R}^3$	Velocity of a motion of Ω
$\mathbf{a}\colon [0,T] \times \Omega \to \mathbb{R}^3$	Acceleration of a motion of Ω

Elasticity

$\mathbf{F} = \mathrm{D}\boldsymbol{\varphi}$	Deformation gradient
$J = \det(\mathbf{F})$	Jacobian
$\mathbf{B} = \mathbf{F}\mathbf{F}^\top$	Left Cauchy-Green stress
$\mathbf{C} = \mathbf{F}^\top\mathbf{F}$	Right Cauchy-Green stress
$\mathbf{E} = \frac{1}{2}(\mathbf{C} - \mathbf{I})$	Green-St. Venant strain
$\mathbf{t}$	Cauchy stress vector
$\mathbf{T}$	Cauchy stress tensor
$\mathbf{P} = J\mathbf{T}\mathbf{F}^{-\top}$	First Piola-Kirchhoff stress
$\mathbf{S} = \mathbf{F}^{-1}\mathbf{P}$	Second Piola-Kirchhoff stress
$\mathcal{T}_\mathbf{x}, \mathcal{P}_\mathbf{x}, \mathcal{S}_\mathbf{x}$	Constitutive equation at $\mathbf{x} \in \Omega$
$\mathcal{T}, \mathcal{P}, \mathcal{S}$	Elastic constitutive equation on Ω
$W_\mathbf{P}, W_\mathbf{S}, W_{\boldsymbol{\iota}}$	Stored energy function for hyperelastic materials
W_{iso}	Isochoric part of the stored energy function
W_{vol}	Volumetric part of the stored energy function

Cardiac electrophysiology

$v_{\mathrm{i,e}}\colon [0,T] \times \Omega \to \mathbb{R}$	Intra- and extracellular potential
$v\colon [0,T] \times \Omega \to \mathbb{R}$	Transmembrane voltage
C_m	Capacitance
I_{ion}	Total ionic transmembrane current
I_{ext}	External applied stimulus current
$\mathbf{w}\colon [0,T] \times \Omega \to \mathbb{R}^{d_\mathbf{w}}$	Vector of gating variables w_i, $i = 1, \ldots, d_\mathbf{w}$
$\mathbf{c}\colon [0,T] \times \Omega \to \mathbb{R}^{d_\mathbf{c}}$	Vector of concentrations variables c_i, $i = 1, \ldots, d_\mathbf{c}$
$\mathbf{D}_{\mathrm{i,e}}$	Intra-/extracellular conductivity tensor
$\sigma^{\mathrm{i,e}}_{\mathbf{f},\mathbf{s},\mathbf{t}}$	Intra-/extracellular conductivities along $\mathbf{f}, \mathbf{s}, \mathbf{t}$
$\mathbf{k}\colon [0,T] \times \Omega \to \mathbb{R}^{d_\mathbf{c}}$	Vector of tension variables k_i, $i = 1, \ldots, d_\mathbf{c}$
$\gamma_\mathbf{f}\colon [0,T] \times \Omega \to \mathbb{R}$	Microscopic fibre stretch

$\Gamma_{\mathrm{D}} \subset \Gamma$	Dirichlet boundary
$\Gamma_{\mathrm{N}} \subset \Gamma$	Endocardial surface boundary
$\Gamma_{\mathrm{P}} \subset \Gamma$	Boundary connected to the pericardial surface
$p\colon [0,T] \times \Gamma_N \to \mathbb{R}$	Cardiac cavity pressure

Cardiac elasticity

$\rho\colon [0,T] \times \Omega \to \mathbb{R}^d$	Mass density
$\mathbf{b}\colon [0,T] \times \Omega \to \mathbb{R}^d$	Body load in Ω
$\mathbf{g}\colon [0,T] \times \Gamma \to \mathbb{R}$	Surface load on Ω
$\mathcal{F}$	Body load potential
$\mathcal{G}$	Surface load potential
$\mathcal{K}$	Kinetic energy
$\mathcal{E}$	Potential energy
$\mathcal{I}$	Total energy $\mathcal{I} = \mathcal{K} + \mathcal{E}$
$\mathbf{F}_{\mathrm{vol}} = J^{\frac{1}{3}}\mathbf{I}$	Volumetric part of $\mathbf{F}$
$\mathbf{F} = \mathbf{F}_{\mathrm{vol}}\overline{\mathbf{F}}$	Flory decomposition
$\mathbf{F} = \mathbf{F}_{\mathrm{E}}\mathbf{F}_{\mathrm{A}}$	Active strain decomposition

Discretization

$\mathcal{B}(\mathcal{V}, \mathcal{W})$	Continuous bilinear forms $b\colon \mathcal{V} \times \mathcal{W} \to \mathbb{R}$
$\mathcal{V}$	Solution space
$\mathcal{W}$	Test space
$\mathbb{S}^{l,p}$	Lagrange finite elements of degree l with global mappings in $\mathcal{H}^p$
Ω_h	Triangulation of Ω
Π_h	Interpolation operator on Ω_h
Λ_h	Integration operator on Ω_h
$\mathcal{V}_h$	Finite dimensional solution space $\mathcal{V}_h \subset \mathcal{V}$
$\mathcal{W}_h$	Finite dimensional test space $\mathcal{W}_h \subset \mathcal{W}$
T	End time
Δt	Uniform stepsize
$\mathcal{T}$	Discretized interval $[0,T]$

LIST OF FIGURES

LIST OF TABLES

CHAPTER

ONE

INTRODUCTION

In this chapter we illustrate the topics of this thesis. Beginning with the motivation of the research problem, an overview of the current research field is given. Subsequentially, we highlight the contributions of this work and outline its structure.

1.1 Motivation

Cardiovascular diseases are the primary contributors to morbidity and mortality in the European Union [158]. In Germany, acute myocardial infarction, chronic ischemic heart disease, heart failure, hypertensive heart disease and atrial arrhythmias cause 38.4% of all deaths [48]. With the improvement of diagnostic tools and therapeutic options, the computational modeling of the cardiovascular system has advanced in the recent decades [42, 101, 115]. These models already have a clinical impact in diagnosis [5], risk stratification [11], therapy planning [68, 105, 126] and intraprocedural support [103].

An essential characteristic of the human heart is its complexity, i.e., the multitude of different phenomena acting on various temporal and spatial scales and interacting with each other. Cardiac electrophysiology describes the depolarization and repolarization sequence of cardiac tissue with a reaction-diffusion model. Beginning at the sinoatrial node, an electric impulse is given which, on the microscopic or cellular level, triggers a reaction model first described by Hodgkin and Huxley [84]. This signal then propagates through the cardiac tissue where it is modeled on the macroscopic level as a diffusion-type equation [70, 92].

Electrically activated myocardial cells contract [107], the effect of which is modeled on a macroscopic scale by cardiac mechanics. The corresponding mathematical models are based on elasticity theory [38, 106, 173]. In isolation, such models are well-understood for small deformations, especially in a static setting. The mechanics of cardiac deformation however are described by large deformations, where the mathematical assumptions for regularity become more restrictive. Realistic representations of tissue deformation account for the orientation of the cardiac fibres [51]. As fiber distribution is not measured in clinical routine, rule-based algorithms [25, 166] are often applied to assign fibre fields. From a mathematical point of view, the modeling of these fibre fields leads to anisotropic constitutive materials [149].

Lastly, the contraction and relaxation of the heart is intimately connected to the circulatory system and blood flow [46]. The flow of blood is modeled by a Navier-Stokes equation [34] or, more general, as a non-Newtonian fluid, where the boundary of the circulatory domain satisfies a coupling condition with the mechanical domain boundary [133].

Multi-physics models allow the investigation of interdependencies between these mechanisms to deduce more holistic studies [1]. Due to the complexity of the full multi-physics problem, only few cardiac simulation frameworks have been proposed that solve the complete system. Santiago et al. [141] presented and simulated such a full multiphysics problem, using simplified models for electrophysiology and passive material response, while Nordsletten et al. [117] and Sugiura et al. [154] presented an FSI coupling for the left ventricle. Quarteroni et al. [128, 129] describe the necessary steps for the fluid-structure coupling in great detail, but refrain from a numerical simulation of the full model.

More common approaches replace the FSI representation by a phenomenological model such as 0D lumped parameter models [15, 74, 75, 83, 94, 122, 138, 144]. Such models take the form of systems of ordinary differential equations [169] or differential-algebraic equations [63], which allow a computational efficient coupling to cardiac mechanics.

The reduction of the FSI physics allow for a more detailed description of the interactions between electrophysiology and cardiac mechancs. Additionally, numerical simulations of these models within clinically relevant time frames become feasible [122]. Dedè et al. [47, 64, 129] present multiple schemes for cardiac elastodynamics in the left ventricle. To reduce the computational load of the matrix-multiplication in $\mathbb{R}^{3\times3}$, Garcia-Blanco et al. [61, 62] describe an efficient framework to handle passive material formulations. More recently, reduced circulatory models for the full heart have been developed [15, 63, 83, 90, 132].

Still, reduced electro-mechanical systems consist of phenomena acting on different time and spatial scales which need to be addressed. Since the discretization in space and time for the electrophysiological system needs to be of orders of magnitude finer than the one for the mechanical system [99, 114], choosing a single time- and space scale for all systems is sub-optimal. Segregated solution methods of this coupled system require a discrete uncoupling of the corresponding equations, the effects of which become an increasing research focus [47, 131].

1.2 Objectives and contribution

The goal of this work is to provide a full mathematical model for the electrophysiology and mechanics of the human heart. Commonly used physiological constitutive equations used in cardiac mechanics [43, 85] are investigated in detail on their mathematical properties and categorized within the framework of elastodynamics. We show how common approaches, such as a volumetric splitting [56, 140] of stored energy functionals, the coupling of microscopic fibre shortening by an active stress [119] or active strain [135] and physiological boundary conditions [121, 168], fit into the context of hyperelastic materials. In a joint research effort, we described the mathematical fundamentals together with Gerach et al. [63]. Within said work, a full model of the human heart was presented and evaluated with respect to its agreement on clinical data. However, as was mentioned in the disscussion section, neither analytical nor numerical results on stability or convergence were obtained. We derive a framework for a coupled system similar to the one given in [63], allowing for a systematic approach of the investigation on such topics.

Despite the incredible progress made with respect to modeling and simulation of coupled cardiac problems, as described in the previous section, there are only few contributions which embed these models with their proper mathematical theory. Andreianov, Bendahmane, Quarteroni and Ruiz-Baier [6] proved an existence result for static, linearized elasticity with only traction boundary conditions. Moreover, Bendahmane et al. [29] showed a similar result for more involved electrophysiological models and boundary conditions, but still using linearized cardiac elasticity.

We aim to elevate the mathematical description of the previously mentioned work and give a precise and comprehensive mathematical formulation of coupled cardiac elastodynamics, including the physiological boundary conditions developed in recent years. The full mathematical description of this coupled model allows a detailed formulation of a discretization scheme in space and time for the electro-elastodynamical model. The classification of the coupled model within the context of variational formulations is presented and a time-segregated numerical approximation method for the full system is derived.

Besides the formulation of the mathematical model and the numerical scheme for coupled cardiac elastodynamics, we additionally aim to investigate its numerical properties. Since very little theory is applicable to the elastodynamical system, we provide experimental results on numerical convergence behaviour. Suitable test cases are formulated to analyze the dependencies of the solution of the elastodynamical part on the different coupling mechanisms, including material properties, boundary conditions and electrophysiological coupling.

1.3 Structure of the thesis

We start by presenting the constitutive theory leading to the description of nonlinear finite elasticity. In chapter 2, we summarize the fundamental mathematical concepts which will be needed in the discussion of three-dimensional elasticity. This includes the theory of Fréchet derivatives and basic concepts of tangents on smooth manifolds. With the presented definitions, we briefly discuss general integral formulations relating to functions acting on manifolds.

The abstract concepts of the previous chapter are then specified in chapter 3. We introduce the basics of continuum mechanics and define the concepts of motions, velocities and accelerations on continuum bodies. The spatial derivative of a motion, the deformation gradient, will emerge as a relevant quantity. We utilize it to develop how balance laws, the mathematical description of physical axioms such as the conservation of mass, can be written by only using the initial configuration of the continuum body. Finally, we establish the Cauchy stress principle as the core assumption in elasticity.

In chapter 4, we build on the Cauchy stress tensor introduced in the preceding chapter and formulate additional mathematical and physical assumptions describing said tensor. These constitutive equations lead to the concept of hyperelasticity, where materials are defined by their stored energy functions. We present the fundamental theory of invariants to describe the concepts of anisotropic, fibre-reinforced and incompressible materials. Subsequentially, some common materials used within the context of cardiac elasticity are presented and their restrictions regarding large deformations are pointed out.

In chapter 5, we introduce the basic anatomy of the human heart. Starting with the electrophysilogical depolarization, mathematical models for both microscopic action potentials and their macroscopic propagation within cardiac tissue are presented. The shift in ion concentrations resulting from the electrical excitation of cardiac cells leads to a microscopic contraction in each excited muscle cell. We discuss the coupling of this microscopic phenomenon to the macroscopic formulations of elasticity. Additionally, the relevant boundary conditions within this setting are described. We will see that for a proper mathematical model, the pressure within the cardiac chambers ought to be realized as a fluid-structure interaction model. However, since our focus lies only on the mechanical deformation of the tissue, we adopt a surrogate model for the circulatory system and conclude with the fully coupled model of cardiac electro- and elastodynamics.

Chapter 6 is dedicated to the numerical approximation of the previously defined model. Beginning with a variational setting, we postulate the assumptions needed for existence of solutions of the coupled model. We then present the discretizations in time and space of the electrophysiological and mechanical model. Again, we focus on the elastodynamics, where

we present a conforming and a mixed finite element approach. Lastly, some numerical analysis of the coupled model is provided.
The theoretical considerations are then complemented by numerical studies in chapter 7. Since no exact solutions for the specific models in cardiac elasticity are known, we verify our framework by comparison to publicly available static benchmarks [99]. We present evaluation methods for the coupled dynamic setting and perform experiments to estimate the convergence order of the active strain coupled system.
Finally, we give a summary of the achieved results and describe further improvements and future research prospects.

1.4 Acknowledgement

The prelimary results of this work were obtained within the research project *"Ein integriertes Herz-Modell–Kopplung von Elektrophysiologie, Elastomechanik, Fluss und Kreislauf"* (05M16VKA) funded by the German Federal Ministry of Education and Research. We gratefully acknowledge the financial support by the BMBF and would like to emphasize that the collaboration within this research group had a major impact on this work.
Furthermore, the development and numerical tests presented in this theses were in large parts performed on the supercomputers "ForHLR II" and "HoreKa", funded by the Ministry of Science, Research and the Arts Baden-Württemberg and by the Federal Ministry of Education and Research.

CHAPTER

TWO

PRELIMINARIES

In this chapter, we introduce the basic notation and definitions used throughout this thesis. The concept of Fréchet derivatives is depicted as a generalization of differentiabilty on normed vector spaces. This allows us to consider differentiable mappings on manifolds. The chapter concludes with the introduction of k-forms and the resulting integral equations on smooth manifolds which are fundamental for the rest of this thesis.

2.1 Notation

Throughout this work, mappings may be scalar-, vector-, or tensor-valued. We denote scalar-valued properties by lowercase letters f, vector-valued properties by bold lowercase letters $\mathbf{f}$ and tensor-valued properties by bold uppercase letters $\mathbf{F}$.

Notation 2.1: If not further specified, we denote by

$$\|\cdot\| : \mathbb{R}^{n\times n} \to \mathbb{R}\,, \qquad \|\mathbf{A}\| \mapsto \operatorname{tr}(\mathbf{A}^\top \mathbf{A})$$

the euclidean norm.

Definition 2.2: Let $\mathbf{A} \in \mathbb{R}^{n\times n}$ be regular. We call

$$\operatorname{Cof}(\mathbf{A}) \coloneqq \det(\mathbf{A})\mathbf{A}^{-\top}$$

the *Cofactor matrix* of $\mathbf{A}$.

Definition 2.3: Let $\mathbf{A} \in \mathbb{R}^{n\times n}_{\text{sym}}$ and $\mathbf{B} \in \mathbb{R}^{n\times n}_{\text{sym}}$ be positive semi-definite, such that $\mathbf{B}^2 = \mathbf{A}$. We then call $\mathbf{B}$ *square root* of $\mathbf{A}$ and denote

$$\mathbf{A}^{\frac{1}{2}} \coloneqq \mathbf{B}\,.$$

Every symmetric, positive definite matrix $\mathbf{A}$ has a square root $\mathbf{A}^{\frac{1}{2}}$ (see e.g. [38, theorem 3.2-1]).

Notation 2.4: Let $\mathcal{X}, \mathcal{Y}$ be normed vector spaces. We denote by

$$\mathcal{M}ap(\mathcal{X};\mathcal{Y}) := \{f\colon \mathcal{X} \to \mathcal{Y}\}$$

the space of all mappings from $\mathcal{X}$ to $\mathcal{Y}$.

2.2 Fréchet derivatives

In this section, we outline the concepts of differentiabilty in general normed vector spaces. For more details, we refer to [3]. Let $\mathcal{X}$, $\mathcal{Y}$ be normed vector spaces and $\mathcal{D} \subset \mathcal{X}$ be open. We denote by $\mathcal{C}(\mathcal{X};\mathcal{Y})$ the space of all continuous mappings $f\colon \mathcal{X} \to \mathcal{Y}$. The subset $\mathcal{L}in(\mathcal{X};\mathcal{Y}) \subset \mathcal{C}(\mathcal{X};\mathcal{Y})$ denotes the set of all *linear* continuous mappings from $\mathcal{X}$ to $\mathcal{Y}$.

Definition 2.5: A mapping $f\colon \mathcal{D} \to \mathcal{Y}$ is called *differentiable* in $\mathbf{x} \in \mathcal{D}$, if there exists $\mathrm{D}f(\mathbf{x}) \in \mathcal{L}in(\mathcal{X};\mathcal{Y})$, such that

$$f(\mathbf{x}+\mathbf{h}) = f(\mathbf{x}) + (\mathrm{D}f(\mathbf{x}))\,(\mathbf{h}) + o(\|\mathbf{h}\|)\,, \qquad \mathbf{h} \in \mathcal{X}\,, \mathbf{x}+\mathbf{h} \in \mathcal{D}\,.$$

We call $\mathrm{D}f(\mathbf{x})$ the *Fréchet derivative* of f at the point $\mathbf{x}$. If f is differentiable at all points of $\mathcal{D}$, we call f differentiable in $\mathcal{D}$.

If a mapping $f\colon \mathcal{X} \to \mathcal{Y}$ is differentiable and $\mathrm{D}f\colon \mathcal{X} \to \mathcal{L}in(\mathcal{X};\mathcal{Y})$ is continuous, we call f *continuously differentiable*. The set of all continuously differentiable mappings is denoted by $\mathcal{C}^1(\mathcal{X};\mathcal{Y})$. In this context, we also set $\mathcal{C}^0(\mathcal{X};\mathcal{Y}) := \mathcal{C}(\mathcal{X};\mathcal{Y})$.

Definition 2.6: A mapping $f\colon \mathcal{D} \to \mathcal{Y}$ is called *differentiable in* $\mathbf{x} \in \mathcal{D}$ *in the direction* $\mathbf{h} \in \mathcal{X}$, if the limit

$$\mathrm{D}f(\mathbf{x})[\mathbf{h}] := \lim_{\varepsilon \to 0} \frac{f(\mathbf{x}+\varepsilon\mathbf{h}) - f(\mathbf{x})}{\varepsilon} \in \mathcal{Y}$$

exists. We call $\mathrm{D}f(\mathbf{x})[\mathbf{h}]$ the *directional derivative* of f in the direction $\mathbf{h}$.

For our purposes, as we will later see, it is more convenient to work with the directional derivative, especially because it is easier to compute.

Lemma 2.7: *Let* $f\colon \mathcal{D} \to \mathcal{Y}$ *be differentiable in* $\mathbf{x} \in \mathcal{D}$*. Then* f *is differentiable in* $\mathbf{x}$ *in all directions* $\mathbf{h} \in \mathcal{X}$ *and*

$$(\mathrm{D}f(\mathbf{x}))\,(\mathbf{h}) = \mathrm{D}f(\mathbf{x})[\mathbf{h}]\,.$$

Proof. For $\mathbf{x} \in \mathcal{D}$, $\mathbf{h} \in \mathcal{X}$, it holds

$$\begin{aligned} \mathrm{D}f(\mathbf{x})[\mathbf{h}] = \lim_{\varepsilon \to 0} \frac{f(\mathbf{x} + \varepsilon \mathbf{h}) - f(\mathbf{x})}{\varepsilon} &= \lim_{\varepsilon \to 0} \frac{f(\mathbf{x}) + (\mathrm{D}f(\mathbf{x}))\,(\varepsilon \mathbf{h}) + o(\|\varepsilon \mathbf{h}\|) - f(\mathbf{x})}{\varepsilon} \\ &= \lim_{\varepsilon \to 0} \frac{\varepsilon\,(\mathrm{D}f(\mathbf{x}))\,(\mathbf{h})}{\varepsilon} + \lim_{\varepsilon \to 0} \frac{o(\varepsilon\,\|\mathbf{h}\|)}{\varepsilon} \\ &= (\mathrm{D}f(\mathbf{x}))\,(\mathbf{h}) \end{aligned}$$

□

The classical chain rule applies to Fréchet derivatives as well.

Theorem 2.8 (Chain rule): *Let $\mathcal{X}$, $\mathcal{Y}$, $\mathcal{Z}$ be normed vector spaces and $\mathcal{U} \subset \mathcal{X}$, $\mathcal{V} \subset \mathcal{Y}$ be open. Further let $f \colon \mathcal{U} \to \mathcal{V}$ be differentiable in $\mathbf{x} \in \mathcal{U}$ and $g \colon \mathcal{V} \to \mathcal{Z}$ be differentiable in $\mathbf{y} := f(\mathbf{x}) \in \mathcal{V}$. Then the mapping $g \circ f \colon \mathcal{U} \to \mathcal{Z}$ is differentiable in $\mathbf{x}$ and*

$$(g \circ f)'(\mathbf{x}) = (\mathrm{D}g(f(\mathbf{x})))(\mathrm{D}f(\mathbf{x}))\,.$$

For $\mathbf{h} \in \mathcal{X}$, the corresponding directional derivative reads

$$\mathrm{D}(g \circ f)(\mathbf{x})[\mathbf{h}] = \mathrm{D}g(f(\mathbf{x}))\left[\mathrm{D}f(\mathbf{x})[\mathbf{h}]\right].$$

Proof. Since f and g are differentiable, it holds

$$\begin{aligned} f(\mathbf{x} + \mathbf{h}) &= f(\mathbf{x}) + (\mathrm{D}f(\mathbf{x}))(\mathbf{h}) + o_f(\|\mathbf{h}\|_{\mathcal{X}}) \\ &= \mathbf{y} + (\mathrm{D}f(\mathbf{x}))(\mathbf{h}) + o_f(\|\mathbf{h}\|_{\mathcal{X}})\,, \\ g(\mathbf{y} + \mathbf{k}) &= g(\mathbf{y}) + (\mathrm{D}g(\mathbf{y}))(\mathbf{k}) + o_g(\|\mathbf{k}\|_{\mathcal{Y}}) \end{aligned}$$

for $\mathbf{h} \in \mathcal{X}, \mathbf{k} \in \mathcal{Y}$ such that $\mathbf{x} + \mathbf{h} \in \mathcal{U}$, $\mathbf{y} + \mathbf{k} \in \mathcal{V}$. By setting $\mathbf{k} = (\mathrm{D}f(\mathbf{x}))(\mathbf{h}) + o_f(\|\mathbf{h}\|)$, we see that

$$\begin{aligned} \|\mathbf{k}\|_{\mathcal{Y}} &\leq \left(\|(\mathrm{D}f(\mathbf{x}))\|_{\mathcal{M}ap(\mathcal{X};\mathcal{Y})} + \left\| \frac{o_f(\|\mathbf{h}\|_{\mathcal{X}})}{\|\mathbf{h}\|_{\mathcal{X}}} \right\| \right) \|\mathbf{h}\|_{\mathcal{X}} \\ &= \Big(\|(\mathrm{D}f(\mathbf{x}))\|_{\mathcal{M}ap(\mathcal{X};\mathcal{Y})} + \|o_f(1)\| \Big) \|\mathbf{h}\|_{\mathcal{X}} \end{aligned}$$

For this $\mathbf{k}$, we then have

$$\begin{aligned} (g \circ f)(\mathbf{x} + \mathbf{h}) &= g(f(\mathbf{x}) + (\mathrm{D}f(\mathbf{x}))(\mathbf{h}) + o_f(\|\mathbf{h}\|_{\mathcal{X}})) \\ &= g(\mathbf{y} + \mathbf{k}) \\ &= g(\mathbf{y}) + (\mathrm{D}g(\mathbf{y}))\big((\mathrm{D}f(\mathbf{x}))(\mathbf{h}) + o_f(\|\mathbf{h}\|_{\mathcal{X}})\big) + o_g(\|\mathbf{k}\|_{\mathcal{Y}}) \\ &= g(\mathbf{y}) + (\mathrm{D}g(\mathbf{y}))\big((\mathrm{D}f(\mathbf{x}))(\mathbf{h})\big) + (\mathrm{D}g(\mathbf{y}))\big(o_f(\|\mathbf{h}\|_{\mathcal{X}})\big) + o_g(\|\mathbf{k}\|_{\mathcal{Y}}) \\ &= g(\mathbf{y}) + (\mathrm{D}g(\mathbf{y}))\big((\mathrm{D}f(\mathbf{x}))(\mathbf{h})\big) + \psi(\mathbf{h})\,, \end{aligned}$$

where we use the linearity of $\mathrm{D}g(\mathbf{y})$ and

$$\psi(\mathbf{h}) = (\mathrm{D}g(\mathbf{y}))\big(o_f(\|\mathbf{h}\|)\big) + o_g(\|\mathbf{h}\|_{\mathcal{X}}) \,.$$

Using the same estimate as for the norm of $\mathbf{k}$, we see that $\psi(\mathbf{h}) = o(\|\mathbf{h}\|_{\mathcal{X}})$. Thus $g \circ f$ is differentiable. The formula for the directional derivative follows from the equation above. □

For the sake of completeness, we briefly mention the concept of higher order Fréchet derivatives.

Definition 2.9: Let $f\colon \mathcal{D} \to \mathcal{Y}$ be differentiable in $\mathcal{D}$ with derivative mapping

$$\mathrm{D}f(\mathbf{x})\colon \mathcal{D} \to \mathcal{L}in(\mathcal{X};\mathcal{Y}) \,.$$

We call f *twice differentiable in* $\mathbf{x} \in \mathcal{D}$, if $\mathrm{D}f(\mathbf{x})$ is differentiable in $\mathbf{x}$. We call

$$\mathrm{D}^2 f(\mathbf{x}) \coloneqq \mathrm{D}(\mathrm{D}f)(\mathbf{x}) \in \mathcal{L}in(\mathcal{X}, \mathcal{L}in(\mathcal{X};\mathcal{Y}))$$

the *second derivative* of f in $\mathbf{x}$.
If f is twice differentiable for all $\mathbf{x} \in \mathcal{D}$, we call f twice differentiable in $\mathcal{D}$.

Again, if the second derivative of f is continuous, we call the mapping f twice continuously differentiable and write

$$f \in \mathcal{C}^2(\mathcal{X};\mathcal{Y}) \,.$$

Similar to above, the notation using directional derivatives is more useful:

Lemma 2.10: *Let $f\colon \mathcal{D} \to \mathcal{Y}$ be twice differentiable. Then its second derivative is a symmetric bilinear mapping, in the sense that*

$$\mathrm{D}^2 f(\mathbf{x})[\mathbf{h};\mathbf{k}] = \mathrm{D}\big(\mathrm{D}f(\mathbf{x})[\mathbf{h}]\big)[\mathbf{k}] = \mathrm{D}\big(\mathrm{D}f(\mathbf{x})[\mathbf{k}]\big)[\mathbf{h}] = \mathrm{D}^2 f(\mathbf{x})[\mathbf{k};\mathbf{h}] \,, \qquad \mathbf{h},\mathbf{k} \in \mathcal{X} \,.$$

Proof. Direct calculation using the definition of the directional derivative. □

We denote by

$$\mathcal{L}in_r(\mathcal{X};\mathcal{Y}) = \mathcal{L}in(\mathcal{X}, \mathcal{L}in_{r-1}(\mathcal{X};\mathcal{Y})) \,, \qquad r \geq 2 \,,$$

the space of all continuous r-linear mappings from $\mathcal{X}$ to $\mathcal{Y}$ and set $\mathcal{L}in_1(\mathcal{X};\mathcal{Y}) = \mathcal{L}in(\mathcal{X};\mathcal{Y})$. Higher-order derivates are then defined iteratively:

Definition 2.11: Let $f\colon \mathcal{D} \to \mathcal{Y}$ be $(r-1)$-times differentiable with $(r-1)$th derivative mapping

$$\mathrm{D}^{(r-1)} f\colon \mathcal{D} \to \mathcal{L}in_{r-1}(\mathcal{X};\mathcal{Y}) \,, \qquad \mathbf{x} \mapsto f^{(r-1)}(\mathbf{x}) \,.$$

Then f is called *r-times differentiable* in $\mathbf{x} \in \mathcal{D}$, if $f^{(r-1)}$ is differentiable in $\mathbf{x}$. We call its derivative

$$\mathrm{D}^r f(\mathbf{x}) \coloneqq \mathrm{D}(\mathrm{D}f)(\mathbf{x}) \in \mathcal{Lin}_r(\mathcal{X}, \mathcal{Lin}(\mathcal{X}; \mathcal{Y}))$$

the r-th derivative.
If f is r-times differentiable for all $\mathbf{x} \in \mathcal{D}$, we call f r-times differentiable in $\mathcal{D}$.

If the r-th derivative of f is continuous, we say that the mapping f is r-times continuously differentiable and write

$$f \in \mathcal{C}^r(\mathcal{X}; \mathcal{Y}) \, .$$

Lemma 2.12: *Let $\Omega \subset \mathbb{R}^n$ be a region with smooth boundary and let*

$$\mathcal{X} = \mathcal{C}^r(\overline{\Omega}; \mathbb{R}^n) \, , \qquad \mathcal{Y} = \mathcal{C}^{k-1}(\overline{\Omega}; \mathbb{R}^n)$$

for $1 \leq k < \infty$. Let further be

$$W \in \mathcal{C}^r \left(\overline{\Omega} \times \mathcal{Map}(\mathbb{R}^n; \mathbb{R}^n) \to \mathbb{R}^n \right)$$

with $r \geq k - 1 - l \geq 0$. Then the function

$$f \colon \mathcal{X} \to \mathcal{Y} \, , \qquad \mathbf{f}(u)(\mathbf{x}) = W(\mathbf{x}, \mathrm{D}u(\mathbf{x}))$$

is in $\mathcal{C}^l$ and

$$(Df(u)[v])(\mathbf{x}) = \mathrm{D}_{\mathrm{D}u} W(\mathbf{x}, \mathrm{D}u(\mathbf{x}))[\mathrm{D}v(\mathbf{x})]$$

Proof. We only show $r = k = 1$. Since

$$\begin{aligned} (Df(u)[v])(\mathbf{x}) &= \lim_{\varepsilon \to 0} \frac{1}{\varepsilon} \left(f(u + \varepsilon v)(\mathbf{x}) - f(u)(\mathbf{x}) \right) \\ &= \frac{1}{\varepsilon} \left(W(\mathbf{x}, \mathrm{D}u(\mathbf{x}) + \varepsilon \mathrm{D}v(\mathbf{x})) - W(\mathbf{x}, \mathrm{D}u(\mathbf{x})) \right) \\ &= \mathrm{D}_{\mathrm{D}u} W(\mathbf{x}, \mathrm{D}u(\mathbf{x}))[\mathrm{D}v(\mathbf{x})] \end{aligned}$$

and $W \in \mathcal{C}^1$, it follows $\mathrm{D}f \in \mathcal{C}^0$. Therefore $f \in \mathcal{C}^1(\mathcal{X}; \mathcal{Y})$. □

2.3 Tangent maps

For a proper definition of the relevant mathematical objects in continuum mechanics, we use basic definitions in differential geometry to introduce tangents on manifolds. We will then see that deformations of a three-dimensional body are a special case of the representations below. We avoid the coordinate free description, as we will use all definitions in Euclidean space. For a more general form and proofs, we refer to [106].

Definition 2.13: A *smooth n-manifold* is a set $\mathcal{M}$, such that

(i) For each $\mathbf{x} \in \mathcal{M}$ there is a subset $\mathcal{U} \subset \mathcal{M}$ with $\mathbf{x} \in \mathcal{U}$ and an injective mapping

$$\mathbf{X} \colon \mathcal{U} \to \mathcal{V} \subset \mathbb{R}^n .$$

Such a mapping $\mathbf{X}$ is called *chart*.

(ii) If $\mathbf{X}$ and $\overline{\mathbf{X}}$ are two charts of a subset $\mathcal{U}$, the change in coordinates

$$\mathbf{X}(\mathcal{U}) \to \overline{\mathbf{X}}(\mathcal{U})$$

has to be in $C^\infty(\mathbf{X}(\mathcal{U}); \overline{\mathbf{X}}(\mathcal{U}))$.

Remark 2.14: Any open set $\mathcal{M} \subset \mathbb{R}^n$ is a n-manifold with the chart

$$\mathbf{X} \colon \mathcal{M} \to \mathcal{M}\,, \qquad \mathbf{x} \mapsto \mathbf{x}$$

being applicable for all subsets $\mathcal{U} \subset \mathcal{M}$. Additionally, each C^∞ mapping is then also a chart of $\mathcal{M}$.

We will continue to pose defintions and theorems for general n-manifolds $\mathcal{M}, \mathcal{N}$. We will later use them for open subsets of $\mathbb{R}^3$.

Definition 2.15: A manifold $\mathcal{M}$ is called *oriented*, if for all pairs of charts $\mathbf{X}, \overline{\mathbf{X}}$ of $\mathcal{M}$, the corresponding change in coordinates $\boldsymbol{\psi}_{\mathbf{X},\overline{\mathbf{X}}} \colon \mathbf{X}(\mathcal{M}) \to \overline{\mathbf{X}}(\mathcal{M})$ is *orientation preserving*, that is

$$\det(\mathrm{D}\boldsymbol{\psi}_{\mathbf{X},\overline{\mathbf{X}}}) > 0\,.$$

The term *orientation preserving* can be extended to any mapping between two manifolds $\boldsymbol{\phi} \colon \mathcal{M} \to \mathcal{N}$.

Definition 2.16: Let $\mathcal{M}$ be a n-manifold and $\mathbf{x} \in \mathcal{M}$.

1. The vector space $\mathbb{R}^n$ of all vectors originating at $\mathbf{x} \in \mathcal{M}$ is called *tangent space* $T_{\mathbf{x}}\mathcal{M}$ of $\mathcal{M}$ in $\mathbf{x}$.

2. The product $T\mathcal{M} = \mathcal{M} \times \mathbb{R}^n$ consisting of pairs of points $\mathbf{x} \in \mathcal{M}$ and associated tangent vectors $\mathbf{W} \subset \mathbb{R}^n$ is called the *tangent bundle* of $\mathcal{M}$.

Definition 2.17: Let $\mathcal{M}$ be a n-manifold and $\boldsymbol{\phi} \in C^1(\mathcal{M}; \mathcal{N})$. Then the *tangent map* of $\boldsymbol{\phi}$ is defined as

$$T\boldsymbol{\phi} \colon T\mathcal{M} \to T\mathcal{N}\,, \qquad (\mathbf{x}, \mathbf{W}) \mapsto (\boldsymbol{\phi}(\mathbf{x})\,, \mathrm{D}\boldsymbol{\phi}(\mathbf{x})[\mathbf{W}])\,.$$

For a fixed $\mathbf{x} \in \Omega$, the restriction $\mathrm{D}\boldsymbol{\phi}\big|_{T_{\mathbf{x}}\mathcal{M}}$ is a linear map.

Lemma 2.18: *Let $\mathcal{U}$, $\mathcal{V}$, $\mathcal{W}$ be manifolds and $\boldsymbol{\phi} \in C^r(\mathcal{U}, \mathcal{V})$, $\psi \in C^r(\mathcal{V}, \mathcal{W})$ with $r \geq 1$. Then*

$$\psi \circ \boldsymbol{\phi} \in C^r(\mathcal{U}, \mathcal{W}) \qquad \textit{with} \qquad T(\psi \circ \boldsymbol{\phi}) = T\psi \circ T\boldsymbol{\phi}\,.$$

Proof. Let $(\mathbf{x}, \mathbf{W}) \in T\mathcal{U}$. Then

$$\begin{aligned}
T(\psi \circ \boldsymbol{\phi})(\mathbf{x}, \mathbf{W}) &= (\psi(\boldsymbol{\phi}(\mathbf{x})), \mathrm{D}(\psi \circ \boldsymbol{\phi})(\mathbf{x})[\mathbf{W}]) \\
&= (\psi(\boldsymbol{\phi}(\mathbf{x})), \mathrm{D}\psi(\boldsymbol{\phi}(\mathbf{x}))\,[\mathrm{D}\boldsymbol{\phi}(\mathbf{x})[\mathbf{W}]]) \\
&= T(\psi)\,(\boldsymbol{\phi}(\mathbf{x}), \mathrm{D}\boldsymbol{\phi}(\mathbf{x})[\mathbf{W}]) \\
&= T(\psi)\,(T(\boldsymbol{\phi}(\mathbf{x}), \mathbf{W}))
\end{aligned}$$

by the chain rule. □

Definition 2.19: Let $\mathcal{M}$ be a n-manifold. We call a mapping

$$\mathbf{v} \colon \mathcal{M} \to T\mathcal{M}$$

a *vector field* on $\mathcal{M}$, if $\mathbf{v}(\mathbf{x}) \in T_{\mathbf{x}}\mathcal{M}$ for all $\mathbf{x}$ in $\mathcal{M}$.

Definition 2.20: Let $\mathcal{M}$ be a n-manifold and $\boldsymbol{\phi} \in C^1(\mathcal{M}; \mathcal{N})$.

- Let $\mathbf{v}$ be a vectorfield on $\mathcal{M}$. Then

  $$\boldsymbol{\phi}_* \mathbf{v} := T\boldsymbol{\phi} \circ \mathbf{v} \circ \boldsymbol{\phi}^{-1}$$

  is called the *push-forward* of $\mathbf{v}$ by $\boldsymbol{\phi}$.

- Let $\mathbf{v}^{\phi}$ be a vectorfield on $\boldsymbol{\phi}(\mathcal{M})$ and $\boldsymbol{\phi}^{-1} \in C^1(\mathcal{N}; \mathcal{M})$. Then

  $$\boldsymbol{\phi}^* \mathbf{v}^{\phi} := T(\boldsymbol{\phi}^{-1}) \circ \mathbf{v}^{\phi} \circ \boldsymbol{\phi}$$

  is called the *pull-back* of $\mathbf{v}^{\phi}$ by $\boldsymbol{\phi}$.

Remark 2.21: If $\mathbf{v}$ and $\mathbf{v}^{\phi}$ are vectorfields on $\mathcal{M}$ and $\boldsymbol{\phi}(\mathcal{M})$, respectively, then

$$\begin{aligned}
\boldsymbol{\phi}_* \mathbf{v} &\colon \boldsymbol{\phi}(\mathcal{M}) \to T\boldsymbol{\phi}(\mathcal{M})\,, & \mathbf{x}^{\phi} &\mapsto \left(\mathbf{x}^{\phi}, \mathrm{D}\boldsymbol{\phi}(\mathbf{x})\left[\mathbf{v}(\boldsymbol{\phi}^{-1}(\mathbf{x}^{\phi}))\right]\right)\,, \\
\boldsymbol{\phi}^* \mathbf{v}^{\phi} &\colon \mathcal{M} \to T\mathcal{M}\,, & \mathbf{x} &\mapsto \left(\mathbf{x}, \mathrm{D}\boldsymbol{\phi}^{-1}(\mathbf{x}^{\phi})\left[\mathbf{v}^{\phi}(\boldsymbol{\phi}(\mathbf{x}))\right]\right)
\end{aligned}$$

are vectorfields on $\boldsymbol{\phi}(\mathcal{M})$ and $\mathcal{M}$, respectively.

2.4 Differential forms

In the previous section we introduced the concept of manifolds. We continue by briefly discussing k-forms and their connection to integral formulations in three-dimensional space. If not further specified, we always consider $\mathcal{M}$ and $\mathcal{N}$ to be a n-manifolds and $\boldsymbol{\phi} \in C^1(\mathcal{M};\mathcal{N})$. A more extensive study of the topic is given in [17].

Definition 2.22: A *differential k-form* is a mapping $\boldsymbol{\alpha}$ of the form $\mathbf{x} \mapsto \boldsymbol{\alpha}_{\mathbf{x}}$, where

$$\boldsymbol{\alpha}_{\mathbf{x}} \colon \underbrace{T_{\mathbf{x}}\mathcal{M} \times \cdots \times T_{\mathbf{x}}\mathcal{M}}_{k-\text{times}} \to \mathbb{R}$$

is multilinear and skew symmetric, i.e.

$$\boldsymbol{\alpha}_{\mathbf{x}}(\mathbf{W}_{\pi(1)}, \ldots, \mathbf{W}_{\pi(k)}) = \operatorname{sgn}(\pi)\boldsymbol{\alpha}_{\mathbf{x}}(\mathbf{W}_1, \ldots, \mathbf{W}_k)\,, \qquad \mathbf{W}_1, \ldots, \mathbf{W}_k \in T_{\mathbf{x}}\mathcal{M}$$

for any permutation π on $\{1, \ldots, k\}$.

We omit the index $\mathbf{x}$ of $\boldsymbol{\alpha}_{\mathbf{x}}$ for better readability, noting that the tangents $\mathbf{W}_i$, $i = 1, \ldots, k$, always depend on their origin $\mathbf{x}$.

Definition 2.23: Let $\boldsymbol{\alpha}$ be a k-form and $\boldsymbol{\beta}$ be a l-form. Their *exterior product*

$$\begin{aligned}
&\boldsymbol{\alpha} \wedge \boldsymbol{\beta}(\mathbf{W}_1, \ldots, \mathbf{W}_k, \mathbf{W}_{k+1}, \ldots, \mathbf{W}_{k+l}) \\
&\quad := \frac{1}{k!l!} \sum_{\pi} \operatorname{sgn}(\pi)\boldsymbol{\alpha}(\mathbf{W}_{\pi(1)}, \ldots, \mathbf{W}_{\pi(k)})\boldsymbol{\beta}(\mathbf{W}_{\pi(k+1)}, \ldots, \mathbf{W}_{\pi(k+l)})
\end{aligned}$$

defines a $(k+l)$-form $\boldsymbol{\alpha} \wedge \boldsymbol{\beta}$.

Definition 2.24: Let $d \in \mathbb{N}$ and $f \in C^1(\mathcal{M};\mathbb{R}^d)$ such that

$$Tf \colon T\mathcal{M} \to T\mathbb{R}^d = \mathbb{R}^d \times \mathbb{R}^d\,, \qquad (\mathbf{x}, \mathbf{W}) \mapsto (f(\mathbf{x}), \mathrm{D}f(\mathbf{x})[\mathbf{W}])\,.$$

We call the 1-form

$$\mathbf{d}f := \mathbf{d}f_{\mathbf{x}} \colon T_{\mathbf{x}}\mathcal{M} \to \mathbb{R}^d\,, \qquad \mathbf{W} \mapsto \mathrm{D}f(\mathbf{x})[\mathbf{W}]$$

the *differential of f*.

Definition 2.25: For $k = 1, \ldots, n$, we call the 1-forms

$$\mathbf{dx}^k \colon T_{\mathbf{x}}\mathcal{M} \to \mathbb{R}\,, \qquad \mathbf{W} \mapsto W_k$$

the *coordinate differential forms*, where W_k ist the k-th component of $\mathbf{W} \in \mathbb{R}^n$.

Theorem 2.26: *There exists a unique linear operator* $\mathbf{d}$*, such that for all k-forms* $\boldsymbol{\alpha}$ *on* $\mathcal{M}$*,* $\mathbf{d}\boldsymbol{\alpha}$ *is a* $(k+1)$*-form on* $\mathcal{M}$ *and* *(i)* $\mathbf{d}(\mathbf{d}\boldsymbol{\alpha}) = 0$.

(ii) $\mathbf{d}(\boldsymbol{\alpha} \wedge \boldsymbol{\beta}) = (\mathbf{d}\boldsymbol{\alpha}) \wedge \boldsymbol{\beta} + (-1)^k \boldsymbol{\alpha} \wedge (\mathbf{d}\boldsymbol{\beta})$.

(iii) *For a scalar function* $f\colon \mathcal{M} \to \mathbb{R}$*,* $\mathbf{d}f$ *coincides with the differential from definition 2.24.*

Proof. See [106, chapter 1, theorem 7.4]. □

Definition 2.27: Let $\boldsymbol{\alpha}^\phi$ be a k-form on $\boldsymbol{\phi}(\mathcal{M})$. Then

$$(\boldsymbol{\phi}^* \boldsymbol{\alpha}^\phi)(\mathbf{W}_1, \ldots, \mathbf{W}_k) = \boldsymbol{\alpha}(\boldsymbol{\phi}_* \mathbf{W}_1, \ldots \boldsymbol{\phi}_* \mathbf{W}_k) , \qquad \mathbf{W}_1, \ldots, \mathbf{W}_k \in T_{\mathbf{x}}\mathcal{M}$$

is called the *pull-back of* $\boldsymbol{\alpha}^\phi$ on $\mathcal{M}$.

Lemma 2.28: *Let* $\boldsymbol{\alpha}^\phi$ *be a* k*-form on* $\boldsymbol{\phi}(\mathcal{M})$*. Then*

$$(\boldsymbol{\phi}^* \mathbf{d}\boldsymbol{\alpha}^\phi) = \mathbf{d}(\boldsymbol{\phi}^* \boldsymbol{\alpha}^\phi) .$$

Proof. See [106, chapter 1, proposition 7.5]. □

We finalize this chapter by stating some key theorems about integration on manifolds.

Lemma 2.29: *Let* $\boldsymbol{\alpha}$ *be a* k*-form on* $\mathcal{M}$*. Then there exists a unique function* $f\colon \mathcal{M} \to \mathbb{R}$*, such that*

$$\boldsymbol{\alpha}_{\mathbf{x}} = f(\mathbf{x}) \mathbf{dx}^1 \wedge \cdots \wedge \mathbf{dx}^k , \qquad \mathbf{x} \in \mathcal{M} .$$

Proof. See [102, proposition 15.29]. □

The lemma above leads to the conclusion, that there exists a k-form on $\mathcal{M}$ of the form

$$\mathrm{d}V := \mathbf{dx}^1 \wedge \cdots \wedge \mathbf{dx}^n .$$

We call $\mathrm{d}V$ the *volume element* of $\mathcal{M}$.

Theorem 2.30: *Let* $\boldsymbol{\phi}$ *be orientation-preserving and* $\boldsymbol{\alpha}^\phi$ *a* n*-form on the* n*-manifold* $\boldsymbol{\phi}(\mathcal{M})$*. Then*

$$\int_{\phi(\mathcal{M})} \boldsymbol{\alpha}^\phi = \int_{\mathcal{M}} \boldsymbol{\phi}^* \boldsymbol{\alpha}^\phi .$$

Proof. See [106, chapter 1, theorem 7.12]. □

For the following theorems, we consider the boundary $\partial\mathcal{M}$ of the manifold $\mathcal{M}$. The boundary is itself a $(n-1)$-manifold.

Theorem 2.31: *Let* $\partial\mathcal{M}$ *be positively oriented and* $\boldsymbol{\alpha}$ *be a* $(n-1)$*-form on* $\partial\mathcal{M}$*. Then*

$$\int_{\partial\mathcal{M}} \boldsymbol{\alpha} = \int_{\mathcal{M}} \mathbf{d}\boldsymbol{\alpha} .$$

Proof. See [102, theorem 16.11]. □

We call $\mathrm{d}A := \mathbf{dx}^1 \wedge \cdots \wedge \mathbf{dx}^{n-1}$ the *area element* on $\partial\mathcal{M}$. It depicts the „volume element" of the $(n-1)$-manifold $\partial\mathcal{M}$.

Theorem 2.32: *Let* $\mathbf{v}\colon \mathcal{M} \to T\mathcal{M}$ *be differentiable on* $\mathcal{M}$*. Then*

$$\int_{\mathcal{M}} \operatorname{div}(\mathbf{v})\,\mathrm{d}V = \int_{\partial\mathcal{M}} \mathbf{v}\cdot\mathbf{n}\,\mathrm{d}A\,,$$

where $\mathbf{n}$ *is the unit outward normal on* $\partial\mathcal{M}$*.*

Proof. See [106, chapter 1, theorem 7.17]. □

Corollary 2.33: *Let* $\mathbf{v}\colon \mathcal{M} \to T\mathcal{M}$ *be a differentiable vectorfield on* $\mathcal{M}$ *and* $w\colon \mathcal{M} \to \mathbb{R}$ *be a differentiable scalar function. Then*

$$\int_{\mathcal{M}} \operatorname{div}(\mathbf{v})\,w\,\mathrm{d}V = -\int_{\mathcal{M}} \mathbf{v}\cdot\mathrm{D}w\,\mathrm{d}V + \int_{\partial\mathcal{M}} \mathbf{v}\cdot\mathbf{n}\,w\,\mathrm{d}A\,,$$

where $\mathbf{n}$ *is the unit outward normal on* $\partial\mathcal{M}$*.*

Proof. Using the chain rule of the divergence operator, i.e., $\operatorname{div}(w\mathbf{v}) = w\operatorname{div}(\mathbf{v}) + \mathbf{v}\cdot\mathrm{D}w$, we get

$$\int_{\mathcal{M}} \operatorname{div}(\mathbf{v})\,w\,\mathrm{d}V = -\int_{\mathcal{M}} \mathbf{v}\cdot\mathrm{D}w\,\mathrm{d}V + \int_{\mathcal{M}} \operatorname{div}(w\mathbf{v})\,\mathrm{d}V \overset{2.31}{=} -\int_{\mathcal{M}} \mathbf{v}\cdot\mathrm{D}w\,\mathrm{d}V + \int_{\partial\mathcal{M}} \mathbf{v}\cdot\mathbf{n}\,w\,\mathrm{d}A\,.$$

□

Remark 2.34: By lemma 2.29, differential forms can be described with scalar valued mappings $f\colon \mathcal{M} \to \mathbb{R}$ by

$$f(\mathbf{x})\mathbf{dx}^1 \wedge \cdots \wedge \mathbf{dx}^k\,, \qquad \mathbf{x} \in \mathcal{M}\,.$$

When using cartesian coordinates, the defintions above can be extended to vector-valued functions $\mathbf{f}\colon \mathcal{M} \to \mathbb{R}^d$, $d \in \mathbb{N}$. We interpret the corresponding vector-valued k-forms and integrals component-wise.

CHAPTER

THREE

FOUNDATIONS OF NONLINEAR CONTINUUM MECHANICS

This chapter introduces basic definitions and concepts of nonlinear kinematics, utilizing concepts of differential geometry similar to the ones used in [106]. The derivation of balance laws and the equations of motion in the initial configuration for elastodynamics follow the structure of [38], where these concepts are well introduced for static problems. More details used in this chapter can be studied further in [41].

3.1 Kinematic motion

In continuum mechanics, we consider bodies with continuous mass density occupying a subset of three-dimensional space. *Kinematics* describes the deformation of these bodies given external or internal forces. We begin by defining the basic objects we will consider throughout this work.

Definition 3.1: A *continuum body* is an open set $\Omega \subset \mathbb{R}^3$. A *configuration* of the body Ω is a map

$$\boldsymbol{\phi} \colon \Omega \to \mathbb{R}^3 \,.$$

We denote by $\boldsymbol{\Phi} = \boldsymbol{\Phi}(\Omega)$ the set of all configurations of Ω.

Definition 3.2: A *motion* of a continuum body Ω is a mapping

$$\boldsymbol{\varphi} \colon [0,T] \to \boldsymbol{\Phi}(\Omega)\,, \qquad t \mapsto \boldsymbol{\varphi}_t(\Omega)\,.$$

where $\boldsymbol{\varphi}_t$ are configurations of Ω.

The concept of a motion represents the transformation, rotation and deformation of a body over time. This definition does not need to specify the initial configuration $\boldsymbol{\varphi}_0(\Omega)$.

However, we will throughout this work always assume $\boldsymbol{\varphi}_0(\Omega) = \Omega$, i.e., no deformation has taken place at the time $t = 0$.

Definition 3.3: A motion $\boldsymbol{\varphi}$ of Ω is called *regular*, if $\boldsymbol{\varphi}_t(\Omega)$ is open and $\boldsymbol{\varphi}_t$ is invertible for all $t \in [0, T]$. A motion $\boldsymbol{\varphi}$ of Ω is called $\mathcal{C}^r$*-regular* or r*-regular*, if $\boldsymbol{\varphi}_t^{-1} \in \mathcal{C}^r(\boldsymbol{\varphi}_t(\Omega); \Omega)$ for all $t \in [0, T]$.

The regularity of $\boldsymbol{\varphi}$ indicates the „niceness" of the physical deformation of Ω. Events such as ripping, pinching or interpenetration of matter cannot be described by regular motions.

Remark 3.4: The definition of regularity allows self-contact, since $\boldsymbol{\varphi}_t(\Omega)$ is open. In this case however, we cannot extend $\boldsymbol{\varphi}_t$ to the boundary of Ω.

For every *material point* $\mathbf{x} \in \Omega$, we characterize the corresponding *spatial point* by

$$\mathbf{x}^{\varphi} := \mathbf{x}^{\varphi}(t) := \boldsymbol{\varphi}(t, \mathbf{x}) \in \boldsymbol{\varphi}_t(\Omega) \,.$$

Though each motion of a body is a curve in $\boldsymbol{\Phi}$, it is for our purposes more convenient to rewrite motions as mappings in space and time, i.e.

$$\boldsymbol{\varphi}\colon [0, T] \times \Omega \to \boldsymbol{\Phi}(\Omega) \,, \qquad (t, \mathbf{x}) \mapsto \mathbf{x}^{\varphi} \,.$$

Definition 3.5: Let $\boldsymbol{\varphi}\colon [0, T] \times \Omega \to \boldsymbol{\Phi}(\Omega)$ be a motion. We call

$$\mathbf{u}(t, \mathbf{x}) := \mathbf{x}^{\varphi} - \mathbf{x} \,.$$

the *displacement* of $\mathbf{x}$.

By this definition, we can also reformulate $\boldsymbol{\varphi}$ to $\boldsymbol{\varphi}(t, \mathbf{x}) = \mathbf{x} + \mathbf{u}(t, \mathbf{x})$.

Definition 3.6: Let $\boldsymbol{\varphi}\colon [0, T] \times \Omega \to \boldsymbol{\Phi}(\Omega)$ be a 1-regular motion. We call the mapping

$$\mathbf{v}\colon [0, T] \times \Omega \to \mathbb{R}^3 \,, \qquad \mathbf{v}(t, \mathbf{x}) := \frac{\partial \boldsymbol{\varphi}}{\partial t}(t, \mathbf{x}) = \frac{\partial \mathbf{u}}{\partial t}(t, \mathbf{x})$$

the *material velocity* of $\boldsymbol{\varphi}$.

Note that the material velocity is only defined on the initial body Ω. We can formulate the velocity on a configuration $\boldsymbol{\varphi}_t(\Omega)$ as the parametrization $\mathbf{v}^{\varphi}(t, \boldsymbol{\varphi}(t, \mathbf{x}))$:

Definition 3.7: Let $\boldsymbol{\varphi}\colon [0, T] \times \Omega \to \boldsymbol{\Phi}(\Omega)$ be a 1-regular motion. We call the mapping

$$\mathbf{v}^{\varphi}\colon [0, T] \times \boldsymbol{\Phi}(\Omega) \to \mathbb{R}^3 \,, \qquad \mathbf{v}^{\varphi}(t, \mathbf{x}^{\varphi}) = \mathbf{v}(t, \boldsymbol{\varphi}^{-1}(t, \mathbf{x}^{\varphi}))$$

the *spatial velocity* of $\boldsymbol{\varphi}$.

Intuitively, we often need to reverse the above definition: The velocity associated with a given motion is "measured" on the configuration $\boldsymbol{\varphi}_t(\Omega)$. We would like to formulate this velocity in the coordinates of the original configuration Ω. This gives us the relationship

$$\mathbf{v}(t,\mathbf{x}) = \mathbf{v}^{\varphi}(t,\boldsymbol{\varphi}(t,\mathbf{x}))\,.$$

Definition 3.8: Let $\boldsymbol{\varphi}\colon [0,T]\times\Omega \to \boldsymbol{\Phi}(\Omega)$ be a 1-regular motion and

$$\mathbf{f}^{\varphi}\colon [0,T]\times\boldsymbol{\Phi}(\Omega)\to\mathbb{R}^3\,,\qquad (t,\mathbf{x}^{\varphi})\to\mathbf{f}^{\varphi}_t(\mathbf{x}^{\varphi})$$

be a mapping with $\mathbf{f}^{\varphi}_t \in C^1(\boldsymbol{\varphi}_t(\Omega);\mathbb{R}^3)$ for all $t\in[0,T]$. Then

$$\frac{\mathrm{d}\mathbf{f}^{\varphi}}{\mathrm{d}t}(t,\mathbf{x}^{\varphi}) = \frac{\partial\mathbf{f}^{\varphi}}{\partial t}(t,\mathbf{x}^{\varphi}) + \mathrm{D}^{\varphi}\mathbf{f}^{\varphi}(t,\mathbf{x}^{\varphi})\mathbf{v}^{\varphi}(t,\mathbf{x}^{\varphi})$$

is called the *material (time) derivative* of $\mathbf{f}^{\varphi}$.

By D^{φ} we denote the derivate in space with respect to $\mathbf{x}^{\varphi}$. We always distinguish between the derivative D with respect to the material coordinates $\mathbf{x}$ and the derivative D^{φ} with respect to $\mathbf{x}^{\varphi}$. For any spatial mapping $\mathbf{f}^{\varphi}$ as above, we can set the corresponding material mapping

$$\mathbf{f}\colon [0,T]\times\Omega\to\mathbb{R}^3\,,\qquad \mathbf{f}(t,\mathbf{x}) \coloneqq \mathbf{f}^{\varphi}(t,\mathbf{x}^{\varphi})\,.$$

By the chain rule, it holds

$$\frac{\partial\mathbf{f}}{\partial t}(t,\mathbf{x}) = \frac{\mathrm{d}\mathbf{f}^{\varphi}}{\mathrm{d}t}(t,\mathbf{x}^{\varphi})\,.$$

Definition 3.9: Let $\boldsymbol{\varphi}\colon [0,T]\times\Omega \to \boldsymbol{\Phi}(\Omega)$ be a 1-regular motion. We call the mapping $\mathbf{a}(t,\mathbf{x}) \coloneqq \frac{\partial\mathbf{v}}{\partial t}(t,\mathbf{x})$ *material acceleration* of $\boldsymbol{\varphi}$ and $\mathbf{a}^{\varphi}(t,\mathbf{x}^{\varphi}) = \mathbf{a}(t,\mathbf{x})$ the *spatial acceleration* of $\boldsymbol{\varphi}$.

With the material derivative, we see that

$$\mathbf{a}(t,\mathbf{x}) = \frac{\partial\mathbf{v}^{\varphi}}{\partial t}(t,\mathbf{x}^{\varphi}) + \mathrm{D}^{\varphi}\mathbf{v}^{\varphi}(t,\mathbf{x}^{\varphi})\mathbf{v}^{\varphi}(t,\mathbf{x}^{\varphi})$$

Remark 3.10: The object $\mathrm{D}^{\varphi}\mathbf{v}^{\varphi}(t,\mathbf{x}^{\varphi})$ is called *velocity gradient tensor*. Using the concepts of the following chapters, more convenient descriptions of this tensor can be derived. Though we will not need it within the context of this work, the velocity gradient tensor is crucial when considering viscoelastic materials [73].

3.2 Deformation gradient

The local deformation of the continuum body is described by the *deformation gradient* of $\boldsymbol{\varphi}$. We motivate this object as the tangent of $\boldsymbol{\varphi}$, using the more abstract formulations

introduced in section 2.3: As an open subset of $\mathbb{R}^3$, the domain Ω is a 3-manifold with unit vector basis $\{\mathbf{e}^1, \mathbf{e}^2, \mathbf{e}^3\}$.
With these abstract definitions, we are well-equipped to define the relevant objects for our three-dimensional special case.

Definition 3.11: Let $\boldsymbol{\phi}\colon \Omega \to \boldsymbol{\Phi}(\Omega)$ be a $\mathcal{C}^1$-configuration of Ω. The tangent $T\boldsymbol{\phi}$ of $\boldsymbol{\phi}$ is denoted by $\mathbf{F}$ and called the *deformation gradient* of $\boldsymbol{\phi}$. For $\mathbf{x} \in \Omega$, the restriction

$$\mathbf{F}(\mathbf{x}) := \mathbf{F}_{\mathbf{x}}\colon T_{\mathbf{x}}\Omega \to T_{\mathbf{x}^{\varphi}}\mathbb{R}^n\,, \qquad \mathbf{y} \mapsto \mathbf{F}(\mathbf{x})\mathbf{y}$$

is a linear transformation.

The deformation gradient is well-defined for any 1-regular motion $\boldsymbol{\varphi}\colon [0,T] \times \Omega \to \boldsymbol{\Phi}(\Omega)$, where we set $\mathbf{F}(t,\mathbf{x})$ as the tangent $T\boldsymbol{\varphi}_t$ of $\boldsymbol{\varphi}_t$ for all $t \in [0,T]$. Again, it is more convenient to write $\mathbf{F}$ as a tensor-valued function

$$\mathbf{F}\colon [0,T] \times \Omega \to \mathbb{R}^{3\times 3}\,, \qquad (t,\mathbf{x}) \mapsto \mathbf{F}(t,\mathbf{x})\,.$$

Lemma 3.12: *Let $\boldsymbol{\varphi}\colon [0,T] \times \Omega \to \boldsymbol{\Phi}(\Omega)$ be a 1-regular motion. Then its deformation gradient for $t \in [0,T]$ and $\mathbf{x} \in \Omega$ is given by*

$$\mathbf{F} := \mathbf{F}(t,\mathbf{x}) = \begin{pmatrix} \frac{\partial\varphi_1}{\partial x_1} & \frac{\partial\varphi_1}{\partial x_2} & \frac{\partial\varphi_1}{\partial x_3} \\ \frac{\partial\varphi_2}{\partial x_1} & \frac{\partial\varphi_2}{\partial x_2} & \frac{\partial\varphi_2}{\partial x_3} \\ \frac{\partial\varphi_3}{\partial x_1} & \frac{\partial\varphi_3}{\partial x_2} & \frac{\partial\varphi_3}{\partial x_3} \end{pmatrix} (t,\mathbf{x})$$

The deformation gradient describes local changes between the material and spatial configuration and most macroscopic properties of a motion rely on it. One particular property is the change of volume discussed in section 4.3. We will see that the volume of a configuration $\boldsymbol{\varphi}_t(\Omega)$ is connected to the determinant of $\mathbf{F}$.

Definition 3.13: Let $\boldsymbol{\varphi}\colon [0,T] \times \Omega \to \boldsymbol{\Phi}(\Omega)$ be a 1-regular motion. The function

$$J\colon [0,T] \times \Omega \to \mathbb{R}\,, \qquad (t,\mathbf{x}) \mapsto \det(\mathbf{F}(t,\mathbf{x}))$$

is called *Jacobian.*

Since the motion $\boldsymbol{\varphi}$ is regular, its deformation gradient is invertible for all $(t,\mathbf{x}) \in [0,T]\times\Omega$, i.e.

$$J := J(t,\mathbf{x}) = \det(\mathbf{F}) \neq 0 \qquad \forall\ (t,\mathbf{x}) \in [0,T] \times \Omega\,.$$

Furthermore, since the determinant is continuous and $\mathbf{F} = \mathbf{I}$ for $t = 0$, it holds

$$J(t,\mathbf{x}) > 0 \qquad \forall\ (t,\mathbf{x}) \in [0,T] \times \Omega\,.$$

Lemma 3.14: *Let $\boldsymbol{\varphi}\colon [0,T]\times\Omega \to \boldsymbol{\Phi}(\Omega)$ be a 1-regular motion with Jacobian J. Then*

$$\mathrm{D}_{\mathbf{F}} J(t,\mathbf{x}) = J(t,\mathbf{x})\mathbf{F}^{-\top}(t,\mathbf{x})\,, \qquad \frac{\partial J}{\partial t}(t,\mathbf{x}) = J(t,\mathbf{x})\mathrm{div}^{\varphi}(\mathbf{v}^{\varphi}(t,\mathbf{x}^{\varphi}))\,.$$

Proof. Let $\mathbf{H}\in\mathbb{R}^{3\times3}$ be arbitrary. Since $J>0$, $\mathbf{F}$ is invertible and it holds

$$\det(\mathbf{F}+\varepsilon\mathbf{H}) = \det(\mathbf{F})\det(\mathbf{I}+\varepsilon\mathbf{F}^{-1}\mathbf{H}) = \det(\mathbf{F})(1+\varepsilon\,\mathrm{tr}(\mathbf{F}^{-1}\mathbf{H})+o(\varepsilon^2))\,,$$

where the last expansion results from the definition of the determinant. Then

$$\mathrm{D}_{\mathbf{F}}\det(\mathbf{F})[\mathbf{H}] = \lim_{\varepsilon\to0}\frac{\det(\mathbf{F}+\varepsilon\mathbf{H})-\det(\mathbf{F})}{\varepsilon} = \det(\mathbf{F})\,\mathrm{tr}(\mathbf{F}^{-1}\mathbf{H}) = J\mathbf{F}^{-\top}:\mathbf{H}\,.$$

With this result, we use the chain rule on the determinant to get

$$\begin{aligned}\frac{\partial}{\partial t}\det(\mathbf{F}) &= \mathrm{D}_{\mathbf{F}}\det(\mathbf{F})[\frac{\partial}{\partial t}\mathbf{F}] = \det(\mathbf{F})\,\mathrm{tr}\left(\mathbf{F}^{-1}\mathrm{D}\mathbf{v}\right)\\ &= \det(\mathbf{F})\,\mathrm{tr}\left(\mathrm{D}^{\varphi}\mathbf{v}^{\varphi}\mathbf{F}\mathbf{F}^{-1}\right) = J\,\mathrm{div}^{\varphi}(\mathbf{v}^{\varphi})\,,\end{aligned}$$

where we used [41, proposition 2.1] to get $\mathrm{D}\mathbf{v} = \mathrm{D}^{\varphi}\mathbf{v}^{\varphi}\mathbf{F}$. □

We close this section by giving the definitions of two tensors commonly used in elasticity.

Definition 3.15: Let $\boldsymbol{\varphi}\colon[0,T]\times\Omega\to\mathbb{R}^3$ be a 1-regular motion. The symmetric tensor

$$\mathbf{B}\colon T\Omega\to T\Omega\,, \qquad \mathbf{B} := \mathbf{F}\mathbf{F}^{\top}$$

is called *left Cauchy-Green strain tensor.*

We mostly use the left Cauchy-Green strain tensor for some theorems in the upcoming chapter.

Definition 3.16: Let $\boldsymbol{\varphi}\colon[0,T]\times\Omega\to\mathbb{R}^3$ be a 1-regular motion. The symmetric tensor

$$\mathbf{C}\colon T\Omega\to T\Omega\,, \qquad \mathbf{C} := \mathbf{F}^{\top}\mathbf{F}$$

is called *right Cauchy-Green strain tensor.*

The right Cauchy-Green strain tensor introduces a positive definite quadratic form which we will later use to compute lengths. Let $\mathbf{f}\in\mathbb{R}^3$ be a vector starting at $\mathbf{x}\in\Omega$ with length $|\mathbf{f}| = \sqrt{\mathbf{f}\cdot\mathbf{f}}$. The corresponding deformed vector $\mathbf{f}^{\varphi} = \mathbf{F}(\mathbf{x})\mathbf{f}$ then has the length

$$|\mathbf{f}^{\varphi}| = \sqrt{\mathbf{F}\mathbf{f}\cdot\mathbf{F}\mathbf{f}} = \sqrt{\mathbf{f}^{\top}\mathbf{C}\mathbf{f}}\,.$$

Definition 3.17: Let $\boldsymbol{\varphi}\colon[0,T]\times\Omega\to\mathbb{R}^3$ be a 1-regular motion. The tensor

$$\mathbf{E}\colon T\Omega\to T\Omega\,, \qquad \mathbf{E} := \frac{1}{2}(\mathbf{C}-\mathbf{I})$$

is called *Green-St. Venant strain tensor.*

As shown in [38, section 1.8], the Green-St. Venant strain tensor illustrates the "deviation" of $\boldsymbol{\varphi}$ to a purely rigid deformation.

3.3 Equations of equilibrium

From this point on, we consider $\boldsymbol{\varphi}\colon [0,T] \times \Omega \to \boldsymbol{\Phi}(\Omega)$ to be a motion on the continuum body Ω with intermediate configurations $\boldsymbol{\varphi}(t,\Omega) = \boldsymbol{\varphi}_t(\Omega)$. We set $\boldsymbol{\varphi}(t,\mathbf{x}) = \mathbf{x}^{\varphi}$. If not further specified, we assume $\boldsymbol{\varphi}$ to be regular enough to allow the upcoming definitions and theorems.

This section describes the basic axioms of continuum mechanics, namely the conservation of mass and momentum. These fundamental laws of physics will provide a set of equations which will be the basis of our mathematical model.

Lemma 3.18: *Let $f^{\varphi}\colon [0,T] \times \boldsymbol{\Phi}(\Omega) \to \mathbb{R}$ be a spatial mapping with corresponding material mapping $f\colon [0,T] \times \Omega \to \mathbb{R}$ and let $\mathcal{D} \subset \Omega$ be open. Then*

$$\int_{\boldsymbol{\varphi}_t(\mathcal{D})} f^{\varphi}(t,\mathbf{x}^{\varphi})\,\mathrm{d}V^{\varphi} = \int_{\mathcal{D}} f(t,\mathbf{x})J(t,\mathbf{x})\,\mathrm{d}V\,, \qquad t \in [0,T]\,.$$

Proof. This follows from 2.30 with $\boldsymbol{\alpha} = f^{\varphi}\,\mathrm{d}V^{\varphi}$ and $\boldsymbol{\varphi}^{*}\,\mathrm{d}V^{\varphi} = J\,\mathrm{d}V$. For a more in-depth proof, we refer to [49, section V.4]. □

Definition 3.19 (Piola transform): Let $\mathbf{f}^{\varphi}$ be a vectorfield on $\boldsymbol{\varphi}_t(\Omega)$. Then the vectorfield

$$\mathbf{f}(t,\mathbf{x}) = J(t,\mathbf{x})(\boldsymbol{\varphi}^{*}\mathbf{f}^{\varphi})(t,\mathbf{x}) = J(t,\mathbf{x})\mathbf{f}^{\varphi}(t,\mathbf{x}^{\varphi})\mathbf{F}^{-\top}(t,\mathbf{x})\,, \qquad (t,\mathbf{x}) \in [0,T] \times \Omega\,,$$

on Ω is called its *Piola transform.*

The Piola transform is essential for the transformation of vector- and tensor-valued vectorfields into the reference configuration Ω, due to the following properties. The proofs of these identities are not difficult, but somewhat technical, which is why we refer to [38, section 1.7].

Lemma 3.20 (Piola identity): *Let $\boldsymbol{\varphi}[0,T] \times \Omega \to \mathbb{R}^3$ be a 1-regular motion. Then*

$$\operatorname{div}\Big((J(t,\mathbf{x})\mathbf{F}^{-\top}(t,\mathbf{x})\Big) = 0$$

Lemma 3.21: *Let $\mathbf{f}^{\varphi}$ be a vectorfield on $\boldsymbol{\varphi}_t(\Omega)$ with Piola transform $\mathbf{f}$. Then*

$$\operatorname{div}(\mathbf{f}(t,\mathbf{x})) = J(t,\mathbf{x})\operatorname{div}^{\varphi}(\mathbf{f}^{\varphi}(t,\mathbf{x}^{\varphi}))\,,$$

Lemma 3.22: *Let $\mathbf{f}^{\varphi}$ be a vectorfield on $\boldsymbol{\varphi}_t(\Omega)$ with Piola transform $\mathbf{f}$ and let $\mathcal{D} \subset \Omega$ be open. Then*

$$\int_{\partial\boldsymbol{\varphi}_t(\mathcal{D})} \mathbf{f}^{\varphi} \cdot \mathbf{n}^{\varphi}\,\mathrm{d}A^{\varphi} = \int_{\partial\mathcal{D}} \mathbf{f} \cdot \mathbf{n}\,\mathrm{d}A\,.$$

Remark 3.23: From lemma 3.22, we conclude two properties related to the area elements of $\mathcal{D}$ and $\varphi_t(\mathcal{D})$:

(i) If $\mathbf{n}$ and $\mathbf{n}^\varphi$ are the outer normal vectors at $\mathbf{x}$ and $\mathbf{x}^\varphi$, then $\mathbf{n}^\varphi = \frac{\mathrm{Cof}(\mathbf{F})\mathbf{n}}{|\mathrm{Cof}(\mathbf{F})\mathbf{n}|}$.

(ii) The area elements are related by $\mathrm{d}A^\varphi = \mathrm{Cof}\,(\mathbf{F})\,\mathrm{d}A$.

The equations of equilibrium dictate that certain quantities stay constant over time. We will therefore examine the time derivative of integrals over time-dependant functions. The corresponding relation on moving geometries is given by *Reynolds transport theorem*:

Theorem 3.24 (Reynolds transport theorem): *Let $f^\varphi\colon [0,T]\times \mathbf{\Phi}(\Omega)\to\mathbb{R}$ be a $\mathcal{C}^1$ mapping and $\mathcal{D}\subset\Omega$ open. Then*

$$\frac{\partial}{\partial t}\int_{\varphi_t(\mathcal{D})} f^\varphi\,\mathrm{d}V^\varphi = \int_{\varphi_t(\mathcal{D})} \frac{\mathrm{d}f^\varphi}{\mathrm{d}t} + f^\varphi \mathrm{div}^\varphi \mathbf{v}^\varphi\,\mathrm{d}V^\varphi = \int_{\varphi_t(\mathcal{D})} \frac{\partial f^\varphi}{\partial t} + \mathrm{div}^\varphi\left(f^\varphi \mathbf{v}^\varphi\right)\mathrm{d}V^\varphi$$

Proof. Using 3.18, it holds

$$\begin{aligned}
\frac{\partial}{\partial t}\int_{\varphi_t(\mathcal{D})} f^\varphi\,\mathrm{d}V^\varphi &= \int_{\mathcal{D}}\frac{\partial}{\partial t}(f(t,\mathbf{x})J(t,\mathbf{x}))\,\mathrm{d}V\\
&= \int_{\mathcal{D}}\left(\frac{\partial f}{\partial t}(t,\mathbf{x})J(t,\mathbf{x})\right) + \left(f(t,\mathbf{x})\frac{\partial J}{\partial t}(t,\mathbf{x})\right)\mathrm{d}V\\
&\overset{3.14}{=} \int_{\mathcal{D}}\left(\frac{\partial f}{\partial t}(t,\mathbf{x}) + f(t,\mathbf{x})\mathrm{div}^\varphi(\mathbf{v}^\varphi(t,\boldsymbol{\varphi}(t,\mathbf{x})))\right)J(t,\mathbf{x})\,\mathrm{d}V\\
&= \int_{\varphi_t(\mathcal{D})}\frac{\mathrm{d}f^\varphi}{\mathrm{d}t}(t,\mathbf{x}^\varphi) + f^\varphi(t,\mathbf{x}^\varphi)\mathrm{div}^\varphi(\mathbf{v}^\varphi(t,\mathbf{x}^\varphi))\,\mathrm{d}V^\varphi
\end{aligned}$$

□

Definition 3.25: Let $a^\varphi, b^\varphi\colon [0,T]\times\mathbf{\Phi}(\Omega)\to\mathbb{R}$ and $\mathbf{c}^\varphi\colon[0,T]\times\mathbf{\Phi}(\Omega)\to\mathbb{R}^3$. The mappings a^φ, b^φ and $\mathbf{c}^\varphi$ satisfy the *spatial master balance law*, if for any open $\mathcal{D}\subset\Omega$ with sufficiently smooth boundary $\partial\mathcal{D}$, the equation

$$\frac{\mathrm{d}}{\mathrm{d}t}\int_{\varphi_t(\mathcal{D})} a^\varphi\,\mathrm{d}V^\varphi = \int_{\varphi_t(\mathcal{D})} b^\varphi\,\mathrm{d}V^\varphi + \int_{\partial\varphi_t(\mathcal{D})}\mathbf{c}^\varphi\cdot\mathbf{n}^\varphi\,\mathrm{d}A^\varphi$$

is well defined and holds for all $t\in[0,T]$.

The term "sufficiently smooth" is usually fulfilled if $\partial\mathcal{D}$ is piecewise $\mathcal{C}^1$ [106, chapter 2.1]. However, some of the upcoming statements may require additional regularity of $\partial\mathcal{D}$. Since we are not interested in the specific regularity requirements on subsets $\mathcal{D}\subset\Omega$, we omit them for the sake of brevity and always assume $\mathcal{D}$ is sufficiently smooth.

Theorem 3.26: *Let $a^\varphi\in\mathcal{C}^1([0,T]\times\mathbf{\Phi}(\Omega);\mathbb{R})$, $b^\varphi\in\mathcal{C}^0([0,T]\times\mathbf{\Phi}(\Omega);\mathbb{R})$ and $\mathbf{c}^\varphi\in\mathcal{C}^1([0,T]\times\mathbf{\Phi}(\Omega);\mathbb{R}^3)$. The mappings satisfy the spatial master balance law if and only if*

$$\frac{\partial a^\varphi}{\partial t} + \mathrm{div}^\varphi(a^\varphi\mathbf{v}^\varphi) = b^\varphi + \mathrm{div}^\varphi(\mathbf{c}^\varphi)\,. \tag{3.1}$$

Proof. With theorems 3.24 and 2.32, the master balance law is equivalent to

$$\frac{\mathrm{d}}{\mathrm{d}t}\int_{\varphi_t(\mathcal{D})}\frac{\partial a^\varphi}{\partial t}+\operatorname{div}^\varphi(a^\varphi\mathbf{v}^\varphi)\,\mathrm{d}V^\varphi=\int_{\varphi_t(\mathcal{D})}b^\varphi\,\mathrm{d}V^\varphi+\int_{\varphi_t(\mathcal{D})}\operatorname{div}^\varphi(\mathbf{c}^\varphi)\,\mathrm{d}V^\varphi\,,\qquad\mathcal{D}\subset\Omega\,.$$

Thus, if (3.1) holds, the master balance law has to hold. Conversely, since $\mathcal{D}$ is arbitrary, equation (3.1) holds if a^φ, b^φ and $\mathbf{c}^\varphi$ satisfy the master balance law. □

Definition 3.27: Let $a, b\colon [0,T]\times\Omega\to\mathbb{R}$ and $\mathbf{c}\colon [0,T]\times\Omega\to\mathbb{R}^3$ and let J be the Jacobian of $\boldsymbol{\varphi}$. The mappings a, b and $\mathbf{c}$ satisfy the *material master balance law*, if for any open $\mathcal{D}\subset\Omega$, the equation

$$\frac{\mathrm{d}}{\mathrm{d}t}\int_{\mathcal{D}}a\,J\,\mathrm{d}V=\int_{\mathcal{D}}b\,J\,\mathrm{d}V+\int_{\partial\mathcal{D}}\mathbf{c}\cdot\mathbf{n}\,\mathrm{d}A$$

is well defined and holds for all $t\in[0,T]$.

Theorem 3.28: *Let J be the Jacobian of $\boldsymbol{\varphi}$ and $(a\,J)\in\mathcal{C}^1([0,T]\times\Omega;\mathbb{R})$, $(b\,J)\in\mathcal{C}^0([0,T]\times\Omega;\mathbb{R})$ and $\mathbf{c}\in\mathcal{C}^1([0,T]\times\Omega;\mathbb{R}^3)$. The mappings satisfy the material master balance law if and only if*

$$\frac{\partial}{\partial t}(a\,J)=b\,J+\operatorname{div}(\mathbf{c})\,.\tag{3.2}$$

Proof. This follows analogously to the proof of theorem 3.26. □

With spatial and material definitions of the same principle, we lastly need to know how to switch from a spatial to a material setting (and vice versa).

Theorem 3.29: *Let the mappings $a^\varphi, b^\varphi, \mathbf{c}^\varphi$ and $a, b, \mathbf{c}$ from above be related by*

$$a(t,\mathbf{x})=a^\varphi(t,\mathbf{x}^\varphi)\,,\qquad b(t,\mathbf{x})=b^\varphi(t,\mathbf{x}^\varphi)\,,\qquad \mathbf{c}(t,\mathbf{x})=J\mathbf{c}^\varphi(t,\mathbf{x}^\varphi)\mathbf{F}^{-\top}\,.$$

Then $a^\varphi, b^\varphi, \mathbf{c}^\varphi$ satisfy the spatial master balance law if and only if $a, b, \mathbf{c}$ satisfy the material master balance law.

Proof. Using conversion 3.18 for a and b and the divergence theorem 2.32 together with the divergence property of the Piola transform 3.21 for $\mathbf{c}$, we get

$$\frac{\mathrm{d}}{\mathrm{d}t}\int_{\varphi_t(\mathcal{D})}a^\varphi\,\mathrm{d}V^\varphi-\int_{\varphi_t(\mathcal{D})}b^\varphi\,\mathrm{d}V^\varphi-\int_{\partial\varphi_t(\mathcal{D})}\mathbf{c}^\varphi\cdot\mathbf{n}^\varphi\,\mathrm{d}A^\varphi=\frac{\mathrm{d}}{\mathrm{d}t}\int_{\mathcal{D}}a\,J\,\mathrm{d}V-\int_{\mathcal{D}}b\,J\,\mathrm{d}V-\int_{\partial\mathcal{D}}\mathbf{c}\cdot\mathbf{n}\,\mathrm{d}A\,.$$

□

Theorem 3.30 (Cauchy): *Let $a^\varphi\in\mathcal{C}^1([0,T]\times\boldsymbol{\Phi}(\Omega);\mathbb{R})$, $b^\varphi\in\mathcal{C}^0([0,T]\times\boldsymbol{\Phi}(\Omega);\mathbb{R})$ and $c^\varphi\in\mathcal{C}^0([0,T]\times T\boldsymbol{\Phi}(\Omega);\mathbb{R})$. Assume that for all open $\mathcal{D}\subset\Omega$, $a^\varphi, b^\varphi, c^\varphi$ satisfy*

$$\frac{\mathrm{d}}{\mathrm{d}t}\int_{\varphi_t(\mathcal{D})}a^\varphi(t,\mathbf{x}^\varphi)\,\mathrm{d}V^\varphi=\int_{\varphi_t(\mathcal{D})}b^\varphi(t,\mathbf{x}^\varphi)\,\mathrm{d}V^\varphi+\int_{\partial\varphi_t(\mathcal{D})}c^\varphi(t,\mathbf{x}^\varphi,\mathbf{n}^\varphi)\,\mathrm{d}A^\varphi\,,\qquad t\in[0,T]\,.$$

Then there exists a unique vectorfield $\mathbf{c}^\varphi\in\mathcal{C}^1([0,T]\times\boldsymbol{\Phi}(\Omega);\mathbb{R}^3)$, such that

$$c^\varphi(t,\mathbf{x}^\varphi,\mathbf{n}^\varphi)=\mathbf{c}^\varphi(t,\mathbf{x}^\varphi)\cdot\mathbf{n}^\varphi\,,\qquad\forall\,t\in[0,T],\ \mathbf{x}^\varphi\in\varphi_t(\Omega),\ \mathbf{n}^\varphi\in T\varphi_t(\Omega)$$

and $a^\varphi, b^\varphi, \mathbf{c}^\varphi$ satisfy the spatial master balance law.

Proof. See [106, section 2.1]. □

Remark 3.31: A similar statement holds for material quantities and the material master balance law.

The master balance laws and Cauchys theorem are still only abstract integral equations on a deformed continuum body. We continue by presenting the laws of physics mentioned at the beginning of this section as integral equations.

Definition 3.32: A mapping $\rho^\varphi \colon [0,T] \times \boldsymbol{\Phi}(\Omega) \to \mathbb{R}$ is said to obey the *conservation of mass*, if for all open $\mathcal{D} \subset \Omega$, it holds

$$\frac{\mathrm{d}}{\mathrm{d}t} \int_{\varphi_t(\mathcal{D})} \rho^\varphi(t, \mathbf{x}^\varphi) \, \mathrm{d}V^\varphi = 0\,, \qquad t \in [0,T]\,.$$

We call ρ^φ the *mass density* and $m(\boldsymbol{\varphi}_t(\mathcal{D})) \coloneqq \int_{\boldsymbol{\varphi}_t(\mathcal{D})} \rho^\varphi \, \mathrm{d}V^\varphi$ the *mass* of $\boldsymbol{\varphi}_t(\mathcal{D})$.

The conservation of mass states that the mass of a continuum body does not change under deformations, i.e.,

$$m(\boldsymbol{\varphi}_t(\mathcal{D})) \coloneqq \int_{\varphi_t(\mathcal{D})} \rho^\varphi(t, \mathbf{x}^\varphi) \, \mathrm{d}V^\varphi = \int_{\mathcal{D}} \rho(\mathbf{x}) \, \mathrm{d}V = m(\mathcal{D})\,, \qquad t \in [0,T]$$

with the reference mass density $\rho \colon \Omega \to \mathbb{R}$. We naturally set $\rho^\varphi(0, \boldsymbol{\varphi}(0,\mathbf{x})) = \rho(\mathbf{x})$.

Lemma 3.33: *Let $f^\varphi \colon [0,T] \times \boldsymbol{\Phi}(\Omega) \to \mathbb{R}$ be a $\mathcal{C}^1$ mapping and $\mathcal{D} \subset \Omega$ open. Let conservation of mass hold with mass density ρ^φ. Then for the mapping $\rho^\varphi f^\varphi$, the transport theorem 3.24 simplifies to*

$$\frac{\mathrm{d}}{\mathrm{d}t} \int_{\varphi_t(\mathcal{D})} \rho^\varphi f^\varphi \, \mathrm{d}V^\varphi = \int_{\varphi_t(\mathcal{D})} \rho^\varphi \frac{\mathrm{d}f^\varphi}{\mathrm{d}t} \, \mathrm{d}V^\varphi\,.$$

Proof. Using the transport theorem 3.24 only for the mass density ρ^φ, we get

$$0 = \frac{\mathrm{d}}{\mathrm{d}t} \int_{\varphi_t(\mathcal{D})} \rho^\varphi \, \mathrm{d}V^\varphi = \int_{\varphi_t(\mathcal{D})} \frac{\mathrm{d}\rho^\varphi}{\mathrm{d}t} + \rho^\varphi \mathrm{div}^\varphi(\mathbf{v}^\varphi) \, \mathrm{d}V^\varphi\,.$$

Since $\mathcal{D}$ is arbitrary, it follows

$$\frac{\mathrm{d}\rho^\varphi}{\mathrm{d}t} + \rho^\varphi \, \mathrm{div}(\mathbf{v}) \equiv 0\,.$$

With this, we evaluate the integral

$$\begin{aligned}
\frac{\mathrm{d}}{\mathrm{d}t} \int_{\varphi_t(\mathcal{D})} \rho^\varphi f^\varphi \, \mathrm{d}V^\varphi &\overset{3.24}{=} \int_{\varphi_t(\mathcal{D})} \frac{\partial \rho^\varphi f^\varphi}{\partial t} + \mathrm{div}^\varphi(\rho^\varphi f^\varphi \mathbf{v}^\varphi) \, \mathrm{d}V^\varphi \\
&= \int_{\varphi_t(\mathcal{D})} \frac{\partial \rho^\varphi}{\partial t} f^\varphi + \frac{\partial f^\varphi}{\partial t} \rho^\varphi + \mathrm{D}(\rho^\varphi f^\varphi) \cdot \mathbf{v}^\varphi + \rho^\varphi f^\varphi \mathrm{div}^\varphi(\mathbf{v}^\varphi) \, \mathrm{d}V^\varphi \\
&= \int_{\varphi_t(\mathcal{D})} \rho^\varphi \frac{\mathrm{d}f^\varphi}{\mathrm{d}t} + \left(\frac{\partial \rho^\varphi}{\partial t} f^\varphi + f^\varphi \mathrm{D}\rho^\varphi \cdot \mathbf{v}^\varphi + \rho^\varphi f^\varphi \mathrm{div}^\varphi(\mathbf{v}^\varphi) \right) \mathrm{d}V^\varphi \\
&= \int_{\varphi_t(\mathcal{D})} \rho^\varphi \frac{\mathrm{d}f^\varphi}{\mathrm{d}t} + \Bigg(\underbrace{\frac{\mathrm{d}\rho^\varphi}{\mathrm{d}t} + \rho^\varphi \mathrm{div}^\varphi(\mathbf{v}^\varphi)}_{=0} \Bigg) f^\varphi \, \mathrm{d}V^\varphi\,.
\end{aligned}$$

□

Up until now, we have stated all definitions and theorems for scalar functions and vector-valued vectorfields. However, as mentioned in remark 2.34, the results so far can be transferred to vector-valued functions and tensor-valued vectorfields. We then interpret integrals component-wise and, for any tensor $\mathbf{F}\colon \Omega \to \mathbb{R}^{3\times 3}$, denote with $\operatorname{div}(\mathbf{F}) \in \mathbb{R}^3$ the vector of divergences of the rows of $\mathbf{F}$.

Definition 3.34: Let φ be a deformation resulting from exterior forces.

(i) The function $\mathbf{b}^\varphi\colon [0,T] \times \mathbf{\Phi}(\Omega) \to \mathbb{R}^3$ describing all forces per unit volume acting on $\varphi_t(\Omega)$ is called *applied body force* per unit volume.

(ii) The function $\mathbf{g}^\varphi\colon [0,T] \times \mathbf{\Phi}(\Gamma) \to \mathbb{R}^3$ describing the union of all forces acting on subsets $\Gamma_t^\varphi \subset \partial\varphi_t(\Omega)$ of the boundary is called *applied surface force*.

Let $\mathcal{D}$ be an open subset of Ω.

3. The *sum of all forces* acting on $\varphi_t(\mathcal{D})$ is defined by

$$F(\varphi_t(\mathcal{D})) \coloneqq \int_{\varphi_t(\mathcal{D})} \rho^\varphi \mathbf{b}^\varphi \,\mathrm{d}V^\varphi + \int_{\partial\varphi_t(\mathcal{D})\cap\Gamma_t^\varphi} \mathbf{g}^\varphi \,\mathrm{d}A^\varphi\,, \qquad t \in [0,T]\,.$$

4. The *torque of all forces* with respect to the origin acting on $\varphi_t(\mathcal{D})$ is defined by

$$T(\varphi_t(\mathcal{D})) \coloneqq \int_{\varphi_t(\mathcal{D})} \rho^\varphi (\mathbf{x}^\varphi \times \mathbf{b}^\varphi) \,\mathrm{d}V^\varphi + \int_{\partial\varphi_t(\mathcal{D})\cap\Gamma_t^\varphi} \mathbf{x}^\varphi \times \mathbf{g}^\varphi \,\mathrm{d}A^\varphi\,, \qquad t \in [0,T]\,.$$

For a continuum body with mass density ρ^φ, we may write the applied body forces as $\mathbf{f}^\varphi \coloneqq \rho^\varphi \mathbf{b}^\varphi$.

Definition 3.35: Let φ be the resulting deformation from applied forces $\mathbf{b}^\varphi, \mathbf{g}^\varphi$. The forces are said to obey the *conservation of linear momentum*, if for all open $\mathcal{D} \subset \Omega$, it holds

$$\frac{\mathrm{d}}{\mathrm{d}t} \int_{\varphi_t(\mathcal{D})} \rho^\varphi \mathbf{v}^\varphi \,\mathrm{d}V^\varphi = F(\varphi_t(\mathcal{D}))\,, \qquad t \in [0,T]\,.$$

We call $M_{\mathrm{L}}(\varphi_t(\mathcal{D})) \coloneqq \int_{\varphi_t(\mathcal{D})} \rho^\varphi \mathbf{v}^\varphi \,\mathrm{d}V^\varphi$ the *linear momentum* of $\mathcal{D}$ under φ.

Remark 3.36: The definition above is equivalent to Newtons second law of motion, which states that the change of linear momentum $M_{\mathrm{L}}(\varphi_t(\mathcal{D}))$ over time is equal to the sum of applied forces $F(\varphi_t(\mathcal{D}))$.

Definition 3.37: Let φ be the resulting deformation from applied forces $\mathbf{b}^\varphi, \mathbf{g}^\varphi$. The forces are said to obey the *conservation of angular momentum*, if for all open $\mathcal{D} \subset \Omega$, it holds

$$\frac{\mathrm{d}}{\mathrm{d}t} \int_{\varphi_t(\mathcal{D})} \rho^\varphi (\mathbf{x}^\varphi \times \mathbf{v}^\varphi) \,\mathrm{d}V^\varphi = T(\varphi_t(\mathcal{D}))\,, \qquad t \in [0,T]\,.$$

We call $M_{\mathrm{A}}(\varphi_t(\mathcal{D})) \coloneqq \int_{\varphi_t(\mathcal{D})} \rho^\varphi (\mathbf{x}^\varphi \times \mathbf{v}^\varphi) \,\mathrm{d}V^\varphi$ the *angular momentum* of $\mathcal{D}$ under φ.

The following assumption, called the *Stress Principle of Euler and Cauchy* is the fundamental concept of continuum mechanics, which is why we formulate it as an axiom. It postulates the existence of a vector-valued function, such that for each time $t \in [0,T]$, any subset of $\boldsymbol{\varphi}_t(\Omega)$, including $\boldsymbol{\varphi}_t(\Omega)$ itself, is in a static equilibrium.

Axiom 3.38: *Let $\mathcal{S}^1 \subset \mathbb{R}^3$ be the space of all vectors with unit-length and let $\boldsymbol{\varphi}$ be a motion on a body Ω. Let the deformed body $\boldsymbol{\varphi}_t(\Omega)$ have a mass density $\rho^\varphi \colon \boldsymbol{\varphi}_t(\Omega) \to \mathbb{R}$ and be subjected to applied forces $\mathbf{b}^\varphi \colon \boldsymbol{\varphi}_t(\Omega) \to \mathbb{R}^3$ and $\mathbf{g}^\varphi \colon \boldsymbol{\varphi}_t(\Gamma) \to \mathbb{R}^3$. Then there exists a vectorfield $\mathbf{t}^\varphi \colon [0,T] \times \boldsymbol{\Phi}(\Omega) \times \mathcal{S}^1 \to \mathbb{R}^3$, such that for all open subsets $\mathcal{D} \subset \Omega$, it holds*

$$\mathbf{t}^\varphi(t, \mathbf{x}^\varphi, \mathbf{n}^\varphi) = \mathbf{g}^\varphi(t, \mathbf{x}^\varphi)\,, \qquad \forall\, t \in [0,T],\ \mathbf{x}^\varphi \in \boldsymbol{\varphi}_t(\mathcal{D}),\ \mathbf{n}^\varphi \in \partial\boldsymbol{\varphi}_t(\mathcal{D}) \cap \Gamma_t^\varphi$$

and $\mathbf{b}^\varphi$, $\mathbf{g}^\varphi$ obey the conservation of linear and angular momentum.

We call $\mathbf{t}^\varphi$ the *Cauchy stress vector.*

3.4 The Cauchy stress principle

In the last section, we introduced balance laws and the fundamental axiom of continuum mechanics. Combined, they imply major consequences, concluding in the partial differential equation relating the exterior forces $\mathbf{b}^\varphi$, $\mathbf{g}^\varphi$ and the motion $\boldsymbol{\varphi}$.
Throughout the rest of this chapter, let $\boldsymbol{\varphi} \colon [0,T] \times \Omega \to \boldsymbol{\Phi}(\Omega)$ be a motion with applied forces $\mathbf{b}^\varphi \colon [0,T] \times \boldsymbol{\Phi}(\Omega) \to \mathbb{R}^3$ and $\mathbf{g}^\varphi \colon [0,T] \times \boldsymbol{\Phi}(\Gamma) \to \mathbb{R}^3$ and let $\rho^\varphi \colon [0,T] \times \boldsymbol{\Phi}(\Omega) \to \mathbb{R}$ be a mass density on $\boldsymbol{\varphi}(\Omega)$.

Theorem 3.39: *Let the stress principle 3.38 and the balance of linear momentum 3.35 hold. Let $\boldsymbol{\varphi} \in \mathcal{C}^1([0,T] \times \Omega; \mathbb{R}^3)$ and the Cauchy stress vector $\mathbf{t}^\varphi$ be continuous. Then there exists a unique tensorfield $\mathbf{T}^\varphi \colon [0,T] \times \boldsymbol{\Phi}(\Omega) \to \mathbb{R}^{3\times 3}$ satisfying*

$$\mathbf{t}^\varphi(t, \mathbf{x}^\varphi \mathbf{n}^\varphi) = \mathbf{T}^\varphi(t, \mathbf{x}^\varphi)\mathbf{n}^\varphi\,, \qquad \forall\, t \in [0,T]\,,\ \mathbf{x}^\varphi \in \boldsymbol{\varphi}_t(\Omega)\,,\ \mathbf{n}^\varphi \in T\boldsymbol{\varphi}_t(\Omega)\,.$$

We call $\mathbf{T}^\varphi$ the Cauchy stress tensor.

Proof. Let $\mathcal{D} \subset \Omega$ and $\mathbf{e}_i \in \mathbb{R}^3$ be a unit vector. The balance of linear momentum is equivalent to the spatial master balance law

$$\frac{\mathrm{d}}{\mathrm{d}t} \int_{\boldsymbol{\varphi}_t(\mathcal{D})} \rho^\varphi \mathbf{v}^\varphi \cdot \mathbf{e}_i \,\mathrm{d}V^\varphi = \int_{\boldsymbol{\varphi}_t(\mathcal{D})} \rho^\varphi (\mathbf{b}^\varphi \cdot \mathbf{e}_i) \,\mathrm{d}V^\varphi + \int_{\partial\boldsymbol{\varphi}_t(\mathcal{D}) \cap \Gamma_t^\varphi} \mathbf{t}^\varphi \cdot \mathbf{e}_i \,\mathrm{d}A^\varphi\,.$$

Defining the scalar-valued function $c_i^\varphi(t, \mathbf{x}^\varphi, \mathbf{n}^\varphi) := \mathbf{t}^\varphi(t, \mathbf{x}^\varphi, \mathbf{n}^\varphi) \cdot \mathbf{e}_i$, Cauchys theorem 3.30 implies the existence of a unique vectorfield $\mathbf{c}_i^\varphi$, such that

$$c_i^\varphi(t, \mathbf{x}^\varphi, \mathbf{n}^\varphi) = \mathbf{c}_i^\varphi(t, \mathbf{x}^\varphi) \cdot \mathbf{n}^\varphi\,.$$

We then set $\mathbf{T}^\varphi$ as the tensor with rows $\mathbf{c}_i^\varphi$ for $i = 1, \ldots, 3$, i.e. $\mathbf{T}^\varphi = (c_1^\varphi \mid c_2^\varphi \mid c_3^\varphi)^\top$. This defines a unique tensorfield $\mathbf{T}^\varphi \colon [0,T] \times \mathbf{\Phi}(\Omega) \to \mathbb{R}^{3\times 3}$, and it holds component-wise

$$(\mathbf{T}^\varphi(t, \mathbf{x}^\varphi)\mathbf{n}^\varphi) \cdot \mathbf{e}_i = \mathbf{c}_i^\varphi(t, \mathbf{x}^\varphi) \cdot \mathbf{n}^\varphi = \mathbf{t}^\varphi(t, \mathbf{x}^\varphi, \mathbf{n}^\varphi) \cdot \mathbf{e}_i \,.$$

This implies $\mathbf{t}^\varphi(t, \mathbf{x}^\varphi \mathbf{n}^\varphi) = \mathbf{T}^\varphi(t, \mathbf{x}^\varphi)\mathbf{n}^\varphi$. □

The existence of the Cauchy stress tensor is the basis of the partial differential equation we motivate throughout the remainder of this chapter. We always assume the assumptions of theorem 3.39 to hold.

Theorem 3.40: *The Cauchy stress tensor $\mathbf{T}^\varphi$ is symmetric if and only if the balance of angular momentum 3.37 holds.*

Proof. See [106, section 2.2]. □

Theorem 3.41: *Let the conservation of mass hold. Then*

$$\rho^\varphi \mathbf{a}^\varphi = \rho^\varphi \mathbf{b}^\varphi + \operatorname{div}^\varphi(\mathbf{T}^\varphi) \,, \qquad \textit{in } \boldsymbol{\varphi}_t(\Omega) \,, \tag{3.3a}$$

$$\mathbf{T}^\varphi \mathbf{n}^\varphi = \mathbf{g}^\varphi \,, \qquad \textit{on } \boldsymbol{\varphi}_t(\Gamma) \,. \tag{3.3b}$$

Proof. Let $\mathcal{D} \subset \Omega$ be arbitrary. Using lemma 3.33, the balance of linear momentum

$$\frac{\mathrm{d}}{\mathrm{d}t} \int_{\boldsymbol{\varphi}_t(\mathcal{D})} \rho^\varphi \mathbf{v}^\varphi \,\mathrm{d}V^\varphi = \int_{\boldsymbol{\varphi}_t(\mathcal{D})} \rho^\varphi \mathbf{b}^\varphi \,\mathrm{d}V^\varphi + \int_{\partial\boldsymbol{\varphi}_t(\mathcal{D}) \cap \Gamma_t^\varphi} \mathbf{T}^\varphi \mathbf{n}^\varphi \,\mathrm{d}A^\varphi$$

simplifies to

$$\int_{\boldsymbol{\varphi}_t(\mathcal{D})} \rho^\varphi \frac{\mathrm{d}\mathbf{v}^\varphi}{\mathrm{d}t} \,\mathrm{d}V^\varphi = \int_{\boldsymbol{\varphi}_t(\mathcal{D})} \rho^\varphi \mathbf{b}^\varphi \,\mathrm{d}V^\varphi + \int_{\partial\boldsymbol{\varphi}_t(\mathcal{D}) \cap \Gamma_t^\varphi} \mathbf{T}^\varphi \mathbf{n}^\varphi \,\mathrm{d}A^\varphi$$

Using $\frac{\mathrm{d}\mathbf{v}^\varphi}{\mathrm{d}t} = \mathbf{a}^\varphi$ and theorem 3.26, this is equivalent to

$$\rho^\varphi \frac{\mathrm{d}\mathbf{a}^\varphi}{\mathrm{d}t} = \rho^\varphi \mathbf{b}^\varphi + \operatorname{div}(\mathbf{T}^\varphi) \,, \qquad \text{in } \boldsymbol{\varphi}_t(\Omega) \,.$$

The equality on $\boldsymbol{\varphi}_t(\Gamma)$ follows directly from $\mathbf{g}^\varphi(t, \mathbf{x}^\varphi) = \mathbf{t}^\varphi(t, \mathbf{x}^\varphi, \mathbf{n}^\varphi) = \mathbf{T}^\varphi \mathbf{n}^\varphi$. □

The system (3.3) is given in the material configuration $\boldsymbol{\varphi}_t(\Omega)$, as the forces and the Cauchy stress tensor $\mathbf{T}^\varphi$ are applied on the deformed geometry. In practice, the deformation $\boldsymbol{\varphi}$ is usually the unknown, making the system unsuitable for applications. It is therefore advantageous to rewrite (3.3) in material coordinates.

Definition 3.42: Let $\mathbf{T}^\varphi$ be the Cauchy stress tensor of a motion $\boldsymbol{\varphi}$. We call

$$\mathbf{P}(t, \mathbf{x}) \coloneqq J(t, \mathbf{x})\mathbf{T}^\varphi(t, \boldsymbol{\varphi}(t, \mathbf{x}))\mathbf{F}^{-\top}(t, \mathbf{x}) \,, \qquad (t, \mathbf{x}) \in [0,T] \times \Omega \,,$$

the *first Piola-Kirchhoff stress tensor.*

With the first Piola-Kirchhoff stress tensor, we are now able to state the equations of motion in the reference configuration.

Theorem 3.43: *Let the conservation of mass hold. Then the following statements are equivalent:*

(i) The balance of linear momentum holds.

(ii) For any open set $\mathcal{D} \subset \Omega$, it holds

$$\frac{\mathrm{d}}{\mathrm{d}t} \int_{\mathcal{D}} \rho \mathbf{v} \,\mathrm{d}V = \int_{\mathcal{D}} \rho \mathbf{b} \,\mathrm{d}V + \int_{\partial\mathcal{D} \cap \Gamma} \mathbf{P}\mathbf{n} \,\mathrm{d}A \,.$$

(iii) The first Piola-Kirchhoff stress $\mathbf{P}$ satisfies

$$\rho \mathbf{a} = \rho \mathbf{b} + \operatorname{div}(\mathbf{P}) \,, \qquad \text{in } \Omega \,, \tag{3.4a}$$

$$\mathbf{P}\mathbf{n} = \mathbf{g} \,, \qquad \text{on } \Gamma \,. \tag{3.4b}$$

Proof. This follows directly from the conversion 3.29. □

One downside of working with the first Piola-Kirchhoff stress tensor is the loss of symmetry, due to $\mathbf{F}$ not being symmetric. In most literature, this is rectified by working with the following tensor instead:

Definition 3.44: Let $\mathbf{P}$ be the first Piola-Kirchhoff stress tensor of a motion $\boldsymbol{\varphi}$. Then the symmetric mapping

$$\mathbf{S}(t, \mathbf{x}) := \mathbf{F}^{-1}(t, \mathbf{x})\mathbf{P}(t, \mathbf{x}) \,, \qquad (t, \mathbf{x}) \in [0, T] \times \Omega$$

is called the *second Piola-Kirchoff stress tensor*.

The second Piola-Kirchhoff stress tensor $\mathbf{S}$ will be useful in some proofs in the upcoming chapter due to its symmetry. In general, we use the the first Piola-Kirchhoff stress tensor $\mathbf{P}$ in the equations of motion in the reference configuration.

CHAPTER

FOUR

CONSTITUTIVE MODELS OF PASSIVE SOFT TISSUES

Given the partial differential equation for kinematic motion, this chapter introduces the concept of hyperelasticity to match the number of equations to the number of unknowns. Different constitutive models, formulating a relation between the Cauchy stress tensor and the deformation, are presented. We later focus on conditions and materials relevant for the modeling of soft tissue, which will be relevant in the description of cardiac electromechanics.

Throughout this chapter, we consider $\Omega \subset \mathbb{R}^3$ to be open and $\boldsymbol{\varphi}\colon [0,T] \times \Omega \to \boldsymbol{\Phi}(\Omega)$ be a motion on Ω with deformation gradient $\mathbf{F}$ and Jacobian J and use the terminology as defined in the previouos chapter. We assume $\boldsymbol{\varphi}$ to be regular enough to allow for all definitions and theorems and consider the external forces $\mathbf{b}$ and $\mathbf{g}$ to be given.

4.1 Hyperelastic materials

At the end of the previous chapter, we were left with a partial differential equation dependant on the motion $\boldsymbol{\varphi}$ and its Cauchy stress tensor $\mathbf{T}^{\boldsymbol{\varphi}}$. However, this system only consists of three equations (one for each component) and nine unknowns: Three components of $\boldsymbol{\varphi}$ and six components of the symmetric tensor $\mathbf{T}^{\boldsymbol{\varphi}}$. To circumvent this issue, we introduce *constitutive equations*, which state a relation between the Cauchy stress and the underlying motion. To better specify different material types, we introduce basic axioms of continuum physics and material assumptions, such as elasticity and hyperelasticity.

For a more thorough definition of constitutive theory, we refer to [106]. We state the axiom of objectivity as in [116, 159]. Lastly, the definitions and statements for (hyper)elasticity are depicted as in [38, chapter 3].

If $\boldsymbol{\varphi}$ is r-regular for $r \in \mathbb{N}$ or $r = \infty$, we set the *set of all past motions* up to time t to be

$$\mathcal{M}_t \coloneqq \{\boldsymbol{\phi} \colon (-\infty, t] \times \Omega \to \boldsymbol{\Phi}(\Omega) \mid \boldsymbol{\phi} \text{ is } r\text{-regular for all } -\infty < \tau < t\} .$$

With this we define the set of *past histories* by

$$\mathcal{H} \coloneqq \bigcup_{t \in \mathbb{R}} (\{t\} \times \mathcal{M}_t) .$$

Definition 4.1: We call a mapping $\mathcal{T}_{\mathbf{x}} \colon \mathcal{H} \to \mathbb{R}^{3\times 3}_{\text{sym}}$ a *constitutive equation* for the Cauchy stress tensor at $\mathbf{x} \in \Omega$, if $\mathbf{T}^{\varphi}$ can be written as

$$\mathbf{T}^{\varphi}(t, \boldsymbol{\varphi}(t, \mathbf{x})) = \mathcal{T}_{\mathbf{x}}(t, \boldsymbol{\varphi}_{[t]}) .$$

Note that the mapping $\mathcal{T}_{\mathbf{x}}$ depends not only on the values of $\boldsymbol{\varphi}$, but on $\boldsymbol{\varphi}$ as a whole, which is denoted by $\boldsymbol{\varphi}_{[t]}$. This includes the possible derivatives of $\boldsymbol{\varphi}$, the relevance of which will become clear by the end of this section.

Remark 4.2: If $\mathcal{T}_{\mathbf{x}}$ is a constitutive equation for $\mathbf{T}^{\varphi}$ at $\mathbf{x} \in \Omega$, then

$$\mathcal{P}_{\mathbf{x}} \colon \mathcal{H} \to \mathbb{R}^{3\times 3} , \qquad \mathcal{P}_{\mathbf{x}} \coloneqq J \mathcal{T}_{\mathbf{x}} \mathbf{F}^{-\top} ,$$

is a constitutive equation for the first Piola-Kirchhoff stress $\mathbf{P}$ at $\mathbf{x}$ and

$$\mathcal{S}_{\mathbf{x}} \colon \mathcal{H} \to \mathbb{R}^{3\times 3}_{\text{sym}} , \qquad \mathcal{S}_{\mathbf{x}} \coloneqq \mathbf{F}^{-1} \mathcal{P}_{\mathbf{x}} ,$$

is a constitutive equation for the second Piola-Kirchhoff stress $\mathbf{S}$ at $\mathbf{x}$.

A constitutive equation describes intrinsic properties of the continuum body Ω, i.e. how it behaves when exposed to specific deformations. The definition above allows for the inclusion of rate and memory effects, which are important for viscose or plastic materials. However, the elastic behaviour of the heart is similar to a sponge and such effects can thus be neglected for the application in cardiac elastodynamics. We therefore drop them and formulate constitutive equations for pure elasticity:

Definition 4.3: An *elastic constitutive equation* for the first Piola-Kirchhoff stress $\mathbf{P}$ at a point $\mathbf{x}$ is a mapping $\mathcal{P}_{\mathbf{x}} \colon \boldsymbol{\Phi}(\Omega) \to \mathbb{R}^{3\times 3}$, such that

$$\mathbf{P}(t, \mathbf{x}) = \mathcal{P}_{\mathbf{x}}(\boldsymbol{\varphi}_{[t]}) , \qquad \forall\, t \in [0, T] .$$

Lastly, the local definitions can be extended to the whole domain Ω.

Definition 4.4: We call a mapping

$$\mathcal{T} \colon \Omega \to \mathcal{C}(\boldsymbol{\Phi}(\Omega); \mathbb{R}^{3\times 3}) , \qquad \mathbf{x} \mapsto \mathcal{T}_{\mathbf{x}}$$

an *elastic constitutive equation* for $\mathbf{T}^{\varphi}$, if $\mathcal{T}_{\mathbf{x}}$ are constitutive equations for $\mathbf{T}^{\varphi}$ for all $\mathbf{x} \in \Omega$.

This definition of constitutive equations is deliberately abstract, as it can be applied on a multitude of physical problems other than elastodynamics, such as thermodynamics, plasticity or even electromagnetism [8, section 12.10]. Within this work, we focus on elastodynamical constitutive equations for continuum bodies. Such constitutive equations describe physical properties of the body Ω and are mainly related to the material it consists of. We therefore associate the two and continue to describe material properties which are both motivated by the physical context and mathematically convenient.

Definition 4.5: A material is called *elastic*, if there exists an elastic constitutive equation $\widehat{\mathbf{T}}$ for $\mathbf{T}^{\varphi}$ of the form

$$\mathbf{T}^{\varphi}(t, \boldsymbol{\varphi}(t, \mathbf{x})) = \widehat{\mathbf{T}}(\mathbf{x}, \mathbf{F}(t, \mathbf{x})), \qquad \forall\, t \in [0, T],\ \mathbf{x} \in \Omega .$$

We call $\widehat{\mathbf{T}}$ the *response function* of $\mathbf{T}^{\varphi}$.

Remark 4.6: As with general constitutive equations, if $\widehat{\mathbf{T}}$ is a response function of $\mathbf{T}$, then

$$\widehat{\mathbf{P}} \coloneqq J\widehat{\mathbf{T}}\mathbf{F}^{-\top}, \qquad \widehat{\mathbf{S}} \coloneqq J\mathbf{F}^{-1}\widehat{\mathbf{T}}\mathbf{F}^{-\top}$$

are response functions of the first and second Piola-Kirchhoff stress tensors, respectively.

For the sake of brevity, we use the term constitutive equation and response function for $\mathbf{T}^{\varphi}$, $\mathbf{P}$ and $\mathbf{S}$ synonymously.

Definition 4.7: An elastic material with response function $\widehat{\mathbf{P}} \colon \Omega \times T\Omega \to \mathbb{R}^{3\times 3}$ is called *hyperelastic*, if there exists a mapping $W_{\mathbf{P}} \colon \Omega \times \mathbb{R}^{3\times 3} \to \mathbb{R}$, which is differentiable with respect to the second argument, such that

$$\mathbf{P}(\mathbf{x}, \mathbf{F}) = \mathrm{D}_{\mathbf{F}} W_{\mathbf{P}}(\mathbf{x}, \mathbf{F}), \qquad \forall\, \mathbf{x} \in \Omega,\ \mathbf{F} \in T\Omega .$$

The mapping $W_{\mathbf{P}}$ is called *stored energy function.*

A general requirement in physics is that any deformation $\boldsymbol{\varphi}$ is unaffected by the direction from which is it looked at. This assumption is called the *axiom of frame indifference* or *axiom of objectivity.* For our mathematical framework, this means that any intrinsic property of the regarded body Ω, such as its mass density, is independent of the orthogonal basis in which it is computed. We introduce the concept of objectivity similar to [116].

Definition 4.8: A *change of frame* $\{\mathbf{c}, \mathbf{Q}, a\}$ is a triple of mappings

$$\mathbf{c} \colon [0, T] \to \mathbb{R}^3, \qquad \mathbf{Q} \colon [0, T] \to \mathbb{SO}(3), \qquad a \colon [0, T] \to \mathbb{R},$$

such that each time and point $(t, \mathbf{x})$ are transformed into another pair $(t', \mathbf{x}')$ by

$$\begin{aligned} \mathbf{x}' &= \mathbf{c}(t) + \mathbf{Q}(t)\mathbf{x}, \\ t' &= t - a(t). \end{aligned}$$

If $\mathbf{v}\colon [0,T] \times \Omega \to \mathbb{R}^3$ is a vector-valued mapping, it is transformed according to

$$\mathbf{v}'(t', \mathbf{x}) = \mathbf{Q}(t)\mathbf{v}(t, \mathbf{x})\,.$$

In the above definition, the mapping $\mathbf{c}$ depicts a translation in euclidian space, $\mathbf{Q}$ a rotation of Ω and a a change of rate of time. Vector-valued mappings on Ω are only affected by the rotational part of the change of frame. A similar observation can be made for tensor-valued mappings:

Remark 4.9: Let $\mathbf{A}\colon [0,T] \times \Omega \to \mathbb{R}^{3\times 3}$ be a tensor-valued mapping. Defining its change of frame transformation $\mathbf{A}'$ by the property

$$\mathbf{A}'\mathbf{v}' = (\mathbf{A}\mathbf{v})'\,, \qquad \forall\, \mathbf{v} \in \mathbb{R}^3\,,$$

we get

$$\mathbf{A}'(t', \mathbf{x}) = \mathbf{Q}(t, \mathbf{x})\mathbf{A}(t, \mathbf{x})\mathbf{Q}^\top(t, \mathbf{x})\,.$$

Definition 4.10: Let $\boldsymbol{\psi}$ be a motion of same regularity as $\boldsymbol{\varphi}$ and let $\mathcal{T}^{\varphi}, \mathcal{T}^{\psi}$ be elastic constitutive equations for the corresponding Cauchy stress tensors. We call the motions $\boldsymbol{\varphi}$ and $\boldsymbol{\psi}$ *equivalent*, if there exists a change of frame $\{\mathbf{c}, \mathbf{Q}, a\}$, such that

$$\begin{aligned} \boldsymbol{\psi}(t', \mathbf{x}) &= \mathbf{c}(t) + \mathbf{Q}(t)\boldsymbol{\varphi}(t, \mathbf{x})\,, \\ \mathcal{T}^{\psi}(\mathbf{x}) &= \mathbf{Q}(t)\mathcal{T}^{\varphi}(\mathbf{x})\mathbf{Q}^\top(t)\,. \end{aligned}$$

Two motions are equivalent, if they only differ by a change of frame. With this, we can finally state the axiom of frame indifference:

Axiom 4.11 (Objectivity): *Let $\{\boldsymbol{\varphi}, \mathcal{T}^{\varphi}\}$ be a motion with $\mathcal{T}^{\varphi}$ being an elastic constitutive equation for $\mathbf{T}^{\varphi}$. Then for any equivalent motion $\{\boldsymbol{\psi}, \mathcal{T}^{\psi}\}$, $\mathcal{T}^{\psi}$ is a constitutive equation for $\mathbf{T}^{\psi}$.*

With the axiom of objectivity, we can state some fundamental relations between the response functions of $\mathbf{T}^{\varphi}$, $\mathbf{P}$ and $\mathbf{S}$. The proofs of the following theorems can be found in [38].

Theorem 4.12: *The response function $\widehat{\mathbf{T}}$ of an elastic material satisfies the axiom of objectivity 4.11 if and only if*

$$\widehat{\mathbf{T}}(\mathbf{x}, \mathbf{Q}\mathbf{F}) = \mathbf{Q}\widehat{\mathbf{T}}(\mathbf{x}, \mathbf{F})\mathbf{Q}^\top\,, \qquad \forall\, \mathbf{x} \in \Omega,\ \mathbf{Q} \in \mathbb{SO}(3)\,.$$

Theorem 4.13: *The response function $\widehat{\mathbf{T}}$ of an elastic material satisfies the axiom of objectivity 4.11 if and only if there exists a mapping $\tilde{\mathbf{S}}\colon \Omega \times \mathbb{R}^{3\times 3}_{\text{sym}} \to \mathbb{R}^{3\times 3}_{\text{sym}}$, such that*

$$\widehat{\mathbf{S}}(\mathbf{x}, \mathbf{F}) = \tilde{\mathbf{S}}(\mathbf{x}, \mathbf{F}^\top\mathbf{F})\,, \qquad \forall\, \mathbf{F} \in \mathbb{R}^{3\times 3}\,.$$

Theorem 4.14: *Let $W_{\mathbf{P}}$ be the stored energy function of a hyperelastic material. The following statements are equivalent:*

(i) *$W_{\mathbf{P}}$ satisfies the axiom of objectivity 4.11.*

(ii) *For all $\mathbf{x} \in \Omega$, $\mathbf{F} \in \mathbb{R}^{3\times 3}$, it holds*

$$W_{\mathbf{P}}(\mathbf{x}, \mathbf{QF}) = W_{\mathbf{P}}(\mathbf{x}, \mathbf{F})\,.$$

(iii) *There exists a mapping $W_{\mathbf{S}} \colon \Omega \times \mathbb{R}^{3\times 3}_{\mathrm{sym}} \to \mathbb{R}$, such that*

$$W_{\mathbf{P}}(\mathbf{x}, \mathbf{F}) = W_{\mathbf{S}}(\mathbf{x}, \mathbf{F}^{\top}\mathbf{F}) \qquad \forall\, \mathbf{x} \in \Omega,\ \mathbf{F} \in \mathbb{R}^{3\times 3}\,.$$

Theorem 4.15: *Let $W_{\mathbf{P}}$ be the stored energy function of a hyperelastic material which satisfies the axiom of objectivity 4.11. Let $W_{\mathbf{S}} \colon \Omega \times \mathbb{R}^{3\times 3}_{\mathrm{sym}} \to \mathbb{R}$ be defined by*

$$W_{\mathbf{S}}(\mathbf{x}, \mathbf{C}) \coloneqq W_{\mathbf{P}}(\mathbf{x}, \mathbf{C}^{\frac{1}{2}})\,, \qquad \mathbf{C} \in \mathbb{R}^{3\times 3}_{\mathrm{sym}}\,,$$

and assume without loss of generality that $\mathrm{D}_{\mathbf{C}} W_{\mathbf{S}}$ is symmetric. Then

$$\widehat{\mathbf{S}}(\mathbf{x}, \mathbf{F}) = \tilde{\mathbf{S}}(\mathbf{x}, \mathbf{F}^{\top}\mathbf{F}) = 2\mathrm{D}_{\mathbf{C}} W_{\mathbf{S}}(\mathbf{x}, \mathbf{F}^{\top}\mathbf{F})\,, \qquad \mathbf{F} \in \mathbb{R}^{3\times 3}\,.$$

Theorem 4.16: *Let $\widehat{S}$ be the response function of an elastic material which satisfies the axiom of objectivity 4.11. If there exisits a mapping $W_{\mathbf{S}} \colon \Omega \times \mathbb{R}^{3\times 3}_{\mathrm{sym}} \to \mathbb{R}$ such that*

$$\widehat{\mathbf{S}}(\mathbf{x}, \mathbf{F}) = 2\mathrm{D}_{\mathbf{C}} W_{\mathbf{S}}(\mathbf{x}, \mathbf{F}^{\top}\mathbf{F}),, \qquad \mathbf{F} \in \mathbb{R}^{3\times 3}\,,$$

then the material is hyperelastic with stored energy function

$$W_{\mathbf{P}}(\mathbf{x}, \mathbf{F}) = W_{\mathbf{S}}(\mathbf{x}, \mathbf{F}^{\top}\mathbf{F})\,, \qquad \mathbf{F} \in \mathbb{R}^{3\times 3}\,.$$

Material models such as the ones for cardiac tissue described in section 4.4 are typically defined by a differentiable stored energy function W. Using the fundamental theorems above ensures the objectivity and hyperelasticity of the material model. We therefore always associate a material with its corresponding stored energy function W.

4.2 Anisotropy

In the previous section, we restricted the form of the response function and the stored energy, respectively, by enforcing the axiom of objectivity. We want to impose another property on the given material, namely orthotropy, to account for similar material responses given rotated or mirrored deformations. The structure below is loosely based on [31, section 1, 7].

Definition 4.17: Let $G \subset \mathbb{O}^{3\times 3}$ be a subgroup of the group of orthogonal mappings and

$$\iota\colon \underbrace{\mathbb{R}^{3\times 3}_{\mathrm{sym}} \times \cdots \times \mathbb{R}^{3\times 3}_{\mathrm{sym}}}_{N \text{ times}} \times \underbrace{\mathbb{R}^3 \times \cdots \times \mathbb{R}^3}_{M \text{ times}} \to \mathbb{R}$$

be a mapping depending on N symmetric tensors and M vectors. For $\mathbf{A} \in \mathbb{R}^{3\times 3}_{\mathrm{sym}}$ and $\mathbf{a} \in \mathbb{R}^3$, set

$$\overline{\mathbf{A}} := \mathbf{Q}\mathbf{A}\mathbf{Q}^\top , \qquad \overline{\mathbf{a}} := \mathbf{Q}\mathbf{a} , \qquad \mathbf{Q} \in G .$$

We call ι *invariant under* G, if for all $\mathbf{Q} \in G$, it holds

$$\iota(\mathbf{A}_1, \ldots, \mathbf{A}_N, \mathbf{a}_1, \ldots, \mathbf{a}_M) = \iota(\overline{\mathbf{A}}_1, \ldots, \overline{\mathbf{A}}_N, \overline{\mathbf{a}}_1, \ldots, \overline{\mathbf{a}}_M)$$

for all $\mathbf{A}_n \in \mathbb{R}^{3\times 3}_{\mathrm{sym}}$, $n = 1, \ldots, N$ and $\mathbf{a}_m \in \mathbb{R}^3$, $m = 1, \ldots, M$.

Invariance under specific orthogonal transformations is a key feature of materials. Preferably, we would like the response function to be invariant under all orthogonal transformations (see definition 4.25). As we will see in section 4.4, this condition is too restrictive for material models used in cardiac elasticity.
We continue to develop a basic invariant theory to specify the largest subgroup under which the response function of such models is invariant. Within this section, we say ι is an *invariant*, if there exists a subgroup $G \subset \mathbb{O}^{3\times 3}$, such that ι is invariant under G. Multiple invariants in the same context are always assumed to be invariant under the same subgroup $G \subset \mathbb{O}^{3\times 3}$.

Lemma 4.18: *Let $\boldsymbol{\iota} = \{\iota_1, \ldots, \iota_K\}$ be a set of invariants. Then any mapping resulting from arbitrary concatenations and combinations of $\iota_1, \ldots, \iota_K$ is also an invariant.*

Proof. See [159, section 11]. □

Since any combination of invariants is again an invariant, the question arises when the reverse is true: For any invariant ι, is there a set of invariants $\boldsymbol{\iota}$, such that ι can be represented by the components of $\boldsymbol{\iota}$? We begin with some basic definitions as in [52, part III].

Definition 4.19: Let ι be an invariant. If there exists a finite set of invariants

$$\boldsymbol{\iota} = \{\iota_1, \ldots, \iota_K\} , \qquad K \in \mathbb{N} ,$$

such that ι can be expressed as a function in $\iota_1, \ldots, \iota_K$, we call ι *reducible*. If there exists no such set of other invariants, ι is said to be *irreducible*.

Definition 4.20: Let $\boldsymbol{\iota} = \{\iota_1, \ldots, \iota_K\}$ be a set of invariants.

(i) If any invariant can be expressed as a polynomial in the members of $\boldsymbol{\iota}$, then $\boldsymbol{\iota}$ is called an *integrity basis*.

(ii) If any invariant ι can be expressed as a function $\iota = \varphi(\iota_1, \ldots, \iota_K)$, then $\boldsymbol{\iota}$ is called a *functional basis*.

We call $\boldsymbol{\iota}$ *minimal*, if there exists no other integrity basis with fewer members.

Theorem 4.21: *Let $\boldsymbol{\iota}$ be an integrity basis. Then $\boldsymbol{\iota}$ is a functional basis.*

Proof. See [123]. ☐

It should be obvious that the size of any integrity basis depends on the argument counts N and M of tensors and vectors, respectively. Our goal is to find a minimal functional basis to describe the response function of an elastic or fibre-reinforced material. For an arbitrary number of tensors and vectors, integrity bases have been calculated in [148, 150, 151]. We discuss only results relevant for the characterization of cardiac tissue and therefore set $N = 1$ and $M = 3$.

Lemma 4.22: *Let ι be an invariant depending on $\mathbf{A}, \mathbf{a}_1, \mathbf{a}_2, \mathbf{a}_3$. Then there exists an invariant $\bar{\iota}$ depending on four symmetric tensors, such that*

$$\iota(\mathbf{A}, \mathbf{a}_1, \mathbf{a}_2, \mathbf{a}_3) = \bar{\iota}(\mathbf{A}, \mathbf{a}_1 \otimes \mathbf{a}_1, \mathbf{a}_2 \otimes \mathbf{a}_2, \mathbf{a}_3 \otimes \mathbf{a}_3)\,.$$

Proof. See the derivation made in [31, section 1]. ☐

A relevant simplification of the integrity basis arises if the three vectors are mutually orthogonal:

Lemma 4.23: *Let $\boldsymbol{\iota}$ be an integrity basis of $\mathbf{A}, \mathbf{a}_1, \mathbf{a}_2, \mathbf{a}_3$ and let $\mathbf{a}_1, \mathbf{a}_2, \mathbf{a}_3$ be mutually orthogonal. Then the members of $\boldsymbol{\iota}$ depending on $\mathbf{a}_3$ are reducible.*

Proof. Since $\mathbf{a}_1, \mathbf{a}_2, \mathbf{a}_3$ are mutually orthogonal, it holds

$$\mathbf{a}_1 \otimes \mathbf{a}_1 + \mathbf{a}_2 \otimes \mathbf{a}_2 + \mathbf{a}_3 \otimes \mathbf{a}_3 = \mathbf{I}\,.$$

Hence $\mathbf{a}_3 \otimes \mathbf{a}_3$ is a polynomial in $\mathbf{a}_1 \otimes \mathbf{a}_1$ and $\mathbf{a}_2 \otimes \mathbf{a}_2$. This property propagates to all invariants depending on $\mathbf{a}_3 \otimes \mathbf{a}_3$ in $\boldsymbol{\iota}$. ☐

This observation leaves us with a minimal integrity basis for invariants depending on one tensor and three mutually orthogonal vectors.

Theorem 4.24: *Let* $\mathbf{A} \in \mathbb{R}^{3\times 3}_{\mathrm{sym}}$ *and* $\mathbf{a}_1, \mathbf{a}_2, \mathbf{a}_3 \in \mathbb{R}^3$ *be mutually orthogonal. Then a minimal integrity basis for* $\mathbf{A}, \mathbf{a}_1, \mathbf{a}_2, \mathbf{a}_3$ *is given by*

$$\boldsymbol{\iota}_{\mathbf{A},\mathbf{a}_1,\mathbf{a}_2} = \left\{ \begin{array}{lll} \iota_1 := \mathrm{tr}(\mathbf{A})\,, & \iota_2 := \frac{1}{2}(\mathrm{tr}(\mathbf{A})^2 - \mathrm{tr}(\mathbf{A}^2))\,, & \iota_3 := \det(\mathbf{A})\,, \\ \iota_{4,\mathbf{a}_1} := \mathrm{tr}(\mathbf{A}(\mathbf{a}_1 \otimes \mathbf{a}_1))\,, & \iota_{5,\mathbf{a}_1} := \mathrm{tr}(\mathbf{A}^2(\mathbf{a}_1 \otimes \mathbf{a}_1))\,, & \\ \iota_{4,\mathbf{a}_2} := \mathrm{tr}(\mathbf{A}(\mathbf{a}_2 \otimes \mathbf{a}_2))\,, & \iota_{5,\mathbf{a}_2} := \mathrm{tr}(\mathbf{A}^2(\mathbf{a}_2 \otimes \mathbf{a}_2))\,. & \end{array} \right\} \tag{4.1}$$

Proof. See [149, chapter 1]. □

We will continue to use the notation of the single invariants $\iota_{(\cdot)}$ for all integrity basis of a symmetric tensor and two orthogonal vectors without specifying the tensor in the notation of $\iota_{(\cdot)}$. The integrity basis to which the single invariants belong to should be clear within the context.
The observations made for general invariants now allow us to specify material behaviour under orthogonal transformations:

Definition 4.25: Let $\widehat{\mathbf{T}} \colon \Omega \times \mathbb{R}^{3\times 3} \to \mathbb{R}^{3\times 3}$ be the response function of an elastic material. We call the material *isotropic*, if $\widehat{\mathbf{T}}$ is invariant under the full orthogonal group $\mathbb{O}^{3\times 3}$, i.e., for all $\mathbf{Q} \in \mathbb{O}^{3\times 3}$ it holds

$$\widehat{\mathbf{T}}(\mathbf{x}, \mathbf{F}\mathbf{Q}) = \widehat{\mathbf{T}}(\mathbf{x}, \mathbf{F})\,, \qquad \forall\, \mathbf{F} \in \mathbb{R}^{3\times 3}\,. \tag{4.2}$$

Isotropy is a common assumption in continuum mechanics. It illustrates the property, that deformations related by transformations of a certain group, i.e. rotations or reflections, yield the same stress response. For a hyperelastic material, isotropy leads to very convenient formulations of the stored energy function W.

Lemma 4.26: *Let* $\mathbf{A} \in \mathbb{R}^{3\times 3}$ *be invertible. Then there exist* $\alpha_0(\boldsymbol{\iota}_{\mathbf{A}}), \alpha_1(\boldsymbol{\iota}_{\mathbf{A}}), \alpha_2(\boldsymbol{\iota}_{\mathbf{A}}) \in \mathbb{R}$, *such that*

$$\mathbf{A}^{-1} = \alpha_0(\boldsymbol{\iota}_{\mathbf{A}})\mathbf{I} + \alpha_1(\boldsymbol{\iota}_{\mathbf{A}})\mathbf{A} + \alpha_2(\boldsymbol{\iota}_{\mathbf{A}})\mathbf{A}^2\,.$$

Proof. The Cayley-Hamilton theorem states, that for $\mathbf{A} \in \mathbb{R}^{3\times 3}$, it holds

$$-\mathbf{A}^3 + \iota_1\mathbf{A}^2 - \iota_2\mathbf{A} + \iota_3\mathbf{I} = \mathbf{0}\,,$$

where the representatation with $\iota_1, \ldots, \iota_3$ is calculated in [38, chapter 1]. The assertion then follows by multiplying with $\mathbf{A}^{-1}$ and rearranging the arguments. □

Theorem 4.27: *The following statements are equivalent:*

(i) An elastic material is objective and isotropic, i.e.

$$\widehat{\mathbf{T}}(\mathbf{x}, \mathbf{Q}\mathbf{F}) = \mathbf{Q}\widehat{\mathbf{T}}(\mathbf{x}, \mathbf{F})\mathbf{Q}^\top \qquad \textit{and} \qquad \widehat{\mathbf{T}}(\mathbf{x}, \mathbf{F}\mathbf{Q}) = \widehat{\mathbf{T}}(\mathbf{x}, \mathbf{F}) \qquad \forall\, \mathbf{F} \in \mathbb{R}^{3\times 3}\,,\ \mathbf{Q} \in \mathbb{O}^{3\times 3}\,.$$

(ii) There exists a mapping $\overline{\mathbf{T}}\colon \Omega \times \mathbb{R}^{3\times 3}_{\mathrm{sym}} \to \mathbb{R}^{3\times 3}_{\mathrm{sym}}$ *of the form*

$$\overline{\mathbf{T}}(\mathbf{x},\mathbf{B}) = \beta_0(\boldsymbol{\iota}_{\mathbf{B}})\mathbf{I} + \beta_1(\boldsymbol{\iota}_{\mathbf{B}})\mathbf{B} + \beta_2(\boldsymbol{\iota}_{\mathbf{B}})\mathbf{B}^2\,,$$

such that $\widehat{\mathbf{T}}(\mathbf{x},\mathbf{F}) = \overline{\mathbf{T}}(\mathbf{x},\mathbf{F}\mathbf{F}^\top)$ *for all* $\mathbf{F} \in \mathbb{R}^{3\times 3}$.

(iii) There exists a mapping $\tilde{\mathbf{S}}\colon \Omega \times \mathbb{R}^{3\times 3}_{\mathrm{sym}} \to \mathbb{R}^{3\times 3}_{\mathrm{sym}}$ *of the form*

$$\tilde{\mathbf{S}}(\mathbf{x},\mathbf{C}) = \gamma_0(\boldsymbol{\iota}_{\mathbf{C}})\mathbf{I} + \gamma_1(\boldsymbol{\iota}_{\mathbf{C}})\mathbf{C} + \gamma_2(\boldsymbol{\iota}_{\mathbf{C}})\mathbf{C}^2\,,$$

such that $\widehat{\mathbf{S}}(\mathbf{x},\mathbf{F}) = \tilde{\mathbf{S}}(\mathbf{x},\mathbf{F}^\top\mathbf{F})$ *for all* $\mathbf{F} \in \mathbb{R}^{3\times 3}$.

Proof. See [38, section 3.6]. □

Physiological response functions of cardiac tissue are expressed with additional dependencies on the cardinal directions of the muscle tissue, called fibre directions. Such response functions are categorized within a certain set of materials:

Definition 4.28: Let $\mathbf{f},\mathbf{s},\mathbf{t}\colon \Omega \to \mathbb{R}^3$ be mappings, such that $\mathbf{f}(\mathbf{x}),\mathbf{s}(\mathbf{x}),\mathbf{t}(\mathbf{x})$ are linearly independent for all $\mathbf{x} \in \Omega$. We call a material *fibre-reinforced*, if there exists an elastic constitutive equation $\widehat{\mathbf{T}}$ for $\mathbf{T}^\varphi$ of the form

$$\mathbf{T}^\varphi(t,\boldsymbol{\varphi}(t,\mathbf{x})) = \widehat{\mathbf{T}}(\mathbf{x},\mathbf{F}(t,\mathbf{x}),\mathbf{f}(\mathbf{x}),\mathbf{s}(\mathbf{x}),\mathbf{t}(\mathbf{x}))\,, \qquad \forall\, t \in [0,T]\,,\ \mathbf{x} \in \Omega\,.$$

As with elastic materials, $\widehat{\mathbf{T}}$ is called *response function* of $\mathbf{T}^\varphi$.

For the sake of readability, we omit the dependency of $\mathbf{x}$ of the directions $\mathbf{f},\mathbf{s},\mathbf{t}$.

Remark 4.29: Let the fibres of a fibre-reinforced material $\mathbf{f},\mathbf{s},\mathbf{t}$ be mutually orthogonal. Then the response function $\widehat{\mathbf{T}}$ reduces to

$$\mathbf{T}^\varphi(t,\boldsymbol{\varphi}(t,\mathbf{x})) = \widehat{\mathbf{T}}(\mathbf{x},\mathbf{F}(t,\mathbf{x}),\mathbf{f}(\mathbf{x}),\mathbf{s}(\mathbf{x}))\,, \qquad \forall\, t \in [0,T]\,,\ \mathbf{x} \in \Omega\,.$$

Evidently, fibre-reinforced materials are not isotropic. The largest subgroup of orthogonal transformations, for which the response function of fibre-reinforced materials is invariant, is given, among others, in [31, chapter 1]:

Definition 4.30: Let $\mathbf{f},\mathbf{s},\mathbf{t} \in \mathbb{R}^3$ be mutually orthogonal and $\mathbf{R}^{\boldsymbol{\ell}} \in \mathbb{O}^{3\times 3}$ be the reflection along the plane normal to $\boldsymbol{\ell}$ for $\boldsymbol{\ell} = \mathbf{f},\mathbf{s},\mathbf{t}$. We then call

$$\mathbb{O}^{3\times 3}_{\mathrm{orth}} \coloneqq \{\mathbf{I},\mathbf{R}^{\mathbf{f}},\mathbf{R}^{\mathbf{s}},\mathbf{R}^{\mathbf{t}},\mathbf{R}^{\mathbf{f}}\mathbf{R}^{\mathbf{s}},\mathbf{R}^{\mathbf{s}}\mathbf{R}^{\mathbf{t}},\mathbf{R}^{\mathbf{f}}\mathbf{R}^{\mathbf{t}},-\mathbf{I}\} \subset \mathbb{O}^{3\times 3}$$

the *orthotropic symmetry group*.

Definition 4.31: We call a fibre-reinforced material with fibre fields $\mathbf{f},\mathbf{s},\mathbf{t}$ *orthotropic*, if $\widehat{\mathbf{T}}$ is invariant under the orthotropic symmetry group, i.e., for all $\mathbf{Q} \in \mathbb{O}^{3\times 3}_{\mathrm{orth}}$ it holds

$$\widehat{\mathbf{T}}(\mathbf{x},\mathbf{F}\mathbf{Q},\mathbf{Q}\mathbf{f},\mathbf{Q}\mathbf{s}) = \widehat{\mathbf{T}}(\mathbf{x},\mathbf{F},\mathbf{f},\mathbf{s})\,.$$

As we have seen in theorem 4.27, the response functions of isotropic materials can be stated purely in terms of a symmetric tensor and its invariants. This leads to a useful application for hyperelastic materials, as we will see below. A similar statement can be drawn for fibre-reinforced materials, where we use the arguments from [149, chapter 1].
Let $\mathbf{f}\colon \Omega \to \mathbb{R}^3$ be a fibre field with unit length. For any given motion $\boldsymbol{\varphi}$ with deformation gradient $\mathbf{F}$, the fibre field on $\boldsymbol{\varphi}_t(\Omega)$ is then given by $\mathbf{Ff}$. However, since $\boldsymbol{\varphi}_t$ may involve a stretching or shortening of the body Ω, $\mathbf{Ff}$ may not have unit length. We therefore introduce the normalized fibre field

$$\mathbf{f}^{\varphi} := \frac{1}{\lambda}\mathbf{Ff}\,, \qquad \lambda = \sqrt{\mathbf{f}\cdot\mathbf{Cf}}\,,$$

where we omitted the dependence of t and $\mathbf{x}$ for readability.

Theorem 4.32: *The following statements are equivalent:*

(i) A fibre-reinforced material is objective and orthotropic, i.e. for all $\mathbf{F}\in\mathbb{R}^{3\times 3}$ *and* $\mathbf{Q}\in\mathbb{O}^{3\times 3}_{\mathrm{orth}}$ *it holds*

$$\widehat{\mathbf{T}}(\mathbf{x},\mathbf{QF},\mathbf{f},\mathbf{s}) = \mathbf{Q}\widehat{\mathbf{T}}(\mathbf{x},\mathbf{F},\mathbf{f},\mathbf{s})\mathbf{Q}^{\top} \qquad \textit{and} \qquad \widehat{\mathbf{T}}(\mathbf{x},\mathbf{FQ},\mathbf{Qf},\mathbf{Qs}) = \widehat{\mathbf{T}}(\mathbf{x},\mathbf{F},\mathbf{f},\mathbf{s})\,.$$

(ii) There exists a mapping $\overline{\mathbf{T}}\colon \Omega\times\mathbb{R}^{3\times 3}_{\mathrm{sym}}\times\mathbb{R}^3\times\mathbb{R}^3\to\mathbb{R}^{3\times 3}_{\mathrm{sym}}$ *of the form*

$$\begin{aligned}\overline{\mathbf{T}}(\mathbf{x},\mathbf{B},\mathbf{f},\mathbf{s}) = {}& \beta_0(\boldsymbol{\iota}_{\mathbf{B},\mathbf{f},\mathbf{s}})\mathbf{I} + \beta_1(\boldsymbol{\iota}_{\mathbf{B},\mathbf{f},\mathbf{s}})\mathbf{B} + \beta_2(\boldsymbol{\iota}_{\mathbf{B},\mathbf{f},\mathbf{s}})\mathbf{B}^2\\ &+ \beta_3(\boldsymbol{\iota}_{\mathbf{B},\mathbf{f},\mathbf{s}})\mathbf{f}^{\varphi}\otimes\mathbf{f}^{\varphi} + \beta_4(\boldsymbol{\iota}_{\mathbf{B},\mathbf{f},\mathbf{s}})\mathbf{s}^{\varphi}\otimes\mathbf{s}^{\varphi}\\ &+ \beta_5(\boldsymbol{\iota}_{\mathbf{B},\mathbf{f},\mathbf{s}})\left(\mathbf{f}^{\varphi}\otimes\mathbf{B}\mathbf{f}^{\varphi} + \mathbf{B}\mathbf{f}^{\varphi}\otimes\mathbf{f}^{\varphi}\right) + \beta_6(\boldsymbol{\iota}_{\mathbf{B},\mathbf{f},\mathbf{s}})\left(\mathbf{s}^{\varphi}\otimes\mathbf{B}\mathbf{s}^{\varphi} + \mathbf{B}\mathbf{s}^{\varphi}\otimes\mathbf{s}^{\varphi}\right)\,,\end{aligned}$$

such that $\widehat{\mathbf{T}}(\mathbf{x},\mathbf{F},\mathbf{f},\mathbf{s}) = \overline{\mathbf{T}}(\mathbf{x},\mathbf{F}\mathbf{F}^{\top},\mathbf{f},\mathbf{s})$ *for all* $\mathbf{F}\in\mathbb{R}^{3\times 3}$.

(iii) There exists a mapping $\tilde{\mathbf{S}}\colon \Omega\times\mathbb{R}^{3\times 3}_{\mathrm{sym}}\to\mathbb{R}^{3\times 3}_{\mathrm{sym}}$ *of the form*

$$\begin{aligned}\tilde{\mathbf{S}}(\mathbf{x},\mathbf{x},\mathbf{C}) = {}& \gamma_0(\boldsymbol{\iota}_{\mathbf{C},\mathbf{f},\mathbf{s}})\mathbf{I} + \gamma_1(\boldsymbol{\iota}_{\mathbf{C},\mathbf{f},\mathbf{s}})\mathbf{C} + \gamma_2(\boldsymbol{\iota}_{\mathbf{C},\mathbf{f},\mathbf{s}})\mathbf{C}^2\\ &+ \gamma_3(\boldsymbol{\iota}_{\mathbf{C},\mathbf{f},\mathbf{s}})\mathbf{f}^{\varphi}\otimes\mathbf{f}^{\varphi} + \gamma_4(\boldsymbol{\iota}_{\mathbf{C},\mathbf{f},\mathbf{s}})\mathbf{s}^{\varphi}\otimes\mathbf{s}^{\varphi}\\ &+ \gamma_5(\boldsymbol{\iota}_{\mathbf{C},\mathbf{f},\mathbf{s}})\left(\mathbf{f}^{\varphi}\otimes\mathbf{C}\mathbf{f}^{\varphi} + \mathbf{C}\mathbf{f}^{\varphi}\otimes\mathbf{f}^{\varphi}\right) + \gamma_6(\boldsymbol{\iota}_{\mathbf{C},\mathbf{f},\mathbf{s}})\left(\mathbf{s}^{\varphi}\otimes\mathbf{C}\mathbf{s}^{\varphi} + \mathbf{C}\mathbf{s}^{\varphi}\otimes\mathbf{s}^{\varphi}\right)\,,\end{aligned}$$

such that $\widehat{\mathbf{S}}(\mathbf{x},\mathbf{F}) = \tilde{\mathbf{S}}(\mathbf{x},\mathbf{F}^{\top}\mathbf{F})$ *for all* $\mathbf{F}\in\mathbb{R}^{3\times 3}$.

Proof. The equivalence for (i) and (ii) is shown in [69]. The equivalence of (ii) and (iii) follows by the same arguments as in the proof of theorem 4.27. □

Theorem 4.32 is especially useful, as it provides a convenient expression for the second Piola-Kirchhoff stress tensor $\mathbf{S}$ and does not require any regularity conditions on the functionals γ_i, $i = 0,\ldots,6$.
Still, its main advantage is providing a method for directly calculating $\mathbf{S}$ for hyperelastic materials, where hyperelasticity is similarly defined for fibre-reinforced materials as in definition 4.7.

Definition 4.33: A fibre-reinforced material with fibre fields $\mathbf{f}, \mathbf{s}, \mathbf{t}$ and response function $\widehat{\mathbf{P}}$ is called *hyperelastic*, if there exists a mapping $W_{\mathbf{P}}$, which is differentiable with respect to its second argument, such that

$$\mathbf{P}(\mathbf{x}, \mathbf{F}, \mathbf{f}, \mathbf{s}, \mathbf{t}) = \mathrm{D}_{\mathbf{F}} W_{\mathbf{P}}(\mathbf{x}, \mathbf{F}, \mathbf{f}, \mathbf{s}, \mathbf{t})\,, \qquad \forall\, \mathbf{x} \in \Omega,\ \mathbf{F} \in T\Omega\,.$$

The main result of this section is the relation between the second Piola-Kirchhoff stress tensor and the stored energy function of a hyperelastic material. For convenience, let

$$\boldsymbol{\iota}(\mathbb{R}^{3\times 3}_{\mathrm{sym}}; \mathbb{R}^3; \mathbb{R}^3) \coloneqq \{\boldsymbol{\iota}_{\mathbf{A},\mathbf{a}_1,\mathbf{a}_2} \text{ is an integrity basis} \mid \mathbf{A} \in \mathbb{R}^{3\times 3}_{\mathrm{sym}}, \mathbf{a}_1 \in \mathbb{R}^3, \mathbf{a}_2 \in \mathbb{R}^3\}$$

be the set of all integrity basis for one symmetric tensor and two vectors.

Theorem 4.34:

(i) *A hyperelastic material is objective and isotropic if and only if there exists a mapping* $W_{\boldsymbol{\iota}} \colon \Omega \times \boldsymbol{\iota}(\mathbb{R}^{3\times 3}_{\mathrm{sym}}) \to \mathbb{R}$, *such that*

$$W_{\mathbf{P}}(\mathbf{x}, \mathbf{F}) = W_{\boldsymbol{\iota}}(\mathbf{x}, \boldsymbol{\iota}_{\mathbf{F}^\top\mathbf{F}}) = W_{\boldsymbol{\iota}}(\mathbf{x}, \boldsymbol{\iota}_{\mathbf{F}\mathbf{F}^\top})\,, \qquad \forall\, \mathbf{F} \in \mathbb{R}^{3\times 3}\,.$$

(ii) *A hyperelastic, fibre-reinforced material is objective and orthotropic if and only if there exists a mapping* $W_{\boldsymbol{\iota}} \colon \Omega \times \boldsymbol{\iota}(\mathbb{R}^{3\times 3}_{\mathrm{sym}}; \mathbb{R}^3; \mathbb{R}^3) \to \mathbb{R}$, *such that*

$$W_{\mathbf{P}}(\mathbf{x}, \mathbf{F}, \mathbf{f}, \mathbf{s}) = W_{\boldsymbol{\iota}}(\mathbf{x}, \boldsymbol{\iota}_{\mathbf{F}^\top\mathbf{F},\mathbf{f},\mathbf{s}}) = W_{\boldsymbol{\iota}}(\mathbf{x}, \boldsymbol{\iota}_{\mathbf{F}\mathbf{F}^\top,\mathbf{f},\mathbf{s}})\,, \qquad \forall\, \mathbf{F} \in \mathbb{R}^{3\times 3}\,.$$

Proof. The proof for (i) can be found in [38, section 4.4]. The proof of (ii) follows analoguously. □

Hyperelastic, orthotropic materials therefore always admit to an invariant based formulation of the stored energy function. Such stored energy functions allow for a convenient formulation of the first and second Piola-Kirchhoff stress tensors.

Theorem 4.35: *Let* $W_{\boldsymbol{\iota}}$ *be the stored energy function of a hyperelastic, orthotropic material. If* $W_{\boldsymbol{\iota}}$ *is differentiable at* $\boldsymbol{\iota}_{\mathbf{F}^\top\mathbf{F},\mathbf{f},\mathbf{s}}$, *then the second Piola-Kirchhoff stress tensor admits to the formulation*

$$\begin{aligned} \frac{1}{2}\tilde{\mathbf{S}}(\mathbf{x}, \mathbf{C}) = \quad & (W_1 + \iota_1 W_2 + \iota_2 W_3)\mathbf{I} - (W_2 + \iota_1 W_3)\mathbf{C} + W_3\mathbf{C}^2 \\ +\ & W_{4,\mathbf{f}}(\mathbf{f} \otimes \mathbf{f}) + W_{5,\mathbf{f}}(\mathbf{f} \otimes \mathbf{C}\mathbf{f} + \mathbf{f}\mathbf{C} \otimes \mathbf{f}) \\ +\ & W_{4,\mathbf{s}}(\mathbf{s} \otimes \mathbf{s}) + W_{5,\mathbf{s}}(\mathbf{s} \otimes \mathbf{C}\mathbf{s} + \mathbf{s}\mathbf{C} \otimes \mathbf{s})\,, \end{aligned}$$

where $W_{(\cdot)}(\mathbf{x}) \coloneqq D_{\iota_{(\cdot)}} W(\mathbf{x}, \boldsymbol{\iota}_{\mathbf{F}^\top\mathbf{F}}, \mathbf{f}, \mathbf{s})$.

Proof. Since the stored energy admits to an invariant based description $W_{\boldsymbol{\iota}}$, the material must be objective and orthotropic (see theorem 4.34). By theorem 4.15, there exists a stored energy function $W_{\mathbf{S}}$, such that

$$W_{\mathbf{P}}(\mathbf{x}, \mathbf{F}, \mathbf{f}, \mathbf{s}) = W_{\mathbf{S}}(\mathbf{x}, \mathbf{C}, \mathbf{f}, \mathbf{s}) \qquad \text{and} \qquad \frac{1}{2}\tilde{\mathbf{S}}(\mathbf{x}, \mathbf{C}) = \mathrm{D}_{\mathbf{C}} W_{\mathbf{S}}(\mathbf{x}, \mathbf{C}, \mathbf{f}, \mathbf{s})\,, \qquad \mathbf{C} = \mathbf{F}^\top \mathbf{F}\,.$$

By the chain rule, we then have to calculate

$$\mathrm{D}_{\mathbf{C}} W_{\mathbf{S}}(\mathbf{x}, \mathbf{C}, \mathbf{f}, \mathbf{s}) = \mathrm{D}_{\mathbf{C}} W_{\boldsymbol{\iota}}(\mathbf{x}, \boldsymbol{\iota}_{\mathbf{C},\mathbf{f},\mathbf{s}}) = \sum_{\iota_k \in \boldsymbol{\iota}_{\mathbf{C},\mathbf{f},\mathbf{s}}} \mathrm{D}_{\iota_k}\left(W_{\boldsymbol{\iota}}(\mathbf{x}, \boldsymbol{\iota}_{\mathbf{C},\mathbf{f},\mathbf{s}})\right) \mathrm{D}_{\mathbf{C}}\left(\iota_k\right)\,. \tag{4.3}$$

With the fundamentals shown in [38, chapter 1], it holds

$$\begin{aligned} \mathrm{D}_{\mathbf{C}}\left(\iota_1\right) &= \mathbf{I}\,, & \mathrm{D}_{\mathbf{C}}\left(\iota_2\right) &= \operatorname{tr}(\mathbf{C})\mathbf{I} - \mathbf{C} = \iota_1 \mathbf{I} - \mathbf{C}\,, \\ \mathrm{D}_{\mathbf{C}}\left(\iota_{4,\mathbf{a}}\right) &= (\mathbf{a} \otimes \mathbf{a})\mathbf{I}\,, & \mathrm{D}_{\mathbf{C}}\left(\iota_{5,\mathbf{a}}\right) &= \mathbf{C}(\mathbf{a} \otimes \mathbf{a}) + (\mathbf{a} \otimes \mathbf{a})\mathbf{C}\,, \\ \mathrm{D}_{\mathbf{C}}\left(\iota_3\right) &= \det(\mathbf{C})\mathbf{C}^{-\top} = \det(\mathbf{C})\mathbf{C}^{-1} = \mathbf{C}^2 - \iota_1 \mathbf{C} + \iota_2 \mathbf{I}\,. \end{aligned}$$

Using $W_k = \mathrm{D}_{\iota_k} W_{\boldsymbol{\iota}}(\boldsymbol{\iota}_{\mathbf{C},\mathbf{f},\mathbf{s}})$ and inserting the derivatives into the sum in (4.3), we get the desired result. □

Corollary 4.36: *Let $W_{\boldsymbol{\iota}}$ be the stored energy function of a hyperelastic, orthotropic material. If $W_{\boldsymbol{\iota}}$ is differentiable at $\boldsymbol{\iota}_{\mathbf{F}^\top\mathbf{F},\mathbf{f},\mathbf{s}}$, then the first Piola-Kirchhoff stress tensor admits to the formulation*

$$\begin{aligned} \frac{1}{2}\widehat{\mathbf{P}}(\mathbf{x}, \mathbf{F}) = \;& (W_1 + \iota_1 W_2 + \iota_2 W_3)\mathbf{F} - (W_2 + \iota_1 W_3)\mathbf{F}\mathbf{F}^\top\mathbf{F} + W_3 \mathbf{F}\mathbf{F}^\top\mathbf{F}\mathbf{F}^\top\mathbf{F} \\ &+ W_{4,\mathbf{f}}\mathbf{F}(\mathbf{f} \otimes \mathbf{f}) + W_{5,\mathbf{f}}\left((\mathbf{F}\mathbf{f} \otimes \mathbf{F}\mathbf{f})\mathbf{F}^\top + \mathbf{F}(\mathbf{f}\mathbf{F}^\top \otimes \mathbf{f}\mathbf{F}^\top)\right) \\ &+ W_{4,\mathbf{s}}\mathbf{F}(\mathbf{s} \otimes \mathbf{s}) + W_{5,\mathbf{s}}\left((\mathbf{F}\mathbf{s} \otimes \mathbf{F}\mathbf{s})\mathbf{F}^\top + \mathbf{F}(\mathbf{s}\mathbf{F}^\top \otimes \mathbf{s}\mathbf{F}^\top)\right)\,, \end{aligned}$$

Proof. Using the formulation given by theorem 4.35 and $\mathbf{P}(\mathbf{F}) = \mathbf{F}\mathbf{S}(\mathbf{F}^\top\mathbf{F})$, we get the result by direct calculation. □

For the remainder of this thesis, we omit the dependence on $\mathbf{x}$ for constituive equations and stored energy functions.

4.3 Incompressibility

Throughout this section, we consider the stored energy function $W_{\mathbf{P}} \colon \Omega \times T\Omega \to \mathbb{R}$ of a hyperelastic, objective and isotropic or orthotropic material.

Definition 4.37: We call a motion $\boldsymbol{\varphi} \colon [0, T] \times \Omega \to \boldsymbol{\Phi}(\Omega)$ *volume-preserving*, *isochoric* or *incompressible*, if

$$\int_{\varphi_t(\Omega)} 1 \,\mathrm{d}V^{\varphi} = \int_{\Omega} 1 \,\mathrm{d}V \qquad \forall\, t \in [0, T]\,.$$

The property of being volume-preserving is usually enforced by the type of material which is considered in the elastic material model. Common examples of incompressible materials are rubber or water. While the modeling of water would better fit in the category of fluid dynamics, objects filled with water also behave isochoric. This approximately applies to muscle tissue, which is comprised mainly of water.

Lemma 4.38: *The following statements are equivalent:*

(i) $\boldsymbol{\varphi}$ *is volume-preserving.*

(ii) $J(t, \mathbf{x}) = 1$ *for all* $t \in [0, T]$, $\mathbf{x} \in \Omega$.

Proof. For the identity mapping, it holds by lemma 3.18, that

$$\int_{\varphi_t(\mathcal{D})} \mathrm{d}V^{\varphi} = \int_{\mathcal{D}} J(t, \mathbf{x})\, \mathrm{d}V\,, \qquad t \in [0, T]\,,\ \mathcal{D} \subset \Omega\,.$$

The equivalence of (i) and (ii) directly follows from this equation. □

The stored energy function of incompressible materials does not rely on $\iota_3 = \det(\mathbf{F})$ and is only defined for deformations with $J \equiv 1$. Our goal in this section is to formulate stored energy functions which are well-defined for arbitrary motions, but penalize non-isochoric behaviour.

Definition 4.39: We call a convex mapping $W_{\mathrm{vol}} \colon \mathbb{R}_+ \backslash \{0\} \to \mathbb{R}_+$ satisfying

$$W_{\mathrm{vol}}(1) = 0\,, \qquad \lim_{J \to 0} W_{\mathrm{vol}}(J) = \infty\,, \qquad \lim_{J \to \infty} W_{\mathrm{vol}}(J) = \infty\,,$$

a *volumetric energy function.*

The first proposal for the integration of the incompressibiliy restriction into the material formulation was given by Flory [56]. Let $\mathbf{F}$ be the deformation gradient of a motion $\boldsymbol{\varphi}$. Consider the multiplicative decompostition

$$\mathbf{F} = \mathbf{F}_{\mathrm{vol}} \overline{\mathbf{F}}\,, \qquad \mathbf{F}_{\mathrm{vol}} = J^{\frac{1}{3}} \mathbf{I}\,.$$

into a purely volumetric and an isochoric part. Then $\det(\mathbf{F}_{\mathrm{vol}}) = J = \det(\mathbf{F})$, leaving $\det(\overline{\mathbf{F}}) = 1$. We then assume there exists an additive decomposition of the stored energy function [26] of the form

$$W_{\boldsymbol{\iota}}(\boldsymbol{\iota}_{\mathbf{C},\mathbf{f},\mathbf{s}}) = W_{\mathrm{iso}}(\iota_1, \iota_2) + W_{\mathrm{vol}}(\iota_3)\,,$$

with a volumetric energy W_{vol}. Lastly, we enforce isochority of the first part by calculating

$$\overline{W_{\boldsymbol{\iota}}}(\boldsymbol{\iota}_{\mathbf{C},\mathbf{f},\mathbf{s}}) = W_{\mathrm{iso}}(\bar{\iota}_1, \bar{\iota}_2) + W_{\mathrm{vol}}(\iota_3)\,,$$

where $\bar{\iota}_{(\cdot)} = \iota_{(\cdot)}(\overline{\mathbf{F}}^{\top} \overline{\mathbf{F}}) = \iota_{(\cdot)}(J^{-\frac{2}{3}} \mathbf{C})$.

Remark 4.40: All considerations and statements for $W_{\mathbf{P}}$ are equally valid for a fibre-reinforced material with fibre fields $\mathbf{f}, \mathbf{s}$, as (near-)incompressibility only affects the deformation gradient of $\boldsymbol{\varphi}$. However, as suggested by Sansour et al. [140], the Flory split should only be applied to the full isotropic part, namely

$$W_{\mathbf{P}}(\mathbf{F}, \mathbf{f}, \mathbf{s}) = W_{\boldsymbol{\iota}}(\boldsymbol{\iota}_{\mathbf{C},\mathbf{f},\mathbf{s}}) = W_{\text{iso}}(\bar{\iota}_1, \bar{\iota}_2) + W_{\text{ani}}(\iota_{4,\mathbf{f}}, \iota_{5,\mathbf{f}}, \iota_{4,\mathbf{s}}, \iota_{5,\mathbf{s}}) + W_{\text{vol}}(\iota_3)\,.$$

4.4 Passive models for cardiac tissue

At the beginning of this chapter, we introduced constitutive equations to describe the properties of a continuum body Ω when deformed into a configuration $\boldsymbol{\varphi}_t(\Omega)$. As we have seen in section 4.1, determining the constitutive equation of a hyperelastic material coincides with determining its stored energy function.
In the literature, materials are often described merely by their corresponding stored energy function. We close this chapter by introducing the energy functions commonly used to characterize cardiac tissue.

4.4.1 Ogden materials

Definition 4.41: Let $M, N \in \mathbb{N}$ and $a_m > 0, \alpha_m \geq 1$ for $m = 1, \dots, M$ and $b_n > 0, \beta_n \geq 1$ for $n = 1, \dots N$. We call a material with the stored energy function

$$W_{\mathbf{S}}(\mathbf{C}) = \sum_{n=1}^{N} a_n \operatorname{tr}(\mathbf{C})^{\frac{\alpha_n}{2}} + \sum_{m=1}^{M} b_m \operatorname{tr}(\operatorname{Cof}(\mathbf{C}))^{\frac{\beta_m}{2}} + W_{\text{vol}}(\det(\mathbf{C})^{\frac{1}{2}})\,,$$

where W_{vol} is a volumetric energy as in definition 4.39, *Ogden material.* [118]

Remark 4.42: Ogden materials are objective and isotropic, since

$$W_{\mathbf{S}}(\mathbf{C}) = W_{\boldsymbol{\iota}}(\boldsymbol{\iota}_{\mathbf{C}}) = \sum_{n=1}^{N} a_n \sqrt{\iota_1^{\alpha_n}} + \sum_{m=1}^{M} b_m \sqrt{\iota_2^{\beta_m}} + W_{\text{vol}}(\sqrt{\iota_3})\,.$$

Definition 4.43: We call a material with the stored energy function

$$W_{\boldsymbol{\iota}}(\boldsymbol{\iota}_{\mathbf{C}}) = a\iota_1 + W_{\text{vol}}(\sqrt{\iota_3})\,, \qquad a > 0$$

compressible Neo-Hooke material.

Definition 4.44: We call a material with the stored energy function

$$W_{\boldsymbol{\iota}}(\boldsymbol{\iota}_{\mathbf{C}}) = a\iota_1 + b\iota_2 + W_{\text{vol}}(\sqrt{\iota_3})\,, \qquad a, b > 0$$

compressible Mooney-Rivlin material.

Remark 4.45: Neo-Hooke and Mooney-Rivlin materials with $W_{\text{vol}} \equiv 0$ are called incompressible.

4.4.2 Guccione materials

Cardiac muscle cells, similar to skeletal muscle, are long and cylindrical, arranged in fibre bundles [30, chapter 10]. The contraction of such fibre bundles is mainly one-directional, and experimental observations have shown that the directions of these bundles has to be modeled within the stored energy function [60]. Guccione et al. [71] proposed a fibre-reinforced material model, which is still widely used. The following definition uses the adapted alignment derived in [43].

Definition 4.46: Let $\mathbf{f}, \mathbf{s}$ be the fibre fields of an orthotropic material. Let

$$\mathbf{Q} \colon \Omega \to \mathbb{SO}(3)\,, \qquad \mathbf{Q}(\mathbf{x}) = (\mathbf{f}(\mathbf{x}) \mid \mathbf{s}(\mathbf{x}) \mid \mathbf{f}(\mathbf{x}) \times \mathbf{s}(\mathbf{x}))$$

be the rotation aligning the frame of reference at $\mathbf{x}$ with the fibre directions $\mathbf{f}, \mathbf{s}$. For a given deformation gradient $\mathbf{F}$ with Green-St. Venant strain $\mathbf{E}$, let further

$$\mathbf{E_f} = \mathbf{QEQ}^\top = \frac{1}{2}\mathbf{Q}(\mathbf{I} - \mathbf{C})\mathbf{Q}^\top \in \mathbb{R}^{3\times 3}_{\mathrm{sym}}$$

be the aligned Green-St. Venant strain with entries E_{ij}, $i, j = 1, 2, 3$. If the material adheres to the stored energy function

$$W_{\mathbf{S}}(\mathbf{C}, \mathbf{f}, \mathbf{s}) = \frac{1}{2} C_{\mathrm{G}} \left(\exp\left(Q_{\mathbf{f}}(\mathbf{E_f})\right) - 1\right)\,, \qquad C_{\mathrm{G}} > 0\,,$$

where $Q \colon \mathbb{R}^{3\times 3} \to \mathbb{R}$ is a mapping of the form

$$Q_{\mathbf{f}}(\mathbf{E_f}) = b_{\mathbf{f}}(E_{11}^2) + b_{\mathbf{s}}(E_{22}^2 + E_{33}^2 + E_{23}^2 + E_{32}^2) + b_{\mathbf{f},\mathbf{s}}(E_{12}^2 + E_{21}^2 + E_{13}^2 + E_{31}^2)\,, \qquad b_{\mathbf{f}}, b_{\mathbf{s}}, b_{\mathbf{f},\mathbf{s}} > 0\,,$$

it is called *Guccione material.*

The material formulation in definition 4.46 has two drawbacks: It lacks a volumetric energy needed for modeling near-incompressibility and its description is in fibre coordinates rather than global coordinates. However, we can reformulate the stored energy function to suit our needs:

Lemma 4.47: *Let $W_{\mathbf{S}}$ be the stored energy function of a Guccione material. Then there exists a stored energy function W_{ι}, such that*

$$W_{\mathbf{S}}(\mathbf{C}, \mathbf{f}, \mathbf{s}) = W_{\iota}(\iota_{\mathbf{C},\mathbf{f},\mathbf{s}})\,.$$

Proof. We follow the idea of [61, Appendix B], where the functional $Q_{\mathbf{f}}$ is rewritten to use the Green-St. Venant strain $\mathbf{E}$ in global coordinates: With unit vector basis $\{\mathbf{e}_1, \mathbf{e}_2, \mathbf{e}_3\}$ of $\mathbb{R}^3$, it holds

$$Q_{\mathbf{f}}(\mathbf{E_f}) = 4c_1\left(\mathbf{e}_1^\top \mathbf{E_f} \mathbf{e}_1\right)^2 + 4c_2 \operatorname{tr}\left(\mathbf{e}_1^\top \mathbf{E_f}^\top \mathbf{E_f} \mathbf{e}_1\right) + 4c_3 \operatorname{tr}\left(\mathbf{E_f}^\top \mathbf{E_f}\right)$$

with

$$c_1 = \frac{1}{4}(b_{\mathbf{f}} - 2b_{\mathbf{f},\mathbf{s}} + b_{\mathbf{s}})\,, \qquad c_2 = \frac{1}{2}(b_{\mathbf{f},\mathbf{s}} - b_{\mathbf{s}})\,, \qquad c_3 = \frac{1}{4}b_{\mathbf{s}}\,.$$

Since $\mathbf{E} = \mathbf{Q}^\top \mathbf{E}_{\mathbf{f}} \mathbf{Q}$, we define the global functional

$$Q(\mathbf{E}) \coloneqq 4c_1 \left(\mathbf{f}^\top \mathbf{E} \mathbf{f}\right)^2 + 4c_2 \operatorname{tr}\left(\mathbf{f}^\top \mathbf{E}^\top \mathbf{E} \mathbf{f}\right) + 4c_3 \operatorname{tr}\left(\mathbf{E}^\top \mathbf{E}\right)\,. \tag{4.4}$$

Lastly, we use $\mathbf{E} = \frac{1}{2}(\mathbf{I} - \mathbf{C})$ to get the depency on the invariants of $\mathbf{C}$. It holds

$$\begin{aligned}
\left(\mathbf{f}^\top \mathbf{E} \mathbf{f}\right) &= \frac{1}{2}\left(\operatorname{tr}\left(\mathbf{f}^\top \mathbf{f}\right) - \operatorname{tr}\left(\mathbf{f}^\top \mathbf{C} \mathbf{f}\right)\right) &&= \frac{1}{2}(1 - \iota_{4,\mathbf{f}})\,,\\
\operatorname{tr}\left(\mathbf{f}^\top \mathbf{E}^\top \mathbf{E} \mathbf{f}\right) &= \frac{1}{4}\left(\operatorname{tr}\left(\mathbf{f}^\top \mathbf{f}\right) - 2\operatorname{tr}\left(\mathbf{f}^\top \mathbf{C} \mathbf{f}\right) + \operatorname{tr}\left(\mathbf{f}^\top \mathbf{C}^2 \mathbf{f}\right)\right) &&= \frac{1}{4}(1 - 2\iota_{4,\mathbf{f}} + \iota_{5,\mathbf{f}})\\
\operatorname{tr}\left(\mathbf{E}_{\mathbf{f}}^\top \mathbf{E}_{\mathbf{f}}\right) &= \frac{1}{4}(3 - 2\operatorname{tr}(\mathbf{C}) + \operatorname{tr}(\mathbf{C}^2)) &&= \frac{1}{4}\left(2 + (1 - \iota_1)^2 - 2\iota_2\right)\,.
\end{aligned}$$

Subsequently, we obtain the mapping $Q_{\boldsymbol{\iota}} \colon \boldsymbol{\iota}(\mathbb{R}^{3\times3}_{\mathrm{sym}}; \mathbb{R}^3; \mathbb{R}^3) \to \mathbb{R}$, defined by

$$Q_{\boldsymbol{\iota}}(\boldsymbol{\iota}_{\mathbf{C},\mathbf{f},\mathbf{s}}) = 2c_1(1 - \iota_{4,\mathbf{f}}) + c_2(1 - 2\iota_{4,\mathbf{f}} + \iota_{5,\mathbf{f}}) + c_3(2 + (1 - \iota_1)^2 - 2\iota_2)\,,$$

satisfying $Q(\mathbf{E}) = Q_{\boldsymbol{\iota}}(\boldsymbol{\iota}_{\mathbf{C},\mathbf{f},\mathbf{s}})$ and

$$W_{\boldsymbol{\iota}}(\boldsymbol{\iota}_{\mathbf{C},\mathbf{f},\mathbf{s}}) \coloneqq \frac{1}{2}C_{\mathrm{G}}(\exp(Q_{\boldsymbol{\iota}}(\boldsymbol{\iota}_{\mathbf{C},\mathbf{f},\mathbf{s}}) - 1) = \frac{1}{2}C_{\mathrm{G}}(\exp(Q_{\mathbf{f}}(\mathbf{E}_{\mathbf{f}})) - 1) = W_{\mathbf{S}}(\mathbf{C}, \mathbf{f}, \mathbf{s})\,.$$

□

Remark 4.48: The stored energy function of a Guccione material does not depend on the change of volume ι_3. From a modeling point of view, the material is considered incompressible, i.e. it should only be used with the constraint $J = 1$. As indicated in remark 4.45, we can define a *compressible Guccione material* by adding a volumetric energy W_{vol}. We therefore consider

$$W_{\boldsymbol{\iota}}(\boldsymbol{\iota}_{\mathbf{C},\mathbf{f},\mathbf{s}}) = \frac{1}{2}C(\exp(Q_{\boldsymbol{\iota}}(\boldsymbol{\iota}_{\mathbf{C},\mathbf{f},\mathbf{s}}) - 1) + W_{\mathrm{vol}}(\iota_3)\,.$$

4.4.3 Holzapfel-Ogden Materials

Lemma 4.49: *Let* $\mathbf{A} \in \mathbb{R}^{3\times3}_{\mathrm{sym}}$ *and* $\mathbf{a}_1, \mathbf{a}_2, \mathbf{a}_3 \in \mathbb{R}^3$ *with* $\mathbf{a}_3$ *being orthogonal to* $\mathbf{a}_1$ *and* $\mathbf{a}_2$*. Then*

$$\iota_{8,\mathbf{a}_1,\mathbf{a}_2} = \iota_{8,\mathbf{a}_1,\mathbf{a}_2}(\mathbf{A}) \coloneqq (\mathbf{a}_1 \cdot \mathbf{a}_2)\operatorname{tr}(\mathbf{A}(\mathbf{a}_1 \otimes \mathbf{a}_2))$$

is an invariant.

Proof. See [149, chapter 1]. □

Definition 4.50: Consider a material with (arbitrary) fibre fields $\mathbf{a}_1, \mathbf{a}_2 \in \mathbb{R}^3$ and let $a, b, a_1, b_1, a_2, b_2, a_{1,2}, b_{1,2} > 0$. We call a material with the stored energy function

$$\begin{aligned} W_{\iota}(\boldsymbol{\iota}_{\mathbf{C},\mathbf{a}_1,\mathbf{a}_2}) = &\ \frac{a}{2b}\left[\exp\Big(b(\iota_1 - 3)\Big) - 1\right] + \sum_{i=1,2}\frac{a_i}{2b_i}\left[\exp\Big(b_i(\iota_{4,\mathbf{a}_i} - 1)^2\Big) - 1\right] \\ &+ \frac{a_{1,2}}{2b_{1,2}}\left[\exp\Big(b_{1,2}\iota_{8,\mathbf{a}_1,\mathbf{a}_2}^2\Big) - 1\right] \end{aligned} \tag{4.5}$$

Holzapfel-Ogden material. [85]

For an orthotropic material with fibre fields $\mathbf{f}, \mathbf{s}, \mathbf{t}$, it holds

$$\iota_{8,\mathbf{f},\mathbf{s}} = 0\,,$$

since $\mathbf{f}$ and $\mathbf{s}$ are orthogonal. We therefore omit the last term in (4.5) for orthotropic materials.

Remark 4.51: In most literature, the stored energy functions is written in dependence of $\bar{\iota}_{8,\mathbf{f},\mathbf{s}} := \operatorname{tr}(\mathbf{A}(\mathbf{f}\otimes\mathbf{s}))$ for orthotropic materials with fibre fields $\mathbf{f}, \mathbf{s}, \mathbf{t}$. However, $\bar{\iota}_{8,\mathbf{f},\mathbf{s}}$ is not an invariant: Let $\mathbf{Q} \in \mathbb{O}^{3\times 3}$ be the reflection at the plane spanned by $\mathbf{s}$ and $\mathbf{t}$. Then

$$\bar{\mathbf{f}} = \mathbf{Q}\mathbf{f} = -\mathbf{f} \quad \text{ and } \bar{\mathbf{s}} = \mathbf{Q}\mathbf{s} = \mathbf{s}\,,$$

since the fibre directions are mutually orthogonal. For the identity matrix $\mathbf{I} \in \mathbb{R}^{3\times 3}_{\text{sym}}$, we get

$$\bar{\iota}_{8,\bar{\mathbf{f}},\bar{\mathbf{s}}}(\bar{\mathbf{I}}) = \operatorname{tr}\Big((\mathbf{Q}\mathbf{I}\mathbf{Q}^{\top})(-\mathbf{f}\otimes\mathbf{s})\Big) = -\operatorname{tr}(\mathbf{I}(\mathbf{f}\otimes\mathbf{s})) = -\bar{\iota}_{8,\mathbf{f},\mathbf{s}}(\mathbf{I})\,.$$

Remark 4.52: As before, Holzapfel-Ogden materials are considered to be incompressible. We again define the *compressible Holzapfel-Ogden material* by adding a volumetric energy W_{vol} and consider

$$W_{\iota}(\boldsymbol{\iota}_{\mathbf{C},\mathbf{f},\mathbf{s}}) = \frac{a}{2b}\left[\exp\Big(b(\iota_1 - 3)\Big) - 1\right] + \sum_{\ell=\mathbf{f},\mathbf{s}}\frac{a_\ell}{2b_\ell}\left[\exp\Big(b_\ell(\iota_{4,\ell} - 1)^2\Big) - 1\right] + W_{\text{vol}}(\iota_3)\,.$$

for orthotropic materials with fibre fiels $\mathbf{f}, \mathbf{s}, \mathbf{t}$.

4.5 Constitutive restrictions for large strains

Constitutive equations for the Cauchy-Stress tensor should, additionaly to appropriately modeling material specific behaviour, reflect proper physical restrictions. We conclude this chapter by formulating two central constraints, which are both mathematically convenient and physically reasonable [8, chapter 13]:

(i) Extreme strains should be ensued by extreme stresses.

(ii) An increase in a component of strain should be accompanied by an increase in a corresponding component in stress.

The mathematical descriptions of these constraints can of course be formulated for arbitrary functions. Since we are only interested in the consequences for our constitutive equations, we always consider a hyperelastic material with stored energy function $W_{\mathbf{P}}$.
A common measure of strain are the eigenvalues $\lambda(\mathbf{F}^\top\mathbf{F})$, where very large or very small eigenvalues correspond to "extreme" strains. Item (i) states the requirement, that $W_{\mathbf{P}}$ approaches ∞ as any eigenvalue $\lambda(\mathbf{F}^\top\mathbf{F})$ approaches 0 or ∞. A detailed mathematical description is given in [124]:

Definition 4.53: We say a stored energy function $W_{\mathbf{P}}$ follows the *growth conditions*, if

$$\det(\mathbf{F}) \to 0 \Rightarrow W_{\mathbf{P}}(\mathbf{F}) \to \infty \qquad \text{and} \qquad \|\mathbf{F}\| \to \infty \Rightarrow W_{\mathbf{P}}(\mathbf{F}) \to \infty\,.$$

While the growth conditions theoretically satisfy the premise of ensuring extreme stresses under extreme strains, some problems additionally require a sufficiently fast growth of stresses (see for example [7, 146]).

Definition 4.54: We call a stored energy function $W_{\mathbf{P}}$ *coercive*, if there exist $A > 0$, $a > 1$ and $b \in \mathbb{R}$ such that

$$W_{\mathbf{P}}(\mathbf{F}) \geq A\,\mathrm{tr}(\mathbf{F})^{\frac{a}{2}} + b\,.$$

As we will see in chapter 6, coercivity is a necessary assumption to guarantee the existence of a solution of theorem 3.43 in a weak sense. The definition above is the same as in [8] for homogeneous materials and, as shown in [124], equivalent to the one given in [21, 38].

Definition 4.55: Let $W_{\mathbf{P}}$ be two times continuously differentiable. We say $W_{\mathbf{P}}$ satisfies the *Legendre-Hadamard condition*, if

$$\mathrm{D}^2_{\mathbf{F}} W_{\mathbf{P}}(\mathbf{F})[\mathbf{H};\mathbf{H}] \geq 0 \qquad \text{for all } \mathbf{F} \in \mathbb{R}^{3\times 3}\,,\ \mathbf{H} \in \mathbb{R}^{3\times 3}\,. \tag{4.6}$$

Lemma 4.56: *Let $W_{\mathbf{P}}$ be two times continuously differentiable. Then $W_{\mathbf{P}}$ is coercive if and only if it satisfies the Legendre-Hadamard condition.*

Proof. See [67]. □

For the mathematical desciption of (ii), we follow the arguments given in [8, chapter 13]. The most desirable assumption would be for $\mathbf{P}$ to be strictly monotone, which for hyperelastic materials is equivalent for $W_{\mathbf{P}}$ to be strictly convex:

Definition 4.57: A subset $\mathcal{U}$ of a vector space $\mathcal{V}$ is called *convex*, if

$$\{\lambda\mathbf{u} + (1-\lambda)\mathbf{v} \colon \lambda \in [0,1]\} \subset \mathcal{U}\,, \qquad \text{for all } \mathbf{u}, \mathbf{v} \in \mathcal{U}\,.$$

A function $f \colon \mathcal{U} \to \mathbb{R}$ defined on a convex subset $\mathcal{U} \subset \mathcal{V}$ is called *convex* on $\mathcal{U}$, if

$$f(\lambda\mathbf{u} + (1-\lambda)\mathbf{v}) \leq \lambda f(\mathbf{u}) + (1-\lambda) f(\mathbf{v})\,, \qquad \text{for all } \mathbf{u}, \mathbf{v} \in \mathcal{U} \text{ and } \lambda \in [0,1]$$

and *strictly convex* on $\mathcal{U}$, if additionally

$$f(\lambda\mathbf{u} + (1-\lambda)\mathbf{v}) < \lambda f(\mathbf{u}) + (1-\lambda) f(\mathbf{v})\,, \qquad \text{for } \mathbf{u} \neq \mathbf{v} \text{ and } \lambda \in (0,1)\,.$$

Unfortunately, $W_{\mathbf{P}}$ can not be convex for two reasons. First, the definition space of $W_{\mathbf{P}}$ is not convex, hence it is not convex in the sense of definition 4.57. This follows directly from the following theorem.

Theorem 4.58: *Let* $\operatorname{co}(\mathcal{U})$ *be the convex hull of a subset* $\mathcal{U} \subset \mathcal{V}$ *and define*

$$\mathbb{R}^{3\times3}_{+} := \{\mathbf{F} \in \mathbb{R}^{3\times3} \colon \det(\mathbf{F}) > 0\}\,.$$

Then

(i) $\operatorname{co}(\mathbb{R}^{3\times3}_{+}) = \mathbb{R}^{3\times3}\,,$

(ii) $\operatorname{co}\left(\left\{(\mathbf{F}, \operatorname{Cof}(\mathbf{F}), \det(\mathbf{F})) \in \mathbb{R}^{3\times3} \times \mathbb{R}^{3\times3} \times \mathbb{R}_{+} \colon \mathbf{F} \in \mathbb{R}^{3\times3}_{+}\right\}\right) = \mathbb{R}^{3\times3} \times \mathbb{R}^{3\times3} \times \mathbb{R}_{+}\,.$

Proof. See [21]. □

Since we only allow $\boldsymbol{\varphi}$ to be a 1-regular motion, its deformation gradient is in the non-convex subspace $\mathbb{R}^{3\times3}_{+}$, which was outlined in the remarks after definition 3.13. However, we can extend convexity to functions defined on non-convex sets:

Lemma 4.59: *Let* $\mathcal{U} \subset \mathcal{V}$ *be a subset on a vector space* $\mathcal{V}$ *and* $f \colon \mathcal{U} \to \mathbb{R}$*. Then the function*

$$\overline{f} \colon \mathcal{V} \to \mathbb{R} \cup \{\infty\}\,, \qquad \mathbf{v} \mapsto \begin{cases} f(\mathbf{v}) & \text{if } \mathbf{v} \in \mathcal{U}\,, \\ \infty & \text{if } \mathbf{v} \notin \mathcal{U} \end{cases}$$

is convex if and only if $\mathcal{U}$ *is convex and* f *is convex.*

Proof. See [38, theorem 4.7-9]. □

We can therefore theoretically define stored energy functionals $W_{\mathbf{P}}$, such that the extended functional $\overline{W_{\mathbf{P}}}$ is convex. This leads to the second, and more crucial, reason why this is not possible within the scope of large strain elasticity. For the sake of readability, we identify $W_{\mathbf{P}}$ with $\overline{W_{\mathbf{P}}}$ in the context of convexity.

Lemma 4.60: *Let $W_{\mathbf{P}}$ be convex. Then $W_{\mathbf{P}}$ can not obey the growth conditions 4.53.*

Proof. See [38, theorem 4.8-1]. □

To unite the concepts of convexity and the growth conditions, we present the condition of polyconvexity, first introduced by Ball [21]:

Definition 4.61: Let $W_{\mathbf{P}}$ be the stored energy function $W_{\mathbf{P}}$ of a hyperelastic material. We call $W_{\mathbf{P}}$ *polyconvex*, if there exists a convex function

$$\mathbb{W}\colon \mathbb{R}^{3\times 3} \times \mathbb{R}^{3\times 3} \times \mathbb{R} \to \mathbb{R}\,,$$

such that

$$W_{\mathbf{P}}(\mathbf{F}) = \mathbb{W}(\mathbf{F}, \mathrm{Cof}\,(\mathbf{F})\,, \det(\mathbf{F})) \qquad \text{for all } \mathbf{F} \in \mathbb{R}^{3\times 3}\,.$$

Lemma 4.62: *Let $W_{\mathbf{P}}$ satisfy the growth conditions 4.53 and be polyconvex. Then $W_{\mathbf{P}}$ is coercive.*

Proof. See [45, theorem 5.3]. □

Polyconvex materials still allow for existence and uniqueness results in a weak sense, for the details we again refer to chapter 6. Similar results hold for other assumptions on $W_{\mathbf{P}}$, such as the weaker quasiconvexity [109] or stronger uniform polyconvexity [147]. We focus on the concept of polyconvexity, mainly because conventional stored-energy formulations satisfy definition 4.61 as well as the growth conditions 4.53. As Ball [22] points out, it is still unclear whether useful classes of quasiconvex stored-energy functions exist.
We finalize this section by giving some short statements on the stored-energy functions defined in section 4.4.

Theorem 4.63: *Ogden materials with the stored energy function as in definition 4.41 are polyconvex.*

Proof. See [38, theorem 4.9-2]. □

Theorem 4.64: *Guccione materials with the stored energy function as in definition 4.46 are not polyconvex.*

Proof. Wilber et al. [172] provide necessary conditions for a broader class of stored energy functions to satisfy the Legendre-Hadamard condition. We will outline the parts relevant for Guccione materials: Let $Q\colon \mathbb{R}^{3\times 3}_{\mathrm{sym}} \to \mathbb{R}$ be defined by

$$Q(\mathbf{E}) := \sum_{i,j=1}^{3} A_{ij} E_{ii} E_{jj} + \sum_{i,j=1, i<j}^{3} \overline{A}_{ij} E_{ij}^2\,.$$

Then, if the function $\mathbf{E} \mapsto C \exp(Q(\mathbf{E}))$ satisfies the Legendre-Hadamard condition, it holds

$$\begin{aligned}
\left(A_{11}A_{12}(A_{13}+\overline{A}_{13})\right)^{\frac{1}{3}} &\geq \frac{1}{3}\left(A_{11}+A_{12}+A_{13}\right), & \left(A_{12}A_{22}(A_{23}+\overline{A}_{23})\right)^{\frac{1}{3}} &\geq \frac{1}{3}\left(A_{12}+A_{22}+A_{23}\right),\\
\left(A_{1}(A_{23}+\overline{A}_{23})A_{33}\right)^{\frac{1}{3}} &\geq \frac{1}{3}\left(A_{13}+A_{23}+A_{33}\right), & \left(A_{11}(A_{12}+\overline{A}_{12})A_{13}\right)^{\frac{1}{3}} &\geq \frac{1}{3}\left(A_{11}+A_{12}+A_{13}\right),\\
\left((A_{12}+\overline{A}_{12})A_{22}A_{23}\right)^{\frac{1}{3}} &\geq \frac{1}{3}\left(A_{12}+A_{22}+A_{23}\right), & \left((A_{13}+\overline{A}_{13})A_{23}A_{33}\right)^{\frac{1}{3}} &\geq \frac{1}{3}\left(A_{13}+A_{23}+A_{33}\right).
\end{aligned}$$

For a Guccione material, we have $A_{12} = A_{13} = A_{23} = 0$. Therefore the left hand sides above are always zero, leading to $A_{11} = A_{22} = A_{33} = 0$. Since $A_{11} = b_{\mathbf{f}} > 0$, the Guccione material does not satisfy the equations above. By [172, theorem 5.7] and lemma 4.56, the Guccione material is not coercive and thus by lemma 4.62 not polyconvex. $\square$

Theorem 4.65: *Holzapfel materials with the stored energy function*

$$W_{\boldsymbol{\iota}}(\boldsymbol{\iota}_{\mathbf{C},\mathbf{f},\mathbf{s}}) = \frac{a}{2b}\left[\exp\left(b(\iota_1-3)\right)-1\right] + \sum_{\boldsymbol{\ell}=\mathbf{f},\mathbf{s}} \frac{a_{\boldsymbol{\ell}}}{2b_{\boldsymbol{\ell}}}\left[\exp\left(b_{\boldsymbol{\ell}}(\iota_{4,\boldsymbol{\ell}}-1)^2\right)-1\right] + W_{\mathrm{vol}}(\iota_3)\,.$$

are polyconvex for all $\mathbf{F} \in \mathbb{R}^{3\times 3}_{+}$ *with* $\iota_{4,\boldsymbol{\ell}}(\mathbf{F}^\top\mathbf{F}) > 1$, $\boldsymbol{\ell} = \mathbf{f}, \mathbf{s}$.

Proof. We can write the stored energy function of a Holzapfel-Ogden material as

$$W_{\mathbf{P}}(\mathbf{F}) = W_1(\mathbf{F}) + W_2(\mathrm{Cof}\,(\mathbf{F})) + W_3(\det(\mathbf{F})) + W_{4,\mathbf{f}}(\mathbf{F}) + W_{4,\mathbf{s}}(\mathbf{F})\,,$$

where

$$W_1(\mathbf{F}) = W_{\iota_1}(\iota_1)\,, \quad W_2(\mathrm{Cof}\,(\mathbf{F})) = W_{\iota_2}(\iota_2) = 0\,, \qquad W_3(\det(\mathbf{F}))) = W_{\mathrm{vol}}(\iota_3)\,,$$
$$W_{4,\boldsymbol{\ell}} = W_{\iota_{4,\boldsymbol{\ell}}}(\iota_{4,\boldsymbol{\ell}})\,,\ \boldsymbol{\ell} = \mathbf{f}, \mathbf{s}\,,$$

are the corresponding parts of the additive energy functional. As Schröder et al. [143] point out, $W_{\mathbf{P}}$ is polyconvex if the W_i, $i = 1, 2, 3, \{4, \mathbf{f}\}, \{4, \mathbf{s}\}$, are convex in their respective argument and show further that W_1,W_2,W_3 are convex. Holzapfel et al. [86] show that the $W_{4,\ell}$, $\ell = \mathbf{f}, \mathbf{s}$ are convex for $\iota_{4,\boldsymbol{\ell}} > 1$ and $a_{\boldsymbol{\ell}}, b_{\boldsymbol{\ell}} > 0$. $\square$

Remark 4.66: The condition $\iota_{4,\boldsymbol{\ell}} > 1$ physically resembles an extension along $\boldsymbol{\ell}$. In order to accomodate contractions within our deformations, let

$$\langle\cdot\rangle : \mathbb{R} \to \mathbb{R}_+\,, \qquad x \mapsto \begin{cases} x\,, & \text{if } x > 0 \\ 0\,, & \text{otherwise} \end{cases}.$$

We use the modified stored energy function [85]

$$W_{\boldsymbol{\iota}}(\boldsymbol{\iota}_{\mathbf{C},\mathbf{f},\mathbf{s}}) = \frac{a}{2b}\left[\exp\left(b(\iota_1-3)\right)-1\right] + \sum_{\boldsymbol{\ell}=\mathbf{f},\mathbf{s}} \frac{a_{\boldsymbol{\ell}}}{2b_{\boldsymbol{\ell}}}\left[\exp\left(b_{\boldsymbol{\ell}}\langle\iota_{4,\boldsymbol{\ell}}-1\rangle^2\right)-1\right] + W_{\mathrm{vol}}(\iota_3)\,. \quad (4.7)$$

Theorem 4.67: *The modified Holzapfel constituve model* (4.7) *is polyconvex.*

Proof. Schröder et al. [142] show that the function

$$\frac{a_{\boldsymbol{\ell}}}{2b_{\boldsymbol{\ell}}} \exp\left(b_{\boldsymbol{\ell}}\langle\iota_{4,\boldsymbol{\ell}} - 1\rangle^2\right) , \qquad \boldsymbol{\ell} = \mathbf{f}, \mathbf{s}$$

is convex for $a_\ell, b_\ell > 0$. By the same argument as in the proof of theorem 4.65, it follows that the functional (4.7) is polyconvex. $\square$

CHAPTER

FIVE

AN INTEGRATED HUMAN HEART MODEL

In this chapter, we introduce the mathematical models used to describe a healthy human heart. Beginning with a short outline of the anatomy of the heart, the three main parts in coupled cardiac modeling are described: The electrophysiological propagation of an action potential through cardiac tissue, the following active contraction of the heart and the interaction of the cardiac cycle with the cardiovascular pressure. We finalize the chapter by summarizing the components and discuss a coupled cardiac model.

5.1 Physiological foundations

”The heart is a hollow organ that pumps the blood into the arteries” [129]. It is separated into the right heart, which drives deoxygenated blood into the lungs, and the left heart, which pumps oxygenated blood through the body. We refer to these two circulations as the pulmonary and the systemic circulation. Each side of the heart consists of an atrium and a ventricle, separated by valves.

The cardiac wall is comprised of three layers: The inner layer is called the *endocardium* and similar in structure to the inner layer of blood vessels. The outer layer is called the *epicardium*. Between these two layers lies the *myocardium*, which is the thickest of the three and consists of muscular tissue. The whole heart is contained within a fibrous sac called the *pericardium*, containing the motion of the heart and preventing excessive enlargement [37].

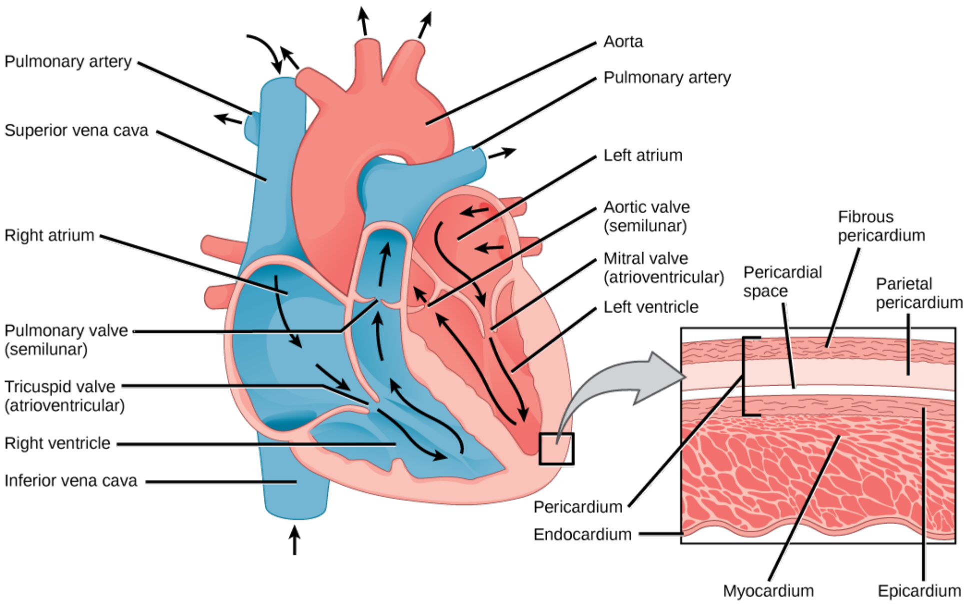

Figure 5.1: Structure of the heart and the cardiac wall [39, Figure 40.11(a), CC BY 4.0].

Cardiac cells are contractible in a similar fashion to skeletal muscle tissue. In addition, they are excitable, meaning they enable an electric signal to propagate throughout the tissue. This signal, called *action potential*, causes the cells to contract, which in turn enable the pumping action of the heart.

The action potential is initiated in a cluster of cells named the *sinoatrial node* (SA node). These cells are autonomous oscillators and initiate an electric signal about once per second in a resting human body. The action potential then propagates through the atria only, which are separated from the ventricles by a septum composed of non-excitable cells. To reach the ventricles, the electric current has to reach the *atrioventricular node* (AV node). From here, it propagates through the *bundle of HIS*, the bundle branches and fascicular branches leading to the Purkinje fibres, ending in the endocardial surface of the ventricles [93].

Through these propagation mechanisms, the action potential follows a predefined path. The resulting excitation of cardiac cells initiates the contraction and subsequentially the relaxation of the cardiac muscle in a specific pattern, the cardiac cycle. Starting in a relaxed stated, the *diastole*, blood flows into the heart chambers. The cardiac diastole is followed by the contraction (*systole*) of the atria, pushing blood into the ventricles and concluding with the closing of the atrioventricular valves. Atrial diastole begins immediately and the ventricular systole ensues after a short delay, pumping blood out of the heart.

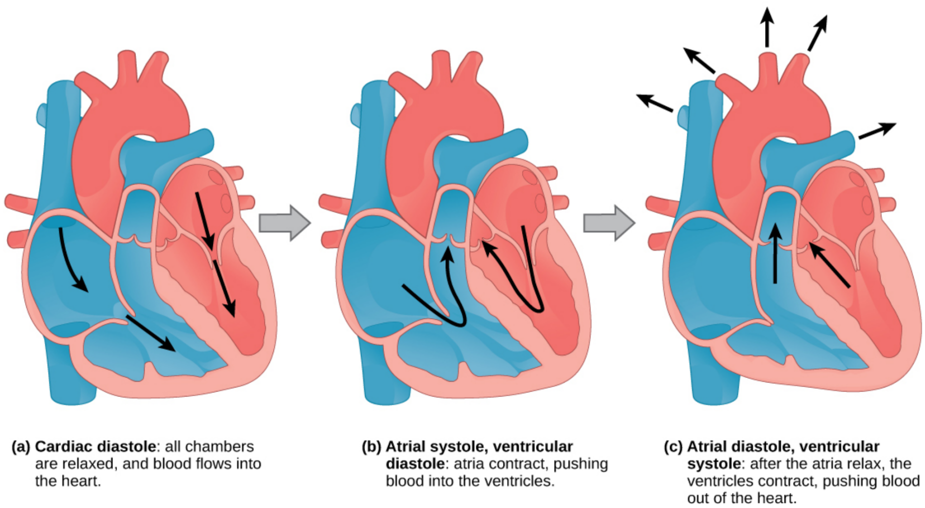

Figure 5.2: Flow direction of blood during the phases of a cardiac cycle [39, Figure 40.12, CC BY 4.0].

The phases of the cardiac cycle can be represented in more detail with a Wiggers diagram [108, 170]. We reiterate the explanation given in [129, section 4.2] and follow the phases as shown in Figure 5.3, starting with the systole of the left ventricle.

1. *Isovolumic contraction:* The active contraction of the left ventricle starts. Since both valves are closed, a fast increase in ventricular pressure can be observed.

2. *Ventricular ejection:* The pressure inside the ventricle is higher than the aortic pressure, allowing the aortic valve to open. Since the ventricular systole is not finished yet, pressure continues to increase. During the end of systole, the ventricular and aortic pressure align, resulting in the closing of the aortic valve.

3. *Isovolumic relaxation:* The diastole of the ventricle starts with both valves closed. The abscence of external cardiovascular pressure results in a decrease in ventricular pressure.

4. *Ventricular filling:* With the opening of the mitral valve, blood starts entering the left ventricle. Combined with the muscle relaxation, we observe an increase in ventricular volume, gradually slowing down until the end of diastasis. The filling ends with the contraction of the atria, forcing additional blood into the left ventricle and leading to a short peak of ventricular volume and pressure. As atrial systole is finished, the mitral valve closes and the next cardiac cycle begins.

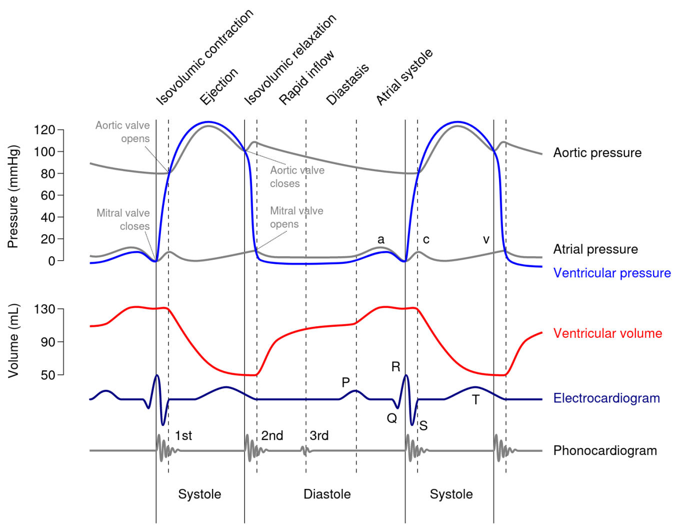

Figure 5.3: Wiggers diagram, showing an idealized cardiac cycle [171, CC BY-SA 2.5].

5.2 Electrophysiological depolarization waves

As outlined in the previous section, the contraction of the heart is mainly driven by the propagated action potential. In this section, we formalize the concept of electrophysiological depolarization and repolarization by first introducing mathematical models of action potentials of a single cardiac cell, also referred to as *cardiomyocyte*. We continue by establishing a macroscopical model of action potential propagation in cardiac tissue and conclude by introducing reduced models which are later used within the coupled context.

5.2.1 Cardiac cell models

Each cell in the human body has a resting electical potential difference across its cell membrane, the *transmembrane voltage*. This rest potential ensures the maintenance of the cell volume, which would otherwise increase without bound due to osmosis effects. Specialized cells, such as neurons or cardiomyocytes, can manipulate this potential difference to send electrical signals to neighbouring cells. [70]

Mathematically, this change of transmembrane voltage can be formulated with the equations of an electrical ciruit model of the form

$$C_{\mathrm{m}} \frac{\partial}{\partial t} v = -I_{\mathrm{ion}}(v, \mathbf{w}, \mathbf{c}) + I_{\mathrm{ext}}(t)\,, \qquad t \in (0, T)\,. \tag{5.1}$$

The capacitive current $C_{\mathrm{m}} \frac{\partial}{\partial t} v$ with *capacitance* C_{m} balances any *external applied stimulus current* I_{ext} and the *total ionic transmembrane current* I_{ion}, depending on the transmembrane voltage v, the state variable of transmembrane ion channels $\mathbf{w}$ and cellular ion concentrations $\mathbf{c}$.

The first mathematical model to accurately describe cellular action potentials and the underlying permeability changes was proposed by Hodgkin and Huxley [84]. Though their model was initially described for nerve action potentials, the formalism passed to cardiac tissue and enabled a multitude of different transmembrane current models. We first present this formalism and will comment on some cell models of particular interest.

Definition 5.1: Let $v\colon [0,T] \to \mathbb{R}$ be the transmembrane voltage in a cardiomyocyte and $N \in \mathbb{N}$. Let $\mathbf{w}\colon [0,T] \to \mathbb{R}^{d_\mathbf{w}}$ be a vector with $d_\mathbf{w}$ *gating variables* w_i, $i = 1,\dots,d_\mathbf{w}$, described by the system of ODEs

$$\begin{cases} \frac{\partial}{\partial t} w_i(t) & = \alpha_i(v(t))(1-w_i(t)) - \beta_i(v(t))w_i(t)\,, \quad t \in (0,T)\,, \\ w_i(t) & \in [0,1]\,, \qquad\qquad\qquad\qquad\qquad\quad t \in [0,T]\,, \\ w_i(0) & = w_0\,, \\ \alpha_i(v), \beta_i(v) & > 0\,, \qquad\qquad\qquad\qquad\qquad\qquad v \in \mathbb{R}\,. \end{cases} \tag{5.2}$$

and $\mathbf{c}\colon [0,T] \to \mathbb{R}^{d_\mathbf{c}}$ be a vector of intracellular *concentration variables* c_j, $j = 1,\dots,d_\mathbf{c}$ following

$$\begin{cases} \frac{\partial}{\partial t} c_j(t) = -\frac{I_{c_j}(v(t),\mathbf{w}(t))\cdot A_\mathrm{cap}}{V_{c_j} z_{c_j} F}\,, \quad t \in (0,T) \\ w_j(0) = c_0\,, \end{cases} \tag{5.3}$$

with capacitive membrane area A_cap, compartment volume V_{c_j}, valence z_{c_j}, Faraday constant F and I_{c_j} being the sum of ionic currents carrying ion c_j. To ease notation, we will omit the time dependence of all variables for the remainder of this chapter. We call

$$I_\mathrm{ion}(v,\mathbf{w},\mathbf{c}) = \sum_{n=1}^{N} \left[G_n(v,\mathbf{c}) \prod_{i=1}^{d_\mathbf{w}} w_i^{p_{n,i}} (v - v_n(\mathbf{c})) \right] + I_\mathrm{static}(v,\mathbf{w},\mathbf{c})\,, \qquad p_{n,i} \in \mathbb{N}\,,$$

a *general ionic current model* with N currents. The current I_static accounts for time independent fluxes.

For the sake of readability, we declare the main functions in (5.2) and (5.3) by

$$\begin{aligned} \mathbf{G}_\mathbf{w}(v,\mathbf{w}) &:= \left(\alpha_i(v(t))(1-w_i) - \beta_i(v)w_i\right)_{i=1,\dots,d_\mathbf{w}}\,, \\ \mathbf{G}_\mathbf{c}(v,\mathbf{w},\mathbf{c}) &:= \left(-\frac{I_{c_j}(v,\mathbf{w})\cdot A_\mathrm{cap}}{V_{c_j} z_{c_j} F}\right)_{j=1,\dots,d_\mathbf{w}}\,. \end{aligned}$$

Definition 5.2: Let v, $\mathbf{w}$, $\mathbf{c}$ be as in definition 5.1. Then the evolution of the transmembrane potential of a single myocyte is given by

$$C_\mathrm{m} \frac{\partial}{\partial t} v + I_\mathrm{ion}(v,\mathbf{w},\mathbf{c}) = I_\mathrm{ext} \qquad \text{in } (0,T)\,, \tag{5.4a}$$

$$\frac{\partial}{\partial t}\mathbf{w} = \mathbf{G}_\mathbf{w}(t,v,\mathbf{w}) \qquad \text{in } (0,T)\,, \tag{5.4b}$$

$$\frac{\partial}{\partial t}\mathbf{c} = \mathbf{G}_\mathbf{c}(t,v,\mathbf{w},\mathbf{c}) \qquad \text{in } (0,T)\,, \tag{5.4c}$$

$$v = v_0\,, \qquad \mathbf{w} = \mathbf{w}_0\,, \qquad \mathbf{c} = \mathbf{c}_0 \qquad \text{for } t = 0\,. \tag{5.4d}$$

This general formalism and the corresponding system of equations (5.4) does not portray the entirety of cellular transmembrane current models. Simple evolution models for transmembrane voltage, for example the one presented by FitzHugh [55], set $d_{\mathbf{w}} = 1$, $d_{\mathbf{c}} = 0$ and use an affine function $\mathbf{G}_{\mathbf{w}}$ to model a system of the type

$$\begin{cases} \frac{\partial}{\partial t} v = f(v, w)\,, \\ \frac{\partial}{\partial t} w = g(v, w)\,. \end{cases}$$

These models only offer a basic qualitative transmembrane voltage evolution. However, they are still widely used due to their low computational cost and the multitude of existing theory on existence, uniqueness and numerical treatment within the macroscopic excitation propagation (see section 5.2.2). More involved models, such as the atrial cell model proposed by Courtemanche et al. [44] and the ventricular cell model introduced by ten Tusscher et al. [161, 162], do not follow the strict formalism described above. These models consist of additional ODEs as well as algebraic equations, making the system a differential algebraic system. We do not go into detail on such systems, but refer to an extensive discussion on the topic in [79].

5.2.2 Macroscale models of cardiac excitation propagation

Within cardiac tissue, transmembrane voltage does not occur in isolation. The action potentials of myocytes depend on and interact with neighbouring cells, since the intracellular spaces are connected via low resistance gap junctions. The extracellular and intracellular spaces are intertwined, but separated by a membrane boundary. This arrangement permits a flow of ionic currents between cells and allows a macroscopic excitation propagation. [160]

Following the formalism established in [65], we depict cardiac tissue to be bounded by intra- and extracellular spaces and denote by $\Omega \subset \mathbb{R}^3$ the collection of cardiomyocytes connecting the two domains. In theory, this allows the view of single myocytes at each $\mathbf{x} \in \Omega$. Because of the microscopic lengths of these cells, which are typically around 100μm long and separated by about 250 angstroms [93, section 12.3], this approach is not feasible in practice. For that matter, we regard each point $\mathbf{x} \in \Omega$ as the homogenization of several hundreds or thousands of cells. While the detailed mathematical analysis of this homogenization process as well as further references can be found in [57, section 3.2], we continue by giving a brief description of the physiological concepts leading to the model describing excitation propagation.

Abusing notation, we extend the vectors of ion concentrations $\mathbf{c}$ and gating variables $\mathbf{w}$ on Ω by assuming

$$\mathbf{c}\colon [0, T] \times \Omega \to \mathbb{R}^{d_{\mathbf{c}}}\,, \qquad \mathbf{w}\colon [0, T] \times \Omega \to \mathbb{R}^{d_{\mathbf{w}}}$$

are evaluated in the sense that for each $\mathbf{x} \in \Omega$, $\mathbf{c}(\cdot, \mathbf{x}), \mathbf{w}(\cdot, \mathbf{x})$ follow the cell models presented in the previous section. The introduced concepts of electromagnetic field theory can be viewed in more detail for example in [104] and its connection to cardiac electrophysiology in [156, chapter 2]. We omit the dependencies of t and $\mathbf{x}$ for the sake of readability.

Lemma 5.3: *Let $\mathcal{D} \subset \mathbb{R}^3$ and $v \in \mathcal{C}^2(\mathcal{D}; \mathbb{R})$ be a scalar field. Then*

$$\operatorname{curl}(\nabla v) = \mathbf{0}\,.$$

Conversely, if $\operatorname{curl}(\mathbf{E}) = \mathbf{0}$ for any vector field $\mathbf{E} \in \mathcal{C}^1(\mathcal{D}; \mathbb{R}^3)$ with $\mathcal{D} \subset \mathbb{R}^3$ open and 1-connected, then there exists a scalar field v with $\mathbf{E} = -\nabla v$.

The intra- and extracellular spaces can be modeled as volume conductors. Using the subscripts "$\mathrm{i,e}$" to denote intra- and extracellular space, respectively, the relation between electric and magnetic fields is given by the first Maxwell equation

$$\nabla \times E_{\mathrm{i,e}} + \frac{\partial}{\partial t} B_{\mathrm{i,e}} = \mathbf{0} \qquad \text{in } (0,T) \times \Omega\,.$$

In the context of volume conductor theory, the temporal variations in electric and magnetic fields within cardiac tissue are so slow that their coupling can be neglected. This leaves us with the *quasistationary* case of the Maxwell equations, namely

$$\nabla \times \mathbf{E}_{\mathrm{i,e}} = \mathbf{0}\,.$$

Using lemma 5.3, there exists an electric potential $v_{\mathrm{i,e}}$, such that

$$\mathbf{E}_{\mathrm{i,e}} = -\nabla v_{\mathrm{i,e}}\,.$$

Definition 5.4: Let $\mathbf{f}, \mathbf{s}, \mathbf{t}$ be fibre fields on Ω and $\sigma^{\mathrm{i}}_{\mathbf{f}}, \sigma^{\mathrm{i}}_{\mathbf{s}}, \sigma^{\mathrm{i}}_{\mathbf{t}} > 0$ representing the intracellular conductivities along the respective axis. We call

$$\mathbf{D}_{\mathrm{i}} := \sigma^{\mathrm{i}}_{\mathbf{f}}\, \mathbf{f} \otimes \mathbf{f} + \sigma^{\mathrm{i}}_{\mathbf{s}}\, \mathbf{s} \otimes \mathbf{s} + \sigma^{\mathrm{i}}_{\mathbf{t}}\, \mathbf{t} \otimes \mathbf{t}\,, \qquad \text{in } \Omega$$

the *intracellular anisotropic conductivity tensor.*
Analogously, the *extracellular anisotropic conductivity tensor* $\mathbf{D}_{\mathrm{e}}$ is defined for conductivities $\sigma^{\mathrm{e}}_{\mathbf{f}}, \sigma^{\mathrm{e}}_{\mathbf{s}}, \sigma^{\mathrm{e}}_{\mathbf{t}} > 0$.

We denote by $\mathbf{j}_{\mathrm{i,e}} \colon [0,T] \times \Omega \to \mathbb{R}^3$ the intra- and extracellular current densities flowing across the membrane surface. According to Ohm's law, the relation between the current density and electric field is given by

$$\mathbf{j}_{\mathrm{i,e}} = \mathbf{D}_{\mathrm{i,e}} \mathbf{E}_{\mathrm{i,e}} = -\mathbf{D}_{\mathrm{i,e}} \nabla v_{\mathrm{i,e}}\,. \tag{5.5}$$

The current density $\mathbf{j}_{\mathrm{i,e}}$ follows the law of conservation of charge, which states that the current leaving $\mathcal{D}$ must be equal to the rate of change of charge Q within $\mathcal{D}$. This is expressed as

$$I_{\mathrm{M}}^{\mathrm{i,e}} := \frac{\partial}{\partial t} Q_{\mathrm{i,e}} = -\operatorname{div}(\mathbf{j}_{\mathrm{i,e}})\,. \tag{5.6}$$

We call $I_{\mathrm{M}}^{\mathrm{i,e}}\colon [0,T]\times\Omega \to \mathbb{R}$ the *total transmembrane current*, which is determined by three factors:

- the accumulation of charge $\frac{\partial}{\partial t} q_{\mathrm{i,e}}$,
- the ion transmembrane current I_{ion},
- external applied stimuli $I_{\mathrm{ext}}^{\mathrm{i,e}}$.

The quasistationary case of the Maxwell equations implies that there is no accumulation in charge at any point. Since the myocyte tissue is modeled as an insulator between the intra- and extracellular spaces, there may be some accumulation of charge in the separate domains. However, because of the small thickness of the membranes, each accumulation of charge in one layer immediately attracts an opposite charge in the other layer, resulting in

$$\frac{\partial}{\partial t}(q_{\mathrm{i}} + q_{\mathrm{e}}) = 0\,. \tag{5.7}$$

Definition 5.5: Let $v_{\mathrm{i,e}}\colon [0,T]\times\Omega \to \mathbb{R}$ be the respective potentials on the intra- and extracellular spaces. We call

$$v\colon [0,T]\times\Omega \to \mathbb{R}\,, \qquad (t,\mathbf{x}) \mapsto v_{\mathrm{i}}(t,\mathbf{x}) - v_{\mathrm{e}}(t,\mathbf{x})$$

the *transmembrane voltage.*

Lastly, we address the issue of different scales: The ion transmembrane current as well as the membrance capacitance C_{m} are given per unit area of the cell membrane, while the potentials $v_{\mathrm{i}}, v_{\mathrm{e}}$, charges $q_{\mathrm{i}}, q_{\mathrm{e}}$ and the external stimuli $I_{\mathrm{ext}}^{\mathrm{i,e}}$ are given per unit volume of the macroscale tissue. To unify these scales, we introduce a geometric parameter χ representing the scale conversion and get the formula for the total transmembrane current:

$$I_{\mathrm{M}}^{\mathrm{i,e}} = \frac{\partial}{\partial t} q_{\mathrm{i,e}} + \chi I_{\mathrm{ion}}(v,\mathbf{w},\mathbf{c}) - \chi I_{\mathrm{ext}}^{\mathrm{i,e}}\,. \tag{5.8}$$

Lemma 5.6: *Let* $q = \frac{1}{2}(q_{\mathrm{i}} - q_{\mathrm{e}})$ *be the transmembrane rate of charge, related to the transmembrane current by* $\chi C_{\mathrm{m}} \frac{\partial}{\partial t} v = \frac{\partial}{\partial t} q$. *Then*

$$\begin{aligned}
\operatorname{div}(\mathbf{j}_{\mathrm{i}}) &= -\chi C_{\mathrm{m}} \frac{\partial}{\partial t} v - \chi I_{\mathrm{ion}}(v,\mathbf{w},\mathbf{c}) + \chi I_{\mathrm{ext}}^{\mathrm{i}}\,,\\
\operatorname{div}(\mathbf{j}_{\mathrm{e}}) &= \chi C_{\mathrm{m}} \frac{\partial}{\partial t} v + \chi I_{\mathrm{ion}}(v,\mathbf{w},\mathbf{c}) - \chi I_{\mathrm{ext}}^{\mathrm{e}}\,.
\end{aligned}$$

Proof. By (5.6), we know that $\operatorname{div}(\mathbf{j}_\mathrm{i}) = -I_\mathrm{M}^\mathrm{i}$. Using (5.7) yields the relation

$$\chi C_\mathrm{m} \frac{\partial}{\partial t} v = \frac{\partial}{\partial t} q_\mathrm{i} = -\frac{\partial}{\partial t} q_\mathrm{e} \,.$$

Inserting both terms in (5.8) results in

$$\operatorname{div}(\mathbf{j}_\mathrm{i}) = -I_\mathrm{M}^\mathrm{i} = -\chi C_\mathrm{m} \frac{\partial}{\partial t} v - \chi I_\mathrm{ion}(v, \mathbf{w}, \mathbf{c}) + I_\mathrm{ext}^\mathrm{i} \,.$$

Analoguously, the equation for $\operatorname{div}(\mathbf{j}_\mathrm{e})$ is derived. □

Remark 5.7: In some literature, $I_\mathrm{ext}^\mathrm{i,e}$ may be given in the macroscopic scale and the preceding χ is dropped. Since I_ext may be regarded for a singular cell model as well, we find it more coherent to present the applied current in the microscale.

Taking into account a suitable model for the cellular ionic transmembrane potential I_ion at each point $\mathbf{x} \in \Omega$, we can now use (5.5) and summarize the equations of the bidomain model as follows:

Problem 5.8 (Parabolic-parabolic bidomain equations):
Let $I_\mathrm{ext}^\mathrm{i,e} \colon (0, T) \times \Omega \to \mathbb{R}$ be the applied intra- and extracellular currents per unit volume. Find the intra- and extracellular potentials $v_\mathrm{i}, v_\mathrm{e} \colon (0, T) \times \Omega \to \mathbb{R}$ satisfying

$$C_\mathrm{m} \frac{\partial}{\partial t} v - \operatorname{div}\left(\mathbf{D}_\mathrm{i} \nabla v_\mathrm{i}\right) = -I_\mathrm{ion}(v, \mathbf{w}, \mathbf{c}) + I_\mathrm{ext}^\mathrm{i} \qquad \text{in } (0,T) \times \Omega \,, \tag{5.9a}$$

$$-C_\mathrm{m} \frac{\partial}{\partial t} v - \operatorname{div}\left(\mathbf{D}_\mathrm{e} \nabla v_\mathrm{e}\right) = I_\mathrm{ion}(v, \mathbf{w}, \mathbf{c}) - I_\mathrm{ext}^\mathrm{e} \qquad \text{in } (0,T) \times \Omega \,, \tag{5.9b}$$

$$\frac{\partial}{\partial t} \mathbf{w} = \mathbf{G}_\mathbf{w}(v, \mathbf{w}) \qquad \text{in } (0,T) \times \Omega \,, \tag{5.9c}$$

$$\frac{\partial}{\partial t} \mathbf{c} = \mathbf{G}_\mathbf{c}(v, \mathbf{w}, \mathbf{c}) \qquad \text{in } (0,T) \times \Omega \,, \tag{5.9d}$$

$$(\mathbf{D}_{i,e} \nabla v_{i,e}) \cdot \mathbf{n} = 0 \qquad \text{on } (0,T) \times \Gamma \,, \tag{5.9e}$$

$$v = v_0 \,, \qquad \mathbf{w} = \mathbf{w}_0 \,, \qquad \mathbf{c} = \mathbf{c}_0 \qquad \text{on } \{0\} \times \Omega \,, \tag{5.9f}$$

where $\mathbf{D}$ is the anisotropic conductivity tensor scaled by $\frac{1}{\chi}$.

The homogeneous Neumann boundary (5.9e) constitutes that no current passes through the boundary $\partial\Omega$. This is a reasonable assumption, since cells outside the cardiac tissue Ω are not excitable and will therefore not conduct any action potential. Since the system (5.9) depends on $v = v_\mathrm{i} - v_\mathrm{e}$, it can be more convenient to reformulate it to depend on the transmembrane voltage v and the extracellular potential v_e only.

Lemma 5.9 (Parabolic-elliptic bidomain equations):
The system (5.9) is equivalent to the parabolic-elliptic bidomain equations

$$
\begin{aligned}
C_\mathrm{m}\frac{\partial}{\partial t}v - \operatorname{div}(\mathbf{D}_\mathrm{i}\nabla v) - \operatorname{div}(\mathbf{D}_\mathrm{i}\nabla v_\mathrm{e}) &= -I_\mathrm{ion}(v,\mathbf{w},\mathbf{c}) + I^\mathrm{i}_\mathrm{ext} && \textit{in } (0,T)\times\Omega\,, && (5.10a)\\
-\operatorname{div}(\mathbf{D}_\mathrm{i}\nabla v_\mathrm{e}) - \operatorname{div}((\mathbf{D}_\mathrm{i}+\mathbf{D}_\mathrm{e})\nabla v_\mathrm{e}) &= I_\mathrm{ion}(v,\mathbf{w},\mathbf{c}) + I^\mathrm{i}_\mathrm{ext} + I^\mathrm{e}_\mathrm{ext} && \textit{in } (0,T)\times\Omega\,, && (5.10b)\\
\frac{\partial}{\partial t}\mathbf{w} &= \mathbf{G}_\mathbf{w}(v,\mathbf{w}) && \textit{in } (0,T)\times\Omega\,, && (5.10c)\\
\frac{\partial}{\partial t}\mathbf{c} &= \mathbf{G}_\mathbf{c}(v,\mathbf{w},\mathbf{c}) && \textit{in } (0,T)\times\Omega\,, && (5.10d)\\
(\mathbf{D}_i\nabla(v+v_\mathrm{e}))\cdot\mathbf{n} &= 0 && \textit{on } (0,T)\times\Gamma\,, && (5.10e)\\
((\mathbf{D}_i+\mathbf{D}_e)\nabla v_e)\cdot\mathbf{n} + (\mathbf{D}_i\nabla v)\cdot\mathbf{n} &= 0 && \textit{on } (0,T)\times\Gamma\,, && (5.10f)\\
v(0) = v_0\,, \qquad \mathbf{w}(0) = \mathbf{w}_0\,, \qquad \mathbf{c}(0) &= \mathbf{c}_0 && \textit{in } \Omega\,. && (5.10g)
\end{aligned}
$$

Proof. Inserting $v_\mathrm{i} = v + v_\mathrm{e}$ in (5.9) yields the result. □

Remark 5.10: The solutions $v_\mathrm{i}, v_\mathrm{e}$ of both (5.9) and (5.10) are only unique up to an additive constant $\nu\colon [0,T] \to \mathbb{R}$ due to the given initial conditions [156, theorem 3.5]. One possibility to obtain a unique solution is by requiring

$$\int_\Omega v_\mathrm{e}\,\mathrm{d}\mathbf{x} = 0\,.$$

This does not affect the usefulness of the bidomain model, since only potential differences v can be measured in applications [70].

5.2.3 Reduced macroscopic models

The bidomain model introduced in the previous section entails several disadvantages limiting numerical simulations. The homogenized bidomain equations are intended to model a full heartbeat lasting about 0.8 seconds. However, the ionic currents I_ion used at each point $\mathbf{x} \in \Omega$ simulate concentration shifts and ion channel opening and closing, requiring a timescale of at least 0.01 ms. Additionally, the bidomain model is ill-conditioned due to the pure Neumann boundary conditions. [57, chapter 4]
A common simplifying assumption, which we will also employ, is that the ratios of the entries of the conductivity tensors $\mathbf{D}_\mathrm{i,e}$ are equal. Though this variation is not based on physiological foundations, the resulting patterns of action potentials v are very similar to the full bidomain model, baring external stimuli such as defibrillation [40, 125]. The result is a single parabolic reaction-diffusion equation coupled with the same cellular potential models.

Theorem 5.11 (Monodomain equations): *Consider the system* (5.10). *Suppose there exists a* $\lambda \in \mathbb{R}$, *such that* $\mathbf{D}_\mathrm{e} = \lambda \mathbf{D}_\mathrm{i}$. *Then the system* (5.10) *is equivalent to*

$$C_\mathrm{m} \frac{\partial}{\partial t} v - \operatorname{div}(\mathbf{D}\nabla v) + I_\mathrm{ion}(v, \mathbf{w}, \mathbf{c}) = I_\mathrm{ext} \qquad \text{in } (0,T)\times\Omega\,, \tag{5.11a}$$

$$\frac{\partial}{\partial t}\mathbf{w} = \mathbf{G}_\mathbf{w}(v, \mathbf{w}) \qquad \text{in } (0,T)\times\Omega\,, \tag{5.11b}$$

$$\frac{\partial}{\partial t}\mathbf{c} = \mathbf{G}_\mathbf{c}(v, \mathbf{w}, \mathbf{c}) \qquad \text{in } (0,T)\times\Omega\,, \tag{5.11c}$$

$$(\mathbf{D}\nabla v)\cdot \mathbf{n} = 0 \qquad \text{on } (0,T)\times\Gamma\,, \tag{5.11d}$$

$$v(0) = v_0\,, \qquad \mathbf{w}(0) = \mathbf{w}_0\,, \qquad \mathbf{c}(0) = \mathbf{c}_0 \qquad \text{in } \Omega\,, \tag{5.11e}$$

with $\mathbf{D} = \frac{\lambda}{1+\lambda}\mathbf{D}_\mathrm{i}$ *and* $I_\mathrm{ext} = \frac{\lambda I^\mathrm{i}_\mathrm{ext} + I^\mathrm{e}_\mathrm{ext}}{1+\lambda}$.

Proof. Inserting $\mathbf{D}_\mathrm{e} = \lambda \mathbf{D}_\mathrm{i}$ in (5.10) yields the result. □

5.3 Constitutive elasticity models

Modeling the contraction of the human heart poses some distinct challenges regarding the equations of elasticity (3.4). The types of stored energy functions used in this context have already been discussed in section 4.4. We complete the system of equations by detailing the specific boundary conditions of cardiac functions, incorporating the contraction of carciomyocytes resulting from the electrophysiological transmembrane voltage and introducing a systematic approach for choosing initial conditions.

5.3.1 Boundary conditions in cardiac elasticity

Consider the domain of the heart Ω and its boundary $\Gamma = \partial\Omega$. We denote by $\Gamma_\mathrm{D} \subset \Gamma$ the *Dirichlet boundary*, i.e., it holds

$$\mathbf{u}(t, \mathbf{x}) = \mathbf{u}_0(t, \mathbf{x}) \qquad \text{on } (0,T)\times\Gamma_\mathrm{D}\,.$$

The fixation of some part of Ω is necessary to ensure the stability of the system in a mechanical sense. We continue with the boundary condition corresponding to the cardiovascular pressure pushing onto the endocardial surface.

Definition 5.12: Let $\Gamma_\mathrm{LV}, \Gamma_\mathrm{RV}, \Gamma_\mathrm{LA}, \Gamma_\mathrm{RA}$ be the endocardial surface of the left and right ventricle and atria, respectively, and let $p_\mathrm{C}\colon [0,T] \to \mathbb{R}_+$ be the pressure inside the chambers $\mathrm{C} \in \{\mathrm{LV}, \mathrm{RV}, \mathrm{LA}, \mathrm{RA}\}$. The *endocardial surface pressure* is described by the boundary condition

$$\mathbf{P}(\mathbf{F})\mathbf{n} = -p_\mathrm{C}(t)\operatorname{Cof}(\mathbf{F})\,\mathbf{n} \qquad \text{on } (0,T)\times\Gamma_\mathrm{C} \qquad \text{for } \mathrm{C} \in \{\mathrm{LV}, \mathrm{RV}, \mathrm{LA}, \mathrm{RA}\}\,.$$

We follow the general convention that a positive pressure p_C corresponds to a push on the respective surface. Since the normal $\mathbf{n}$ points outwards, i.e., it points inside the cardiac chamber, the negative sign is included to ensure the correct behaviour.

Remark 5.13: To increase readability, we combine the endocardial surfaces by setting

$$\Gamma_\mathrm{N} := \Gamma_\mathrm{LV} \cup \Gamma_\mathrm{RV} \cup \Gamma_\mathrm{LA} \cup \Gamma_\mathrm{RA}$$

and defining $p\colon [0,T] \times \Gamma_\mathrm{N} \to \mathbb{R}$ by

$$p(t, \mathbf{x}) = p_\mathrm{C}(t)\,, \quad \text{if } \mathbf{x} \in \Gamma_\mathrm{C} \qquad \text{for C} \in \{\mathrm{LV}, \mathrm{RV}, \mathrm{LA}, \mathrm{RA}\}\,.$$

The specifics of the function p are discussed in section 5.4. However, as we have seen in Figure 5.3, it can be roughly described by a positive base value which rapidly increases and then decreases to its initial value. This boundary condition on its own would result in the inflation and subsequential deflation of the heart chambers. Again refering to Figure 5.3, a counterpart is needed for the chamber volumes to decrease simultaneously.

While the decrease in volume is mostly due to the active contraction depicted in the following section, the movement of the epicardium during the cardiac cycle is additionally constrained by the *pericardium*, a serous membrane divided into visceral and parietal pericardium. The inner layer, the visceral pericardium, is connected to the epicardium of the heart tissue. The parietal pericardium is reinforced by an outer layer of dense, irregular connected collagen fibres. The small gap between these two layers is called the pericardial cavity. It is filled with pericardial fluid, which acts as a lubricant and negates friction between the moving visceral and the mostly static parietal pericardium [107, chapter 21]. During diastole, the pericardium mostly acts as a barrier to prevent extensive expansions of the heart chamber. During systole, the contracting chambers mostly stay adherent to the pericardium. The behaviour of the epicardium along the parietal pericardium can be better described as a sliding motion. [121].

A physiologically accurate method of modeling this boundary condition was implemented by Fritz et al. [58]. Here, a frictionless contact boundary condition using a bidirectional penalty term was implemented. The contact boundary was generated by adding the physical pericardium to the domain Ω. While the outer layer of this additional volumetric domain is fixated, the inner layer acts as a counterpart for the epicardial boundary condition. However, this method is computationally expensive as it requires larger geometries due to the added pericardium and costly evaluations of the sliding boundary condition.

Therefore, we adopt the model of the pericardial boundary presented by Pfaller et al. [121]. Here, the epicardial surface is modeled as a spring and a dashpot in parallel at each point. Mathematically, we write this as follows:

Definition 5.14: Let $\varphi \in \mathcal{D}$ be a motion with displacement $\mathbf{u}$ and velocity $\mathbf{v}$. For an outwards-facing normal $\mathbf{n} \in S_1$, let

$$q_{\mathrm{P}}(\mathbf{u}, \mathbf{v}, \mathbf{n}) \coloneqq k_{\mathrm{P}} \mathbf{u} \cdot \mathbf{n} + c_{\mathrm{P}} \mathbf{v} \cdot \mathbf{n} \,.$$

The *pericardial surface traction* is described by the boundary condition

$$\mathbf{P}(\mathbf{F})\mathbf{n} = q_{\mathrm{P}}(\mathbf{u}, \mathbf{v}, \mathbf{n})\mathbf{n} \qquad \text{on } (0, T) \times \Gamma_{\mathrm{P}} \,,$$

with $k_{\mathrm{P}}, c_{\mathrm{P}} \geq 0$ and Γ_{P} describes the boundary connected to the pericardium.

Remark 5.15: We can reformulate the traction function q_{P} within the boundary condition to be independent of $\mathbf{n}$: Let

$$\mathbf{q}_{\mathrm{P}}(\mathbf{u}, \mathbf{v}) \coloneqq k_{\mathrm{P}} \mathbf{u} + c_{\mathrm{P}} \mathbf{v} \,.$$

Then $q_{\mathrm{P}}(\mathbf{u}, \mathbf{v}, \mathbf{n})\, \mathbf{n} = (\mathbf{n} \otimes \mathbf{n})\, \mathbf{q}_{\mathrm{P}}(\mathbf{u}, \mathbf{v})$.

For large values of k_{P} and c_{P}, the function

$$\mathbf{q}(\mathbf{u}, \mathbf{v}, \mathbf{n}) \coloneqq (\mathbf{n} \otimes \mathbf{n}) \mathbf{q}_{\mathrm{P}}(\mathbf{u}, \mathbf{v})$$

acts as a kind of penalty for large displacements and velocities along the outer normal direction $\mathbf{n}$.

Remark 5.16: Dede et al. [64] supplement this approach by adding a tangential part to $\mathbf{q}$, allowing for a more detailed model description. The traction function then takes the form

$$\mathbf{q}(\mathbf{u}, \mathbf{v}, \mathbf{n}) = (\mathbf{n} \otimes \mathbf{n})\, (k_{\perp} \mathbf{u} + c_{\perp} \mathbf{v}) + (\mathbf{I} - (\mathbf{n} \otimes \mathbf{n})) \left(k_{\parallel} \mathbf{u} + c_{\parallel} \mathbf{v} \right) \,.$$

We will omit this term, as within their experiments, the authors set $k_{\parallel} = c_{\parallel} = 0$ except at a quasi-fixated boundary.

The boundaries corresponding to the respective boundary condition are highlighted in Figure 5.4. Summarizing the conditions used in our cardiac elasticity model yields the following set of equations:

Problem 5.17 (Strong form of cardiac elasticity): *Let* Ω *be a bounded domain. Find* $\mathbf{u} \colon [0, T] \times \Omega \to \mathbf{\Phi}(\Omega)$ *satisfying*

$$\rho \frac{\partial^2}{\partial t^2} \mathbf{u} - \operatorname{div}\left(\mathbf{P}(\mathbf{F})\right) = \mathbf{0} \qquad \text{in } (0, T) \times \Omega \,, \tag{5.12a}$$

$$\mathbf{u} = \mathbf{0} \qquad \text{on } (0, T) \times \Gamma_{\mathrm{D}} \,, \tag{5.12b}$$

$$\mathbf{P}(\mathbf{F})\mathbf{n} = -p(t) \operatorname{Cof}(\mathbf{F})\, \mathbf{n} \qquad \text{on } (0, T) \times \Gamma_{\mathrm{N}} \,, \tag{5.12c}$$

$$\mathbf{P}(\mathbf{F})\mathbf{n} = \mathbf{q}(\mathbf{u}, \frac{\partial}{\partial t} \mathbf{u}, \mathbf{n}) \qquad \text{on } (0, T) \times \Gamma_{\mathrm{P}} \,, \tag{5.12d}$$

$$\mathbf{u} = \mathbf{u}_0 \,, \quad \mathbf{v} = \mathbf{0} \,, \quad \mathbf{a} = \mathbf{0} \qquad \text{on } \{0\} \times \Omega \,, \tag{5.12e}$$

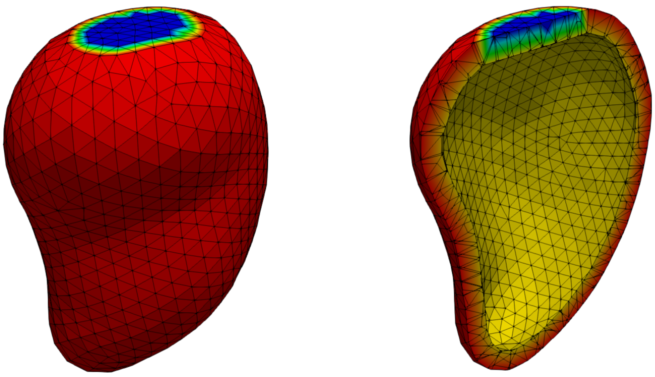

Figure 5.4: Location of boundary values on a left ventricle: Dirichlet Γ_{D} (blue), pressure Γ_{N} (yellow) and traction Γ_{P} (red).

The system (5.12) is complemented with suitable initial conditions. Since we want $t = 0$ to be the beginning of a cardiac cycle, we assume the heart to be in a resting state and therefore set $\mathbf{v}(0) = \mathbf{a}(0) = \mathbf{0}$. Additionally, we want initial displacement $\mathbf{u}_0$ to be zero as well. This in turn would require $p_{\mathrm{C}}(0) = 0$ for $\mathrm{C} \in \{\mathrm{LV}, \mathrm{RV}, \mathrm{LA}, \mathrm{RA}\}$. Because the latter assumption is not applicable in physiological problems [108], we will not enforce $\mathbf{u}_0 = \mathbf{0}$. Suitable methods of modifying (5.12) to obtain $\mathbf{u}_0 = \mathbf{0}$ are presented in section 5.3.4.

5.3.2 Cellular tension development

Muscle tissue can be categorized into three different types: Skeletal, cardiac and smooth muscle tissue. Smooth muscle can be found surrounding blood vessels and vital organs, for example. This type of muscle tissue contracts and relaxes on its own in the sense that their activity is often not triggered by neural activatons or at least it can not be controlled arbitrarily. Skeletal muscle tissue is found in large muscle groups commonly known only as “muscles”. Their activity is triggered actively by the nervous system and can be managed voluntarily. Cardiac muscle tissue is similar to skeletal muscle in structure and the contraction of both relies on an external impulse. [107]

As we have described in the previous section, such an impulse triggers an action potential and, subsequentially, enables a shift in ion concentrations. The process of force generation and the following contraction of single muscle cells is explained by sliding filament theory [89]. The muscle contraction occurs as a result of the relative sliding between thin (*actin*) and thick (*myosin*) filaments. This sliding is caused by cycling cross-bridges, reacting to shifts in ion concentrations within the cell. For a more in-depth overview, we refer to [112].

Cardiomyocytes are thin, cable-like muscle cells [93, section 12.3] and contract mainly along their longitudinal direction $\mathbf{f}$. Our goal is to formulate a mathematical model describing the longitudinal stretch $\gamma_{\mathbf{f}}$ of these cells. As depicted in [93, chapter 15], the active tension $f_{\mathbf{k}}$ resulting in a muscle contraction is generated in small contractile units called *sarcomeres*. Let $\mathbf{w}, \mathbf{c}$ be the vectors of gating variables and ion concentrations introduced in section 5.2. Tension development models are usually of the form

$$\frac{\partial}{\partial t}\mathbf{k} = \mathbf{G}_{\mathbf{k}}(\mathbf{w}, \mathbf{c}, \mathbf{k}, \ell^{\varphi}, \frac{\partial}{\partial t}\ell^{\varphi}) , \tag{5.13}$$

where $\mathbf{k}\colon [0,T] \to \mathbb{R}^{d_{\mathbf{k}}}$ is the vector of tension model variables and ℓ^{φ} is the current length of the myocyte [77, 100, 112, 167].

Remark 5.18: Simpler tension evolution models only rely on the calcium concentration, represented as one entry of $\mathbf{c}$. More involved models, such as the one presented by Land et al. [100], require additional coupling between $\mathbf{c}$, $\mathbf{w}$ and $\mathbf{k}$ [63, section 2.4.1]. We therefore keep the more intricate description for the sake of completeness.

Definition 5.19: Let ℓ be the initial length of a cardiomyocyte with longitudinal direction $\mathbf{f}$. Then, given its current length ℓ^{φ}, we call

$$\gamma_{\mathbf{f}} \coloneqq \frac{\ell^{\varphi} - \ell}{\ell}$$

the *stretch* along $\mathbf{f}$.

Remark 5.20: The stretch is by definition dimensionless and negative for cellular contractions. In physiological setups, we expect $\gamma_{\mathbf{f}} \in [-0.3, 0]$ [135, 136].

We extend equation (5.13) by assuming the macroscopic contraction $\gamma_{\mathbf{f}}$ obeys a general differential equation of the type [137]

$$\frac{\partial}{\partial t}\gamma_{\mathbf{f}} = \mathbf{G}_{\gamma_{\mathbf{f}}}(\mathbf{c}, \mathbf{k}, \gamma_{\mathbf{f}}, \frac{\partial}{\partial t}\gamma_{\mathbf{f}}, \mathbf{F}) \ ,$$

Note that the stretch is also affected by the current state of deformation, represented by the dependence on $\mathbf{F}$. For a specific formulation of $\mathbf{G}_{\gamma_{\mathbf{f}}}$, we follow the arguments presented by Rossi et al. [135]. Using the results of [152], we set

$$\mathbf{G}_{\gamma_{\mathbf{f}}}(\mathbf{c}, \mathbf{k}, \gamma_{\mathbf{f}}, \mathbf{F}) = \frac{1}{\mu c_{\mathrm{Ca}}^2} \left(\alpha\, f_{\mathbf{k}}\, R_{\mathrm{FL}}(\iota_{4,\mathbf{f}}(\mathbf{F}^{\top}\mathbf{F})) + \sum_{j=1}^{5} (-1)^j (j+1)(j+2) \iota_{4,\mathbf{f}}(\mathbf{F}^{\top}\mathbf{F}) \gamma_{\mathbf{f}}^j \right) , \tag{5.14a}$$

where $f_{\mathbf{k}}$ is the active tension generated by contractile force generated by the sarcomere and R_{FL} is the *force length* relationship, experimentally fitted by Strobeck et al. [153], given by

$$R_{\mathrm{FL}}(\lambda) \coloneqq \delta_{\ell^{\varphi} \in [l_{\min}, l_{\max}]} \left[\frac{c_0}{2} + \sum_{j=1}^{3} \Big(c_j \sin(j\sqrt{\lambda} l_0) + d_j \cos(j\sqrt{\lambda} l_0) \Big) \right] , \tag{5.14b}$$

where l_0 is the initial length of the cell and $l_{\min}$, $l_{\max}$ are its minimal and maximum possible length. The symbol $\delta_{(\cdot)}$ represents the Kronecker-operator, ensuring no additional force is generated if the myocyte cant contract or elongate further. The active tension $f_{\mathbf{k}}$ is a component of the tension vector $\mathbf{k}$. This leaves us with defining a model for calculating the components of $\mathbf{k}\colon [0,T] \to \mathbb{R}^{d_{\mathbf{k}}}$ containing the variables of the specific cellular tension model. Some possible models were already cited above. To ease the analysis of the coupled model, we keep the simple phenomenological model from [135]. We set $d_{\mathbf{k}} = 1$, leading $\mathbf{k}$ to only consist of the contractile force $f_{\mathbf{k}}$, which will be set by the equation

$$\mathbf{G}_{\mathbf{k}}(\mathbf{w}, \mathbf{c}, \mathbf{k}, \gamma_{\mathbf{f}}, \frac{\partial}{\partial t}\gamma_{\mathbf{f}}) = f_{\mathbf{k}}(\mathbf{c}) := \left(c_{\mathrm{Ca}}(t) - c_{\mathrm{Ca}}(0)\right)^2 , \qquad t \in [0,T] . \tag{5.15}$$

Remark 5.21: Note that in contrast to the general tension development model (5.13) presented at the beginning of this section, the equation for $f_{\mathbf{k}}$ is not an ordinary differential equation. More involved electrophysiological activation models [44, 161] and tension development models [100] similarly use algebraic updates for some entries of $\mathbf{c}, \mathbf{w}$ or $\mathbf{k}$, respectively. This formalism is known as *differential algebraic equation* [79] (DAE). For the time being, we abuse the notation of $\mathbf{G}_{\mathbf{k}}$ to express both differential and algebraic equations used to calculate $\mathbf{k}$.

To conclude the subject of cellular tension development, we summarize the system of equations calculating the microscopic fibre stretch.

Problem 5.22 (Stretch deveolpment): *Let $\mathbf{F}\colon [0,T] \to \mathbb{R}^{3\times 3}$ be the macroscopic deformation tensor acting on a single cardiomyocyte and let $\mathbf{c}\colon [0,T] \to \mathbb{R}^{d_{\mathbf{c}}}, \mathbf{w}\colon [0,T] \to \mathbb{R}^{d_{\mathbf{w}}}$ be the ion concentration and gating variables over time. Find $\gamma_{\mathbf{f}}\colon [0,T] \to \mathbb{R}$ and $\mathbf{k}\colon [0,T] \to \mathbb{R}^{d_{\mathbf{k}}}$ satisfying*

$$\frac{\partial}{\partial t}\gamma_{\mathbf{f}} = \mathbf{G}_{\gamma_{\mathbf{f}}}(\mathbf{c}, \mathbf{k}, \gamma_{\mathbf{f}}, \frac{\partial}{\partial t}\gamma_{\mathbf{f}}, \mathbf{F}) \qquad \text{in } (0,T) , \tag{5.16a}$$

$$\frac{\partial}{\partial t}\mathbf{k} = \mathbf{G}_{\mathbf{k}}(\mathbf{w}, \mathbf{c}, \mathbf{k}, \gamma_{\mathbf{f}}, \frac{\partial}{\partial t}\gamma_{\mathbf{f}}) \qquad \text{in } (0,T) , \tag{5.16b}$$

$$\mathbf{k}(0) = \mathbf{k}_0 , \quad \gamma_{\mathbf{f}}(0) = 0 , \tag{5.16c}$$

where $\mathbf{G}_{\gamma_{\mathbf{f}}}$ and $\mathbf{G}_{\mathbf{k}}$ are defined as in (5.14) and (5.15), respectively.

The extension of the stretch development model to the domain Ω can be done canonically as was done in section 5.2 by assuming independent stretch developments at each $\mathbf{x} \in \Omega$. We remark an alternative approach presented by Dede et al. [64]:

Problem 5.23 (Regularized stretch deveolpment): *Let* $\mathbf{F}\colon [0,T] \times \Omega \to \mathbb{R}^{3\times 3}$ *be the deformation tensor of a motion* $\boldsymbol{\varphi}$ *and let* $\mathbf{c}\colon [0,T] \times \Omega \to \mathbb{R}^{d_\mathbf{c}}, \mathbf{w}\colon [0,T] \times \Omega \to \mathbb{R}^{d_\mathbf{w}}$ *be the ion concentration and gating variables, resepectively. Find* $\gamma_\mathbf{f}\colon [0,T] \times \Omega \to \mathbb{R}$ *and* $\mathbf{k}\colon [0,T] \times \Omega \to \mathbb{R}^{d_\mathbf{k}}$ *satisfying*

$$\frac{\partial}{\partial t}\gamma_\mathbf{f} - \frac{\varepsilon}{\mu c_{\mathrm{Ca}}^2}\Delta\gamma_\mathbf{f} = \mathbf{G}_{\gamma_\mathbf{f}}(\mathbf{c}, \mathbf{k}, \gamma_\mathbf{f}, \frac{\partial}{\partial t}\gamma_\mathbf{f}, \mathbf{F}) \qquad \text{in } (0,T) \times \Omega\,, \tag{5.17a}$$

$$\frac{\partial}{\partial t}\mathbf{k} = \mathbf{G}_\mathbf{k}(\mathbf{w}, \mathbf{c}, \mathbf{k}, \gamma_\mathbf{f}, \frac{\partial}{\partial t}\gamma_\mathbf{f}) \qquad \text{in } (0,T) \times \Omega\,, \tag{5.17b}$$

$$\nabla\gamma_\mathbf{f} \cdot \mathbf{n} = 0 \qquad \text{on } (0,T) \times \Gamma\,, \tag{5.17c}$$

$$\mathbf{k} = \mathbf{k}_0\,, \quad \gamma_\mathbf{f} = 0 \qquad \text{on } \{0\} \times \Omega\,. \tag{5.17d}$$

The authors clarify that this approach is not motivated by physical considerations. However, it may be interpreted as the result of some homogenization process on Ω. Additionally, the solutions $\gamma_\mathbf{f}$ of (5.17) have higher regularity, assisting the numerical approximation of this system as well as the coupled elasticity problem.

5.3.3 The active strain decomposition

In the previous section, we illustrated the development of microscopic tension $\mathbf{k}$ and stretch development $\gamma_\mathbf{f}$. On the macroscopic level, these lead to an *active* deformation, which has to be incorporated into (5.12). We highlight the two common approaches used in cardiac modeling, the *active stress* and the *active strain* approach, focussing on the latter as it will be used in the simulations in chapter 7.

Within the active stress approach [66, 113, 139], the active shortening of fibres in the material model, the first Piola-Kirchhoff tensor is additively decomposed by

$$\mathbf{P} = \mathbf{P}_\mathrm{P} + \mathbf{P}_\mathrm{A} \tag{5.18}$$

into a passive part $\mathbf{P}_\mathrm{P} = \mathrm{D}_\mathbf{F} W_\mathbf{P}(\mathbf{F})$, corresponding to the derivative of the stored energy function, and an active part

$$\mathbf{P}_\mathrm{A} = T_\mathrm{A}(\mathbf{k})\mathbf{F}\mathbf{f} \otimes \mathbf{f}\,.$$

Remark 5.24: We may interpret $\mathbf{P}_\mathrm{A}$ as the derivative of some functional W_A, as we will see in lemma 6.43. Bonet et al. [61] show that W_A satisfies the Legendre-Hadamard condition (4.6). Since W_A does not depend on $\det(\mathbf{F})$ and is linear in $\mathbf{F}$, we see that $W_\mathbf{P}+W_\mathrm{A}$ is coercive and satisfies the growth conditions 4.53 if and only if $W_\mathbf{P}$ is polyconvex and satisfies the growth conditions.

This observation is not true for arbitrary models of T_A. As Pathmanathan et al. [119] have observed, $W_\mathbf{P} + W_\mathrm{A}$ may not be coercive if T_A depends on the microscopic stretch $\gamma_\mathbf{f}$ or the macroscopic equivalent $\iota_{4,\mathbf{f}}(\mathbf{F})$.

As an alternative to the additive decomposition (5.18), the active strain approach considers a multiplicative split of the deformation gradient. First introduced by Kondaurov and Nikitin [95] for muscle tissue, the approach follows the principle of intermediate configurations used in elastoplasticity [145, chapter 9]. Consider the decomposition

$$\mathbf{F} = \mathbf{F}_{\mathrm{E}}\mathbf{F}_{\mathrm{A}}\,, \tag{5.19}$$

where $\mathbf{F}_{\mathrm{E}}$ is the purely elastic part of the deformation and $\mathbf{F}_{\mathrm{A}}$ consists of the macroscopic active deformation generated by $\gamma_{\mathbf{f}}$. This introduces an intermediate configuration $\widehat{\Omega}$ as depicted in Figure 5.5. The deformation $\mathbf{F}_{\mathrm{A}}$ represents the plastic part of $\mathbf{F}$, e.g. irreversible deformations of Ω. Concurrently, $\widehat{\Omega}$ is assumed to be stress-free. Removing external forces from $\boldsymbol{\varphi}(\Omega)$ would lead to the elastic relaxation $\mathbf{F}_{\mathrm{E}}^{-1}$, again resulting in $\widehat{\Omega}$.

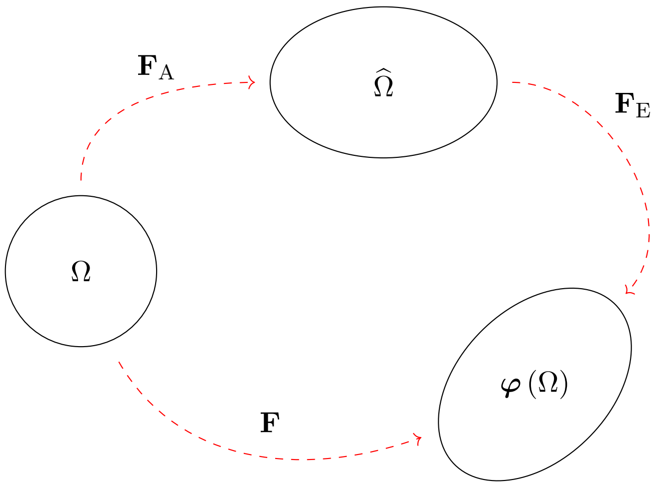

Figure 5.5: Intermediate configuration

For hyperelastic materials, we then choose to only insert the elastic part of the deformation $\mathbf{F}_{\mathrm{E}}$ as argument. With the general form of incompressible stored energy functions $W_{\mathbf{P}}$ detailed in section 4.3, we calculate

$$\overline{W_{\mathbf{P}}(\mathbf{F})} = W_{\mathrm{iso}}(\overline{\mathbf{F}_{\mathrm{E}}}) + W_{\mathrm{vol}}(\det(\mathbf{F}_{\mathrm{E}})) = W_{\mathrm{iso}}(\overline{\mathbf{F}\mathbf{F}_{\mathrm{A}}^{-1}}) + W_{\mathrm{vol}}(\det(\mathbf{F}\mathbf{F}_{\mathrm{A}}^{-1}))\,. \tag{5.20}$$

Remark 5.25: It is customary within the theory of plasticity and the modeling of cardiac elasticity to assume that the plastic flow is isochoric, i.e., $\det(\mathbf{F}_{\mathrm{A}}) = 1$. This reduces (5.20) to

$$\overline{W_{\mathbf{P}}(\mathbf{F})} = W_{\mathrm{iso}}(\overline{\mathbf{F}\mathbf{F}_{\mathrm{A}}^{-1}}) + W_{\mathrm{vol}}(\det(\mathbf{F}))\,.$$

For hyperelastic materials, the active strain approach alters the form of the first Piola-Kirchhoff tensor as well. We will use the nomenclature $\mathbf{P}(\mathbf{F},\mathbf{F}_{\mathrm{A}}) \coloneqq \mathbf{P}(\mathbf{F}\mathbf{F}_{\mathrm{A}}^{-1})$ and similar designations for $\tilde{\mathbf{P}}(\mathbf{C}), \overline{\mathbf{P}}(\mathbf{E})$ and the different variations of $\mathbf{S}$. Following the chain rule, the first Piola-Kirchhoff tensor is then given by

$$\mathbf{P}(\mathbf{F},\mathbf{F}_\mathrm{A}) = \mathbf{P}(\mathbf{F}\mathbf{F}_\mathrm{A}^{-1}) = \mathrm{D}_\mathbf{F} W_\mathbf{P}(\mathbf{F}\mathbf{F}_\mathrm{A}^{-1}) = \mathrm{D}_{\mathbf{F}_\mathrm{E}} W_\mathbf{P}(\mathbf{F}_\mathrm{E})\mathbf{F}_\mathrm{A}^{-1}\,.$$

Active deformation models for $\mathbf{F}_\mathrm{A}$ within cardiac elasticity typically construct a simple transversly isotropic tensor. A popular model is given by Rossi et al. [136]:

Definition 5.26: Let $\mathbf{f},\mathbf{s},\mathbf{t}$ be fibre fields on Ω and $\gamma_\mathbf{f},\gamma_\mathbf{s},\gamma_\mathbf{t}$ be the cellular stretches along these directions. We call

$$\mathbf{F}_\mathrm{A} \coloneqq \mathbf{I} + \gamma_\mathbf{f}\mathbf{f}\otimes\mathbf{f} + \gamma_\mathbf{s}\mathbf{s}\otimes\mathbf{s} + \gamma_\mathbf{t}\mathbf{t}\otimes\mathbf{t}$$

the *active deformation gradient* of the mircostructural contraction.

Since we insert $\mathbf{F}_\mathrm{E} = \mathbf{F}\mathbf{F}_\mathrm{A}^{-1}$ into the stored energy function, we use the analytical form of the inverse of $\mathbf{F}_\mathrm{A}$ as presented in [136].

Lemma 5.27: *Let* $\mathbf{F}_\mathrm{A}$ *be the active deformation gradient. Then*

$$\mathbf{F}_\mathrm{A}^{-1} = \mathbf{I} - \frac{\gamma_\mathbf{f}}{1+\gamma_\mathbf{f}}\mathbf{f}\otimes\mathbf{f} - \frac{\gamma_\mathbf{s}}{1+\gamma_\mathbf{s}}\mathbf{s}\otimes\mathbf{s} - \frac{\gamma_\mathbf{t}}{1+\gamma_\mathbf{t}}\mathbf{t}\otimes\mathbf{t}\,.$$

Proof. For $\boldsymbol{\ell},\mathbf{k}\in\{\mathbf{f},\mathbf{s},\mathbf{t}\}$, it holds

$$(\boldsymbol{\ell}\otimes\mathbf{k})\;(\boldsymbol{\ell}\otimes\mathbf{k}) = \boldsymbol{\ell}\mathbf{k}^\top\boldsymbol{\ell}\mathbf{k}^\top = \begin{cases}\mathbf{0}\,, & \boldsymbol{\ell}\neq\mathbf{k}\,,\\ \boldsymbol{\ell}\otimes\mathbf{k}\,, & \boldsymbol{\ell}=\mathbf{k}\,.\end{cases}$$

Then, a simple calculation shows

$$\begin{aligned}\mathbf{F}_\mathrm{A}\mathbf{F}_\mathrm{A}^{-1} &= \mathbf{F}_\mathrm{A} - \sum_{\boldsymbol{\ell}\in\{\mathbf{f},\mathbf{s},\mathbf{t}\}}\left(\frac{\gamma_\boldsymbol{\ell}}{1+\gamma_\boldsymbol{\ell}} + \frac{\gamma_\boldsymbol{\ell}^2}{1+\gamma_\boldsymbol{\ell}}\right)\boldsymbol{\ell}\otimes\boldsymbol{\ell}\\ &= \mathbf{F}_\mathrm{A} - \sum_{\boldsymbol{\ell}\in\{\mathbf{f},\mathbf{s},\mathbf{t}\}}\left(\frac{(1+\gamma_\boldsymbol{\ell})\gamma_\boldsymbol{\ell}}{1+\gamma_\boldsymbol{\ell}}\right)\boldsymbol{\ell}\otimes\boldsymbol{\ell}\\ &= \mathbf{I}\,.\end{aligned}$$

□

Remark 5.28: As Rossi et al. [135, 136] point out, the values of $\gamma_\mathbf{f},\gamma_\mathbf{s}$ and $\gamma_\mathbf{t}$ are not independent. Experimental observations [130] indicate $\gamma_\mathbf{f}\approx 4\gamma_\mathbf{t}$. We set $\gamma_\mathbf{s} = \frac{1}{(1-\gamma_\mathbf{f})(1-\gamma_\mathbf{t})} - 1$ to ensure $\det(\mathbf{F}_\mathrm{A}) = 1$.

Remark 5.29: As discussed in [129, section 6.2], the stretch along the sheet-normal direction $\mathbf{t}$ is more accurately described by

$$\gamma_\mathbf{t} = k_\mathbf{t}\left(\frac{1}{\sqrt{1+\gamma_\mathbf{f}}} - 1\right)\,,\qquad k_\mathbf{t} > 0\,.$$

Barbarotta et al. [23] proposed a transmurally heterogeneous model, such that $k_\mathbf{t}\colon\Omega\to\mathbb{R}_+$ becomes dependent on the position within the myocardial wall.

Combining the active strain model with the active tension development presented in section 5.3.2 and the boundary conditions discussed in section 5.3.1, we can now state the full system of cardiac elasticity:

Problem 5.30: *Let Ω be a bounded domain and let $\mathbf{c}\colon [0,T]\times\Omega \to \mathbb{R}^{d_c}$ be the function of ion concentrations over time. Find $(\gamma_{\mathbf{f}}, \mathbf{k}, \mathbf{u})$, such that*

$$
\begin{aligned}
\frac{\partial}{\partial t}\gamma_{\mathbf{f}} &= \mathbf{G}_{\gamma_{\mathbf{f}}}(\mathbf{c},\mathbf{k},\gamma_{\mathbf{f}},\frac{\partial}{\partial t}\gamma_{\mathbf{f}},\mathbf{F}) && \textit{in } (0,T)\times\Omega\,, && (5.21a)\\
\frac{\partial}{\partial t}\mathbf{k} &= \mathbf{G}_{\mathbf{k}}(\mathbf{w},\mathbf{c},\mathbf{k},\gamma_{\mathbf{f}},\frac{\partial}{\partial t}\gamma_{\mathbf{f}}) && \textit{in } (0,T)\times\Omega\,, && (5.21b)\\
\mathbf{k} = \mathbf{k}_0\,,&\quad \gamma_{\mathbf{f}} = 0 && \textit{on } \{0\}\times\Omega\,, && (5.21c)\\
\rho\frac{\partial^2}{\partial t^2}\mathbf{u} - \operatorname{div}\left(\mathbf{P}(\mathbf{F}\mathbf{F}_{\mathrm{A}}^{-1})\right) &= \mathbf{0} && \textit{in } \{0\}\times\Omega\,, && (5.21d)\\
\mathbf{u} &= \mathbf{0} && \textit{on } \{0\}\times\Gamma_{\mathrm{D}}\,, && (5.21e)\\
\mathbf{P}(\mathbf{F}\mathbf{F}_{\mathrm{A}}^{-1})\mathbf{n} &= -p(t)\,\mathrm{Cof}\,(\mathbf{F})\,\mathbf{n} && \textit{on } \{0\}\times\Gamma_{\mathrm{N}}\,, && (5.21f)\\
\mathbf{P}(\mathbf{F}\mathbf{F}_{\mathrm{A}}^{-1})\mathbf{n} &= \mathbf{q}(\mathbf{u},\frac{\partial}{\partial t}\mathbf{u},\mathbf{n}) && \textit{on } \{0\}\times\Gamma_{\mathrm{P}}\,, && (5.21g)\\
\mathbf{u} = \mathbf{u}_0\,,\quad \mathbf{v} = \mathbf{0}\,,&\quad \mathbf{a} = \mathbf{0}\,,\quad \gamma_{\mathbf{f}} = 0 && \textit{on } \{0\}\times\Omega\,. && (5.21h)
\end{aligned}
$$

where $\mathbf{F}_{\mathrm{A}} = \mathbf{I} + \gamma_{\mathbf{f}}\mathbf{f}\otimes\mathbf{f} + \gamma_{\mathbf{s}}\mathbf{s}\otimes\mathbf{s} + \gamma_{\mathbf{t}}\mathbf{t}\otimes\mathbf{t}$.

5.3.4 Prestress

A common problem in cardiac modeling including intra-cavital pressure is that the reference domain Ω does not correspond to a stress-free configuration. This is because the endocardial pressure approximately ranges from 5 mmHg to 120 mmHg during a full cardiac cycle in healthy individuals [108], and thus never equals zero. Inserting a pressure $p(0) > 0$ in equations (5.12) or (5.21) yields an initial displacement $\mathbf{u}(0) \neq \mathbf{0}$. To be able to match patient-specific geometries acquired by medical imaging with the corresponding cardiac pressure, two methods have been proposed in literature.

During the process of *pressure preloading* [32], the static variant of the cardiac elasticity problem (5.12) is solved at time step 0, i.e. $\mathbf{v} = \mathbf{0}$ and $\mathbf{a} = \mathbf{0}$. The solution $\mathbf{u}(0)$ is then used as initial value for the simulation of the cardiac cycle. The difficulty with this approach is that the stress-free reference domain Ω does not correspond with the initial geometry given and may be unphysiological [96, section 4.2.1].

An alternative solution is *pressure prestressing* [87], where an initial internal stress $\mathbf{P}_0$ is computed such that $\widetilde{\mathbf{P}}(\mathbf{F}) = \mathbf{P}(\mathbf{F}) + \mathbf{P}_0 = \mathbf{0}$ for $\mathbf{u} = \mathbf{0}$. This approach is presented in more detail in [64, 157]. We define the static mechanical problem

Problem 5.31 (Prestressed cardiac elasticity): *Find* $\mathbf{u}_0 \colon \Omega \to \mathbf{\Phi}(\Omega)$ *with* $\mathbf{F}_0 = \mathrm{D}\mathbf{u}_0$, *such that*

$$\begin{aligned} -\operatorname{div}\left(\mathbf{P}(\mathbf{F}_0, \mathbf{I})\right) &= 0 && \text{in } \Omega\,, && (5.22a)\\ \mathbf{P}(\mathbf{F}_0)\mathbf{n} &= -p(0)\operatorname{Cof}\left(\mathbf{F}_0\right)\mathbf{n} && \text{on } \Gamma_N\,, && (5.22b)\\ \mathbf{P}(\mathbf{F}_0)\mathbf{n} &= \mathbf{q}(\mathbf{u}_0, \frac{\partial}{\partial t}\mathbf{u}_0, \mathbf{n}) && \text{on } \Gamma_P\,. && (5.22c) \end{aligned}$$

The solution of problem 5.31 may be obtained by similar methods to the ones solving the dynamic system, which are presented in section 6.4. This leaves us with the following modified system of cardiac elasticity (5.21):

Lemma 5.32: *Let* $\mathbf{u}_0 \colon \Omega \to \mathbf{\Phi}(\Omega)$ *be the solution of problem 5.31 and set* $\mathbf{P}_0 \coloneqq \mathbf{P}(\mathbf{F}_0, \mathbf{I})$. *Then* $\mathbf{u} = \mathbf{0}$ *solves the prestressed equations of elasticity*

$$\begin{aligned} \rho\frac{\partial^2}{\partial t^2}\mathbf{u} - \operatorname{div}\left(\mathbf{P}(\mathbf{F}, \mathbf{F}_\mathrm{A})\right) &= \operatorname{div}\left(\mathbf{P}_0\right) && \text{in } (0,T)\times\Omega\,, && (5.23a)\\ \mathbf{u} &= \mathbf{0} && \text{on } (0,T)\times\Gamma_D\,, && (5.23b)\\ \mathbf{P}(\mathbf{F}, \mathbf{F}_\mathrm{A})\mathbf{n} &= -p(t)\operatorname{Cof}\left(\mathbf{F}\right)\mathbf{n} && \text{on } (0,T)\times\Gamma_N\,, && (5.23c)\\ \mathbf{P}(\mathbf{F}, \mathbf{F}_\mathrm{A})\mathbf{n} &= \mathbf{q}(\mathbf{u}, \frac{\partial}{\partial t}\mathbf{u}, \mathbf{n}) && \text{on } (0,T)\times\Gamma_P\,, && (5.23d)\\ \mathbf{u} = \mathbf{0}\,, \quad \mathbf{v} = \mathbf{0}\,, \quad \mathbf{a} &= \mathbf{0}\,, \quad \gamma_\mathbf{f} = 0 && \text{on } \{0\}\times\Omega\,, && (5.23e) \end{aligned}$$

where $\widetilde{\mathbf{P}}(\mathbf{F}, \mathbf{F}_\mathrm{A}) = \mathbf{P}(\mathbf{F}, \mathbf{F}_\mathrm{A}) + \mathbf{P}_0$.

5.4 The circulatory system

The contraction of a heart chamber increases the pressure inside it, forcing blood to flow out of that chamber and into the next chamber or the circulatory system, respectively. Conversely, blood flows into the heart chamber during its relaxation phase.

As we have seen in section 5.3.1, the pressure on the endocardial wall is a boundary condition for the equations of motion. In physiological models, this pressure cannot be estimated in isolation, but requires the modeling of the circulatory system as well. The most accurate model would be a fluid-structure-interaction (FSI) problem, where a set of Navier-Stokes equations is solved on the inside of the heart chambers, calculating blood displacement and pressure simultaneously. Such FSI models are usually not feasible to implement for a full heart mesh due to their computational complexity [141, 155]. This problem is aggravated by the rapid movement of the heart valves at certain pressure thresholds [46].

Within this work, we are not concerned with the detailed distribution of blood flow and pressure within the cardiac chambers. Alternative ODE-based surrogate models have been

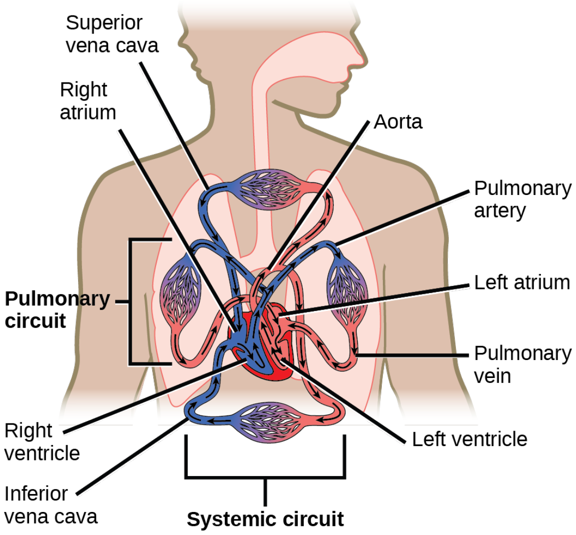

Figure 5.6: Schematic view of the circulatory system [39, Figure 40.10, CC BY 4.0].

proposed in multiple variations and for many types of cardiac simulations [14, 58, 63, 82]. Such models typically describe the circulatory system as a closed electrical circuit. We will describe two such models, one for a single ventricle [64] and one for a full heart [63]. In both cases, pressure and volume of each cavity are intrinsically connected.

5.4.1 Circulatory system for a single ventricle

The typical pressure and volume development within a heart ventricle was schematically shown in the Wiggers diagram (see Figure 5.3). Simple mathematical models of the four phases described in section 5.1 are discussed in [50, 163]. We will reiterate the summary of Dede et al. [64, section 4.1] of the models assigned to their respective phase.

The cavity pressure is not a function known beforehand, but is determined depending on the pressure in and current volume of the ventricle. We will go into more detail on the time discretization in chapter 6. For now, assume p is known at a time t_n, $n \in \mathbb{N}$ and the corresponding volume of the cavity is V_n. The goal is to find the pressure at a suitable time $t_{n+1} > t_n$.

1. *Contraction*: During this phase, the ventricular volume stays mostly constant while the pressure increases rapidly. The pressure $p(t_{n+1})$ is iteratively calculated by

$$p(t_{n+1}) = p(t_n) + \frac{V_{n+1} - V_n}{C_p}, \qquad C_p \ll 0\,. \tag{5.24}$$

until $\frac{|V_{n+1}-V_n|}{|V_n|} < \varepsilon$, where C_p is a constant parameter, called *compliance*, for the volume change. The phase ends if p reaches a peak value of 95mmHg.

2. *Ejection:* The rate of change of p is determined by solving the ODE corresponding to the Windkessel model [168, 169]

$$\frac{\partial}{\partial t}p(t) = \frac{1}{C}\left(-\frac{p(t)}{R} - \frac{\partial}{\partial t}V\right) \qquad \text{in } (t_n, t_{n+1})\,, \tag{5.25a}$$

$$p(t_n) = p_n\,, \tag{5.25b}$$

   where $C, R > 0$ represent the capacitance and compliance resistance in the correspondig electric circuit, see Figure 5.7 .

3. *Isovolumic relaxation*: Similar to the contraction phase, the ventricular volume does not change while the pressure drops within a short timeframe. The pressure update is again modeled with (5.24). The phase ends if p reaches a minimum value of 5mmHg.

4. *Ventricular filling*: Linearly increase the pressure so that the initial value $p(0)$ is again reached at the end of the cardiac cycle.

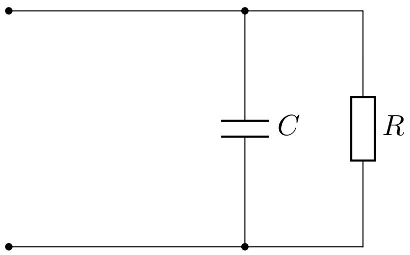

Figure 5.7: Two-element Windkessel model (see [169])

Remark 5.33: As Dede et al. [64] point out, the modeling of ventricular filling does not fully coincide with physiological behaviour. To correctly model this phase, a simulation of the atrium would be necessary. Aligning with the arguments of the authors, we drop the physiological correctness for the upside of having a pressure model applicable to single ventricle models.

5.4.2 Circulatory system for a full heart

In contrast to the single ventricle, we have to model the interaction of pressures and volumes between the four cardiac chambers when simulating a full heart. These interactions consist of the behaviour of the valves and the response of the circulatory system connecting the left and right ventricle to the right and left atrium, respectively. In the following, we present the closed-loop circulatory system as introduced by Gerach et al. [63].

Similar to the Windkessel model (5.25), the whole circulatory system is reinterpreted as a series of transmissions as shown in Figure 5.8. The system consists of algebraic and ordinary differential equations solving for internal volumes, pressures and flows.

Definition 5.34: Let $\mathbf{p}\colon [0,T] \to \mathbb{R}^4$ be the development of the pressure inside the four cardiac chambers given by

$$\mathbf{p} = \begin{pmatrix} p_{\mathrm{LV}} & p_{\mathrm{RV}} & p_{\mathrm{LA}} & p_{\mathrm{RA}} \end{pmatrix}^\top .$$

The equations for a *closed-loop circulatory model* are denoted in the variables of circulatory volumes

$$\mathbf{V}\colon [0,T] \to \mathbb{R}^8 , \qquad t \mapsto (V_{\mathrm{LV}}, V_{\mathrm{RV}}, V_{\mathrm{LA}}, V_{\mathrm{RA}}, V_{\mathrm{SysVen}}, V_{\mathrm{SysArt}}, V_{\mathrm{PulVen}}, V_{\mathrm{PulArt}})^\top$$

and circulatory flows

$$\mathbf{z}\colon [0,T] \to \mathbb{R}^8 , \qquad t \mapsto (Q_{\mathrm{SysArt}}, Q_{\mathrm{SysPer}}, Q_{\mathrm{SysVen}}, Q_{\mathrm{Rav}}, Q_{\mathrm{PulArt}}, Q_{\mathrm{PulPer}}, Q_{\mathrm{PulVen}}, Q_{\mathrm{Lav}})^\top$$

and are given by the equations

$$\partial_t \mathbf{V} = \mathbf{G}_{\mathbf{V}}(\mathbf{p}, \mathbf{V}, \mathbf{z}) \qquad \text{in } (0,T) , \tag{5.26a}$$

$$\mathbf{0} = \mathbf{G}_{\mathbf{z}}(\mathbf{p}, \mathbf{V}, \mathbf{z}) \qquad \text{in } (0,T) . \tag{5.26b}$$

The evolution of $\mathbf{v}$ in (5.26a) is determined by

$$\begin{aligned}
\partial_t V_{\mathrm{LV}} &= Q_{\mathrm{Lav}} - Q_{\mathrm{SysArt}} , & \partial_t V_{\mathrm{SysVen}} &= Q_{\mathrm{SysPer}} - Q_{\mathrm{SysVen}} , \\
\partial_t V_{\mathrm{RV}} &= Q_{\mathrm{Rav}} - Q_{\mathrm{PulArt}} , & \partial_t V_{\mathrm{SysArt}} &= Q_{\mathrm{SysArt}} - Q_{\mathrm{SysPer}} , \\
\partial_t V_{\mathrm{LA}} &= Q_{\mathrm{PulVen}} - Q_{\mathrm{Lav}} , & \partial_t V_{\mathrm{PulVen}} &= Q_{\mathrm{PulPer}} - Q_{\mathrm{PulVen}} , \\
\partial_t V_{\mathrm{RA}} &= Q_{\mathrm{SysVen}} - Q_{\mathrm{Rav}} , & \partial_t V_{\mathrm{PulArt}} &= Q_{\mathrm{PulArt}} - Q_{\mathrm{PulPer}} ,
\end{aligned}$$

while the entries of $\mathbf{G}_{\mathbf{z}}(\mathbf{p}, \mathbf{V}, \mathbf{z})$ in (5.26b) are given by

$$\begin{aligned}
&Q_{\mathrm{SysArt}} - \max\left\{ \frac{p_{\mathrm{LV}} - \frac{V_{\mathrm{SysArt}}}{C_{\mathrm{SysArt}}}}{R_{\mathrm{SysArtValve}} + R_{\mathrm{SysArt}}}, 0 \right\} , && Q_{\mathrm{PulArt}} - \max\left\{ \frac{p_{\mathrm{RV}} - \frac{V_{\mathrm{PulArt}}}{C_{\mathrm{PulArt}}}}{R_{\mathrm{PulArtValve}} + R_{\mathrm{PulArt}}}, 0 \right\} , \\
&Q_{\mathrm{SysPer}} - \frac{\frac{V_{\mathrm{SysArt}}}{C_{\mathrm{SysArt}}} - \frac{V_{\mathrm{SysVen}}}{C_{\mathrm{SysVen}}}}{R_{\mathrm{SysPer}}} , && Q_{\mathrm{PulPer}} - \frac{\frac{V_{\mathrm{PulArt}}}{C_{\mathrm{PulArt}}} - \frac{V_{\mathrm{PulVen}}}{C_{\mathrm{PulVen}}}}{R_{\mathrm{PulPer}}} , \\
&Q_{\mathrm{SysVen}} - \frac{\frac{V_{\mathrm{SysVen}}}{C_{\mathrm{SysVen}}} - p_{\mathrm{RA}}}{R_{\mathrm{SysVen}}} , && Q_{\mathrm{PulVen}} - \frac{\frac{V_{\mathrm{PulVen}}}{C_{\mathrm{PulVen}}} - p_{\mathrm{LA}}}{R_{\mathrm{PulVen}}} , \\
&Q_{\mathrm{Rav}} - \max\left\{ \frac{p_{\mathrm{RA}} - p_{\mathrm{RV}}}{R_{\mathrm{RavValve}}}, 0 \right\} , && Q_{\mathrm{Lav}} - \max\left\{ \frac{p_{\mathrm{LA}} - p_{\mathrm{LV}}}{R_{\mathrm{LavValve}}}, 0 \right\} .
\end{aligned}$$

Remark 5.35: The variables $V_{\mathrm{LV}}, V_{\mathrm{RV}}, V_{\mathrm{LA}}, V_{\mathrm{RA}}, V_{\mathrm{SysVen}}, V_{\mathrm{SysArt}}, V_{\mathrm{PulVen}}, V_{\mathrm{PulArt}}$ correspond to the volumes of the four heart chambers and artificial volumes in the systemic and pulmonary arteries and veins, respectively. The entries of $\mathbf{z}$ represent flow rates between these components. A derivation of the analogy between the electrical circuit model (see Figure 5.8) and the circulatory system is given in [164], where a numerical analysis of the differential-algebraic systems is performed.

The system of equations (5.26) consists of ordinary differential equations and algebraic equations. Such systems are appropriately called systems of differential-algebraic equations (DAEs). We do not go into detail about the mathematical theory of DAEs in this work, again referring to [79].

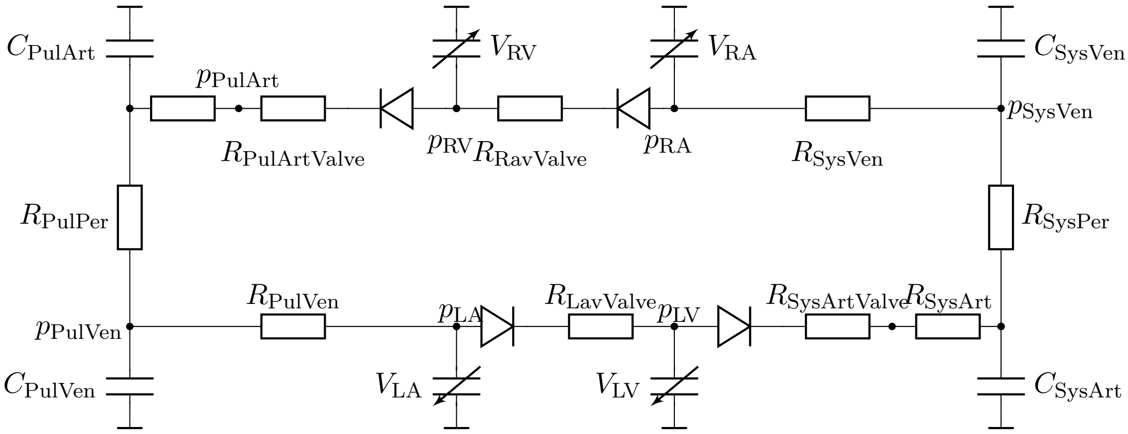

Figure 5.8: Schematic of the 4-chamber circulatory system model with the pressure values of $\mathbf{p}$ and $\mathbf{z}$, resistances R, fixed compliances C and variable compliances V_C with $C \in \{\mathrm{LV}, \mathrm{RV}, \mathrm{LA}, \mathrm{RA}\}$. [63, see Figure 2, CC BY 4.0]

Remark 5.36: From the entries of $\mathbf{G_z}$ in (5.26b), we see that $\mathbf{G_V}$ in (5.26a) is continuous, but not $\mathcal{C}^1$. Typical error estimates for numerical methods of higher order cannot be applied, since they require the right-hand side to be differentiable up to a certain degree as well [78].

5.5 Electro-mechanical coupling mechanisms

In modeling sections 5.2 and 5.3, we have seen that the deformation of the human heart follows the equations of elasticity, where in addition to external boundary conditions, an internal active contraction is introduced as a consequence of the electrical excitation of the cardiac tissue. We conclude this chapter by combining the monodomain equations (5.11) with cardiac elasticity (5.23).

Definition 5.37: Let $\Omega \subset \mathbb{R}^3$ be the domain of a full heart. We call $\Omega_{\mathrm{EP}} \subset \Omega$ the *excitable tissue* of Ω.

It is sufficient to define the transmembrane voltage v as well as the vector-valued functions containing the cellmodel variables only on Ω_{EP}. Since $\Omega \backslash \Omega_{\mathrm{EP}}$ is not excitable, no electrical activation and no entailing active contraction of myofibrills take place.

Remark 5.38: Instead of restricting v to only be defined on Ω_{EP}, we could alternatively define

$$\overline{v}\colon \Omega \to \mathbb{R}\,, \qquad \overline{v}(t,\mathbf{x}) := \begin{cases} v(t,\mathbf{x})\,, & \mathbf{x} \in \Omega_{\mathrm{EP}}\,, \\ 0\,, & \mathbf{x} \in \Omega \backslash \Omega_{\mathrm{EP}}\,. \end{cases}$$

We avoid this approach due to the increased size of the discretized system presented in the following chapter.

Recalling definition 5.4, the conductivity tensor $\mathbf{D}$ depends on the fibre fields $\mathbf{f}, \mathbf{s}, \mathbf{t}$. During the deformation of Ω, the orientation of these fibre fields change. More precisely, the monodomain equation has to be solved in the spatial configuration $\boldsymbol{\varphi}(\Omega)$, i.e.,

$$C_{\mathrm{m}} \frac{\mathrm{d}v^{\varphi}}{\mathrm{d}t} - \mathrm{div}^{\varphi}\left(\mathbf{D}^{\varphi} \nabla^{\varphi} v^{\varphi}\right) = -I_{\mathrm{ion}} + I_{\mathrm{ext}} \qquad \text{in } (0,T) \times \boldsymbol{\varphi}(\Omega_{\mathrm{EP}})\,, \tag{5.27}$$

where $\mathbf{D}^{\varphi}$ is the conductivity tensor along the fibre fields $\mathbf{f}^{\varphi}, \mathbf{s}^{\varphi}, \mathbf{t}^{\varphi}$.
In the equation above, only $\mathbf{D}^{\varphi}$ is actually depending on $\boldsymbol{\varphi}$.

Lemma 5.39: *The material formulation of the monodomain equation* (5.27) *is equivalent to*

$$C_{\mathrm{m}} \frac{\partial}{\partial t}(vJ) - \mathrm{div}\left(J \mathbf{F}^{-1} \mathbf{D} \mathbf{F}^{-\top} \nabla v\right) = J(-I_{\mathrm{ion}} + I_{\mathrm{ext}}) \qquad \textit{in } (0,T) \times \Omega_{\mathrm{EP}}\,. \tag{5.28}$$

Proof. This equivalence is derived in [4, section 2]. We use the tools from chapter 3 to highlight the necessary steps. Without loss of generality, set $C_{\mathrm{m}} = 1$. Let $\mathbf{c}^{\varphi} := \mathbf{D}^{\varphi} \nabla^{\varphi} v^{\varphi}$ and $b^{\varphi} := -I_{\mathrm{ion}} + I_{\mathrm{ext}}$. Then $v^{\varphi}, b^{\varphi}, \mathbf{c}^{\varphi}$ satisfy the spatial master balance law 3.26. By theorem 3.29 the mappings $v(t,\mathbf{x}) = v^{\varphi}(t,\mathbf{x}^{\varphi})$, $b(t,\mathbf{x}) = \mathbf{b}^{\varphi}(t,\mathbf{x}^{\varphi})$ and $\mathbf{c}(t,\mathbf{x}) = J\mathbf{c}^{\varphi}(t,\mathbf{x}^{\varphi})\mathbf{F}^{-\top}$ satisfy

$$\frac{\partial}{\partial t}(vJ) - \mathrm{div}(\mathbf{c}) = bJ\,.$$

It remains to derive the formula for $\mathrm{div}(\mathbf{c})$. Let

$$\mathbf{a}^{\varphi} := \nabla^{\varphi} v^{\varphi} = \mathrm{div}^{\varphi}(v^{\varphi}\mathbf{i})\,,$$

where $\mathbf{i} \in \mathbb{R}^3$ is the vector whose entries are all one. Here we used the basic properties of the divergence. Multiplying by J and using lemma 3.21 on the right-hand side yields

$$J\mathbf{a}^{\varphi} = \mathrm{div}(Jv\mathbf{F}^{-\top})\,,$$

where we again used $v^\varphi(t,\mathbf{x}^\varphi) = v(t,\mathbf{x})$. Substituting this in $\mathbf{c} = J\mathbf{D}^\varphi \mathbf{a}^\varphi \mathbf{F}^{-\top}$ results in

$$\frac{\partial}{\partial t}(vJ) - \operatorname{div}(\mathbf{D}^\varphi \operatorname{div}(Jv\mathbf{F}^{-\top})\mathbf{F}^{-\top}) = bJ\,.$$

Finally, we use

$$\operatorname{div}(\mathbf{D}^\varphi \operatorname{div}(Jv\mathbf{F}^{-\top})\mathbf{F}^{-\top}) = \operatorname{div}(\mathbf{F}^{-1}\mathbf{D}^\varphi \operatorname{div}(Jv\mathbf{F}^{-\top}))$$

and the Piola-identity 3.20 to get

$$\operatorname{div}(Jv\mathbf{F}^{-\top}) = \operatorname{div}(J\mathbf{F}^{-\top}\, v) = J\mathbf{F}^{-\top}\,\nabla v\,.$$

Combining these results leaves the desired result, namely

$$C_\mathrm{m}\frac{\partial}{\partial t}(vJ) - \operatorname{div}\left(J\mathbf{F}^{-1}\mathbf{D}\mathbf{F}^{-\top}\nabla v\right) = Jb\,.$$

□

This concludes the necessary adaptions to couple electrophysiology with the equations of elasticity. This chapter can therefore be summarized by stating the full set of equations of cardiac elastodynamics:

Problem 5.40: *Let Ω be a bounded domain and $\Omega_\mathrm{E} \subset \Omega$ be the subset of excitable tissue. Find $(v, \mathbf{w}, \mathbf{c}, \gamma_\mathbf{f}, \mathbf{u}, \mathbf{V}, \mathbf{z})$ defined as in their respective previous sections, such that*

$$C_\mathrm{m}\frac{\partial}{\partial t}(vJ) - \operatorname{div}\left(J\mathbf{F}^{-1}\mathbf{D}\mathbf{F}^{-\top}\nabla v\right) = J(-I_\mathrm{ion}(v,\mathbf{w},\mathbf{c}) + I_\mathrm{ext}) \quad \textit{in } (0,T)\times\Omega_\mathrm{E}\,, \tag{5.29a}$$

$$\frac{\partial}{\partial t}\mathbf{w} = \mathbf{G}_\mathbf{w}(v,\mathbf{w}) \quad \textit{in } (0,T)\times\Omega_\mathrm{E}\,, \tag{5.29b}$$

$$\frac{\partial}{\partial t}\mathbf{c} = \mathbf{G}_\mathbf{c}(v,\mathbf{w},\mathbf{c}) \quad \textit{in } (0,T)\times\Omega_\mathrm{E}\,, \tag{5.29c}$$

$$\frac{\partial}{\partial t}\gamma_\mathbf{f} = \mathbf{G}_{\gamma_\mathbf{f}}(\gamma_\mathbf{f},\mathbf{F}) \quad \textit{in } (0,T)\times\Omega_\mathrm{E}\,, \tag{5.29d}$$

$$(\mathbf{D}\nabla v)\cdot\mathbf{n} = 0 \quad \textit{on } (0,T)\times\Gamma\,, \tag{5.29e}$$

$$v = v_0\,,\quad \mathbf{w} = \mathbf{w}_0\,,\quad \mathbf{c} = \mathbf{c}_0\,,\quad \gamma_\mathbf{f} = 0 \quad \textit{on } \{0\}\times\Omega\,, \tag{5.29f}$$

$$\rho\frac{\partial^2}{\partial t^2}\mathbf{u} - \operatorname{div}(\mathbf{P}(\mathbf{F},\mathbf{F}_\mathrm{A})) = \operatorname{div}(\mathbf{P}_0) \quad \textit{in } \{0\}\times\Omega\,, \tag{5.29g}$$

$$\mathbf{u} = \mathbf{0} \quad \textit{on } \{0\}\times\Gamma_\mathrm{D}\,, \tag{5.29h}$$

$$\mathbf{P}(\mathbf{F})\mathbf{n} = -p(t)\operatorname{Cof}(\mathbf{F})\,\mathbf{n} \quad \textit{on } \{0\}\times\Gamma_\mathrm{N}\,, \tag{5.29i}$$

$$\mathbf{P}(\mathbf{F})\mathbf{n} = \mathbf{q}(\mathbf{u}, \frac{\partial}{\partial t}\mathbf{u},\mathbf{n}) \quad \textit{on } \{0\}\times\Gamma_\mathrm{P}\,, \tag{5.29j}$$

$$\partial_t\mathbf{V} = \mathbf{G}_\mathbf{V}(\mathbf{p},\mathbf{V},\mathbf{z}) \quad \textit{in } (0,T)\,, \tag{5.29k}$$

$$\mathbf{0} = \mathbf{G}_\mathbf{z}(\mathbf{p},\mathbf{V},\mathbf{z}) \quad \textit{in } (0,T)\,, \tag{5.29l}$$

$$\mathbf{u} = \mathbf{0}\,,\quad \mathbf{v} = \mathbf{0}\,,\quad \mathbf{a} = \mathbf{0} \quad \textit{on } \{0\}\times\Omega\,. \tag{5.29m}$$

The functions $\mathbf{G}_\mathbf{w}, \mathbf{G}_\mathbf{c}, \mathbf{G}_{\gamma_\mathbf{f}}$ are derived from appropiate cellular development models.

Remark 5.41: Note that $\gamma_{\mathbf{f}}$ is only defined on Ω_{EP}, as was justified in remark 5.38, although $\mathbf{F}_\text{A} = \mathbf{F}_\text{A}(\gamma_{\mathbf{f}})$ has to be defined on Ω. Recalling that $\gamma_{\mathbf{f}} = 0$ on $\Omega \backslash \Omega_{\text{EP}}$, we abuse notation and set the active deformation gradient to be

$$\mathbf{F}_\text{A} = \mathbf{F}_\text{A}(\mathbf{x}, \gamma_{\mathbf{f}}) = \begin{cases} \mathbf{I} + \gamma_{\mathbf{f}} \mathbf{f} \otimes \mathbf{f} + \gamma_{\mathbf{s}} \mathbf{s} \otimes \mathbf{s} + \gamma_{\mathbf{t}} \mathbf{t} \otimes \mathbf{t}\,, & \mathbf{x} \in \Omega_{\text{EP}}\,, \\ \mathbf{I}\,, & \mathbf{x} \in \Omega \backslash \Omega_{\text{EP}}\,, \end{cases}$$

where $\gamma_{\mathbf{s}}$ and $\gamma_{\mathbf{t}}$ are calculated as presented in section 5.3.3.

CHAPTER

SIX

FINITE ELEMENT METHODS FOR COUPLED ELASTICITY PROBLEMS

With the mathematical model of the human heart at hand, numerical approximation methods for the coupled equations are presented in this chapter. Since the existence of continuously differentiable solutions of the coupled problem can not be guaranteed, we turn to solutions in a weaker sense. Foundations of Sobolev spaces and variational methods are presented and applied onto the equations of cardiac elastodynamics. The outlined methods can be studied in more detail in [12, 35, 36, 53, 98, 175]. Subsequentially, discretization schemes in space and time are described for the coupled system, where concerns about the interaction between the separate equations are addressed.

6.1 Variational formulations of evolution problems

Classical solutions of the partial differential equations in (5.29) are smooth functions

$$v \in \mathcal{C}^2((0,T)\times\Omega)\cap\mathcal{C}(\overline{[0,T]\times\Omega})\,, \qquad \mathbf{u} \in \mathcal{C}^2((0,T)\times\Omega)\cap\mathcal{C}(\overline{[0,T]\times\Omega})\,.$$

This requires the right-hand sides to be at least in $\mathcal{C}((0,T)\times\Omega)$ and the initial conditions be of the appropriate continuity as well. Still, such conditions do not guarantee the existence of a classical solution [91].

To remove the high smoothness requirements, we shortly introduce the concept of weak solutions of said partial differential equations. We begin by defining the relevant spaces in which such solutions exist and provide the basic concepts of variational formulations. We use these concepts to derive the corresponding formulations for the coupled model (5.29).

6.1.1 Sobolev Spaces

We start by giving a brief overview of Sobolev spaces for functions mapping into vector spaces of higher dimensions. A summary of the relevant concepts is given in [97, Appendix B], whereas we refer to [91, chapter 11] for a more detailed definition of the given spaces. We always assume $\Omega \subset \mathbb{R}^d$ to be open, connected with finite Lebesgue-measure.

Definition 6.1: Let $1 \leq p < \infty$. We call

$$\mathcal{L}^p(\Omega;\mathbb{R}^d) := \left\{ \boldsymbol{\phi} \in \mathcal{M}ap(\Omega;\mathbb{R}^d) \colon \boldsymbol{\phi} \text{ is measurable and } \|\boldsymbol{\phi}\|_p := \left(\int_\Omega |\boldsymbol{\phi}|^p \, \mathrm{d}V \right)^{\frac{1}{p}} < \infty \right\}$$

the *Lebesgue space* of functions which are Lebesgue-integrable to the power p.

By $\mathcal{L}^p$ we always refer to the Lebesgue space defined above equipped with the norm $\|\cdot\|_p$, where $|\cdot|$ depicts the Euclidean norm on $\mathbb{R}^d$.

Remark 6.2: For $p = 2$, $\mathcal{L}^2$ is a Hilbert space with inner product

$$\langle \boldsymbol{\phi}, \boldsymbol{\psi} \rangle_2 := \int_\Omega \boldsymbol{\phi} \cdot \boldsymbol{\psi} \, \mathrm{d}V \,, \qquad \boldsymbol{\phi}, \boldsymbol{\psi} \in \mathcal{L}^2 \,.$$

Definition 6.3: Let $\boldsymbol{\phi} \in \mathcal{M}ap(\Omega;\mathbb{R}^d)$. We call

$$\operatorname{supp}(\boldsymbol{\phi}) := \overline{\{\mathbf{x} \in \Omega \colon \boldsymbol{\phi}(\mathbf{x}) \neq \mathbf{0}\}}$$

the *support* of $\boldsymbol{\phi}$. We say that $\boldsymbol{\phi}$ has *compact support*, if $\operatorname{supp}(\boldsymbol{\phi}) \subset \Omega$.

We will denote by $\mathcal{C}_0^\infty(\Omega;\mathbb{R}^d)$ all functions $\boldsymbol{\phi} \in \mathcal{C}^\infty(\Omega;\mathbb{R}^d)$ with compact support.

Definition 6.4: Let $\boldsymbol{\phi} \in \mathcal{L}^p(\Omega;\mathbb{R}^d)$ and $\boldsymbol{\alpha} = (\alpha_1, \ldots, \alpha_d)$ be a multi index, i.e. $\alpha_i \in \mathbb{N}_0$ for $i = 1, \ldots, d$ and $\alpha := |\boldsymbol{\alpha}| = \alpha_1 + \cdots + \alpha_d$. We call $\mathrm{D}^{\boldsymbol{\alpha}} := \frac{\partial^\alpha \boldsymbol{\phi}}{\partial^{\alpha_1} x_1 \cdots \partial^{\alpha_d} x_d}$ the *distributional derivative* of $\boldsymbol{\phi}$, if

$$\int_\Omega \mathrm{D}^{\boldsymbol{\alpha}} \boldsymbol{\phi} \cdot \boldsymbol{\psi} \, \mathrm{d}V = (-1)^\alpha \int_\Omega \boldsymbol{\phi} \cdot \mathrm{D}^{\boldsymbol{\alpha}} \boldsymbol{\psi} \, \mathrm{d}V \qquad \forall\, \boldsymbol{\psi} \in \mathcal{C}_0^\infty(\Omega;\mathbb{R}^d) \,.$$

With distributional derivatives, we call the vector of first order derivatives

$$\mathrm{D}\boldsymbol{\phi} = \left(\frac{\partial}{\partial x_1} \boldsymbol{\phi}, \ldots, \frac{\partial}{\partial x_d} \boldsymbol{\phi} \right)$$

the *(weak) gradient* of $\boldsymbol{\phi}$. Similarly, for $k \in \mathbb{N}$, we use $\mathrm{D}^k \boldsymbol{\phi}$ to refer to the set of distributional derivatives of $\boldsymbol{\phi}$ for all multi indices $\boldsymbol{\alpha}$ with $|\boldsymbol{\alpha}| \leq k$.

Definition 6.5: Let $1 \leq p \leq \infty$. We call

$$\mathcal{W}^{k,p}(\Omega;\mathbb{R}^d) := \left\{ \boldsymbol{\phi} \in \mathcal{M}ap(\Omega;\mathbb{R}^d) \colon \boldsymbol{\phi} \in \mathcal{L}^p(\Omega;\mathbb{R}^d),\ \mathrm{D}^k \boldsymbol{\phi} \in \mathcal{L}^p(\Omega;\mathbb{R}^{d^k}) \right\}$$

the *Sobolev space* of functions which are in $\mathcal{L}^p$ and all distributional derivates up to the order k are in $\mathcal{L}^p$ as well.

Remark 6.6: Within the definition of $\mathcal{W}^{k,p}$, we implicitly assume the distributional derivatives $\mathrm{D}^k\boldsymbol{\phi}$ of $\boldsymbol{\phi} \in \mathcal{W}^{k,p}$ exist.

Again, $\mathcal{W}^{k,p}$ is equipped with a norm, namely

$$\|\boldsymbol{\phi}\|_{k,p} := \|\boldsymbol{\phi}\|_p + \sum_{j=1}^{k} \left\|\mathrm{D}^j\boldsymbol{\phi}\right\|_p .$$

Note that since $\mathrm{D}^k\boldsymbol{\phi} \in \mathcal{L}^p(\Omega;\mathbb{R}^{d^k})$, the norm of all distributional derivatives is taken into account.

Remark 6.7: For $p = 2$, the Sobolev spaces $\mathcal{W}^{k,2}(\Omega;\mathbb{R}^d)$ are Hilbert spaces with inner product

$$\langle\boldsymbol{\phi},\boldsymbol{\psi}\rangle_{k,2} = \sum_{j=0}^{k}\langle\mathrm{D}^k\boldsymbol{\phi},\mathrm{D}^k\boldsymbol{\psi}\rangle_2\,, \qquad \boldsymbol{\phi},\boldsymbol{\psi} \in \mathcal{W}^{k,2}(\Omega;\mathbb{R}^d)\,.$$

where $\langle\cdot,\cdot\rangle_2$ ist the $\mathcal{L}^2$ inner product. We use the customary notation

$$\mathcal{H}^k(\Omega,\mathbb{R}^d) := \mathcal{W}^{k,2}(\Omega;\mathbb{R}^d)\,.$$

To better describe the variational setting of evolution problems, we use Sobolev spaces of a specific form.

Definition 6.8: Let $1 \le p \le \infty$ and $k \ge 0$. Then the spaces

$$\mathcal{L}^p([0,T];\mathcal{V}) := \left\{\boldsymbol{\phi}\colon [0,T] \to \mathcal{V} \mid \left(\int_0^T \|\boldsymbol{\phi}(t)\|_{\mathcal{V}}^p \,\mathrm{d}t\right)^{\frac{1}{p}} < \infty\right\}.$$

are called *Bochner spaces.*

For an overview of relevant properties of Bochner spaces, we refer to [10]. This definition, as well as the following essential statements are also discussed in detail by Arendt and Urban [9, chapter 8].

Lemma 6.9: *Let $\mathcal{V}$ be a Hilbert space and $f \in \mathcal{L}^1([0,T];\mathcal{V})$. Then there exists a unique $g \in \mathcal{V}$, such that*

$$\int_0^T \langle f(t),\phi\rangle_{\mathcal{V}}\,\mathrm{d}t = \langle g,\phi\rangle_{\mathcal{V}} \qquad \forall\, \phi \in \mathcal{V}\,.$$

Proof. See [9, lemma 8.22] □

We continue with the discussion of Bochner spaces in the context of evolution problems. For the sake of clarity, we use the dot-notation to highlight the weak derivatives with respect to time, i.e., for $\phi\colon [0,T] \to \mathcal{V}$ we set $\dot{\phi} := \frac{\partial}{\partial t}\phi$

Theorem 6.10: *Let*

$$\mathcal{W}^{k,p}([0,T];\mathcal{V}) \coloneqq \left\{\phi \in \mathcal{M}ap([0,T];\mathcal{V})\colon \phi \in \mathcal{L}^p([0,T];\mathcal{V})\,,\ \mathrm{D}^k\phi \in \mathcal{L}^p([0,T];\mathcal{V})\right\}\,,$$

where the existence of the weak derivatives D^k *is implied. Then*

(i) $\mathcal{W}^{1,2}([0,T];\mathcal{V})$ *is a Hilbert space with respect to the inner product*

$$\langle \phi, \psi \rangle_{1,2} \coloneqq \int_0^T \langle \phi(t), \psi(t) \rangle_{\mathcal{V}} + \langle \dot{\phi}(t), \dot{\psi}(t) \rangle_{\mathcal{V}} \mathrm{d}t$$

(ii) Let $\phi \in \mathcal{W}^{1,2}([0,T];\mathcal{V})$. *Then there exists a unique* $u \in \mathcal{C}([0,T);\mathcal{V})$, *such that* $\phi(t) = u(t)$ *almost everywhere. It holds*

$$u(t) = u(0) + \int_0^t \dot{\phi}(\tau)\mathrm{d}\tau \qquad \forall\, t \in [0,T)\,.$$

Proof. See [9, theorem 8.24]. □

As before, we set $\mathcal{H}^k([0,T];\mathcal{V}) \coloneqq \mathcal{W}^{k,2}([0,T];\mathcal{V})$.

Remark 6.11: Lebesgue and Sobolev spaces are also defined for $p = \infty$. The norms in $\mathcal{L}^p(\Omega;\mathbb{R}^d)$ and $\mathcal{W}^{k,p}(\Omega;\mathbb{R}^d)$ are then replaced by

$$\|\boldsymbol{\phi}\|_\infty = \operatorname{ess\,sup}_{\mathbf{x}\in\Omega} |\boldsymbol{\phi}(\mathbf{x})|\,, \qquad \|\boldsymbol{\phi}\|_{k,\infty} = \max\left\{\|\boldsymbol{\phi}\|_\infty\,, \left\|\mathrm{D}^k\boldsymbol{\phi}\right\|_\infty\right\}\,.$$

To ease notation, we often drop the codomain from Sobolev spaces and only write $\mathcal{L}^p(\Omega)$. In these cases, the context should clarify the implied codomain.

6.1.2 Variational problems

We shortly describe the framework of variational formulations for abstract Hilbert spaces $\mathcal{V}, \mathcal{W}$ with norms $\|\cdot\|_{\mathcal{V}}, \|\cdot\|_{\mathcal{W}}$.

Definition 6.12: We call a mapping $b\colon \mathcal{V} \times \mathcal{W} \to \mathbb{R}$ a *bilinear form*, if $b(\cdot,\psi)$ is linear for all $\psi \in \mathcal{W}$ and $b(\phi,\cdot)$ is linear for all $\phi \in \mathcal{V}$.

Definition 6.13: A bilinear form $b\colon \mathcal{V} \times \mathcal{W} \to \mathbb{R}$ is called *continuous*, if there exists an $\alpha > 0$ such that

$$|b(\phi,\psi)| \le \alpha \|\phi\|_{\mathcal{V}} \|\psi\|_{\mathcal{W}}\,.$$

We denote by

$$\mathcal{B}(\mathcal{V},\mathcal{W}) \coloneqq \{b\colon \mathcal{V} \times \mathcal{W} \to \mathbb{R}\colon b \text{ is a continuous bilinear form}\}$$

the set of all continuous bilinear forms. We are interested in the following general type of problem:

Problem 6.14: *Let $b \in \mathcal{B}(\mathcal{V}, \mathcal{W})$ and $\ell \in \mathcal{W}^*$. Find $\phi \in \mathcal{V}$, such that*

$$b(\phi, \psi) = \ell(\psi) \qquad \forall\, \psi \in \mathcal{W}\,. \tag{VP}$$

Definition 6.15 (Hadamard): The variational Problem (VP) is called *well-posed*, if for all $\ell \in \mathcal{W}^*$ there exists a unique solution $\phi = \phi(\ell) \in \mathcal{V}$ and there exists a $c > 0$ such that

$$\|\phi\|_{\mathcal{V}} \le c\,\|\ell\|_{\mathcal{W}^*} \qquad \forall\, \ell \in \mathcal{W}^*\,.$$

When investigating such variational problems, the question arises when (VP) is well-posed.

Definition 6.16: A bilinear form $b\colon \mathcal{V} \times \mathcal{W} \to \mathbb{R}$ is said to satisfy the *inf-sup condition*, if there exists a $\beta > 0$, such that

$$\inf_{\psi \in \mathcal{W}} \sup_{\phi \in \mathcal{V}} \frac{b(\phi, \psi)}{\|\phi\|_{\mathcal{V}}\,\|\psi\|_{\mathcal{W}}} \ge \beta\,. \tag{6.1}$$

We call β the *inf-sup constant.*

Theorem 6.17 (Banach-Nečas-Babuška): *Let $b \in \mathcal{B}(\mathcal{V}, \mathcal{W})$ and $\ell \in \mathcal{W}^*$. Then the variational problem (VP) is well-posed if and only if b satisfies the inf-sup condition (6.1) and*

$$\forall\, \psi \in \mathcal{W}\colon \exists\, \phi \in \mathcal{V}\colon b(\phi, \psi) \neq 0\,.$$

In this case, the solution $\phi \in \mathcal{V}$ of (VP) satisfies

$$\|\phi\|_{\mathcal{V}} \le \frac{1}{\beta}\,\|\ell\|_{\mathcal{W}^*}\,.$$

Proof. See [9, section 4.5.1].

Remark 6.18: Theorem 6.17 still holds if $\mathcal{V}, \mathcal{W}$ are Banach spaces and $\mathcal{V}$ is reflexive [53, section 2.1]. Since we will later use $\mathcal{V} = \mathcal{W} = \mathcal{W}^{k,2}$ for $k = 0, 1$, we will continue to only state results for Hilbert spaces.

Corollary 6.19 (Lax-Milgram): *Let $\mathcal{V} = \mathcal{W}$ and $b \in \mathcal{B}(\mathcal{V}, \mathcal{V})$ be coercive, i.e., there exists $\gamma > 0$ such that*

$$\inf_{\phi \in \mathcal{V}} \frac{b(\phi, \phi)}{\|\phi\|_{\mathcal{V}}^2} \ge \gamma\,.$$

Then the variational problem (VP) is well-posed.

Proof. See [53, section 2.1]. □

We want to apply the essential theorem 6.17 to inhomogeneous evolution equations, specifically the heat equation and the wave equation. This introduction is concluded with two basic well-posedness results for the types of partial differential equations included in the coupled model (5.29).

Theorem 6.20 (Well posedness of the parabolic problem): *Let $a \in \mathcal{B}(\mathcal{V}, \mathcal{V})$ be symmetric and coercive and $f\colon [0,T] \to \mathcal{V}$. Let $\mathbb{V} = \mathcal{H}_0^1([0,T];\mathcal{V}^*) \cap \mathcal{L}^2([0,T];\mathcal{V})$ and $\mathbb{W} = \mathcal{L}^2([0,T];\mathcal{V})$ and let further $b\colon \mathbb{V} \times \mathbb{W} \to \mathbb{R}$ be defined by*

$$b(\phi, \psi) := \int_0^T \langle \dot{\phi}(t), \psi(t) \rangle_2 \,\mathrm{d}t + \int_0^T a(\phi(t), \psi(t)) \,\mathrm{d}t\,.$$

Then the variational Problem

$$b(\phi, \psi) = \ell(\psi) \qquad \forall\, \psi \in \mathbb{W}$$

where the linear form $\ell \in \mathcal{W}^*$ is defined by

$$\ell(\psi) := \int_0^T \langle f(t), \psi(t) \rangle_{\mathbb{W}} \,\mathrm{d}t\,, \qquad \psi \in \mathbb{W}\,,$$

is well posed if $f \in \mathbb{W}$.

Proof. See [98, III, theorem 3.1] □

Theorem 6.21 (Well posedness of the hyperbolic problem): *Let $a \in \mathcal{B}(\mathcal{V}, \mathcal{V})$ be symmetric and coercive and $f\colon [0,T] \to \mathcal{V}$. Let $\mathbb{V} = \mathcal{H}_0^2([0,T];\mathcal{V}^*) \cap \mathcal{L}^2([0,T];\mathcal{V})$ and $\mathbb{W} = \mathcal{H}^1([0,T];\mathcal{V})$ and let further $b\colon \mathbb{V} \times \mathbb{V} \to \mathbb{R}$ be defined by*

$$b(\phi, \psi) := \int_0^T \langle \ddot{\phi}(t), \psi(t) \rangle_2 \,\mathrm{d}t + \int_0^T a(\phi(t), \psi(t)) \,\mathrm{d}t\,.$$

Then the variational problem

$$b(\phi, \psi) = \ell(\psi) \qquad \forall\, \psi \in \mathbb{W}$$

where the linear form $\ell \in \mathcal{W}^*$ is defined by

$$\ell(\psi) := \int_0^T \langle f(t), \psi(t) \rangle_{\mathbb{W}}\,, \qquad \psi \in \mathbb{W} \,\mathrm{d}t\,,$$

is well posed if $f \in \mathbb{W}$.

Proof. See [98, IV, theorem 4.] □

The theorems 6.20 and 6.21 provide the basis for the well-posedness of the weak formulations of cardiac electrophysiology and elasticity, which we present in the following sections.

6.1.3 Weak description of cardiac electrophysiology

Consider the monodomain equations (5.11). We shortly present their variational description along with some existence and regularity results. These results were obtained by Franzone et al. [57] for simple cellular activation models and Mroue [111] for the Beeler-Reuter and Luo-Rudy model. In order to show existence and uniqueness of solutions in a weak sense, the following conditions are assumed to hold:

(M1) The boundary $\Gamma_{\mathrm{EP}} = \partial\Omega_{\mathrm{EP}}$ is Lipschitz.

(M2) The coefficients of $\mathbf{D}$ satisfy $\sigma_{\mathbf{f}}, \sigma_{\mathbf{s}}, \sigma_{\mathbf{t}} \in \mathcal{L}^\infty(\Omega_{\mathrm{EP}})$ and $\sigma_{\mathbf{f}}, \sigma_{\mathbf{s}}, \sigma_{\mathbf{t}} > 0$

(M3) For the external current, it holds $I_{\mathrm{ext}}(t, \cdot) \in \mathcal{L}^2(\Omega_{\mathrm{EP}})$ for a.e. $t > 0$.

(M4) The Sobolev embedding [36, theorem 9.16]

$$\mathcal{W}^{1,2}(\Omega_{\mathrm{EP}}) \subset \mathcal{L}^p(\Omega_{\mathrm{EP}}) \qquad \text{for } 2 \le p \le 6$$

holds.

(M5) The initial data $v_0 \in \mathcal{H}^1(\Omega_{\mathrm{EP}}) \cap \mathcal{L}^\infty(\Omega_{\mathrm{EP}})$, $\mathbf{w}_0 \in \mathcal{L}^2(\Omega_{\mathrm{EP}})^{d_{\mathbf{w}}}$ and $\mathbf{c}_0 \in \mathcal{L}^2(\Omega_{\mathrm{EP}})^{d_{\mathbf{c}}}$ satisfy

$$\begin{aligned} v_{\min} \le v_0 \le v_{\max} &\qquad \text{a.e. in } \Omega_{\mathrm{EP}}\,, \\ \mathbf{w}_{\min} \le \mathbf{w}_0 \le \mathbf{w}_{\max} &\qquad \text{a.e. in } \Omega_{\mathrm{EP}}\,, \\ \mathbf{c}_{\min} \le \mathbf{c}_0 \le \mathbf{c}_{\max} &\qquad \text{a.e. in } \Omega_{\mathrm{EP}}\,, \end{aligned}$$

with suitable values $v_{\min}, v_{\max}, \mathbf{w}_{\min}, \mathbf{w}_{\max}, \mathbf{c}_{\min}, \mathbf{c}_{\max}$, where we interpret the vector-valued inequalities component-wise.

(M6) The transmembrane current I_{ion} and the corresponding evolution functions $\mathbf{G}_{\mathbf{w}}, \mathbf{G}_{\mathbf{c}}$ satisfy suitable regularity conditions.

Remark 6.22: The regularity conditions in (M6) depend on the chosen cellular activation model. Conditions for affine models such as FitzHugh-Nagumo [55], Aliev-Pantilov [2] or Rogers-McCulloch [134] can be found in [57, section 3.5]. Mroue [111] presents necessary conditions for the non-affine model Beeler-Reuter [27] along with the values for the bounds (M5) motivated in [81].

To formulate the variational problem of (5.11), we define

$$m_v\colon \mathcal{L}^2(\Omega_{\mathrm{EP}}) \times \mathcal{L}^2(\Omega_{\mathrm{EP}}) \to \mathbb{R}\,, \qquad m_v(\phi, \psi) := \int_{\Omega_{\mathrm{EP}}} C_{\mathrm{m}} \phi \cdot \psi \,\mathrm{d}V\,, \tag{6.2a}$$

$$a_v\colon \mathcal{H}^1(\Omega_{\mathrm{EP}}) \times \mathcal{H}^1(\Omega_{\mathrm{EP}}) \to \mathbb{R}\,, \quad a_v(\mathbf{w}, \mathbf{c}; \phi, \psi) := \int_{\Omega_{\mathrm{EP}}} (\mathbf{D}\nabla\phi)\nabla\psi + I_{\mathrm{ion}}(\phi, \mathbf{w}, \mathbf{c})\psi \,\mathrm{d}V\,, \tag{6.2b}$$

$$f_v\colon \mathcal{L}^2(\Omega_{\mathrm{EP}}) \to \mathbb{R}\,, \qquad f_v(\psi) := \int_{\Omega_{\mathrm{EP}}} I_{\mathrm{ext}} \cdot \psi \,\mathrm{d}V\,, \tag{6.2c}$$

and choose the standard approach of multiplying (5.11) with suitable testfunctions and integrating over Ω_{EP}.

Remark 6.23: The validity of our variational approach is explained in [36, chapter 10], where additional references are given. However, the results only align if $d_{\mathbf{w}} = 1$, $d_{\mathbf{c}} = 0$ and I_{ion} is affine as assumed in [57]. Again, we refer to [111] for the relation to more involved models.

Definition 6.24: We call the vector of functions $(v, \mathbf{w}, \mathbf{c})$ a *weak solution* of the monodomain equations (5.11), if

$$v \in \mathcal{L}^\infty(\Omega_{\mathrm{EP}}) \cap \mathcal{L}^2([0,T]; \mathcal{H}^1(\Omega_{\mathrm{EP}}))\,, \qquad \mathbf{w} \in \mathcal{L}^2(\Omega_{\mathrm{EP}})^{d_{\mathbf{w}}}\,, \qquad \mathbf{c} \in \mathcal{L}^2(\Omega_{\mathrm{EP}})^{d_{\mathbf{c}}}\,,$$

such that $v, \mathbf{w}, \mathbf{c}$ satisfy the restrictions (M5) and

$$m_v(\frac{\partial}{\partial t} v, \phi) + a_v(\mathbf{w}, \mathbf{c}; v, \phi) = f_v(\phi) \qquad \forall\, \phi \in \mathcal{H}^1_0(\Omega_{\mathrm{EP}})\,, \tag{6.3a}$$

$$\int_{\Omega_{\mathrm{EP}}} \frac{\partial}{\partial t}\mathbf{w} \cdot \boldsymbol{\psi} \,\mathrm{d}V = \int_{\Omega_{\mathrm{EP}}} \mathbf{G}_{\mathbf{w}}(v, \mathbf{w}, \mathbf{c}) \cdot \boldsymbol{\psi} \,\mathrm{d}V \qquad \forall\, \boldsymbol{\psi} \in \mathcal{L}^2_0(\Omega_{\mathrm{EP}})^{d_{\mathbf{w}}}\,, \tag{6.3b}$$

$$\int_{\Omega_{\mathrm{EP}}} \frac{\partial}{\partial t}\mathbf{c} \cdot \boldsymbol{\theta} \,\mathrm{d}V = \int_{\Omega_{\mathrm{EP}}} \mathbf{G}_{\mathbf{c}}(v, \mathbf{w}, \mathbf{c}) \cdot \boldsymbol{\theta} \,\mathrm{d}V \qquad \forall\, \boldsymbol{\theta} \in \mathcal{L}^2_0(\Omega_{\mathrm{EP}})^{d_{\mathbf{c}}}\,. \tag{6.3c}$$

for almost every $t \in [0, T]$.

Theorem 6.25: *Let the regularity assumptions (M1)–(M6) hold. Then there exists a unique solution* $(v, \mathbf{w}, \mathbf{c})$ *of* (6.3).

Proof. See [33] or [165], respectively. □

Remark 6.26: The equations (6.3) miss the weak formulations for the ODEs of $\mathbf{k}$, $\gamma_{\mathbf{f}}$. Since $v, \mathbf{w}, \mathbf{c}$ do not depend on these values, their addition does not require any addition in the regularity assumptions (M1)–(M6). For the coupled formulation, we will later add similar weak formulations for $\mathbf{k}$,$\gamma_{\mathbf{f}}$.

6.1.4 Weak description of cardiac elasticity

Since the conductivities $\sigma_{\mathbf{f},\mathbf{s},\mathbf{t}}$ of $\mathbf{D}$ are assumed to be constant, general theory of parabolic partial differential equations can be applied after treating the term I_{ion}. For small deformations, $\mathbf{P}$ is usually linearized, yielding an equation of the form

$$\rho\mathbf{a} - \operatorname{div}(\mathbb{C}(\mathrm{D}\varepsilon(\mathbf{u}))) = \rho\mathbf{b} \qquad \text{in } (0,T) \times \Omega\,, \tag{6.4}$$

where $\varepsilon(\mathbf{u}) = \operatorname{sym}(\mathrm{D}\mathbf{u})$ and $\mathbb{C}\boldsymbol{\varepsilon} = 2\mu\boldsymbol{\varepsilon} + \lambda\operatorname{tr}(\boldsymbol{\varepsilon})\mathbf{I}$ with suitable parameters $\mu > 0$, $\lambda \geq 0$. Such a linearization is physically motivated by Hooke's law, stating a linear stress response for small displacemenets. The analysis of this wave equation could utilize standard tools for hyperbolic differential equations. This linearization, however, is unsuitable for large deformations.

We will shortly provide the general concept of potential energies leading to a variational formulation of (5.12). This is achieved by showing the existence of differentiable functionals, such that their derivative yields an expression which is equivalent to the classical formulation. The following definitions and conclusions are discussed in more detail in [38, section 4.1] for static problems and in [106, section 5.1] for dynamic problems.

Definition 6.27: Let $\mathbf{b}^{\varphi}\colon \mathbf{\Phi}(\Omega) \to \mathbb{R}^3$ be a body load on $\varphi_t(\Omega)$ and $\mathbf{g}^{\varphi}\colon \mathbf{\Phi}(\Gamma) \to \mathbb{R}^3$ a surface load on $\varphi_t(\Gamma)$. We call $\mathbf{b}^{\varphi}$ a *dead body load*, if its corresponding material formulation $\mathbf{b}\colon \Omega \to \mathbb{R}^3$ is independent of φ, i.e. $\mathbf{b}(t,\mathbf{x})$ is known for all $(t,\mathbf{x})$ in $[0,T] \times \Omega$. Similarly, we call $\mathbf{g}^{\varphi}$ a *dead surface load*, if the material formulation $\mathbf{g}\colon \Gamma \to \mathbb{R}^3$ is independent of φ.

We will use the term *dead load* to mean either one of the terms defined above. A common example for a dead load is the force of gravity, which is independent of the actual configuration of Ω.

Definition 6.28: Let $\mathbf{b}^{\varphi}\colon \mathbf{\Phi}(\Omega) \to \mathbb{R}^3$ be a body load with material formulation $\mathbf{b}\colon \Omega \to \mathbb{R}^3$ in such a way, that

$$\mathbf{b}(t,\mathbf{x}) = \widehat{\mathbf{b}}(t,\mathbf{x},\varphi(t,\mathbf{x}),\mathrm{D}\varphi(t,\mathbf{x}))\,, \qquad \forall\, t \in [0,T],\ \mathbf{x} \in \Omega\,.$$

We call $\mathbf{b}^{\varphi}$ *conservative*, if there exists a functional $\mathcal{F}\colon \mathcal{M}ap(\Omega;\mathbb{R}^3) \to \mathbb{R}$, such that

$$\mathrm{D}\mathcal{F}(\varphi)[\phi] = \int_{\Omega} \rho\widehat{\mathbf{b}}(t,\mathbf{x},\varphi(t,\mathbf{x}),\mathrm{D}\varphi(t,\mathbf{x})) \cdot \phi \,\mathrm{d}V\,.$$

We call $\mathcal{F}$ the *potential* of $\mathbf{b}^{\varphi}$.

Definition 6.29: Let $\mathbf{g}^{\varphi}\colon \mathbf{\Phi}(\Gamma) \to \mathbb{R}^3$ be a surface load with corresponding material formulation $\mathbf{g}\colon \Omega \to \mathbb{R}^3$ in such a way, that

$$\mathbf{g}(t,\mathbf{x}) = \widehat{\mathbf{g}}(t,\mathbf{x},\varphi(t,\mathbf{x}),\mathrm{D}\varphi(t,\mathbf{x}))\,, \qquad \forall\, t \in [0,T],\ \mathbf{x} \in \Omega\,.$$

We call $\mathbf{g}^{\varphi}$ *conservative*, if there exists a functional $\mathcal{G}\colon \mathcal{M}ap(\Gamma;\mathbb{R}^3) \to \mathbb{R}$, such that

$$\mathrm{D}\mathcal{G}(\varphi)[\phi] = \int_{\Gamma} \widehat{\mathbf{g}}(t,\mathbf{x},\varphi(t,\mathbf{x}),\mathrm{D}\varphi(t,\mathbf{x})) \cdot \phi \,\mathrm{d}A\,.$$

We call $\mathcal{G}$ the *potential* of $\mathbf{g}^{\varphi}$.

All dead loads are conservative, since $\mathbf{b}^{\varphi}$ do not depend on φ and therefore $\widehat{\mathbf{b}} = \mathbf{b}^{\varphi}$.

Remark 6.30: It is generally more common to call $\widehat{\mathbf{b}}$ and $\widehat{\mathbf{g}}$ the potentials of $\mathbf{b}^{\varphi}$ and $\mathbf{g}^{\varphi}$, respectively. We will use the term for both and presume the context clarifies which mapping we mean.

Lemma 6.31: *Let* $\mathbf{g}^{\varphi}\colon \mathbf{\Phi}(\Gamma) \to \mathbb{R}^3$ *be the surface load defined by*

$$\mathbf{g}^{\varphi}(t, \mathbf{x}^{\varphi}) := -p(t)\mathbf{n}^{\varphi}(\mathbf{x}^{\varphi}),$$

where $p\colon [0,T] \to \mathbb{R}$ *is a time dependant pressure and* $\mathbf{n}^{\varphi}$ *is the outer normal vector on* Γ*. Then* $\mathbf{g}^{\varphi}$ *is conservative with*

$$\mathcal{G}(t, \boldsymbol{\theta}) = -\frac{p(t)}{3}\int_{\Gamma} \mathrm{Cof}\,(\mathrm{D}\boldsymbol{\theta})\,\mathbf{n} \cdot \boldsymbol{\theta}\,\mathrm{d}A\,.$$

Proof. See [38, theorem 2.7-1]. □

Definition 6.32: Let $\boldsymbol{\varphi}\colon [0,T] \times \Omega \to \mathbb{R}^3$ be a motion subjected to conservative forces $\mathbf{b}^{\varphi}$ and $\mathbf{g}^{\varphi}$ on a hyperelastic material with stored energy function $W_{\mathbf{P}}$. Let $\mathcal{F}, \mathcal{G}$ the potentials of said conservative forces. We then call

$$\mathcal{E}(t, \boldsymbol{\varphi}) := \int_{\Omega} W_{\mathbf{P}}(\mathrm{D}\boldsymbol{\varphi}(t, \mathbf{x}))\,\mathrm{d}\mathbf{x}\,\mathrm{d}V - \mathcal{F}(t, \boldsymbol{\varphi}) - \mathcal{G}(t, \boldsymbol{\varphi})$$

the *potential energy* of $\boldsymbol{\varphi}$ at time $t \in [0,T]$.

Definition 6.33: Let $\boldsymbol{\varphi}\colon [0,T] \times \Omega \to \mathbb{R}^3$ be a motion with velocity $\mathbf{v}$. We call

$$\mathcal{K}(t, \mathbf{v}) := \int_{\Omega} \frac{\rho}{2}\mathbf{v}(t, \mathbf{x}) \cdot \mathbf{v}(t, \mathbf{x})\,\mathrm{d}V$$

the *kinetic energy* of $\boldsymbol{\varphi}$ at time $t \in [0,T]$.

Definition 6.34: Let $\boldsymbol{\varphi}\colon [0,T] \times \Omega \to \mathbb{R}^3$ be a motion with velocity $\mathbf{v}$ as in definitions 6.32 and 6.33. We call

$$\mathcal{I}(t, \boldsymbol{\varphi}, \mathbf{v}) := \mathcal{K}(t, \mathbf{v}) + \mathcal{E}(t, \boldsymbol{\varphi})$$

the *total energy* of $\boldsymbol{\varphi}$ at time $t \in [0,T]$.

For better readability, we drop the dependency on t in the notation for the remainder of this section.

Definition 6.35: Let $\mathcal{J}\colon \mathcal{V} \to \mathbb{R}$ be a differentiable functional. We call an element $\boldsymbol{\varphi} \in \mathcal{V}$ a *critical point* of $\mathcal{J}$, if

$$\mathrm{D}\mathcal{J}(\boldsymbol{\varphi})[\boldsymbol{\phi}] = 0 \qquad \forall\, \boldsymbol{\phi} \in \mathcal{V}\,.$$

We write this as $\mathrm{D}\mathcal{J} = 0$.

Theorem 6.36: *Consider a hyperelastic material with stored energy function* $W_{\mathbf{P}}$ *subjected to conservative body and surface loads* $\mathbf{b}^{\varphi}$ *and* $\mathbf{g}^{\varphi}$*. Then the equations of motion in the reference configuration* (3.4)*, i.e.,*

$$\rho\mathbf{a} - \mathrm{div}\,(\mathrm{D}_{\mathbf{F}} W_{\mathbf{P}}(\mathrm{D}\boldsymbol{\varphi})) = \rho\mathbf{b} \qquad \text{in } (0,T) \times \Omega\,, \tag{6.5a}$$

$$(\mathrm{D}_{\mathbf{F}}) W_{\mathbf{P}}(\mathrm{D}\boldsymbol{\varphi}))\,\mathbf{n} = \mathbf{g} \qquad \text{on } (0,T) \times \Gamma\,, \tag{6.5b}$$

are formally equivalent to

$$\frac{\partial}{\partial t}\mathrm{D}_{\mathbf{v}}\mathcal{K}(\mathbf{v})[\boldsymbol{\phi}] = \mathrm{D}_{\boldsymbol{\varphi}}\mathcal{E}(\boldsymbol{\varphi})[\boldsymbol{\phi}] \qquad \forall\, \boldsymbol{\phi} \in \mathcal{C}_0([0,T]\times\Omega;\mathbb{R}^3)\,,\ t\in[0,T]\,,$$

where we set $\mathbf{v} = \dot{\boldsymbol{\varphi}}$.

Proof. We summarize the discussions from [106, section 5.4] leading to this result. We show that $\boldsymbol{\varphi}$ is a critical point of $\mathcal{I}(\boldsymbol{\varphi},\mathbf{v})$ if and only if the equations of motion (6.5) hold. Using lemma 2.12, it holds

$$\mathrm{D}_{\boldsymbol{\varphi}}\mathcal{E}(\boldsymbol{\varphi})[\boldsymbol{\phi}] = \int_\Omega \mathrm{D}_{\mathbf{F}}W_{\mathbf{P}}(\mathrm{D}\boldsymbol{\varphi})[\mathrm{D}\boldsymbol{\phi}]\,\mathrm{d}V - \mathrm{D}\mathcal{F}(\boldsymbol{\varphi})[\boldsymbol{\phi}] - \mathrm{D}\mathcal{G}(\boldsymbol{\varphi})[\boldsymbol{\phi}]\,,$$

where $\mathcal{F},\mathcal{G}$ are the load and surface potentials. The derivative of $\mathcal{I}$ is then given by

$$\begin{aligned}\mathrm{D}\mathcal{I}(\boldsymbol{\varphi},\dot{\boldsymbol{\varphi}})\left[(\boldsymbol{\phi},\dot{\boldsymbol{\phi}})\right] &= \mathrm{D}_{\dot{\boldsymbol{\varphi}}}\mathcal{I}(\boldsymbol{\varphi},\dot{\boldsymbol{\varphi}})[\dot{\boldsymbol{\phi}}] + \mathrm{D}_{\boldsymbol{\varphi}}\mathcal{I}(\boldsymbol{\varphi},\dot{\boldsymbol{\varphi}})[\boldsymbol{\phi}]\\ &= \mathrm{D}\mathcal{K}(\dot{\boldsymbol{\varphi}})[\dot{\boldsymbol{\phi}}] + \int_\Omega \mathrm{D}_{\mathbf{F}}W_{\mathbf{P}}(\mathrm{D}\boldsymbol{\varphi})[\mathrm{D}\boldsymbol{\phi}]\,\mathrm{d}V - \mathrm{D}\mathcal{F}(\boldsymbol{\varphi})[\boldsymbol{\phi}] - \mathrm{D}\mathcal{G}(\boldsymbol{\varphi})[\boldsymbol{\phi}]\\ &= \int_\Omega \rho\ddot{\boldsymbol{\varphi}}\cdot\boldsymbol{\phi}\,\mathrm{d}V - \int_\Omega \rho\widehat{\mathbf{b}}(\boldsymbol{\varphi},\mathrm{D}\boldsymbol{\varphi})\cdot\boldsymbol{\phi}\,\mathrm{d}V\\ &\quad + \int_\Omega \mathrm{D}_{\mathbf{F}}W_{\mathbf{P}}(\mathrm{D}\boldsymbol{\varphi}) : \mathrm{D}\boldsymbol{\phi}\,\mathrm{d}V - \int_\Gamma \widehat{\mathbf{g}}(\boldsymbol{\varphi},\mathrm{D}\boldsymbol{\varphi})\cdot\boldsymbol{\phi}\,\mathrm{d}A \end{aligned} \tag{6.6}$$

If the equations of elasticity hold, then

$$\begin{aligned}\mathrm{D}\mathcal{I}(\boldsymbol{\varphi},\dot{\boldsymbol{\varphi}})\left[(\boldsymbol{\phi},\dot{\boldsymbol{\phi}})\right] &= \int_\Omega \rho\ddot{\boldsymbol{\varphi}}\cdot\boldsymbol{\phi}\,\mathrm{d}V - \int_\Omega \rho\widehat{\mathbf{b}}(\boldsymbol{\varphi},\mathrm{D}\boldsymbol{\varphi})\cdot\boldsymbol{\phi}\,\mathrm{d}V + \int_\Omega \operatorname{div}\left(\mathrm{D}_{\mathbf{F}}W_{\mathbf{P}}(\mathrm{D}\boldsymbol{\varphi})\right)\cdot\boldsymbol{\phi}\,\mathrm{d}V\\ &= \int_\Omega \Big(\rho\ddot{\boldsymbol{\varphi}} - \rho\widehat{\mathbf{b}}(\boldsymbol{\varphi},\mathrm{D}\boldsymbol{\varphi}) - \operatorname{div}\left(\mathrm{D}_{\mathbf{F}}W_{\mathbf{P}}(\mathrm{D}\boldsymbol{\varphi})\right)\Big)\cdot\boldsymbol{\phi}\,\mathrm{d}V\\ &= \mathbf{0}\,,\end{aligned}$$

therefore $\boldsymbol{\varphi}$ is a critical point of $\mathcal{I}$ and hence

$$\frac{\partial}{\partial t}\mathrm{D}_{\mathbf{v}}\mathcal{K}(\mathbf{v})[\boldsymbol{\phi}] = \mathrm{D}\mathcal{K}(\dot{\boldsymbol{\varphi}})[\dot{\boldsymbol{\phi}}] = \mathrm{D}_{\boldsymbol{\varphi}}\mathcal{E}(\boldsymbol{\varphi},\mathrm{D}\boldsymbol{\varphi})[\boldsymbol{\phi}]\,.$$

On the other hand, if $\boldsymbol{\varphi}\in\mathcal{V}$ is a critical point of $\mathcal{I}$, we have

$$\int_\Omega \rho\ddot{\boldsymbol{\varphi}}\cdot\boldsymbol{\phi}\,\mathrm{d}V - \int_\Omega \mathrm{D}_{\mathbf{F}}W_{\mathbf{P}}(\mathrm{D}\boldsymbol{\varphi}) : \mathrm{D}\boldsymbol{\phi}\,\mathrm{d}V = \int_\Omega \rho\widehat{\mathbf{b}}(\boldsymbol{\varphi},\mathrm{D}\boldsymbol{\varphi})\cdot\boldsymbol{\phi}\,\mathrm{d}V \qquad \forall\,\boldsymbol{\phi}\in\mathcal{V}$$

and, since $\boldsymbol{\phi}\equiv\mathbf{0}$ on Γ,

$$\int_\Omega \mathrm{D}_{\mathbf{F}}W_{\mathbf{P}}(\mathrm{D}\boldsymbol{\varphi}) : \mathrm{D}\boldsymbol{\phi}\,\mathrm{d}V = \int_\Omega \operatorname{div}\left(\mathrm{D}_{\mathbf{F}}W_{\mathbf{P}}(\mathrm{D}\boldsymbol{\varphi})\right)\cdot\boldsymbol{\phi}\,\mathrm{d}V$$

by Greens formula 2.33. Thus the variational formulation of (6.5a) holds for all $\boldsymbol{\phi}$, which is equivalent to

$$\rho\mathbf{a} - \operatorname{div}\left(\mathrm{D}_{\mathbf{F}}W_{\mathbf{P}}(\mathrm{D}\boldsymbol{\varphi})\right) = \rho\mathbf{b} \qquad \text{in } (0,T)\times\Omega\,.$$

Lastly, comparing the variational formulation of (6.5a) with (6.6), we see

$$\int_\Gamma \left(\mathrm{D}_{\mathbf{F}}W_{\mathbf{P}}(\mathrm{D}\boldsymbol{\varphi})\right)\mathbf{n}\cdot\boldsymbol{\phi}\,\mathrm{d}A = \int_\Gamma \widehat{\mathbf{g}}(\boldsymbol{\varphi},\mathrm{D}\boldsymbol{\varphi})\cdot\boldsymbol{\phi}\,\mathrm{d}A \qquad \forall\,\boldsymbol{\phi}\in\mathcal{V}\,,$$

implying the boundary conditions (6.5b) hold. □

Remark 6.37: The space $\mathcal{V}$ in the proof above was intentionally left ambiguous. We will resolve this issue by the end of the section.

By "formally equivalent" we imply that motions $\boldsymbol{\varphi}$ satisfying one of the statements are regular enough for the other statement to be well-defined.

Corollary 6.38: *Let*

$$\mathcal{A}_t := \left\{ \boldsymbol{\phi} \in \mathcal{W}^{1,p}(\Omega)^3 \colon \det(\mathbf{I} + \mathrm{D}\boldsymbol{\phi}) > 0\,,\ \boldsymbol{\phi} = \mathbf{u}_0 \text{ a.e. on } \Gamma_\mathrm{D}\,,\ \mathcal{I}(t, \boldsymbol{\phi}, \frac{\partial}{\partial t}\boldsymbol{\phi}) < \infty \right\}$$

be the set of admissible function *at time* $t \in [0, T]$ *and* $\boldsymbol{\varphi} \in \mathcal{D}$ *be the solution of the minimization problem*

$$\mathcal{I}(\boldsymbol{\varphi}, \dot{\boldsymbol{\varphi}}) = \inf_{\boldsymbol{\phi} \in \mathcal{A}_t} \mathcal{I}(\boldsymbol{\phi}, \dot{\boldsymbol{\phi}})\,. \tag{6.7}$$

If $\boldsymbol{\varphi}$ *is regular enough, then* $\boldsymbol{\varphi}$ *satisfies the equations of motion* (6.5).

Proof. Since $\boldsymbol{\varphi}$ satisfies the minimization problem (6.7), $\boldsymbol{\varphi}$ is a critical point of $\mathcal{I}$ and thus

$$\mathrm{D}\mathcal{I}(\boldsymbol{\varphi}, \dot{\boldsymbol{\varphi}})[\boldsymbol{\phi}] = \mathbf{0} \quad \Leftrightarrow \quad \frac{\partial}{\partial t}\mathrm{D}_\mathbf{v}\mathcal{K}(\mathbf{v})[\boldsymbol{\phi}] = \mathrm{D}_{\boldsymbol{\varphi}}\mathcal{E}(\boldsymbol{\varphi}, \mathrm{D}\boldsymbol{\varphi})[\boldsymbol{\phi}] \qquad \text{for all } \boldsymbol{\phi}\,.$$

The statement then follows with theorem 6.36. □

Remark 6.39: The value of p in the set $\mathcal{A}_t$ depends on the specific boundary conditions of the problem and the stored energy function $W_\mathbf{P}$, specifically if $\mathrm{Cof}\,(\cdot)$ and det need to be well-defined in a weak sense. We leave the value for p open but refer to [18, 20] for a more in-depth analysis of the topic.

Theorem 6.36 justifies the formulation of the following variational problem. We define

$$m_\mathbf{u} \colon \mathcal{L}^2(\Omega)^3 \times \mathcal{L}^2(\Omega)^3 \to \mathbb{R}\,, \qquad m_\mathbf{u}(\boldsymbol{\phi}, \boldsymbol{\psi}) := \int_\Omega \rho \boldsymbol{\phi} \cdot \boldsymbol{\psi} \,\mathrm{d}V\,, \tag{6.8a}$$

$$a_\mathbf{u} \colon \mathcal{W}^{1,p}(\Omega)^3 \times \mathcal{W}^{1,p}(\Omega)^3 \to \mathbb{R}\,, \qquad a_\mathbf{u}(\boldsymbol{\phi}, \boldsymbol{\psi}) := \int_\Omega \mathbf{P}(\mathrm{D}\boldsymbol{\phi}) \colon \boldsymbol{\psi} \,\mathrm{d}V\,, \tag{6.8b}$$

$$f_\mathbf{u} \colon \mathcal{W}^{1,p}(\Omega)^3 \to \mathbb{R}\,, \qquad f_\mathbf{u}(\boldsymbol{\psi}) := \int_\Omega \rho \mathbf{b} \cdot \boldsymbol{\psi} \,\mathrm{d}V + \int_\Gamma \mathbf{g} \cdot \boldsymbol{\psi} \,\mathrm{d}A\,. \tag{6.8c}$$

Definition 6.40: We call $\mathbf{u}$ a *weak solution* of (5.12) with if

$$\mathbf{u} \in \mathcal{L}^2([0, T]; \mathcal{W}^{1,p}(\Omega)^3)$$

and for a.e. $t \in (0, T)$ it holds

$$m_\mathbf{u}(\frac{\partial^2}{\partial t^2}\mathbf{u}, \boldsymbol{\phi}) + a_\mathbf{u}(\mathbf{u}, \boldsymbol{\phi}) = f_\mathbf{u}(\boldsymbol{\phi}) \qquad \forall\, \boldsymbol{\phi} \in \mathcal{H}^1_0(\Omega)^3\,. \tag{6.9}$$

The requirement $\mathbf{u} \in \mathcal{L}^2([0, T]; \mathcal{W}^{1,p}(\Omega)^3)$ is a consequence of weak continuity conditions required for $\mathcal{I}$ (see [21]). These continuity conditions are necessary in the proofs of existence, uniqueness and regularity of the variational formulation. We provide one well-known result.

Definition 6.41: Let $\mathbf{b}^\varphi, \mathbf{g}^\varphi$ be independent of time. We call $\mathbf{u} \in \mathcal{W}^{1,p}(\Omega)^3$ a *weak solution of the static problem*, if

$$a_{\mathbf{u}}(\mathbf{u}, \boldsymbol{\phi}) = f_{\mathbf{u}}(\boldsymbol{\phi}) \qquad \forall\, \boldsymbol{\phi} \in \mathcal{W}_0^{1,p}(\Omega)^3 \,. \tag{6.10}$$

Theorem 6.42: *Consider the static variant* (6.10)*. Let the set of admissible functions*

$$\mathcal{A}_0 = \left\{ \boldsymbol{\phi} \in \mathcal{W}^{1,p}(\Omega)^3 \colon\ \det(\mathbf{I} + \mathrm{D}\boldsymbol{\phi}) > 0 \,,\ \boldsymbol{\phi} = \mathbf{u}_0 \ \text{a.e. on}\ \Gamma_{\mathrm{D}} \,,\ \mathcal{I}(0, \boldsymbol{\phi}, \mathbf{0}) < \infty \right\}$$

be non-empty. Let the material be hyperelastic with polyconvex stored energy function $W_{\mathbf{P}}$ satisfying the growth conditions 4.53 and let $\widehat{\mathbf{b}}, \widehat{\mathbf{g}}$ be continuous and bounded from below. Then there exists a solution of (6.9)*.*

Proof. See [19]. □

Note that theorem 6.42 does not guarantee the uniqueness of a weak solution. In contrast to the problem (6.3), there are only few additional existence and uniqueness results for (6.9). A comprehensive list of literature on the matter is given by Antman [8, section 13.6] and Ball [22]. In recent years, this has led to the approach of defining non-simple materials [76], which include the second derivative of $W_{\mathbf{P}}$ in the material formulations. A comprehensive list of results using this technique for static and dynamic problems is given by Kružík [97]. We nevertheless continue with the classic approach from chapter 4.

6.2 Variational formulation of the coupled system

When employing the active stress approach (5.18), the first Piola-Kirchhoff stress is complemented by an active part $\mathbf{P}_{\mathrm{A}}$. In the context of energy potential, the question arises if $\mathbf{P}_{\mathrm{A}}$ can be interpreted as the derivative of an active stored energy W_{A}. The stored energy $W_{\mathbf{P}} + W_{\mathrm{A}}$ then again would satisfy the equivalence of theorem 6.36.

Lemma 6.43: *Let $\mathbf{f} \colon \Omega \to \mathbb{R}^3$ be a fibre field and $\mathbf{P}_{\mathrm{A}}$ be the active stress given by*

$$\mathbf{P}_{\mathrm{A}}(\mathbf{F}, \lambda) \coloneqq T(\lambda)\mathbf{F}\mathbf{f} \otimes \mathbf{f} \,,$$

where $\mathbf{f}^\varphi = \mathbf{F}\mathbf{f}$ and $T \colon \mathbb{R} \to \mathbb{R}$ is an internal stress dependent on the fiber length $\lambda = \sqrt{\mathbf{F}\mathbf{f} \cdot \mathbf{F}\mathbf{f}}$. Let $W_{\mathrm{A}} \colon \mathbb{R} \to \mathbb{R}$ be a primitive of $\lambda T(\lambda)$ with respect to λ. Then

$$\mathrm{D}_{\mathbf{F}} W_{\mathrm{A}}\big(\sqrt{\mathbf{F}\mathbf{f} \cdot \mathbf{F}\mathbf{f}}\big) = \mathbf{P}_{\mathrm{A}}(\mathbf{F}, \lambda) \,.$$

Proof. We reiterate the arguments given in [110]: First observe that for $\lambda = \sqrt{\|\mathbf{f}^\varphi\|^2}$, it holds

$$\mathrm{D}_{\mathbf{F}}\lambda = \frac{1}{2\lambda}\mathrm{D}_{\mathbf{F}}(\mathbf{f}^\top\mathbf{F}^\top\mathbf{F}\mathbf{f}) = \frac{1}{\lambda}\mathbf{F}\mathbf{f} \otimes \mathbf{f} \,.$$

Let now W_{A} be a primitive of λT, i.e., $\frac{\partial}{\partial\lambda}W_{\mathrm{A}}(\lambda) = \lambda T(\lambda)$. Then for $\lambda = \sqrt{\mathbf{Ff}\cdot\mathbf{Ff}}$, we get

$$\mathrm{D}_{\mathbf{F}}W_{\mathrm{A}}(\lambda) = \mathrm{D}_{\lambda}W_{\mathrm{A}}(\lambda)\mathrm{D}_{\mathbf{F}}\lambda = T(\lambda)\mathbf{Ff}\otimes\mathbf{f}\,.$$

□

Remark 6.44: Since we will not apply the active stress approach, we will not go into detail on the validity of the assumption that a primitive of $\lambda T(\lambda)$ exists. At least for simple phenomenological models, $T\colon \mathbb{R}\to\mathbb{R}$ is given as a continuous function, providing the existence of this primitive.

When considering the active strain approach (5.19), the term containing $\mathbf{P}$ in $a_{\mathbf{u}}$ has to be adapted as well. Instead of $\mathbf{F}$, we insert $\mathbf{F}_{\mathrm{E}} = \mathbf{F}\mathbf{F}_{\mathrm{A}}^{-1}$ into $\mathbf{P}$. Applying the chain rule then yields

$$\begin{aligned}
\mathrm{D}_{\mathbf{F}}W_{\mathbf{P}}(\mathbf{F}\mathbf{F}_{\mathrm{A}}^{-1})\colon \mathrm{D}\boldsymbol{\phi} &= \mathrm{D}_{\mathbf{F}}W_{\mathbf{P}}(\mathbf{F}\mathbf{F}_{\mathrm{A}}^{-1})\,[\mathrm{D}\boldsymbol{\phi}]\\
&= \mathrm{D}_{\mathbf{F}_{\mathrm{E}}}W_{\mathbf{P}}(\mathbf{F}_{\mathrm{E}})\left[(\mathrm{D}_{\mathbf{F}}\mathbf{F}\mathbf{F}_{\mathrm{A}}^{-1})\,[\mathrm{D}\boldsymbol{\phi}]\right]\\
&= \mathrm{D}_{\mathbf{F}_{\mathrm{E}}}W_{\mathbf{P}}(\mathbf{F}_{\mathrm{E}})\left[\mathrm{D}\boldsymbol{\phi}\mathbf{F}_{\mathrm{A}}^{-1}\right]\\
&= \mathrm{D}_{\mathbf{F}_{\mathrm{E}}}W_{\mathbf{P}}(\mathbf{F}_{\mathrm{E}})\colon \mathrm{D}\boldsymbol{\phi}\mathbf{F}_{\mathrm{A}}^{-1}
\end{aligned}$$

With this, we finally formulate the variational setting of cardiac elasticity. By abusing notation, the specific functionals in (6.9) for $t\in(0,T)$ are given by

$$m_{\mathbf{u}}(\boldsymbol{\phi},\boldsymbol{\psi}) = \int_\Omega \rho\boldsymbol{\phi}\cdot\boldsymbol{\psi}\,\mathrm{d}V\,, \tag{6.11a}$$

$$a_{\mathbf{u}}(\gamma_{\mathbf{f}};\boldsymbol{\phi},\boldsymbol{\psi}) = \int_\Omega \mathbf{P}((\mathbf{I}+\mathrm{D}\boldsymbol{\phi})\mathbf{F}_{\mathrm{A}}^{-1})\colon(\mathrm{D}\boldsymbol{\phi}\mathbf{F}_{\mathrm{A}}^{-1})\,\mathrm{d}V - \int_{\Gamma_{\mathrm{P}}}\mathbf{q}(\boldsymbol{\phi},\frac{\partial}{\partial t}\boldsymbol{\phi})\cdot\boldsymbol{\psi}\,\mathrm{d}A\,, \tag{6.11b}$$

$$f_{\mathbf{u}}(\boldsymbol{\psi}) = \int_\Omega \mathbf{P}_0\boldsymbol{\psi}\,\mathrm{d}V - \int_{\Gamma_{\mathrm{N}}} p\mathbf{n}\cdot\boldsymbol{\psi}\,\mathrm{d}A\,, \tag{6.11c}$$

where $\mathbf{P}_0$ is the prestress tensor from section 5.3.4 ensuring $\mathbf{u}_0 = \mathbf{0}$. For the cellular tension $\mathbf{k}$ and stretch $\gamma_{\mathbf{f}}$, we use the same assumptions as in section 6.1.3.

Problem 6.45 (Weak formulation of cardiac elastodynamics): *Let $m_v, a_v, m_{\mathbf{u}}, a_{\mathbf{u}}, f_v, f_{\mathbf{u}}$ be the bilinear and linear forms introduced in (6.2) and (6.11). Find*

$$\begin{aligned}
v &\in \mathcal{L}^2([0,T],\mathcal{H}^1(\Omega_{\mathrm{EP}}))\,, & \mathbf{u} &\in \mathcal{L}^2([0,T];\mathcal{W}^{1,p}(\Omega)^3)\,,\\
\mathbf{w} &\in \mathcal{C}([0,T];\mathcal{L}^2(\Omega_{\mathrm{EP}})^{d_{\mathbf{w}}})\,, & \mathbf{c} &\in \mathcal{C}([0,T];\mathcal{L}^2(\Omega_{\mathrm{EP}})^{d_{\mathbf{c}}})\,,\\
\mathbf{k} &\in \mathcal{C}([0,T];\mathcal{L}^2(\Omega_{\mathrm{EP}})^{d_{\mathbf{k}}})\,, & \gamma_{\mathbf{f}} &\in \mathcal{C}([0,T];\mathcal{L}^2(\Omega_{\mathrm{EP}}))
\end{aligned}$$

with

$$0\le w_i(t,\mathbf{x})\le 1\,,\ i=1,\dots,d_{\mathbf{w}}\,,\qquad c_j(t,\mathbf{x})>0\,,\ j=1,\dots,d_{\mathbf{c}}\qquad \textit{for a.e.}(t,\mathbf{x})\,,$$

such that for almost every $t \in (0,T)$, it holds

$$
\begin{aligned}
m_v(\frac{\partial}{\partial t}v,\phi) + a_v(v,\phi) &= f_v(v,\phi) && \forall\, \phi \in \mathcal{H}^1(\Omega_{\mathrm{EP}})\,, && (6.12a)\\
\int_{\Omega_{\mathrm{EP}}} \frac{\partial}{\partial t}\mathbf{w}\cdot\boldsymbol{\phi}_{\mathbf{w}}\,\mathrm{d}V &= \int_{\Omega_{\mathrm{EP}}} \mathbf{G}_{\mathbf{w}}(v,\mathbf{w},\mathbf{c})\cdot\boldsymbol{\phi}_{\mathbf{w}}\,\mathrm{d}V && \forall \boldsymbol{\phi}_{\mathbf{w}} \in \mathcal{L}^2(\Omega_{\mathrm{EP}})^{d_{\mathbf{w}}}\,, && (6.12b)\\
\int_{\Omega_{\mathrm{EP}}} \frac{\partial}{\partial t}\mathbf{c}\cdot\boldsymbol{\phi}_{\mathbf{c}}\,\mathrm{d}V &= \int_{\Omega_{\mathrm{EP}}} \mathbf{G}_{\mathbf{c}}(v,\mathbf{w},\mathbf{c})\cdot\boldsymbol{\phi}_{\mathbf{c}}\,\mathrm{d}V && \forall \boldsymbol{\phi}_{\mathbf{c}} \in \mathcal{L}^2(\Omega_{\mathrm{EP}})^{d_{\mathbf{c}}}\,, && (6.12c)\\
\int_{\Omega_{\mathrm{EP}}} \frac{\partial}{\partial t}\mathbf{k}\cdot\boldsymbol{\phi}_{\mathbf{k}}\,\mathrm{d}V &= \int_{\Omega_{\mathrm{EP}}} \mathbf{G}_{\mathbf{k}}(\mathbf{w},\mathbf{c},\mathbf{k},\gamma_{\mathbf{f}},\frac{\partial}{\partial t}\gamma_{\mathbf{f}})\cdot\boldsymbol{\phi}_{\mathbf{k}}\,\mathrm{d}V && \forall \boldsymbol{\phi}_{\mathbf{k}} \in \mathcal{L}^2(\Omega_{\mathrm{EP}})^{d_{\mathbf{k}}}\,, && (6.12d)\\
\int_{\Omega_{\mathrm{EP}}} \frac{\partial}{\partial t}\gamma_{\mathbf{f}}\cdot\boldsymbol{\phi}_{\mathbf{w}}\,\mathrm{d}V &= \int_{\Omega_{\mathrm{EP}}} \mathbf{G}_{\gamma_{\mathbf{f}}}(\mathbf{c},\mathbf{k},\gamma_{\mathbf{f}},\frac{\partial}{\partial t}\gamma_{\mathbf{f}},\mathbf{F})\cdot\boldsymbol{\phi}_{\gamma_{\mathbf{f}}}\,\mathrm{d}V && \forall \boldsymbol{\phi}_{\gamma_{\mathbf{f}}} \in \mathcal{L}^2(\Omega_{\mathrm{EP}})\,, && (6.12e)\\
m_{\mathbf{u}}(\mathbf{u},\boldsymbol{\phi}) + a_{\mathbf{u}}(\mathbf{u},\boldsymbol{\phi}) &= f_{\mathbf{u}}(\frac{\partial^2}{\partial t^2}\mathbf{u},\boldsymbol{\phi}) && \forall\, \boldsymbol{\phi} \in \mathcal{W}_0^{1,p}(\Omega)\,. && (6.12f)
\end{aligned}
$$

6.3 Approximation of variational problems

To calculate approximate solutions of a variational problem (VP), we replace the spaces $\mathcal{V},\mathcal{W}$ with finite-dimensional subspaces $\mathcal{V}_h \subset \mathcal{V}$ and $\mathcal{W}_h \subset \mathcal{W}$.

Remark 6.46: For $\mathcal{V}_h \subset \mathcal{V}$, $\mathcal{W}_h \subset \mathcal{W}$, the approximation setting is called *conformal*. Within this work, we only consider conforming methods.

Problem 6.47: *Let $b \in \mathcal{B}(\mathcal{V}_h,\mathcal{W}_h)$ and $\ell \in \mathcal{W}_h^*$. Find $\phi_h \in \mathcal{V}_h$, such that*

$$b(\phi_h,\psi_h) = \ell(\psi_h) \qquad \forall\, \psi_h \in \mathcal{W}_h\,. \tag{VP$_\mathrm{h}$}$$

Just as with the original variational problem (VP), the discrete problem (VP$_\mathrm{h}$) has a unique solution if and only if there exists a $\beta_h > 0$ such that

$$\inf_{\psi_h\in\mathcal{W}_h}\ \sup_{\phi_h\in\mathcal{V}_h} \frac{b(\phi_h,\psi_h)}{\|\phi_h\|_{\mathcal{V}_h}\,\|\psi_h\|_{\mathcal{W}_h}} \geq \beta_h \tag{6.13a}$$

and

$$\forall\, \psi_h \in \mathcal{W}_h \exists\, \phi_h \in \mathcal{V}_h : b(\phi_h,\psi_h) \neq 0\,. \tag{6.13b}$$

Note that (6.1) does not imply (6.13a), since $\mathcal{W}_h \subset \mathcal{W}$. A similar argument holds for the second condition of theorem 6.17.

Lemma 6.48: *Let $\dim(\mathcal{V}_h), \dim(\mathcal{W}_h) < \infty$. Then, if $\dim(\mathcal{V}_h) = \dim(\mathcal{W}_h)$, it holds*

$$(6.13a) \iff (6.13b)\,.$$

Proof. See [53, proposition 2.21] □

Assume that for the spaces $\mathcal{V}$, $\mathcal{W}$, the variational problem (VP) is well-posed. Then the well-posedness of (VP$_\mathrm{h}$) can be examined without explicitly providing the validity of (6.13a).

Lemma 6.49 (Fortin criterion): *Let $\mathcal{V}, \mathcal{W}$ be Hilbert spaces and $\mathcal{V}_h \subset \mathcal{V}$, $\mathcal{W}_h \subset \mathcal{W}$ be closed. Let $b \in \mathcal{B}(\mathcal{V}; \mathcal{W})$ satisfy (6.1). Then, b satisfies the discrete inf-sup condition (6.13a) if and only if there exists a $\Pi_h \in \mathcal{L}in(\mathcal{W}; \mathcal{W}_h)$, such that*

$$b(\phi_h, \Pi_h \psi) = b(\phi_h, \psi) \qquad \forall\, \phi_h \in \mathcal{V}_h, \psi \in \mathcal{W}\,.$$

Proof. See [53, lemma 4.19]. □

We call the operator Π_h in lemma 6.49 *interpolation operator*.

Remark 6.50: Our conforming setting, i.e., assuming $\mathcal{V}_h \subset \mathcal{V}$, $\mathcal{W}_h \subset \mathcal{W}$ are finite dimensional subspaces with $\dim(\mathcal{V}_h) = \dim(\mathcal{W}_h)$, is a special case of lemma 6.49.

We finish the theory of approximation of variational formulations at this point and refer to [12, 53] for a more thourough investigation of approximation theory.

6.4 Discretization in space

We briefly introduce the conforming finite element spaces as approximation spaces for the equations (6.12a)-(6.12f). For an in-depth description of triangulations and conforming finite elements, we refer to [9, 35, 53].
Let Ω_h be an admissible, uniform triangulation of Ω into polyhedral cells with maximum cell diameter h. We write this decomposition as

$$\overline{\Omega} = \bigcup_{K \in \Omega_h} \overline{K}\,.$$

For our purposes, all K will be simplicial elements, i.e. triangles for $d = 2$ and tetrahedrons for $d = 3$.

Definition 6.51: Let $l \in \mathbb{N}$ and let $\mathbb{P}^l(K)$ be the set of all polynomials of degree l defined on a simplex K. We call

$$\mathbb{S}^{l,p}(\Omega_h) \coloneqq \left\{ \phi_h \in \mathcal{H}^p(\Omega) \cap \mathcal{C}(\overline{\Omega}) \colon \phi\big|_K \in \mathbb{P}^l(K) \quad \forall\, K \in \Omega_h \right\}$$

the *Lagrange finite element space*.

Lemma 6.52: *Let Ω_h be a triangulation of Ω into tetrahedra. For $K \in \Omega_h$, let $N_K \in \mathbb{N}$ be the number of nodal points on K within the finite element space $\mathbb{S}^{l,p}(\Omega_h)$ (see Figure 6.1). Then the nodal basis functions $\phi_h \in \mathbb{S}^{l,p}$ are uniquely determined by the interpolation problem*

$$\phi_{h,j}(\mathbf{x}_{K,i}) = \delta_{ij} \qquad i, j = 1, \ldots, N_K \qquad \forall K \in \Omega_h\,.$$

Proof. See [35, section II.5]. □

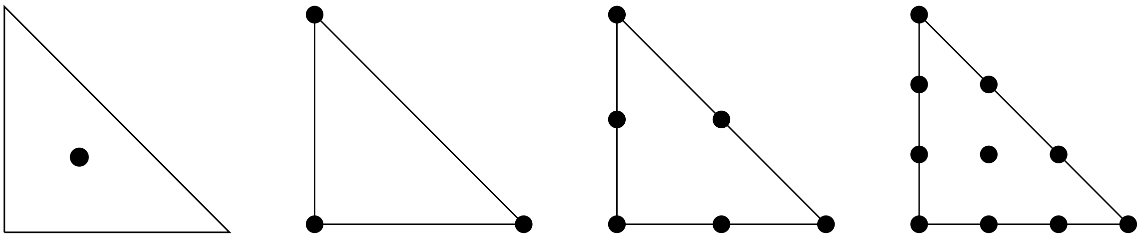

Figure 6.1: Nodal points of the finite element space $\mathbb{S}^{l,p}$ for $l = 0, 1, 2, 3$ on a triangle

We call $\mathcal{N}(\Omega) = \bigcup_{K\in\Omega_h} \{\mathbf{x}_{K,i} \colon i = 1, \ldots N_K\}$ the set of all *nodalpoints* in $\mathbb{S}^{l,p}(\Omega)$.

Theorem 6.53: *Let $1 \le p \le \infty$ and $\phi \in \mathcal{W}^{k+1,p}(\Omega)$. Let further be $0 \le k \le l$. There exists an interpolation operator $\Pi_h \colon \mathcal{W}^{k+1,p}(\Omega) \to \mathbb{S}^{l,p}$ and $C > 0$ such that*

$$\|\phi - \Pi_h\phi\|_{1,p} \le Ch^k \|\phi\|_{k+1,p} .$$

For $p < \infty$ it holds

$$\lim_{h\to 0} \left(\inf_{\phi_h\in\mathbb{S}^{l,p}} \|\phi - \phi_h\|_{1,p} \right) = 0 \qquad \forall\, \phi \in \mathcal{W}^{1,p} .$$

Proof. See [53, corollary 1.110]. Our statement is a special case for Lagrange finite elements, also detailed in the subsequent example. □

For every $K \in \Omega_h$, we choose a quadrature formula with $Q \in \mathbb{N}$ quadrature points $\mathbf{x}_{K,q} \in \overline{K}$ and weights $\omega_{K,q} \ge 0$ for $q = 1, \ldots, Q$, such that

$$\int_K \phi_h(\mathbf{x})\, \mathrm{d}V = \sum_{q=1}^{Q} \omega_{K,q}\phi_h(\mathbf{x}_{K,q}) \qquad \phi_h \in \mathbb{S}^{l,p} . \tag{6.14}$$

Definition 6.54: Consider the quadrature formula (6.14). We call the operator $\Lambda_h \in \mathcal{L}^p(\mathcal{C}(\overline{\Omega}); \mathbb{S}^{l,p}(\Omega_h)^*)$ implicitly defined by the property

$$\int_\Omega \Lambda_h\phi \cdot \psi_h\, \mathrm{d}V = \sum_{K\in\Omega_h} \sum_{q=1}^{Q} \omega_{K,q}\phi(\mathbf{x}_{K,q})\psi_h(\mathbf{x}_{K,q}) , \qquad \phi \in \mathcal{C}(\overline{\Omega}) , \psi_h \in \mathbb{S}^{l,p}(\Omega_h) . \tag{6.15}$$

the *numerical integration operator.*

For the weak coupled formulation (6.12), we choose the finite dimensional subspaces

$$\mathcal{V}_h = \mathcal{W}_h = \mathbb{S}^{l_v,1}(\Omega_{\mathrm{EP},h}) \times \mathbb{S}^{l_v,0}(\Omega_{\mathrm{EP},h}) \times \mathbb{S}^{l_v,0}(\Omega_{\mathrm{EP},h}) \times \mathbb{S}^{l_v,0}(\Omega_{\mathrm{EP},h}) \times \mathbb{S}^{l_v,0}(\Omega_{\mathrm{EP},h}) \times \mathbb{S}^{l_{\mathbf{u}},1}(\Omega_h) . \tag{6.16}$$

Note that this yields to sets of nodalpoints, $\mathcal{N}_{\mathrm{EP},h}$ and $\mathcal{N}_h$, containing N_h and $N_{\mathrm{EP},h}$ points, respectively. For each variable, we get the corresponding nodal basis

$$\phi_i^v, \boldsymbol{\phi}_i^{\mathbf{w}}, \phi_i^{\mathbf{c}}, \phi_i^{\mathbf{k}}, \phi_i^{\gamma_{\mathbf{f}}} , \quad i = 1, \ldots, N_{\mathrm{EP},h} \qquad \text{and} \qquad \boldsymbol{\phi}_j^{\mathbf{u}} , \quad j = 1, \ldots N_h .$$

For every $t \in [0,T]$, we can write $v_h(t,\cdot) \in \mathbb{S}^{l,1}(\Omega_{\mathrm{EP},h})$ in its basis representation

$$v_h(t,\mathbf{x}) = \sum_{i=1}^{N_{\mathrm{EP},h}} v_i(t)\phi_i(\mathbf{x})\,.$$

The discrete basis representation of v_h is therefore given by the vector

$$\widehat{v}(t) = (v_1(t),\ldots,v_{N_{\mathrm{EP},h}}(t))^\top\,.$$

Similarly $\mathbf{w}_h, \mathbf{c}_h, \mathbf{k}_h, \gamma_{\mathbf{f},h}, \mathbf{u}_h$ are discretized in their respective finite element spaces. This yields the following space-discretized system of (6.12)

Problem 6.55 (Space discretized coupled problem): *Let $\mathcal{V}_h = \mathcal{W}_h$ be as in (6.16). Define the following matrices with entries*

$$\begin{aligned}
&(\mathfrak{M}_v)_{ij} := m_v(\phi_i^v,\phi_j^v)\,, && (\mathfrak{A}_v)_{ij} := a_v(\phi_i^v,\phi_j^v)\,, && i,j = 1,\ldots,N_{\mathrm{EP},h}\\
&(\mathfrak{M}_{\mathbf{u}})_{ij} := m_{\mathbf{u}}(\boldsymbol{\phi}_i^{\mathbf{u}},\boldsymbol{\phi}_j^{\mathbf{u}})\,, && (\mathfrak{A}_{\mathbf{u}})_{ij} := a_{\mathbf{u}}(\boldsymbol{\phi}_i^{\mathbf{u}},\boldsymbol{\phi}_j^{\mathbf{u}})\,, && i,j = 1,\ldots,N_h
\end{aligned}$$

and the right-hand sides with entries for $i = 1,\ldots,N_{\mathrm{EP},h}$ and $j = 1,\ldots,N_h$

$$(\mathfrak{f}_v)_i := f_v(\phi_i^v)\,, \qquad (\mathfrak{f}_{\mathbf{u}})_j := f_{\mathbf{u}}(\boldsymbol{\phi}_j^{\mathbf{u}})\,.$$

Find $(v_h, \mathbf{w}_h, \mathbf{c}_h, \mathbf{k}_h, \gamma_{\mathbf{f},h}, \mathbf{u}_h) \in \mathcal{V}_h$ such that the discrete equations

$$\mathfrak{M}_v \frac{\partial}{\partial t}\widehat{v} + \mathfrak{A}_v \widehat{v} = \mathfrak{f}_v\,, \tag{6.17a}$$

$$\frac{\partial}{\partial t}\widehat{\mathbf{w}}_i - \mathbf{G}_{\mathbf{w}}(\widehat{v}_i, \widehat{\mathbf{w}}_i, \widehat{\mathbf{c}}_i) = 0\,, \qquad i = 1,\ldots,N_{\mathrm{EP},h}\,, \tag{6.17b}$$

$$\frac{\partial}{\partial t}\widehat{\mathbf{c}}_i - \mathbf{G}_{\mathbf{c}}(\widehat{v}_i, \widehat{\mathbf{w}}_i, \widehat{\mathbf{c}}_i) = 0\,, \qquad i = 1,\ldots,N_{\mathrm{EP},h}\,, \tag{6.17c}$$

$$\frac{\partial}{\partial t}\widehat{\mathbf{k}}_i - \mathbf{G}_{\mathbf{w}}(\widehat{\mathbf{w}}_i, \widehat{\mathbf{c}}_i, \widehat{\mathbf{k}}_i, \widehat{\gamma_{\mathbf{f}}}_i) = 0\,, \qquad i = 1,\ldots,N_{\mathrm{EP},h}\,, \tag{6.17d}$$

$$\frac{\partial}{\partial t}\widehat{\gamma_{\mathbf{f}}}_i - \mathbf{G}_{\gamma_{\mathbf{f}}}(\widehat{\mathbf{k}}_i, \widehat{\gamma_{\mathbf{f}}}_i, \mathbf{I} + \mathrm{D}\widehat{\mathbf{u}}_i) = 0\,, \qquad i = 1,\ldots,N_{\mathrm{EP},h}\,, \tag{6.17e}$$

$$\mathfrak{M}_{\mathbf{u}} \frac{\partial^2}{\partial t^2}\widehat{v} + \mathfrak{A}_{\mathbf{u}} \widehat{\mathbf{u}} = \mathfrak{f}_{\mathbf{u}} \tag{6.17f}$$

with the initial conditions

$$\begin{aligned}
\widehat{v}(0) &= \Pi_h v_0\,, & \widehat{\mathbf{w}}(0) &= \Pi_h \mathbf{w}_0\,, & \widehat{\mathbf{c}}(0) &= \Pi_h \mathbf{c}_0\,,\\
\widehat{\mathbf{k}}(0) &= \Pi_h \mathbf{k}_0\,, & \widehat{\gamma_{\mathbf{f}}}(0) &= \Pi_h \gamma_{\mathbf{f},0}\,, & \widehat{\mathbf{u}}(0) &= \Pi_h \mathbf{u}_0\,.
\end{aligned} \tag{6.17g}$$

Remark 6.56: Note that the space-discrete formulations (6.17b)–(6.17e) are independently given at each nodal point $\mathbf{x}_i \in \mathcal{N}_{\mathrm{EP},h}$. This stems from the assumption that the intracellular gating mechanisms are independent of one another.

To finalize this section, we apply the integration operator Λ_h from (6.15) on $\mathfrak{M}, \mathfrak{A}$ and $\mathfrak{f}$. For (6.17a), this yields the matrices and vectors with entries for $i, j = 1, \dots, N_{\mathrm{EP},h}$

$$(\mathbb{M}_v)_{ij} = \sum_{K\in\Omega_h} \sum_{q=1}^{Q} \omega_{K,q} \phi_i^v(\mathbf{x}_{K,q}) \phi_j^v(\mathbf{x}_{K,q}) \,, \tag{6.18a}$$

$$(\mathbb{A}_v)_{ij} = \sum_{K\in\Omega_h} \sum_{q=1}^{Q} \omega_{K,q} \left(\mathbf{D}\, \mathrm{D}\phi_i^v(\mathbf{x}_{K,q})\right) \cdot \mathrm{D}\phi_j^v(\mathbf{x}_{K,q}) \,, \tag{6.18b}$$

$$(\mathbb{I}_{\mathrm{ion}})_i = \sum_{K\in\Omega_h} \sum_{q=1}^{Q} \omega_{K,q} I_{\mathrm{ion}} \left(v_h(\mathbf{x}_{K,q}), \mathbf{w}_h(\mathbf{x}_{K,q}), \mathbf{c}_h(\mathbf{x}_{K,q})\right) \phi_i(\mathbf{x}_{K,q}) \,. \tag{6.18c}$$

Similarly, for $i, j = 1, \dots, N_h$, we get the corresponding matrices and vectors for equation (6.17f):

$$(\mathbb{M}_{\mathbf{u}})_{ij} = \sum_{K\in\Omega_h} \sum_{q=1}^{Q} \omega_{K,q} \boldsymbol{\phi}_j^{\mathbf{u}}(\mathbf{x}_{K,q}) \cdot \boldsymbol{\phi}_i^{\mathbf{u}}(\mathbf{x}_{K,q}) \,, \tag{6.18d}$$

$$(\mathbb{A}_{\mathbf{u}})_i = \sum_{K\in\Omega_h} \mathbf{P}\left((\mathbf{I} + \mathrm{D}\mathbf{u}_h(\mathbf{x}_{K,q}))\mathbf{F}_{\mathrm{A}}^{-1}(\gamma_{\mathbf{f},h}(\mathbf{x}_{K,q}))\right) : \mathrm{D}\boldsymbol{\phi}_i^{\mathbf{u}}(\mathbf{x}_{K,q})\mathbf{F}_{\mathrm{A}}^{-1}(\gamma_{\mathbf{f},h}(\mathbf{x}_{K,q})) \,, \tag{6.18e}$$

$$(\mathbb{T}_k)_{ij} = \sum_{K\in\Omega_h\cap\Gamma_{\mathrm{P}}} \sum_{f_K\in K} \sum_{q=1}^{Q_f} \omega_{f_K,q}\, k_{\mathrm{P}}(\mathbf{n}_{f_K} \otimes \mathbf{n}_{f_K}) \boldsymbol{\phi}_j^{\mathbf{u}}(\mathbf{x}_{f_K,q}) \cdot \boldsymbol{\phi}_i^{\mathbf{u}}(\mathbf{x}_{f_K,q}) \,, \tag{6.18f}$$

$$(\mathbb{T}_c)_{ij} = \sum_{K\in\Omega_h\cap\Gamma_{\mathrm{P}}} \sum_{f_K\in K} \sum_{q=1}^{Q_f} \omega_{f_K,q}\, c_{\mathrm{P}}(\mathbf{n}_{f_K} \otimes \mathbf{n}_{f_K}) \boldsymbol{\phi}_j^{\mathbf{u}}(\mathbf{x}_{f_K,q}) \cdot \boldsymbol{\phi}_i^{\mathbf{u}}(\mathbf{x}_{f_K,q}) \,, \tag{6.18g}$$

$$(\mathbb{P})_i = \sum_{K\in\Omega_h\cap\Gamma_{\mathrm{N}}} \sum_{f_K\in K} \sum_{q=1}^{Q_f} \omega_{f_K,q}\, p(t) \mathbf{n}_{f_K} \cdot \boldsymbol{\phi}_i^{\mathbf{u}}(\mathbf{x}_{f_K,q}) \,. \tag{6.18h}$$

The two equations for the PDEs (6.17a) and (6.9) can thus be described by the system

$$\mathbb{M}_v \frac{\partial}{\partial t}\widehat{v}(t) + \mathbb{A}_v \widehat{v}(t) + \mathbb{I}_{\mathrm{ion}}(\widehat{v}(t), \widehat{\mathbf{w}}(t), \widehat{\mathbf{c}}(t)) = \mathbb{I}_{\mathrm{ext}}(t), \tag{6.19a}$$

$$\mathbb{M}_{\mathbf{u}} \frac{\partial^2}{\partial t^2}\widehat{\mathbf{u}}(t) + \mathbb{T}_c \frac{\partial}{\partial t}\widehat{\mathbf{u}}(t) + \mathbb{T}_k \widehat{\mathbf{u}}(t) + \mathbb{A}_{\mathbf{u}}(\widehat{\mathbf{u}}(t), \widehat{\gamma_{\mathbf{f}}}(t)) = \mathbb{P}(t) \,. \tag{6.19b}$$

where we set $\mathbb{I}_{\mathrm{ext}}(t) \coloneqq \Pi_h I_{\mathrm{ext}}(t)$

6.5 Discretization in time

Let $v_h, \mathbf{w}_h, \mathbf{c}_h, \mathbf{k}_h, \gamma_{\mathbf{f},h}, \mathbf{u}_h$ be the space-discretized vectors from the previous section with nodalpoint representations

$$\widehat{v}, \widehat{\mathbf{w}}, \widehat{\mathbf{c}}, \widehat{\mathbf{k}}, \widehat{\gamma_{\mathbf{f}}}, \widehat{\mathbf{u}} \,.$$

The equations for the electrophysiological problem (6.17a)-(6.17e) and the mechanical problem (6.17f) are treated separately with respect to their time discretization. We split the interval $[0,T]$ into $N_T \in \mathbb{N}$ equidistant time steps $t_0 = 0, t_1, \dots, t_N = T$ and denote uniform stepsize by $\Delta t = \frac{T}{N_T}$ and the discretized interval by

$$\mathcal{T} \coloneqq \{t_n = n\Delta t \colon n = 0, \dots, N_T\} .$$

To ease notation, we write for any mapping $f : [0,T] \times \mathcal{X} \to \mathcal{Y}$ that

$$f^n(\mathbf{x}) \coloneqq f(t_n, \mathbf{x}) , \qquad t_n \in \mathcal{T} .$$

We use a semi-implicit decoupled time-stepping scheme for the electrophysiological system similar to the one presented in [54]. This scheme decouples the systems of ODEs (6.17b)-(6.17e) from the parabolic PDE (6.17a). In a first step, the system of ODEs is solved by an explicit method. We use a scheme similar to the one presented in [63]. When using the Beeler-Reuter cell model, the evolution of the components of $\widehat{\mathbf{w}}$ is given by

$$\frac{\partial}{\partial t}\widehat{w}_j = \alpha_j(\widehat{v}) - \widehat{w}_j \cdot (\alpha_j(\widehat{v}) + \beta_j(\widehat{v})) , \qquad j = 1, \dots, 6 . \tag{6.20}$$

Each of these equations is solved exactly with the exponential integrator

$$\begin{aligned} G_j(\widehat{v}, \widehat{w}_j) &\coloneqq \widehat{w}_{j,\infty}(\widehat{v}) + (\widehat{w}_j - \widehat{w}_{j,\infty}(\widehat{v})) \exp\big(- \Delta t(\alpha_j(\widehat{v}) + \beta_j(\widehat{v}))\big) , \\ \widehat{w}_{j,\infty}(\widehat{v}) &= \frac{\alpha_j(\widehat{v})}{\alpha_j(\widehat{v}) + \beta_j(\widehat{v})} . \end{aligned}$$

Then the evolution equations (6.20) are solved exactly on $[t_{n-1}, t_n]$ by

$$\widehat{w}_j^n = G_j(\widehat{v}^{n-1}, \widehat{w}_j^{n-1}) .$$

We therefore set the discretized evolultion operator for $\mathbf{w}$ to

$$\mathbf{G}^n_{\mathbf{w}}(\widehat{v}, \widehat{\mathbf{w}}) \coloneqq \big(G_j(\widehat{v}^{n-1}, \widehat{w}_j^{n-1})\big)_{j=1,\dots,d_{\mathbf{w}}} , \qquad n = 1, \dots, N_T . \tag{6.21}$$

The ordinary differential equations for $\mathbf{c}, \mathbf{k}$ and $\gamma_{\mathbf{f}}$ are solved by a standard explicit Euler method:

$$\widehat{\mathbf{c}}^{n+1} = \widehat{\mathbf{c}}^n + \Delta t \mathbf{G}_{\mathbf{c}}\left(\widehat{v}^n, \widehat{\mathbf{w}}^n, \widehat{\mathbf{c}}^n\right) , \tag{6.22a}$$

$$\widehat{\mathbf{k}}^{n+1} = \widehat{\mathbf{k}}^n + \Delta t \mathbf{G}_{\mathbf{k}}\left(\widehat{\mathbf{w}}^n, \widehat{\mathbf{c}}^n, \widehat{\mathbf{k}}^n, \widehat{\gamma_{\mathbf{f}}}^n\right) , \tag{6.22b}$$

$$\widehat{\gamma_{\mathbf{f}}}^{n+1} = \widehat{\gamma_{\mathbf{f}}}^n + \Delta t \mathbf{G}_{\gamma_{\mathbf{f}}}\left(\widehat{\mathbf{k}}^n, \widehat{\gamma_{\mathbf{f}}}^n, \mathbf{I} + \mathrm{D}\widehat{\mathbf{u}}\right) , \tag{6.22c}$$

We choose this simple method since the ODEs for $\mathbf{c}$, $\mathbf{k}$ and $\gamma_{\mathbf{f}}$ are much less stiff than the one for $\mathbf{w}$. The scheme

$$\widehat{\mathbf{w}}^{n+1} = \mathbf{G}^{n+1}_{\mathbf{w}}(\widehat{v}, \widehat{\mathbf{w}}) \tag{6.23}$$

is only applicable for small timesteps Δt, as the coefficients α_j, β_j, $j = 1, \dots, 6$ are not constant. Because of the high stiffness of (6.17b) for each $i = 1, \dots, N_{\mathrm{EP},h}$, this method is

nevertheless applicable for larger timesteps as a standard explicit method, such as Runge-Kutta methods. Preliminary studies show that a higher order explicit method for (6.22) does not yield better time convergence.
Given the gating and concentration vector $\widehat{\mathbf{w}}^{n+1}, \widehat{\mathbf{c}}^{n+1}$, we solve in a second step the PDE for the transmembrane voltage. We use the generalized scheme presented by Sundnes et al. [156, section 3.2.2]. Consider the system (6.19a), i.e.,

$$\mathbb{M}_v \frac{\partial}{\partial t}\widehat{v} = -\mathbb{A}_v\widehat{v} - \mathbb{I}_{\text{ion}}(\widehat{v}, \widehat{\mathbf{w}}, \widehat{\mathbf{c}}) + \mathbb{I}_{\text{ext}}\,.$$

Define $\mathbb{I}^n_{\text{total}}(\widehat{v}, \widehat{\mathbf{w}}, \widehat{\mathbf{c}}) := \mathbb{I}_{\text{ion}}(\widehat{v}, \widehat{\mathbf{w}}, \widehat{\mathbf{c}}) - \mathbb{I}_{\text{ext}}(t_n)$. For $\theta_{\text{CN}} \in [0, 1]$, we approximate (6.19a) in $[0, T]$ by

$$\mathbb{M}_v \frac{\widehat{v}^{n+1} - \widehat{v}^n}{\Delta t} = \theta_{\text{CN}}\left(-\mathbb{A}_v\widehat{v}^{n+1} - \mathbb{I}^{n+1}_{\text{total}}(\widehat{v}^{n+1}, \widehat{\mathbf{w}}, \widehat{\mathbf{c}})\right) + (1-\theta_{\text{CN}})\left(-\mathbb{A}_v\widehat{v}^n - \mathbb{I}^n_{\text{total}}(\widehat{v}^n, \widehat{\mathbf{w}}, \widehat{\mathbf{c}})\right)\,. \quad (6.24)$$

This method translates to an explicit Euler scheme for $\theta_{\text{CN}} = 0$ and to an implicit Euler scheme for $\theta_{\text{CN}} = 1$. Choosing $\theta_{\text{CN}} = \frac{1}{2}$ yields the *Crank-Nicholson* scheme which is of second order with respect to time. To ease computational load, we choose $\theta_{\text{CN}} = 1$. We then decouple the diffusion part from the reaction part $\mathbb{I}_{\text{ion}}$ by means of a Godunov-Splitting [127], yielding the system

$$\widehat{v}^{n+\frac{1}{2}} = \widehat{v}^n - \Delta t\left(\mathbb{I}_{\text{ion}}(\widehat{v}^n, \mathbf{w}^{n+1}, \mathbf{c}^{n+1}) - \mathbb{I}^n_{\text{ext}}\right)\,, \quad (6.25a)$$

$$(\mathbb{M}_v + \Delta t\mathbb{A}_v)\widehat{v}^{n+1} = \mathbb{M}_v\widehat{v}^{n+\frac{1}{2}}\,. \quad (6.25b)$$

Algorithm 1 Electrophysiological time stepping

Require: $T_{\text{start}}, T_{\text{end}}$

Set $N > 0$ and $t_0 = T_{\text{start}}$, $t_N = T_{\text{end}}$

$$\widehat{v}^0 = \widehat{v}(t_0),\ \widehat{\mathbf{w}}^0 = \widehat{\mathbf{w}}(t_0),\ \widehat{\mathbf{c}}^0 = \widehat{\mathbf{c}}(t_0),\ \widehat{\mathbf{k}}^0 = \widehat{\mathbf{k}}(t_0),\ \widehat{\gamma_{\mathbf{f}}}^0 = \widehat{\gamma_{\mathbf{f}}}(t_0)$$

with the initial conditions (6.17g)

for $n = 0$; $n < N$; $n++$ **do**

Calculate $\mathbf{w}^{n+1}$ by (6.23)

Calculate v^{n+1} by (6.25)

Calculate $\widehat{\mathbf{c}}^{n+1}, \widehat{\mathbf{k}}^{n+1}, \widehat{\gamma_{\mathbf{f}}}^{n+1}$ by (6.22)

end for

return $\widehat{v}^N, \widehat{\mathbf{w}}^N, \widehat{\mathbf{c}}^N, \widehat{\mathbf{k}}^N, \widehat{\gamma_{\mathbf{f}}}^N$

Remark 6.57: As depicted in algorithm 1 and contrary to the schemes detailed above, we first solve for v^{n+1} in (6.25) with $\mathbf{w}^{n+1}, \widehat{\mathbf{c}}^n, \widehat{\mathbf{k}}^n, \widehat{\gamma_{\mathbf{f}}}^n$ and calculate the update of the remaining ODEs afterwards. Preliminary results show that this scheme preserves the order of the initial scheme but is much more stable with respect to the timestep size Δt. We refer to the paper in preparation at our research group.

The time discretization of the elasticity equation (6.17f) is done by employing a general *Newmark β-scheme* [88]. Approximating velocity and acceleration with the terms $\frac{\partial}{\partial t}\widehat{\mathbf{u}}^n(\mathbf{x}) \approx \widehat{\mathbf{v}}^n(\mathbf{x})$ and $\frac{\partial^2}{\partial t^2}\widehat{\mathbf{u}}^n(\mathbf{x}) \approx \widehat{\mathbf{a}}^n(\mathbf{x})$, we choose $\beta_\mathrm{N}, \gamma_\mathrm{N} \in [0,1]$ and define the time integration in $[t_n, t_{n+1}]$ by

$$\widehat{\mathbf{u}}^{n+1} = \widehat{\mathbf{u}}^n + \Delta t \widehat{\mathbf{v}}^n + \Delta t^2 \left(\frac{1-2\beta_\mathrm{N}}{2} \widehat{\mathbf{a}}^n + \beta_\mathrm{N} \widehat{\mathbf{a}}^{n+1} \right), \tag{6.26a}$$

$$\widehat{\mathbf{v}}^{n+1} = \widehat{\mathbf{v}}^n + \Delta t \left((1-\gamma_\mathrm{N}) \widehat{\mathbf{a}}^n + \gamma_\mathrm{N} \widehat{\mathbf{a}}^{n+1} \right). \tag{6.26b}$$

Solving (6.26a) for $\widehat{\mathbf{a}}^{n+1}$ yields

$$\widehat{\mathbf{a}}^{n+1} = \frac{1}{\beta_\mathrm{N} \Delta t} \left(\frac{1}{\Delta t} \left(\widehat{\mathbf{u}}^{n+1} - \widehat{\mathbf{u}}^n \right) - \widehat{\mathbf{v}}^n \right) - \frac{1-2\beta_\mathrm{N}}{2\beta_\mathrm{N}} \widehat{\mathbf{a}}^n . \tag{6.26c}$$

and by insertion into (6.26b), we get

$$\widehat{\mathbf{v}}^{n+1} = \frac{\gamma_\mathrm{N}}{\beta_\mathrm{N} \Delta t} \left(\widehat{\mathbf{u}}^{n+1} - \widehat{\mathbf{u}}^n \right) + (1 - \frac{\gamma_\mathrm{N}}{\beta_\mathrm{N}}) \mathbf{v}^n + \Delta t \left(1 - \gamma_\mathrm{N} (1 + \frac{1-2\beta_\mathrm{N}}{2\beta_\mathrm{N}}) \right) \widehat{\mathbf{a}}^n \tag{6.26d}$$

Applying this formulation of $\widehat{\mathbf{a}}^{n+1}$ and $\widehat{\mathbf{v}}^{n+1}$ on (6.17f) then results in the system

$$\mathbb{M}_\mathbf{u} \widehat{\mathbf{a}}^{n+1} + \mathbb{T}_c \frac{\partial}{\partial t} \widehat{\mathbf{v}}^{n+1} + \mathbb{T}_k \widehat{\mathbf{u}}^{n+1} + \mathbb{A}_\mathbf{u}(\widehat{\mathbf{u}}^{n+1}, \widehat{\gamma_\mathbf{f}}) = \mathbb{P}^{n+1}, \tag{6.27}$$

where we set as usual $\mathbb{P}^{n+1} := \mathbb{P}(t_{n+1})$.

Remark 6.58: We intentionally omitted the time index of $\widehat{\gamma_\mathbf{f}}$. The corresponding coupling to the electrophysiological equation (6.22c) is discussed in the next section.

We now solve (6.27) for $\widehat{\mathbf{u}}^{n+1}$ by inserting (6.26c), (6.26d) to get

$$\begin{aligned} &\frac{1}{\beta_\mathrm{N} \Delta t^2} \mathbb{M}_\mathbf{u} \widehat{\mathbf{u}}^{n+1} + \left(\frac{\gamma_\mathrm{N}}{\beta_\mathrm{N} \Delta t} \mathbb{T}_c + \mathbb{T}_k \right) \widehat{\mathbf{u}}^{n+1} + \mathbb{A}_\mathbf{u}(\widehat{\mathbf{u}}^{n+1}, \widehat{\gamma_\mathbf{f}}) \\ &\quad = \mathbb{P}^{n+1} + \left(\frac{1}{\beta_\mathrm{N} \Delta t^2} \mathbb{M}_\mathbf{u} + \frac{\gamma_\mathrm{N}}{\beta_\mathrm{N} \Delta t} \mathbb{T}_c \frac{\partial}{\partial t} \right) \widehat{\mathbf{u}}^n + \left(\frac{1}{\beta_\mathrm{N} \Delta t} \mathbb{M}_\mathbf{u} - \left(1 - \frac{\gamma_\mathrm{N}}{\beta_\mathrm{N}} \right) \mathbb{T}_c \frac{\partial}{\partial t} \right) \widehat{\mathbf{v}}^n \\ &\qquad + \left(\frac{1-2\beta_\mathrm{N}}{2\beta_\mathrm{N}} \mathbb{M}_\mathbf{u} - \Delta t \left(1 - \gamma_\mathrm{N} \left(1 + \frac{1-2\beta_\mathrm{N}}{2\beta_\mathrm{N}} \right) \right) \mathbb{T}_c \frac{\partial}{\partial t} \right) \widehat{\mathbf{a}}^n . \end{aligned} \tag{6.28}$$

The main advantage of the Newmark β-method is the explicit description (6.28), which allows for an efficient computational implementation. Depending on the values of $\beta_\mathrm{N}, \gamma_\mathrm{N}$, this scheme has additional side-effects and benefits, such as a numerical damping for $\gamma_\mathrm{N} > 0.5$.

Theorem 6.59: *The Newmark β-method is uncoditionally stable for $\beta_\mathrm{N} \geq \frac{\gamma_\mathrm{N}}{2} \geq \frac{1}{4}$.*

Proof. See [28, section 6.3.3] □

We refrain from an in-depth stability analysis of the Newmark β-method for our problem in this work but refer to [28, section 6.6.7] instead.

6.6 A segregated algorithm for the coupled problem

In the last two sections, we have seen the discretized equations of the monodomain and elasticity equations, where we left some open remarks concerning the coupling between (6.17e) and (6.9).
We will present the remaining steps for a fully coupled numerical scheme, starting with the handling of the circulatory systems presented in section 5.4.

6.6.1 Circulatory feedback

The circulatory models presented in 5.4.1 and 5.4.2 calculate a pressure p^n at time t_n depending on the volumes of heart chambers of Ω. We denote these volumes by

$$V_{\mathrm{LV}}(\Omega), V_{\mathrm{RV}}(\Omega), V_{\mathrm{LA}}(\Omega), V_{\mathrm{RA}}(\Omega)$$

and the corresponding cavities by $\Omega_{\mathrm{LV}}, \Omega_{\mathrm{RV}}, \Omega_{\mathrm{LA}}, \Omega_{\mathrm{RA}}$.

Remark 6.60: Since we only simulate the heart tissue, it holds $\Omega_{\mathrm{LV}}, \Omega_{\mathrm{RV}}, \Omega_{\mathrm{LA}}, \Omega_{\mathrm{RA}} \not\subseteq \Omega$.

As we have seen in section 4.3, the volume of these cavities for any configuration $\boldsymbol{\varphi}_t$ is given by

$$V_{\mathrm{C}}(\Omega) = \int_{\boldsymbol{\varphi}_t(\Omega_{\mathrm{C}})} 1 \,\mathrm{d}V = \int_{\Omega_{\mathrm{C}}} J(t, \mathbf{x}) \,\mathrm{d}V\,, \qquad \mathrm{C} \in \{\mathrm{LV}, \mathrm{RV}, \mathrm{LA}, \mathrm{RA}\}\,.$$

If the cavity domains Ω_{C} have closed surfaces, the volumes $V_{\mathrm{C}}(\Omega_h)$ can be calculated by the formula

$$V_{\mathrm{C}}(\Omega_h) = \sum_{f_K \subset \Gamma_{\mathrm{C},h}} \frac{1}{6} \boldsymbol{\varphi}(t, \mathbf{x}_{f_K,1}) \cdot \left((\boldsymbol{\varphi}(t, \mathbf{x}_{f_K,2}) - \boldsymbol{\varphi}(t, \mathbf{x}_{f_K,1})) \times (\boldsymbol{\varphi}(t, \mathbf{x}_{f_K,3}) - \boldsymbol{\varphi}(t, \mathbf{x}_{f_K,1})) \right)\,, \tag{6.29}$$

where $\mathbf{x}_{f_K,1}, \mathbf{x}_{f_K,2}, \mathbf{x}_{f_K,3} \in \mathbf{f}_K$ are the corners of the face f_K of the cell K [176].

Algorithm 2 Elastodynamics with circulatory feedback

Require: $\widehat{\mathbf{u}}^n$
  Set $\mathbf{u}^{n,0} = \mathbf{u}^n$ and $m = 0$
  Get initial pressure $p^{n,0}$ from circulatory model
  repeat
    Calculate $\mathbf{u}^{n,m+1}$ from $\mathbf{u}^{n,m}$, $p^{n,m}$ by (6.28)
    Update Circulatory model with $V_{\mathrm{C}}(\boldsymbol{\varphi}^n(\Omega_h))$
    Set $m = m + 1$
  until $|V_{\mathrm{C}}(\boldsymbol{\varphi}^n(\Omega_h)) - V_{\mathrm{C}}| < \varepsilon$ for $\mathrm{C} \in \{\mathrm{LV}, \mathrm{RV}, \mathrm{LA}, \mathrm{RA}\}$
  return $\widehat{\mathbf{u}}^{n+1} = \widehat{\mathbf{u}}^{n,m}$

6.6.2 Transfer operators

In the coupled system proposed in the previous section, the finite element spaces $\mathbb{S}^{l_v,p}(\Omega_{\mathrm{EP},h})$ and $\mathbb{S}^{l_{\mathbf{u}},p}(\Omega_h)$ are not specified to be of the same polynomial degree or mesh-size. This is intended, as the electrophysiology equations (6.17a)–(6.17e) typically require very small step sizes and fine triangulations of the underlying mesh (see e.g. [114]). On the other hand, as we will see in the following chapter, cardiac elasticity (6.17f) performs well even for coarse meshes and broad time steps, but quadratic polynomials should be used. From an efficiency standpoint, it is unsuitable for coupled system to fully operate with quadratic (or higher order) elements on fine space and time discretizations.
For this reason, we allow different refinements of $\Omega_{\mathrm{EP},h}$ and Ω_h and different polynomial degrees on their respective finite element spaces. This however complicates the inclusion of $\widehat{\mathbf{F}} = \mathrm{D}\hat{\mathbf{u}}$ in (6.17e) and $\widehat{\gamma_{\mathbf{f}}}$ in (6.17f).

Definition 6.61: Let $\Omega_{\mathrm{EP}} \subset \Omega$ and Ω_h, $\Omega_{\mathrm{EP},h}$ be their respective triangulations. We call

$$T_{\mathbf{u}}^{v} \colon \mathbb{S}^{l_{\mathbf{u}},p}(\Omega_h \cap \Omega_{\mathrm{EP},h}) \to \mathbb{S}^{l_v,p}(\Omega_{\mathrm{EP},h})\,, \qquad T_v^{\mathbf{u}} \colon \mathbb{S}^{l_v,p}(\Omega_{\mathrm{EP},h}) \to \mathbb{S}^{l_{\mathbf{u}},p}(\Omega_h)$$

transfer operators between the two corresponding finite element spaces.

Such transfer operators are heavily used when applying adaptive or multiscale methods [120]. Within our framework, it is sufficient to choose two basic transfer operations. Let Ω_h be a given triangulation of Ω. We always assume that $\Omega_{\mathrm{EP},h}$ is generated by taking a subset of Ω_h and further refining this set to the desired grid size. This process ensures that the nodalpoints on Ω_{EP} of the coarse mesh are a subset of the fine mesh, i.e.,

$$\mathcal{N}_h \cap \overline{\Omega_{\mathrm{EP}}} \subset \mathcal{N}_{\mathrm{EP},h}\,. \tag{6.30}$$

The assumption makes the following approach applicable:

Definition 6.62: Let $\theta_h \in \mathbb{S}^{l_v,p}(\Omega_{\mathrm{EP},h})$. The transfer operator from $\Omega_{\mathrm{EP},h}$ to Ω_h is defined by the projection

$$(T_v^{\mathbf{u}}\theta_h)(\mathbf{x}) := \begin{cases} \widehat{\theta_h}(\mathbf{x})\,, & \mathbf{x} \in \mathcal{N}_h\,, \\ 0\,, & \text{else}\,. \end{cases}$$

We later only use this operator on $\widehat{\gamma_{\mathbf{f}}}$. Since the non-excitable tissue $\Omega\backslash\Omega_{\mathrm{EP}}$ does not contract actively, it is reasonable to impose $\gamma_{\mathbf{f}} = 0$ on $\mathcal{N}_h \backslash \mathcal{N}_{\mathrm{EP},h}$.

Definition 6.63: Let $\theta_h \in \mathbb{S}^{l_{\mathbf{u}},p}(\Omega_h)$. The transfer operator from Ω_h to $\Omega_{\mathrm{EP},h}$ is defined by the interpolation

$$(T_{\mathbf{u}}^{v}\theta_h)(\mathbf{x}) := \Pi_h^K(\theta_h(\mathbf{x}))\,, \qquad \mathbf{x} \in K \subset \Omega_h\,,$$

where Π_h^K defines the linear interpolation from the nodal points in K.

Algorithm 3 Coupled time stepping

Require: $T_{\mathrm{start}}, T_{\mathrm{end}}$

Calculate prestress $\mathbf{P}_0$ by as solution of (5.22)

Set $N > 0$, $M > 0$ and $t_0 = T_{\mathrm{start}}$, $t_N = T_{\mathrm{end}}$ Choose $\hat{\mathbf{u}}^0 = \mathbf{0}$

for $n = 0$; $n < N$; $n++$ **do**

Transfer $\hat{\mathbf{u}}_v^n = T_{\mathbf{u}}^v \hat{\mathbf{u}}$

Calculate $\widehat{v}^{n+1}$, $\widehat{\mathbf{w}}^{n+1}$, $\widehat{\mathbf{c}}^{n+1}$, $\widehat{\mathbf{k}}^{n+1}$, $\widehat{\gamma_{\mathbf{f}}}^{n+1}$ on $[t_n, t_{n+1}]$ with M timesteps using $\hat{\mathbf{u}}_{\mathrm{EP}}^n$ with the electrophysiological Algorithm 1

Transfer $\widehat{\mathbf{G}_{\gamma_{\mathbf{f}}\mathbf{f},\mathbf{u}}}^{n+1} = T_v^{\mathbf{u}} \widehat{\gamma_{\mathbf{f}}}^{n+1}$

Calculate $\hat{\mathbf{u}}^{n+1}$ as solution of (6.19b) with $\widehat{\mathbf{G}_{\gamma_{\mathbf{f}}\mathbf{f},\mathbf{u}}}^{n+1}$

end for

return $\widehat{v}^N$, $\widehat{\mathbf{w}}^N$ $\widehat{\mathbf{c}}^N$, $\widehat{\mathbf{k}}^N$, $\widehat{\gamma_{\mathbf{f}}}^N$, $\hat{\mathbf{u}}^N$

This ensures $T_{\mathbf{u}}^v \theta_h(\mathbf{x}) = \theta_h(\mathbf{x})$ for $\mathbf{x} \in \mathcal{N}_h \cap \mathcal{N}_{\mathrm{EP},h}$. The remaining nodalpoints $\mathcal{N}_{\mathrm{EP},h} \backslash \mathcal{N}_h$ are then interpolated according to Π_h^K. This concludes the formulation of the segregated algorithm 3.

CHAPTER

SEVEN

NUMERICAL EXPERIMENTS

To conclude the mathematical modeling and approximation of the human heart, this chapter presents numerical simulations of commonly used geometries. After defining some error quantities for application in cardiac elastodynamics, the static elasticity problem is analyzed. The chapter concludes with first numerical convergence results for dynamic problems on a left ventricle.

The presented numerical experiments have been implemented using the parallel finite element framework M++[24]. The framework as well as the applications for cardiac elasticity described in this chapter are open-source projects and all results were obtained with version 1.0.0 of the *CardMech* framework [59]. The data of the results is accessible via this repository as well.

7.1 Error quantities

There are no analytical solutions of finite elasticity problems for the non-linear materials used within this work. Therefore, we cannot evaluate usual error quantities including the exact solutions, i.e.,

$$\|\mathbf{u}^* - \mathbf{u}_h\|_2 \ ,$$

where $\mathbf{u}^*$ is the exact solution.

Definition 7.1: Let $\{\Omega_h\}$ be a series of uniform mesh refinements with $h \to 0$. We call κ the *convergence rate* of an error quantity e, if

$$e(h) = h^\kappa C \qquad \text{asymptotically for } h \to 0$$

with C independent of h.

Let $\Omega_{h,0}$ be an initial triangulation of Ω. The refinement of $\Omega_{h,0}$ is performed by a bisection of all edges of $\Omega_{h,0}$, yielding a new triangulation $\Omega_{h,1}$. Each refinement $\Omega_{h,l}$ is generated by l iterative bisections of $\Omega_{h,0}$ and we call l the *level* of our refinement. Then $\{\Omega_{h,l}\}$ is a series of uniform mesh refinements. If $\Omega_{h,l}$ consists of N tetrahedra, then $\Omega_{h,l+1}$ contains $N \cdot 2^3$ tetrahedra and its maximum cell diameter h is halved.

Remark 7.2: The optimal convergence rate $\kappa_{\mathcal{L}^2}$ for $\|\cdot\|_2$ is given by $p+1$, where p is the polynomial degree of the finite element space $\mathbb{S}^{p,k}(\Omega_h)$. [16]

Since we cannot compute analytical convergence rates, we have to deduce them from the error quantities of our simulations. From these observation, we state an *experimental order of convergece* (EOC).

Definition 7.3: Let e_l, e_{l+1} be error quantities on subsequent levels. We call

$$R_l = \frac{e_l}{e_{l+1}} = \left(\frac{h_{l+1}}{h_l}\right)^{\mathrm{EOC}} = \left(\frac{1}{2}\right)^{\mathrm{EOC}}$$

the *error ratio.*

The error ratio gives us a simple tool to estimate the convergence rates from error quantities. For the evaluation of cardiac simulations, two such error quantities are of special interest.

Definition 7.4: Let $\Gamma_{\mathrm{endo},h}, \Gamma_{\mathrm{epi},h} \subset \Gamma$ be the endocardial and epicardial wall, respectively. For each $\mathbf{x}^i_{\mathrm{endo}} \in \Gamma_{\mathrm{endo},h}$, we set $\mathbf{x}^i_{\mathrm{epi}} \in \Gamma_{\mathrm{epi},h}$ to be its nearest neighbour on the epicardial wall, i.e.,

$$\mathbf{x}^i_{\mathrm{epi}} = \operatorname{argmin}\left\{\left\|\mathbf{x}^i_{\mathrm{endo}} - \mathbf{x}\right\| : \mathbf{x} \in \Gamma_{\mathrm{epi},h}\right\}.$$

We call

$$\overline{S}(\mathbf{u}) := \sum_{i=1}^{N_h(\Gamma_{\mathrm{endo},h})} \left(\frac{\mathbf{x}^i_{\mathrm{endo}} - \mathbf{x}^i_{\mathrm{epi}}}{\varphi(\mathbf{x}^i_{\mathrm{endo}}) - \varphi(\mathbf{x}^i_{\mathrm{epi}})} - 1\right)$$

the *mean strain* of the myocardial wall.

The myocardial strain at a given point characterizes the relative change in wall thickness. The mean strain therefore can be interpreted as an averaged increase or decrease in thickness.

Definition 7.5: Consider a hyperelastic material with first Piola-Kirchhoff stress $\mathbf{P}$. For a displacement $\mathbf{u}\colon \Omega \to \mathbb{R}^3$, we call

$$\overline{P}(\mathbf{u}) := \left(\int_\Omega \mathbf{P}(\mathbf{F}) : \mathrm{D}\mathbf{u}\,\mathrm{d}V\right)^{\frac{1}{2}}, \qquad \mathbf{F} = \mathbf{I} + \mathrm{D}\mathbf{u}$$

the *strain energy* of $\mathbf{u}$.

For all experiments, we choose the volumetric stored energy function characterized by Ciarlet [38, section 4.10]

$$W_{\mathrm{vol}}(J) = \lambda_{\mathrm{vol}} J^2 - \mu_{\mathrm{vol}} \log(J)\,. \tag{7.1}$$

7.2 Evaluation of the passive materials

To validate the uncoupled elasticity equations, we recreate Problem 2 from the validation experiments performed in [99]. An idealized ventricle, given in the form of a cut ellipsoid, is inflated with a pressure $p > 0$.

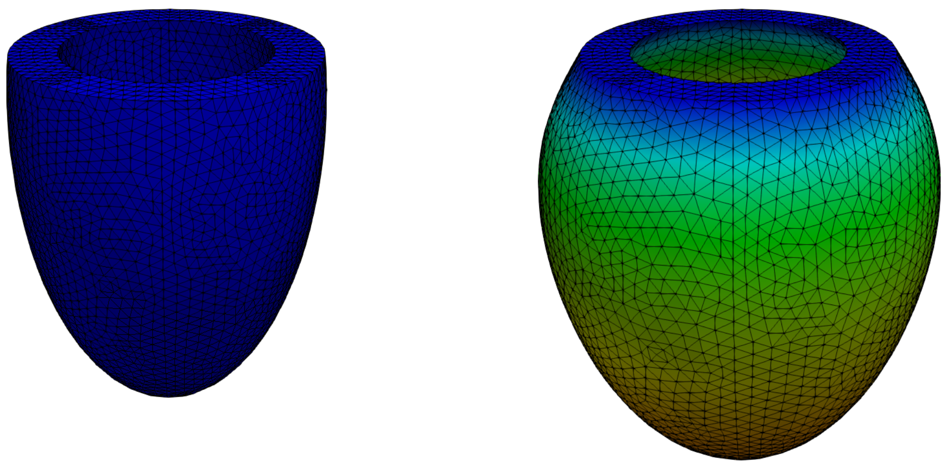

Figure 7.1: Undeformed (left) and deformed (right) ellipsoid geometry Ω_{Ell}

To create Ω, consider the parametrization

$$\mathbf{x} = \begin{pmatrix} r_s \sin u \cos v & r_s \sin u \sin v & r_l \cos u \end{pmatrix}^\top$$

and the three surfaces

- endocardial surface: $r_s = 7$, $r_l = 17$, $u \in [-\pi, \arccos \frac{5}{17}]$, $v \in [-\pi, \pi]$,
- epicardial surface: $r_s = 10$, $r_l = 20$, $u \in [-\pi, \arccos \frac{5}{80}]$, $v \in [-\pi, \pi]$,
- the base plane: $z = 5$:

The truncated ellipsoid is then given by the volume within these three surfaces. We denote this domain by Ω_{Ell}. The ellipsoid is fixated at the base plane and a static pressure ist applied at the endocardial surface, i.e.,

$$\Gamma_{\mathrm{D}} = \{\mathbf{x} \in \partial\Omega_{\mathrm{Ell}} \colon x_3 = 5\} \,,$$

$$\Gamma_{\mathrm{N}} = \left\{ \mathbf{x} \in \partial\Omega_{\mathrm{Ell}} \colon \exists\, u \in [-\pi, \arccos\frac{5}{17}], v \in [-\pi,\pi] \text{ such that } \mathbf{x} = \begin{pmatrix} 7\sin u \sin v \\ 7 \sin u \sin v \\ 17 \cos u \end{pmatrix} \right\} .$$

The problem is complemented with a fibre field $\mathbf{f}$ generated by the function

$$\mathbf{f}(u,v) = \mathbf{N}\left(\frac{\partial \mathbf{x}}{\partial u}(u,v)\right) \sin\alpha(t) + \mathbf{N}\left(\frac{\partial \mathbf{x}}{\partial v}(u,v)\right)\cos\alpha(t)\,,$$

where $\mathbf{N}(\mathbf{v} \coloneqq \frac{\mathbf{v}}{\|\mathbf{v}\|})$ and $\alpha(t) = 90 - 180t$, where $t \in [0,1]$ ranges linearly from 0 on the endocardium to 1 on the epicardium. On Ω_{Ell}, we consider the static elasticity problem, i.e. $\rho \equiv \mathbf{0}$. The variational formulation is given by

$$\int_{\Omega_{\mathrm{Ell}}} \mathrm{D}_{\mathbf{F}} W_{\mathbf{P}}(\mathbf{F}) \colon \mathrm{D}\boldsymbol{\phi}\,\mathrm{d}V = \int_{\Gamma_{\mathrm{N}}} -p\mathbf{n}\,\mathrm{d}A\,,$$

The ellipsoid is inflated by applying a pressure of $p = 10\mathrm{kPa}$ on the endocardial surface. We examine the results for three different materials: The Guccione and Holzapfel-Ogden materials presented in section 4.4 and the *linearized material formulation* already indicated in (6.4), i.e.,

$$W_{\mathrm{Lin}}(\mathbf{F}) = 2\mu\boldsymbol{\varepsilon} + \lambda\,\mathrm{tr}(\boldsymbol{\varepsilon})\mathbf{I}\,, \qquad \boldsymbol{\varepsilon} = \mathrm{sym}(\mathrm{D}\mathbf{u}) = \mathrm{sym}(\mathbf{F}-\mathbf{I})\,.$$

For the three materials, we choose the parameters according to Table 7.1.

Material	Isochoric Parameters					
Linear	$\lambda = 20\mathrm{kPa}$	$\mu = 10\mathrm{kPa}$				
Guccione	$C = 20\mathrm{kPa}$			$b_{\mathbf{f}} = 1$	$b_{\mathbf{s}} = 1$	$b_{\mathbf{f},\mathbf{s}} = 1$
Holzapfel-Ogden	$a = \frac{1}{2}\mathrm{kPa}$	$a_{\mathbf{f}} = 10\mathrm{kPa}$	$a_{\mathbf{s}} = 1\mathrm{kPa}$	$b \quad = 10$	$b_{\mathbf{f}} = 15$	$b_{\mathbf{s}} = 10$

Table 7.1: material parameters for the inflation problem

Additionally, each of the materials is combined with the volumetric penalty function (7.1) with the parameters defined in table 7.2.

We simulate the three materials on levels $l = 0,\dots,4$ for polynomial degrees $p = 1,2$. To estimate the error, we use the solution on the finest mesh $\mathbf{u}_{p,4}$ as a reference for the coarser meshes for their respective polynomial degree p. We show in table 7.3 the results for the linearized material, in 7.4 the results for the Guccione material and in 7.5 the results for the Holzapfel-Ogden material, along with the respective mesh size, degrees of freedom (DoF) and the error ratios.

Material	Volumetric Parameters	
Linear	$\lambda_{\text{vol}} = 0$	$\mu_{\text{vol}} = 0$
Guccione	$\lambda_{\text{vol}} = 20$	$\mu_{\text{vol}} = 20$
Holzapfel-Ogden	$\lambda_{\text{vol}} = 20$	$\mu_{\text{vol}} = 20$

Table 7.2: material parameters for the inflation problem

As indicated in remark 7.2, we expect a convergence rate of $\kappa_2 = p + 1$ in the $\mathcal{L}^2$-norm for the linearized material. Similarly, we expect the convergence rate of $\kappa_p = p$ in the strain energy $\overline{P}$. We can see that the error EOC approximates these convergence rates well for linear finite elements. For quadratic elements, the EOC does not exceed 2 as we should expect.

Level	$l = 0$	$l = 1$	$l = 2$	$l = 3$
Cells	7 013	56 104	448 832	3 590 656
DoF	5 343	35 460	254 181	1 914 663
	$p = 1$			
$\lVert \mathbf{u}_{1,l} - \mathbf{u}^{1,4} \rVert_2$	19.20536	6.54623	1.979646	0.485584
R_l	2.93	3.31	4.08	
$\overline{P}(\mathbf{u}_{1,l} - \mathbf{u}^{1,4})$	30.16462	12.729176	6.389952	2.466499
R_l	2.37	1.99	2.59	
	$p = 2$			
DoF	35 460	254 181	1 914 663	14 840 523
$\lVert \mathbf{u}_{2,l} - \mathbf{u}^{2,4} \rVert_2$	1.741003	0.540143	0.170897	0.045165
R_l	3.22	3.16	3.78	
$\overline{P}(\mathbf{u}_{2,l} - \mathbf{u}^{2,4})$	10.055046	6.98076	3.986164	2.104425
R_l	1.44	1.75	1.89	

Table 7.3: Errors on the oriented ellipsoid with the linearized material W_{Lin}

The Guccione material is in accordance with the corresponding theory regarding convergence rates for linear elements. Again, we notice that the EOC for quadratic elements is not of expected order. The model however is not well-equipped to handle large unphysiological external forces, such as the ones prescribed in this scenario.

Level	$l=0$	$l=1$	$l=2$	$l=3$
		$p=1$		
$\left\lVert \mathbf{u}_{1,l} - \mathbf{u}^{1,4} \right\rVert_2$	10.474307	3.760976	1.139931	0.275482
R_l	2.78	3.3	4.14	
$\overline{P}(\mathbf{u}_{1,l} - \mathbf{u}^{1,4})$	11.537844	4.659333	1.916432	0.665136
R_l	2.48	2.43	2.88	
		$p=2$		
$\left\lVert \mathbf{u}_{2,l} - \mathbf{u}^{2,4} \right\rVert_2$	0.597854	0.173981	0.062065	0.018642
R_l	3.44	2.8	3.33	
$\overline{P}(\mathbf{u}_{2,l} - \mathbf{u}^{2,4})$	2.300186	1.362046	0.732034	0.342045
R_l	1.69	1.86	2.14	

Table 7.4: Errors on the oriented ellipsoid with the Guccione material W_{G}

Level	$l=0$	$l=1$	$l=2$	$l=3$
		$p=1$		
$\left\lVert \mathbf{u}_{1,l} - \mathbf{u}^{1,4} \right\rVert_2$	17.042173	7.28342	2.607279	0.843293
R_l	2.34	2.79	3.09	
$\overline{P}(\mathbf{u}_{1,l} - \mathbf{u}^{1,4})$	84.451375	34.676808	117.625376	4.087412
R_l	2.44	0.29	28.78	
		$p=2$		
$\left\lVert \mathbf{u}_{2,l} - \mathbf{u}^{2,3} \right\rVert_2$	4.471021	2.355663	0.877976	
R_l	1.9	2.68		
$\overline{P}(\mathbf{u}_{2,l} - \mathbf{u}^{2,3})$	20 992 404.81	11 668 675.71	1 024 209.89	
R_l	1.8	11.39		

Table 7.5: Errors on the oriented ellipsoid with the Holzapfel material $W_{\text{H-O}}$

However, the absolute error is reduced by two orders of magnitude on the coarsest mesh when utilizing quadratic elements. With this observation, quadratic elements become more feasible, as exemplary shown in table 7.6. Each calculation was done on 4096 cores on the HoreKa supercomputer.

Discretization	$l = 3$, $p = 1$	$l = 1$, $p = 2$
$\lVert \mathbf{u}_{p,l} - \mathbf{u}^{p,4} \rVert_2$	0.275482	0.173981
Time	217.06s	107.52s

Table 7.6: Computational times and the corresponding errors using W_{G}

For the Holzapfel model, we begin by remarking that due to the increased computational load, $p = 2$ was only refined to level 3. Nevertheless, the EOC follows a similar pattern to the previous two materials considering the $\mathcal{L}^2$-norm Finally, we address the issue of $\overline{P}$. It is clear that no convergence estimates can be derived from the given data. This may be due to the fact that this scenario is not a physiological one. The model of Holzapfel et al. [85] is specifically designed to simulate the passive response of muscle tissue.

7.3 Elastodynamics in a left ventricle

We finish this work by providing a numerical example of coupled elastodynamics. We use Algorithm 3 to solve the dynamic problem without pressure or traction boundary. As domain Ω, we choose the left ventricle geometry provided by Kovacheva [96], which was extracted from a full heart geometry, which in turn was created from MRI data. This left ventricle geometry, which we will denote by Ω_{Ven}, is well suited for convergence studies, as the coarse triangulation $\Omega_{h,0}$ only consists of 5 081 tetrahedra, while retaining a physiological shape.

As a time interval, we choose the length of a typical heartbeat, i.e., 0.8s. We fixate Ω_{Ven} at the base Γ_{D}. The external current function is given by

$$I_{\mathrm{ext}}(t, \mathbf{x}) = \begin{cases} 30\,, & t < 0.3 \text{ and } \left|\mathbf{x} - (8.8, -38.6, -4.8)^{\top}\right| < 15\,, \\ 0\,, & \text{else}\,. \end{cases}$$

We provide a full set of parameters in table 7.7. We run this problem for the linearized material and the Guccione material with the parameters given in table 7.8, where we use the same parameters for W_{G} as Kovacheva [96].

C_m	χ	μ	α	R_FL	
$0.01 \cdot 10^{-6}\,\frac{\mathrm{F}}{\mathrm{mm}^1}$	$140\,\mathrm{mm}^{-1}$	16	6	see [135]	
ρ	β_N	γ_N			
0.001082	0.25	0.5			
$w_1(0)$	$w_2(0)$	$w_3(0)$	$w_4(0)$	$w_5(0)$	$w_6(0)$
0.002980	1.0	0.9877	0.975	0.011	0.0056

$v(0)$	$c_\mathrm{Ca}(0)$	$\sigma_\mathbf{f}$	$\sigma_\mathbf{s} = \sigma_\mathbf{t}$
$-84.57\,\mathrm{mV}$	$0.0000002\,\frac{\mathrm{mol}}{\mathrm{l}}$	$0.0001334177215\mathrm{Smm}^{-1}$	$0.00001760617761\mathrm{Smm}^{-1}$

Table 7.7: Problem parameters

At every timestep t_n, $n = 0, \ldots, N_T$, we calculate the $\mathcal{L}^2$-norm $\|\mathbf{u}\|_h$, the mean strain $\overline{S}(\mathbf{u}_h)$, the strain energy $\overline{P}(\mathbf{u}_h)$ and the cavity volume $V_\mathrm{LV}(\varphi_h(\Omega_\mathrm{Ven}))$. As error ratios we then choose

$$E_l = \sqrt{\frac{1}{N_T}\sum_0^{N_T}(e_l(t) - e_4(t))^2}\,,$$

where e_l represents one of the four mentioned quantities.

Material	Isochoric Parameters				Volumetric Parameters	
Linear	$\lambda = 0.6$kPa	$\mu = 0.3$kPa			$\lambda_\mathrm{vol} = 0$	$\mu_\mathrm{vol} = 0$
Guccione	$C = 0.313$kPa	$b_\mathbf{f} = 17.8$	$b_\mathbf{s} = 7.1$	$b_{\mathbf{f},\mathbf{s}} = 12.4$	$\lambda_\mathrm{vol} = 20$	$\mu_\mathrm{vol} = 20$

Table 7.8: Material parameters for the contraction problem

We again run the simulations for $l = 0, \ldots, 4$ using the algorithm 3 presented in the previous chapter. Due to computational restrictions, we had to omit $l = 4$ for the Guccione material with quadratic elements. As time discretization, we choose $\Delta t_N = 0.005$s for the mechanical timestep and $\Delta t_M = 0.0005$s. All simulations were performed on the HoreKa supercomputer using 4096 CPU cores. The computational times are shown in table 7.9 and the simulation results are shown in tables 7.10 and 7.11.

Level	$l = 0$	$l = 1$	$l = 2$	$l = 3$
CPU-Time (h)	0:11:32	0:21:06	0:50:05	4:15:13
CPU-Time (s)	692	1266	3005	144913
CPU-Time per timestep (s)	4.3	7.9	18.8	905.7

Table 7.9: Computational times for quadratic elements using W_G

For linear elements, we see for both materials an EOC of 1 in the $\mathcal{L}^2$-norm. The remaining error quantities could indicate convergence estimates, but are highly dependent on the used material. For the linearized material, $\overline{P}$ seems to have the same rate as $\|\cdot\|_2$, while for the Guccione material this could be the case for $\overline{S}$ and V_{LV}.

Level	$l=0$	$l=1$	$l=2$	$l=3$	$l=4$
Cells	5 081	40 648	325 184	2 601 472	20 811 776
DoF	5 085	30 471	203 136	1 462 842	11 054 190
			$p=1$		
$\|\mathbf{u}_{1,l}-\mathbf{u}^{1,4}\|_2$	32.726239	19.324948	7.454747	3.111835	
R_l	1.69	2.59	2.4		
$\overline{S}(\mathbf{u}_{1,l}-\mathbf{u}^{1,4})$	18.503477	9.941036	10.102623	8.476877	
R_l	1.86	0.98	1.19		
$\overline{P}(\mathbf{u}_{1,l}-\mathbf{u}^{1,4})$	3.494198	2.209847	0.990644	0.502451	
R_l	1.58	2.23	1.97		
$(V_{\mathrm{LV}}(\boldsymbol{\varphi}_{1,l})-V_{\mathrm{LV}}(\boldsymbol{\varphi}_{1,4}))$	0.793991	0.448844	0.234289	0.191357	
R_l	1.77	1.92	1.22		
			$p=2$		
DoF	30 471	203 136	1 462 842	12 601 472	85 840 086
$\|\mathbf{u}_{2,l}-\mathbf{u}^{2,4}\|_2$	53.264549	47.93663	38.754144	23.091254	
R_l	1.11	1.24	1.68		
$\overline{S}(\mathbf{u}_{2,l}-\mathbf{u}^{2,4})$	86.985761	76.389141	61.918506	36.752958	
R_l	1.14	1.23	1.68		
$\overline{P}(\mathbf{u}_{2,l}-\mathbf{u}^{2,4})$	9.047777	8.116332	6.548042	3.895424	
R_l	1.11	1.24	1.68		
$(V_{\mathrm{LV}}(\boldsymbol{\varphi}_{2,l})-V_{\mathrm{LV}}(\boldsymbol{\varphi}_{2,4}))$	2.289616	2.029508	1.649831	0.987749	
R_l	1.13	1.23	1.67		

Table 7.10: Errors on the left ventricle with the linearized material W_{Lin}

Level	$l=0$	$l=1$	$l=2$	$l=3$
Cells	5 081	40 648	325 184	2 601 472
DoF	5 085	30 471	203 136	1 462 842
	$p=1$			
$\lVert \mathbf{u}_{1,l} - \mathbf{u}^{1,4} \rVert_2$	133.158448	105.236365	54.853488	19.42377
R_l	1.27	1.92	2.82	
$\overline{S}(\mathbf{u}_{1,l} - \mathbf{u}^{1,4})$	217.510795	152.796725	70.952586	25.472463
R_l	1.42	2.15	2.79	
$\overline{P}(\mathbf{u}_{1,l} - \mathbf{u}^{1,4})$	233.016003	225.692899	208.2366	173.905587
R_l	1.03	1.08	1.2	
$(V_{\mathrm{LV}}(\boldsymbol{\varphi}_{1,l}) - V_{\mathrm{LV}}(\boldsymbol{\varphi}_{1,4}))$	6.691143	4.920864	2.395486	0.867453
R_l	1.36	2.05	2.76	
	$p=2$			
DoF	30 471	203 136	1 462 842	12 601 472
$\lVert \mathbf{u}_{2,l} - \mathbf{u}^{2,4} \rVert_2$	55.052192	43.646671	26.495009	
R_l	1.26	1.65		
$\overline{S}(\mathbf{u}_{2,l} - \mathbf{u}^{2,4})$	89.960057	69.249928	42.396271	
R_l	1.3	1.63		
$\overline{P}(\mathbf{u}_{2,l} - \mathbf{u}^{2,4})$	12.842839	10.557681	6.608365	
R_l	1.22	1.6		
$(V_{\mathrm{LV}}(\boldsymbol{\varphi}_{2,l}) - V_{\mathrm{LV}}(\boldsymbol{\varphi}_{2,4}))$	2.382011	1.848279	1.132776	
R_l	1.29	1.63		

Table 7.11: Errors on the left ventricle with the Guccione material W_{G}

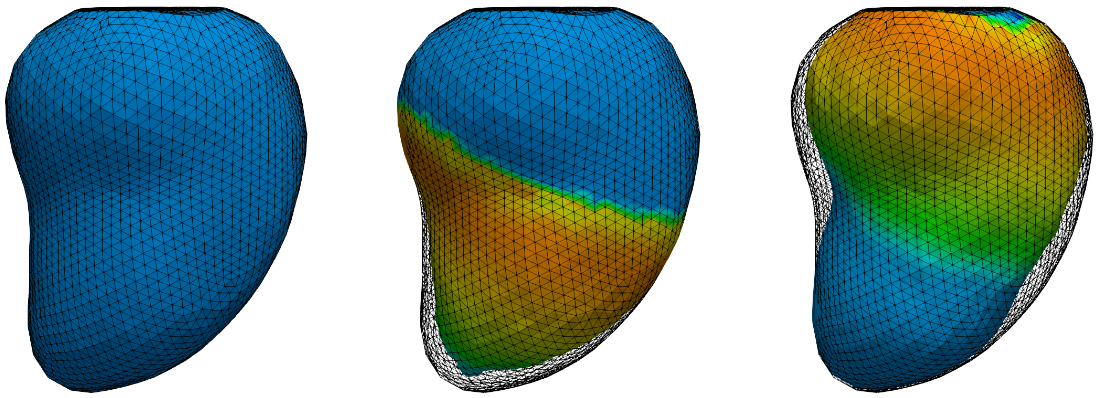

(a) Evolution of v from $v = -84\text{mV}$ (blue) to $v \approx 35\text{mV}$ (orange)

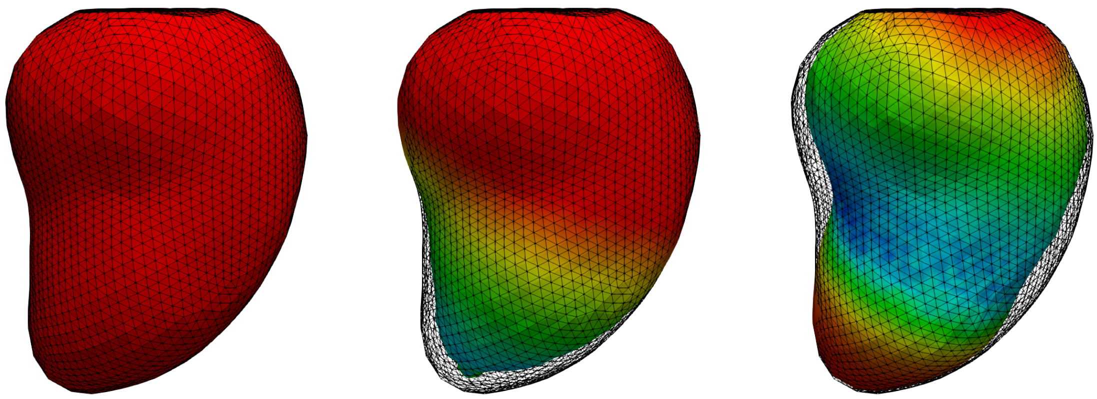

(b) Evolution of $\gamma_{\mathbf{f}}$ from $\gamma_{\mathbf{f}} = 0$ (red) to $\gamma_{\mathbf{f}} \approx 0.18$ (blue)

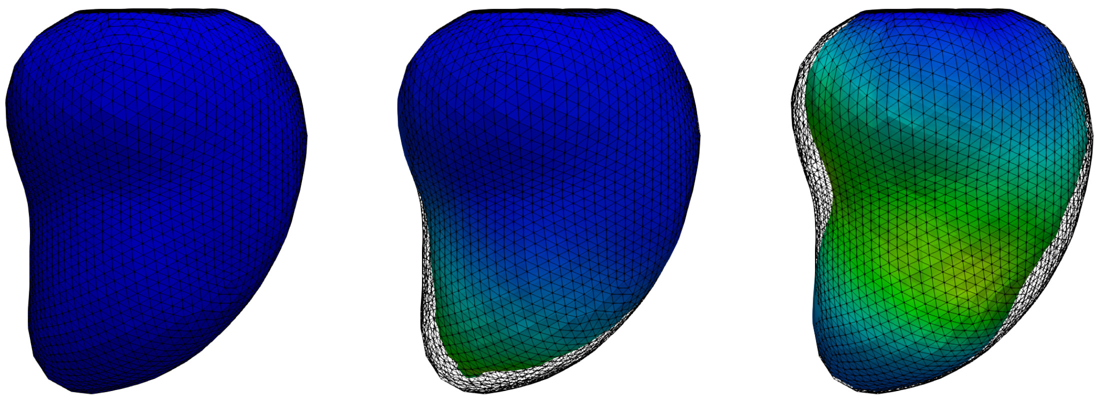

(c) Evolution of $|\mathbf{u}|$ from $|\mathbf{u}| = 0$ (blue) to $|\mathbf{u}| \approx 4$ (green)

Figure 7.2: Evolution of the different quantities at the timesteps $t = 0, 0.3, 0.5$

CHAPTER

EIGHT

CONCLUSION

This final chapter concludes the thesis by giving an overview of the discussed topics and presenting some further research applications.

8.1 Summary

The goal of this work was the precise mathematical description of the full cardiac elastodynamical problem, its classification within the analytical and numerical theory and the development of a numerical method, which allows for a proper computational investigation of the system as a whole and its components.

The mathematical representation of kinematic motion of continuum bodies was introduced by using fundamental concepts of continuum mechanics on manifolds. This framework allowed not only for the description of the elastodynamic balance principles, but later helped properly formulating the electrophysiological model on the reference domain as well. We then established hyperelasticity of materials as a special case of constitutive equations. Using invariant theory, the concept of anisotropy and the special case, orthotropy, for fibre-reinforced materials was provided. This concept enabled the transfer of existence theorems in elasticity from isotropic materials to fibre-reinforced materials. Additionally, incompressibility and polyconvexity of materials used in cardiac mechanics were discussed. We have seen that volumetric splits should only be applied on the isotropic part of a stored energy function and that the commonly used Guccione material is not polyconvex.

From the physiological observations of cardiac functions, mathematical models of cellular excitation propagation, sarcomere force generation, excitation potential diffusion, circulatory feedback and necessary boundary condition were derived. For each system, reasonable assumptions for proper model reduction were discussed and their interaction outlined, resulting in a coupled system of ordinary and partial differential equations. This

coupled system was then analyzed and a corresponding variational formulation derived. Suitable discretizations in space and time were outlined and applied on the weak formulation. Finally, a segregated approximation scheme for the discrete coupled system was presented.
We then performed numerical experiments with the presented segregated scheme. To validate the implementation of the elastodynamical setting, we evaluated a benchmark example with the findings from [99]. The static problem showed that linearized materials conform to the expected convergence results, while the non-linear materials deviate from desired rates. Within the context of dynamical problems, we showed that the space discretizion of Ω_h alone is not enough to improve rates of convergence. In both cases, the absolute error of quadratic elements on the coarsest mesh refinement was lower than the corresponding values for linear elements on finer triangulations, constituting the major advantage of quadratic elements in cardiac elasticity.

8.2 Outlook

Finite element simulations of cardiac elastodynamics are typically done using either linear or quadratic Lagrangian elements [47, 63] or mixed elements [13, 61], the latter implying incompressibility of the cardiac tissue. The modularity of our finite element framework can be used to implement a mixed method as well, allowing for a numerical comparison of the two common approaches. Moreover, to our knowledge, there exists no research on more involved space discretization schemes. Two examples of such methods are discontinuous Galerkin [80] and enriched Galerkin [174] methods.
With the transfer operators presented in section 6.6, it is straightforward to include the deformation gradient into the monodomain equation. The effect of considering the weak form of (5.28) is not only interesting from a numerical standpoint, but allows a more accurate way to model the transmembrane current [72].
Of course the numerical experiments presented in this work only covered few aspects which affect the overall system. The dependency on boundary conditions, especially if they are considered in their proper ”undead” formulation, the feedback of the circulatory system and the interaction between electrophysiological and mechanical systems have to be investigated in much more detail.

APPENDIX

A

THE BEELER-REUTER CELL MODEL

The ventricular cell model introduced by Beeler and Reuter in [27] is defined by the dimensionless vector $\mathbf{w} = (w_1, \ldots, w_6) = (d, f, h, j, m, x_1) \in [0,1]^6$ and the concentration variable $\mathbf{c} = (c_{\mathrm{Ca}}) \in \mathbb{R}_+$, implying $d_{\mathbf{w}} = 6$ and $d_{\mathbf{c}} = 1$. The transmembrane voltage v is measured in mV. The total ionic current $I_{\mathrm{ion}}(v, \mathbf{w}, \mathbf{c})$ is the sum of the two inward currents

$$I_{\mathrm{s}}(v, \mathbf{c}, d, f) = g_{\mathrm{s}} d f (v - E_{\mathrm{s}}(c_{\mathrm{Ca}}))\,, \qquad I_{\mathrm{Na}}(v, m, h, j) = (g_{\mathrm{Na}} m^3 h j + g_{\mathrm{NaC}})(v - E_{\mathrm{Na}})\,,$$

and the two outward currents

$$I_{x_1}(v, x_1) = x_1 \frac{0.8\big(\exp(0.04(v+77)) - 1\big)}{\exp(0.04(v+35))}\,,$$

$$I_{\mathrm{K}}(v) = \frac{1.4\big(\exp(0.04(v+85)) - 1\big)}{\exp(0.08(v+53)) + \exp(0.04(v+53))} + \frac{0.07(v+23)}{1 - \exp(-0.04(v+23))}\,,$$

with the reverse potential $E_{\mathrm{s}}(c_{\mathrm{Ca}}) = -82.3 - 13.0287 \log(c_{\mathrm{Ca}})$ and constant E_{Na}, both meaured in mV. In summary, the total ionic current is given by

$$I_{\mathrm{ion}}(v, \mathbf{w}, \mathbf{c}) = I_{\mathrm{s}}(v, c_{\mathrm{Ca}}, d, f) + I_{\mathrm{Na}}(v, m, h, j) + I_{x_1}(v, x_1) + I_{\mathrm{K}}(v)\,.$$

Corresponding to [27], the constants are set to

$$g_{\mathrm{Na}} = 4\,\mathrm{S/cm}^2\,, \quad g_{\mathrm{NaC}} = 0.003\,\mathrm{S/cm}^2\,, \quad E_{\mathrm{Na}} = 50\,\mathrm{mV}\,, \quad g_{\mathrm{s}} = 0.09\,\mathrm{S/cm}^2\,. \tag{A.1}$$

Depending on positive opening and closing rates $\alpha_j(v)$ and $\beta_j(v)$

$$\alpha_j(v) = \frac{C_1(\alpha_j)\exp(C_2(\alpha_j)(v + C_3(\alpha_j))) + C_4(\alpha_j)(v + C_5(\alpha_j))}{\exp(C_6(\alpha_j)(v + C_3(\alpha_j))) + C_7(\alpha_j)}\,, \tag{A.2}$$

$$\beta_j(v) = \frac{C_1(\beta_j)\exp(C_2(\beta_j)(v + C_3(\beta_j))) + C_4(\beta_j)(v + C_5(\beta_j))}{\exp(C_6(\beta_j)(v + C_3(\beta_j))) + C_7(\beta_j)} \tag{A.3}$$

with the parameters $C_1, \ldots, C_7 \geq 0$ shown in Table A.1, the evolution of $\mathbf{w}$ is determined by

$$\mathbf{G}_{\mathbf{w}}(v, \mathbf{w}) = \Big(G_j(v, w_j)\Big)_{j=1,\ldots,6} \quad \text{with} \quad G_j(v, w_j) = \alpha_j(v) - w_j\big(\alpha_j(v) + \beta_j(v)\big)\,, \tag{A.4}$$

for $j = 1, \ldots, 6$. Remark that for the Beeler-Reuter cell model the gating variables are not directly depending on the intracellular calcium ion concentration. The evolution c_{Ca} is modeled by

$$\partial_t c_{\mathrm{Ca}} = G_{c_{\mathrm{Ca}}}(v, c_{\mathrm{Ca}}, d, f) = -10^{-7} I_{\mathrm{s}}(v, c_{\mathrm{Ca}}, d, f) + 0.07(10^{-7} - c_{\mathrm{Ca}})\,. \tag{A.5}$$

	C_1	C_2	C_3	C_4	C_5	C_6	C_7
α_m	0	0	47	-1	47	-0.1	-1
β_m	40	-0.056	72	0	0	0	0
α_h	0.126	-0.25	77	0	0	0	0
β_h	1.7	0	22.5	0	0	-0.082	1
α_j	0.055	-0.25	78	0	0	-0.2	1
β_j	0.3	0	32	0	0	-0.1	1
α_d	0.095	-0.01	-5	0	0	-0.072	1
β_d	0.07	-0.017	44	0	0	0.05	1
α_f	0.012	-0.008	28	0	0	0.15	1
β_f	0.0065	-0.02	30	0	0	-0.2	1
α_{x_1}	0.0005	0.083	50	0	0	0.057	1
β_{x_1}	0.0013	-0.06	20	0	0	-0.04	1
Unit	$\frac{1}{\mathrm{ms}}$	$\frac{1}{\mathrm{mV}}$	mV	$\frac{1}{\mathrm{mV}\cdot\mathrm{ms}}$	mV	$\frac{1}{\mathrm{mV}}$	-

Table A.1: Constants α_j and β_j of the gate equations in the Beeler-Reuter model

APPENDIX

B

MATERIAL DERIVATIVES

To properly compute the nonlinear materials introduced in section 4.4, we need the first and second derivatives of their respective stored energy function $W_{\mathbf{P}}$. As a convenience for anyone interested in simulating cardiac elasticity, we provide the formal first and second derivatives of the Guccione material W_{G} and the Holzapfel-Ogden material $W_{\text{H-O}}$. The derivatives are given in their native arguments $\mathbf{E}$ or $\mathbf{C}$, respectively. To deduce the corresponding derivatives with respect to $\mathbf{F}$, we provide two basic results. We only outline the proofs and leave the formal calculations as an exercise to the reader.

Lemma B.1: *Consider a hyperelastic material with stored energy functionals*

$$W(\mathbf{F}) = \widetilde{W}(\mathbf{C}) = \widehat{W}(\mathbf{E}), \qquad \mathbf{C} = \mathbf{F}^\top\mathbf{F}, \quad \mathbf{E} = \frac{1}{2}(\mathbf{C} - \mathbf{I}).$$

Then their derivatives follow the relation

$$\mathrm{D}_{\mathbf{F}} W(\mathbf{F}) = 2\mathrm{D}_{\mathbf{C}}\widetilde{W}(\mathbf{C}) = \mathrm{D}_{\mathbf{E}}\widehat{W}(\mathbf{E}).$$

Proof. We first note that, since $\widetilde{W}$ and $\widehat{W}$ are defined on $\mathbb{R}^{3\times3}_{\mathrm{sym}}$, their derivatives are symmetric. The result then follows by using the chain rule on

$$\mathrm{D}_{\mathbf{F}} W(\mathbf{F})[\mathbf{H}] = \mathrm{D}_{\mathbf{F}}\widetilde{W}(\mathbf{F}^\top\mathbf{F})[\mathbf{H}] \qquad \text{or} \qquad \mathrm{D}_{\mathbf{F}} W(\mathbf{F})[\mathbf{H}] = \mathrm{D}_{\mathbf{F}}\widehat{W}(\frac{1}{2}(\mathbf{F}^\top\mathbf{F} - \mathbf{I}))[\mathbf{H}],$$

respectively. □

Lemma B.2: *Consider a hyperelastic material with energy functionals as in lemma B.1. Their respective second derivatives then follow the relation*

$$\begin{aligned}\mathrm{D}^2_{\mathbf{F}} W(\mathbf{F})[\mathbf{G};\mathbf{H}] &= 2\mathrm{D}_{\mathbf{C}}\widetilde{W}(\mathbf{C})[\mathrm{sym}(\mathbf{G}^\top\mathbf{H})] + 4\mathrm{D}^2_{\mathbf{C}}\widetilde{W}(\mathbf{C})[\mathrm{sym}(\mathbf{F}^\top\mathbf{G}); \mathrm{sym}(\mathbf{F}^\top\mathbf{H})] \\ &= \mathrm{D}_{\mathbf{E}}\widehat{W}(\mathbf{E})[\mathrm{sym}(\mathbf{G}^\top\mathbf{H})] + \mathrm{D}^2_{\mathbf{E}}\widehat{W}(\mathbf{E})[\mathrm{sym}(\mathbf{F}^\top\mathbf{G}); \mathrm{sym}(\mathbf{F}^\top\mathbf{H})].\end{aligned}$$

Proof. The result follows from direct calculations using the derivatives from lemma B.1, the product rule and the chain rule similar to the previous proof. □

B.1 Guccione Material

Consider the Guccione material from definition 4.46 with stored energy function

$$\widehat{W}_{\mathrm{G}}(\mathbf{E},\mathbf{f}) = \frac{1}{2}C_{\mathrm{G}}\left(\exp\left(Q(\mathbf{E},\mathbf{f})\right) - 1\right)\,,$$

where Q is given in global coordinate form

$$Q(\mathbf{E},\mathbf{f}) := 4c_1\left(\mathbf{f}^\top\mathbf{E}\mathbf{f}\right)^2 + 4c_2\,\mathrm{tr}\left(\mathbf{f}^\top\mathbf{E}^\top\mathbf{E}\mathbf{f}\right) + 4c_3\,\mathrm{tr}\left(\mathbf{E}^\top\mathbf{E}\right)\,.$$

The derivatives are then given by

$$\begin{aligned}
\mathrm{D}_{\mathbf{E}}\widehat{W}_{\mathrm{G}}(\mathbf{E},\mathbf{f})[\mathbf{H}] &= \left(\frac{1}{2}C_{\mathrm{G}}\exp\left(Q(\mathbf{E},\mathbf{f})\right)\right)\mathrm{D}_{\mathbf{E}}Q(\mathbf{E},\mathbf{f})[\mathbf{H}]\,,\\
\mathrm{D}^2_{\mathbf{E}}\widehat{W}_{\mathrm{G}}(\mathbf{E},\mathbf{f})[\mathbf{H},\mathbf{G}] &= \left(\frac{1}{2}C_{\mathrm{G}}\exp\left(Q(\mathbf{E},\mathbf{f})\right)\right)\left(\mathrm{D}_{\mathbf{E}}Q(\mathbf{E},\mathbf{f})[\mathbf{H}]\;\mathrm{D}_{\mathbf{E}}Q(\mathbf{E},\mathbf{f})[\mathbf{G}] + \mathrm{D}^2_{\mathbf{E}}Q(\mathbf{E},\mathbf{f})[\mathbf{H};\mathbf{G}]\right)\,,
\end{aligned}$$

where the derivatives of Q are

$$\begin{aligned}
\mathrm{D}_{\mathbf{E}}Q(\mathbf{E},\mathbf{f})[\mathbf{H}] &= 8c_1\left(\mathbf{f}^\top\mathbf{E}\mathbf{f}\right)\left(\mathbf{f}^\top\mathbf{H}\mathbf{f}\right) + 8c_2\,\mathrm{sym}\left(\mathbf{E}\mathbf{f}\mathbf{f}^\top\right):\mathbf{H} + 8c_3\mathbf{E}:\mathbf{H}\\
&= 8\,\mathrm{tr}\left(\left(c_1\left(\mathbf{f}^\top\mathbf{E}\mathbf{f}\right)\mathbf{f}\mathbf{f}^\top + c_2\,\mathrm{sym}\left(\mathbf{E}\mathbf{f}\mathbf{f}^\top\right) + c_3\mathbf{E}\right)^\top\mathbf{H}\right)\,,\\
\mathrm{D}^2_{\mathbf{E}}Q(\mathbf{E},\mathbf{f})[\mathbf{H};\mathbf{G}] &= 8c_1\left(\mathbf{f}^\top\mathbf{H}\mathbf{f}\right)\left(\mathbf{f}^\top\mathbf{G}\mathbf{f}\right) + 8c_2\,\mathrm{sym}\left(\mathbf{H}\mathbf{f}\mathbf{f}^\top\right):\mathbf{G} + 8c_3\mathbf{H}:\mathbf{G}\\
&= 8\,\mathrm{tr}\left(\left(c_1\left(\mathbf{f}^\top\mathbf{H}\mathbf{f}\right)\mathbf{f}\mathbf{f}^\top + c_2\,\mathrm{sym}\left(\mathbf{H}\mathbf{f}\mathbf{f}^\top\right) + c_3\mathbf{H}\right)^\top\mathbf{G}\right)\,.
\end{aligned}$$

B.2 Holzapfel-Ogden Material

Consider the Holzapfel-Ogden material from definition 4.50 with the stored energy function

$$\begin{aligned}
\widetilde{W}_{\text{H-O}}(\mathbf{C},\mathbf{f},\mathbf{s}) = {} & \frac{a}{2b}\left[\exp\left(b(\mathrm{tr}(\mathbf{C})-3)\right)-1\right] + \sum_{\boldsymbol{\ell}=\mathbf{f},\mathbf{s}}\frac{a_{\boldsymbol{\ell}}}{2b_{\boldsymbol{\ell}}}\left[\exp\left(b_{\boldsymbol{\ell}}\left(\iota_{4,\boldsymbol{\ell}}(\mathbf{C})\right)^2\right)-1\right]\\
& + \frac{a_{\mathbf{f},\mathbf{s}}}{2b_{\mathbf{f},\mathbf{s}}}\left[\exp\left(b_{\mathbf{f},\mathbf{s}}\left(\iota_{8,\mathbf{f},\mathbf{s}}(\mathbf{C})\right)^2\right)-1\right]\,,
\end{aligned}$$

with $\iota_{4,\boldsymbol{\ell}}(\mathbf{C}) = \langle\boldsymbol{\ell}^\top\mathbf{C}\boldsymbol{\ell} - 1\rangle$ for $\boldsymbol{\ell} = \mathbf{f},\mathbf{s}$ and $\iota_{8,\mathbf{f},\mathbf{s}}(\mathbf{C}) = \frac{1}{2}(\mathbf{f}^\top\mathbf{C}\mathbf{s} + \mathbf{s}^\top\mathbf{C}\mathbf{f}) = \mathbf{C}\,\mathrm{sym}(\mathbf{f}\mathbf{s}^\top)$, where we use modified invariant formulation as indicated in remark 4.66.

Remark B.3: As explained in remark 4.51, the invariant $\iota_{8,\mathbf{f},\mathbf{s}}$ is zero when using mutually orthogonal fibre directions $\mathbf{f},\mathbf{s},\mathbf{t}$. We provide the full description for the sake of completeness.

We rewrite $\widetilde{W}_{\text{H-O}} = \widetilde{W}_{\iota_1} + \widetilde{W}_{\iota_{4,\mathbf{f}}} + \widetilde{W}_{\iota_{4,\mathbf{s}}} + \widetilde{W}_{\iota_8}$ with

$$\begin{aligned}
\widetilde{W}_{\iota_1}(\mathbf{C}) &= \frac{a}{2b}\left[\exp\left(b(\mathrm{tr}(\mathbf{C})-3)\right)-1\right]\,,\\
\widetilde{W}_{\iota_{4,\boldsymbol{\ell}}}(\mathbf{C},\boldsymbol{\ell}) &= \frac{a_{\boldsymbol{\ell}}}{2b_{\boldsymbol{\ell}}}\left[\exp\left(b_{\boldsymbol{\ell}}\left(\iota_{4,\boldsymbol{\ell}}(\mathbf{C})\right)^2\right)-1\right]\,, \qquad \boldsymbol{\ell} = \mathbf{f},\mathbf{s}\,,\\
\widetilde{W}_{\iota_8}(\mathbf{C},\mathbf{f},\mathbf{s}) &= \frac{a_{\mathbf{f},\mathbf{s}}}{2b_{\mathbf{f},\mathbf{s}}}\left[\exp\left(b_{\mathbf{f},\mathbf{s}}\left(\iota_{8,\mathbf{f},\mathbf{s}}(\mathbf{C})\right)^2\right)-1\right]\,.
\end{aligned}$$

The first and second derivative of the isotropic part are given by

$$
\begin{aligned}
\mathrm{D}_{\mathbf{C}}\widetilde{W}_{\iota_1}(\mathbf{C})[\mathbf{H}] &= \frac{a}{2}\left[\exp\Big(b(\mathrm{tr}(\mathbf{C})-3)\Big)-1\right]\mathrm{tr}(\mathbf{H})\,,\\
\mathrm{D}^2_{\mathbf{C}}\widetilde{W}_{\iota_1}(\mathbf{C})[\mathbf{H};\mathbf{G}] &= \frac{a}{2}\left[\exp\Big(b(\mathrm{tr}(\mathbf{C})-3)\Big)-1\right]\mathrm{tr}(\mathbf{H})\,\mathrm{tr}(\mathbf{G})\,,
\end{aligned}
$$

the derivatives of the anisotropic part for $\boldsymbol{\ell} = \mathbf{f}, \mathbf{s}$ are given by

$$
\begin{aligned}
\mathrm{D}_{\mathbf{C}}\widetilde{W}_{\iota_{4,\boldsymbol{\ell}}}(\mathbf{C},\boldsymbol{\ell})[\mathbf{H}] &= a_{\boldsymbol{\ell}}\left[\exp\Big(b_{\boldsymbol{\ell}}\left(\iota_{4,\boldsymbol{\ell}}(\mathbf{C})\right)^2\Big)-1\right]\iota_{4,\boldsymbol{\ell}}(\mathbf{C})\left(\boldsymbol{\ell}^\top\mathbf{H}\boldsymbol{\ell}\right)\,,\\
\mathrm{D}^2_{\mathbf{C}}\widetilde{W}_{\iota_{4,\boldsymbol{\ell}}}(\mathbf{C},\boldsymbol{\ell})[\mathbf{H};\mathbf{G}] &= a_{\boldsymbol{\ell}}\left[\exp\Big(b_{\boldsymbol{\ell}}\left(\iota_{4,\boldsymbol{\ell}}(\mathbf{C})\right)^2\Big)-1\right]\Big(2b_{\boldsymbol{\ell}}\left(\iota_{4,\boldsymbol{\ell}}(\mathbf{C})\right)^2+1\Big)\left(\boldsymbol{\ell}^\top\mathbf{H}\boldsymbol{\ell}\right)\left(\boldsymbol{\ell}^\top\mathbf{G}\boldsymbol{\ell}\right)\,,
\end{aligned}
$$

and, finally, for the invariant $\iota_{8,\mathbf{f},\mathbf{s}}$ we get

$$
\begin{aligned}
\mathrm{D}_{\mathbf{C}}\widetilde{W}_{\iota_8}(\mathbf{C},\mathbf{f},\mathbf{s})[\mathbf{H}] &= \frac{a_{\mathbf{f},\mathbf{s}}}{2}\left[\exp\Big(b_{\mathbf{f},\mathbf{s}}\left(\iota_{8,\mathbf{f},\mathbf{s}}(\mathbf{C})\right)^2\Big)-1\right]\iota_{8,\mathbf{f},\mathbf{s}}(\mathbf{C})\left(\mathbf{f}^\top\mathbf{H}\mathbf{s}+\mathbf{s}^\top\mathbf{H}\mathbf{f}\right)\,,\\
\mathrm{D}^2_{\mathbf{C}}\widetilde{W}_{\iota_8}(\mathbf{C},\mathbf{f},\mathbf{s})[\mathbf{H};\mathbf{G}] &= \frac{a_{\mathbf{f},\mathbf{s}}}{4}\left[\exp\Big(b_{\mathbf{f},\mathbf{s}}\left(\iota_{8,\mathbf{f},\mathbf{s}}(\mathbf{C})\right)^2\Big)-1\right]\Big(2b_{\mathbf{f},\mathbf{s}}\left(\iota_{8,\mathbf{f},\mathbf{s}}(\mathbf{C})\right)^2+1\Big)\\
&\qquad\cdot\left(\mathbf{f}^\top\mathbf{H}\mathbf{s}+\mathbf{s}^\top\mathbf{H}\mathbf{f}\right)\left(\mathbf{f}^\top\mathbf{G}\mathbf{s}+\mathbf{s}^\top\mathbf{G}\mathbf{f}\right)\,.
\end{aligned}
$$

BIBLIOGRAPHY

[1] Ahmad Bakir, A., Al Abed, A., Stevens, M. C., et al. "A Multiphysics Biventricular Cardiac Model: Simulations With a Left-Ventricular Assist Device." In: *Frontiers in physiology* 9 (Jan. 2018), p. 1259. DOI: 10.3389/fphys.2018.01259.

[2] Aliev, R. R. and Panfilov, A. V. "A simple two-variable model of cardiac excitation". In: *Chaos, Solitons & Fractals* 7.3 (1996), pp. 293–301. ISSN: 0960-0779. DOI: https://doi.org/10.1016/0960-0779(95)00089-5.

[3] Amann, H. and Escher, J., eds. *Analysis II.* SpringerLink. Basel: Birkhäuser Basel, 2008. ISBN: 9783764374785.

[4] Ambrosi, D. et al. "Electromechanical Coupling in Cardiac Dynamics: The Active Strain Approach". In: *SIAM Journal on Applied Mathematics* 71.2 (2011), pp. 605–621. DOI: 10.1137/100788379.

[5] Andlauer, R. et al. "Influence of left atrial size on P-wave morphology: differential effects of dilation and hypertrophy". In: *Europace* 20.S3 (Nov. 2018), pp. iii36–iii44. DOI: 10.1093/europace/euy231.

[6] Andreianov, B. et al. "Solvability analysis and numerical approximation of linearized cardiac electromechanics". In: *Math. Models Methods Appl. Sci.* 25.05 (2015), pp. 959–993. DOI: 10.1142/S0218202515500244.

[7] Antman, S. "Existence of Solutions of the Equilibrium Equations for Nonlinearly Elastic Rings and Arches". In: *Indiana University Mathematics Journal* 20 (3 1971), pp. 281–302.

[8] Antman, S. S. *Nonlinear problems of elasticity.* 2. ed. Applied mathematical sciences ; 107. New York, NY: Springer, 2005. ISBN: 0387208801; 9780387208800.

[9] Arendt, W. *Partielle Differenzialgleichungen : eine Einführung in analytische und numerische Methoden.* Ed. by Urban, K. 2. Auflage. Berlin: Springer Spektrum, 2018. ISBN: 9783662583227. DOI: 10.1007/978-3-662-58322-7.

[10] Arendt, W. and Kreuter, M. "Mapping theorems for Sobolev spaces of vector-valued functions". In: *Studia Mathematica* 240.3 (2018), pp. 275–299. ISSN: 1730-6337. DOI: 10.4064/sm8757-4-2017.

[11] Arevalo, H. J., Vadakkumpadan, F., Guallar, E., et al. "Arrhythmia risk stratification of patients after myocardial infarction using personalized heart models". In: *Nature Communications* 7 (Jan. 2016), p. 11437. DOI: 10.1038/ncomms11437.

[12] Atkinson, K. E. and Han, W. *Theoretical numerical analysis : a functional analysis framework*. 2. ed. Texts in applied mathematics ; 39. New York: Springer, 2005. ISBN: 9780387258874.

[13] Augustin, C. M., Neic, A., Liebmann, M., et al. "Anatomically accurate high resolution modeling of human whole heart electromechanics: a strongly scalable algebraic multigrid solver method for nonlinear deformation". In: *J. Computat. Phys.* 305 (2016), pp. 622–646. DOI: 10.1016/j.jcp.2015.10.045.

[14] Augustin, C. M. et al. "A computationally efficient physiologically comprehensive 3D–0D closed-loop model of the heart and circulation". In: *Computer Methods in Applied Mechanics and Engineering* 386 (2021), p. 114092. ISSN: 0045-7825. DOI: 10.1016/j.cma.2021.114092.

[15] Augustin, C. M. et al. *Validation of a 3D-0D closed-loop model of the heart and circulation – Modeling the experimental assessment of diastolic and systolic ventricular properties*. Sept. 2020.

[16] Babuška, L. and Suri, M. "The Optimal Convergence Rate of the p-Version of the Finite Element Method". In: *SIAM Journal on Numerical Analysis* 24.4 (1987), pp. 750–776. DOI: 10.1137/0724049.

[17] Bachman, D. *A Geometric Approach to Differential Forms*. Second. SpringerLink. Boston: Birkhäuser Boston, 2012. ISBN: 9780817683047.

[18] Ball, J., Currie, J., and Olver, P. "Null Lagrangians, weak continuity, and variational problems of arbitrary order". In: *Journal of Functional Analysis* 41.2 (1981), pp. 135–174. ISSN: 0022-1236. DOI: 10.1016/0022-1236(81)90085-9.

[19] Ball, J. and Murat, F. "W1,p-quasiconvexity and variational problems for multiple integrals". In: *Journal of Functional Analysis* 58.3 (1984), pp. 225–253. ISSN: 0022-1236. DOI: 10.1016/0022-1236(84)90041-7.

[20] Ball, J. M. "Convexity conditions and existence theorems in nonlinear elasticity". In: *Archive for Rational Mechanics and Analysis* (1976), pp. 337–403. DOI: 10.1007/BF00279992.

[21] Ball, J. M. “Convexity conditions and existence theorems in nonlinear elasticity”. In: *Arch. Rational Mech. Anal.* 63 (1976), pp. 337–403. DOI: 10.1007/BF00279992.

[22] Ball, J. M. “Some Open Problems in Elasticity”. In: *Geometry, Mechanics, and Dynamics*. Ed. by Newton, P., Holmes, P., and Weinstein, A. New York, NY: Springer New York, 2002, pp. 3–59. ISBN: 978-0-387-21791-8. DOI: 10.1007/0-387-21791-6_1.

[23] Barbarotta, L. et al. “A transmurally heterogeneous orthotropic activation model for ventricular contraction and its numerical validation”. In: *International Journal for Numerical Methods in Biomedical Engineering* 34.12 (2018), e3137. DOI: 10.1002/cnm.3137.

[24] Baumgarten, N. and Wieners, C. “The parallel finite element system M++ with integrated multilevel preconditioning and multilevel Monte Carlo methods”. In: *Computers & Mathematics with Applications* 81 (2021). Development and Application of Open-source Software for Problems with Numerical PDEs, pp. 391–406. ISSN: 0898-1221. DOI: 10.1016/j.camwa.2020.03.004.

[25] Bayer, J. D. et al. “A novel rule-based algorithm for assigning myocardial fiber orientation to computational heart models”. In: *Annals of Biomedical Engineering* 40.10 (Jan. 2012), pp. 2243–2254. DOI: 10.1007/s10439-012-0593-5.

[26] Bednarczyk, H. and Sansour, C. “On the Choice of Integrity Base of Strain Invariants for Constitutive Equations of Isotropic Materials”. In: *Advances in Continuum Mechanics*. Ed. by Brüller, O., Mannl, V., and Najar, J. Berlin, Heidelberg: Springer, 1991, pp. 26–33. ISBN: 978-3-540-53988-9. DOI: https://doi.org/10.1007/978-3-642-48890-0_2.

[27] Beeler, G. W. and Reuter, H. “Reconstruction of the action potential of ventricular myocardial fibres”. In: *The Journal of physiology* 268.1 (1977), pp. 177–210.

[28] Belytschko, T., Liu, W. K., and Moran, B. *Nonlinear finite elements for continua and structures*. Chichester: Wiley, 2000. ISBN: 0471987743.

[29] Bendahmane, M. et al. “Mathematical analysis of cardiac electromechanics with physiological ionic model”. In: *Discrete and Continuous Dynamical Systems - Series B* 24.9 (2019), p. 34. DOI: 10.3934/dcdsb.2019035.

[30] Betts, J. G. et al. *Anatomy and Physiology*. OpenStax Houston, 2020. ISBN: 978-1-947172-04-3. URL: https://openstax.org/details/books/anatomy-and-physiology.

[31] Boehler, J.-P., ed. *Mechanical Behaviour of Anisotropic Solids*. The Hague, Boston, London: Martinus Nijhoff Publishers, 1979. ISBN: 978-94-009-6829-5.

[32] Bols, J. et al. “A computational method to assess the in vivo stresses and unloaded configuration of patient-specific blood vessels”. In: *Journal of Computational and Applied Mathematics* 246 (2013). Fifth International Conference on Advanced COmputational Methods in ENgineering (ACOMEN 2011), pp. 10–17. ISSN: 0377-0427. DOI: 10.1016/j.cam.2012.10.034.

[33] Bourgault, Y., Coudière, Y., and Pierre, C. “Existence and uniqueness of the solution for the bidomain model used in cardiac electrophysiology”. In: *Nonlinear Analysis: Real World Applications* 10.1 (2009), pp. 458–482. URL: https://hal.archives-ouvertes.fr/hal-00101458.

[34] Boyer, F. *Mathematical Tools for the Study of the Incompressible Navier-Stokes Equations and Related Models*. Ed. by Fabrie, P. Applied Mathematical Sciences ; 183SpringerLink. New York, NY: Springer, 2013. ISBN: 9781461459750.

[35] Braess, D. *Finite Elemente: Theorie, schnelle Löser und Anwendungen in der Elastizitätstheorie*. 5th ed. Springer-Lehrbuch MasterclassMasterclassSpringerLinkSpringer eBook Collection. Berlin, Heidelberg: Springer Spektrum, 2013. ISBN: 9783642347979.

[36] Brézis, H. *Functional analysis, Sobolev spaces and partial differential equations*. UniversitextMathematics. New York, NY: Springer, 2011. ISBN: 9780387709130.

[37] Chappell, M. *Physiology for Engineers : Applying Engineering Methods to Physiological Systems*. 2nd ed. Biosystems & Biorobotics. Cham: Springer International Publishing, 2020. ISBN: 978-3-030397-05-0.

[38] Ciarlet, P. G. *Mathematical elasticity ; Volume I. Three-dimensional elasticity*. Studies in mathematics and its applications ; v. 20, 27, 29. Amsterdam: North-Holland, 1988. ISBN: 978-04-447-0259-3.

[39] Clark, M. A., Choi, J., and Douglas, M. *Biology 2e*. OpenStax Houston, 2020. ISBN: 978-1-947172-52-4. URL: https://openstax.org/details/books/biology-2e.

[40] Clayton, R. et al. “Models of cardiac tissue electrophysiology: Progress, challenges and open questions”. In: *Progress in Biophysics and Molecular Biology* 104.1 (2011). Cardiac Physiome project: Mathematical and Modelling Foundations, pp. 22–48. ISSN: 0079-6107. DOI: 10.1016/j.pbiomolbio.2010.05.008.

[41] Coman, C. D. *Continuum Mechanics and Linear Elasticity*. Vol. 238. Solid Mechanics and its Applitcations. Dordrecht: Springer Nature, 2020. ISBN: 978-94-024-1771-5. DOI: https://doi.org/10.1007/978-94-024-1771-5.

[42] Corral-Acero, J., Margara, F., Marciniak, M., et al. “The ’Digital Twin’ to enable the vision of precision cardiology.” In: *European heart journal* (Mar. 2020). DOI: 10.1093/eurheartj/ehaa159.

[43] Costa, K. D. et al. "Modelling cardiac mechanical properties in three dimensions". In: *Philosophical Transactions of the Royal Society of London. Series A: Mathematical, Physical and Engineering Sciences* 359.1783 (2001), pp. 1233–1250. DOI: 10.1098/rsta.2001.0828.

[44] Courtemanche et al. "Ionic mechanisms underlying human atrial action potential properties: insights from a mathematical model". In: *American Journal of Physiology-Heart and Circulatory Physiology* 275.1 (1998), H301–H321.

[45] Dacorogna, B. *Direct methods in the calculus of variations.* Second. Vol. 78. Applied Mathematical Sciences. Springer, New York, 2008. ISBN: 978-0-387-35779-9.

[46] Daub, A., Kriegseis, J., and Frohnapfel, B. "Replication of left ventricular haemodynamics with a simple planar mitral valve model". In: *Biomedical Engineering / Biomedizinische Technik* 65.5 (2020), pp. 595–603. DOI: doi:10.1515/bmt-2019-0175.

[47] Dedè, L., Gerbi, A., and Quarteroni, A. "Segregated Algorithms for the Numerical Simulation of Cardiac Electromechanics in the Left Human Ventricle". In: *The Mathematics of Mechanobiology: Cetraro, Italy 2018.* Ed. by Ambrosi Davideand Ciarletta, P. Cham: Springer International Publishing, 2020, pp. 81–116. ISBN: 978-3-030-45197-4. DOI: 10.1007/978-3-030-45197-4_3.

[48] Deutsche Herzstiftung. *31. Deutscher Herzbericht.* 2019. URL: https://www.herzstiftung.de/system/files/2020-11/DHB19_Herzbericht_2019.pdf.

[49] Elstrodt, J. [*Maß- und Integrationstheorie.* Achte, erweiterte und aktualisierte Auflage. SpringerLinkSpringer eBook Collection. Berlin: Springer Spektrum, 2018. ISBN: 9783662579398.

[50] Eriksson, T. S. E. et al. "Influence of myocardial fiber/sheet orientations on left ventricular mechanical contraction". In: *Mathematics and Mechanics of Solids* 18.6 (2013), pp. 592–606. DOI: 10.1177/1081286513485779.

[51] Eriksson, T. et al. "Influence of myocardial fiber/sheet orientations on left ventricular mechanical contraction". In: *Mathematics and Mechanics of Solids* 18.6 (Jan. 2013), pp. 592–606. DOI: 10.1177/1081286513485779.

[52] Eringen, A. C. et al. "Continuum Physics". In: *Mathematics.* Vol. 1. New York, London: Academic Press, 1971.

[53] Ern, A. and Guermond, J.-L. *Theory and practice of finite elements.* Applied mathematical sciences ; 159. New York: Springer, 2004. ISBN: 9780387205748.

[54] Fernández, M. A. and Zemzemi, N. "Decoupled time-marching schemes in computational cardiac electrophysiology and ECG numerical simulation". In: *Mathematical Biosciences* 226.1 (2010), pp. 58–75. ISSN: 0025-5564. DOI: 10.1016/j.mbs.2010.04.003.

[55] FitzHugh, R. "Impulses and Physiological States in Theoretical Models of Nerve Membrane". In: *Biophysical Journal* 1.6 (1961), pp. 445–466. ISSN: 0006-3495. DOI: 10.1016/S0006-3495(61)86902-6.

[56] Flory, P. J. "Thermodynamic relations for high elastic materials". In: *Trans. Faraday Soc.* 57 (0 1961), pp. 829–838. DOI: 10.1039/TF9615700829.

[57] Franzone, P. C., Pavarino, L. F., and Scacchi, S. *Mathematical cardiac electrophysiology*. Vol. 13. Springer, 2014. DOI: 10.1007/978-3-319-04801-7.

[58] Fritz, T. et al. "Simulation of the contraction of the ventricles in a human heart model including atria and pericardium". In: *Biomechanics and Modeling in Mechanobiology* 13 (2013), pp. 627–641. DOI: 10.1007/s10237-013-0523-y.

[59] Fröhlich, J. *CardMech framework of M++*. 16.02.2022. URL: https://git.scc.kit.edu/mpp/cardmech/-/tree/1.0.0.

[60] Fung, Y. C., Fronek, K., and Patitucci, P. "Pseudoelasticity of arteries and the choice of its mathematical expression". In: *American Journal of Physiology-Heart and Circulatory Physiology* 237.5 (1979), H620–H631. DOI: 10.1152/ajpheart.1979.237.5.H620.

[61] Garcia-Blanco, E., Ortigosa, R., Gil, A. J., et al. "A new computational framework for electro-activation in cardiac mechanics". In: *Computer Methods in Applied Mechanics and Engineering* 348 (2019), pp. 796–845. ISSN: 0045-7825. DOI: 10.1016/j.cma.2019.01.042.

[62] Garcia-Blanco, E. et al. "Towards an efficient computational strategy for electro-activation in cardiac mechanics". In: *Computer Methods in Applied Mechanics and Engineering* 356 (2019), pp. 220–260. ISSN: 0045-7825. DOI: 10.1016/j.cma.2019.06.042.

[63] Gerach, T. et al. "Electro-Mechanical Whole-Heart Digital Twins: A Fully Coupled Multi-Physics Approach". In: *Mathematics* 9.11 (2021). ISSN: 2227-7390. DOI: 10.3390/math9111247. URL: https://www.mdpi.com/2227-7390/9/11/1247.

[64] Gerbi, A., Dedè, L., and Quarteroni, A. "A monolithic algorithm for the simulation of cardiac electromechanics in the human left ventricle". In: *Mathematics in Engineering* 1.Mine-01-01-001 (2019), p. 1. ISSN: 2640-3501. DOI: http://dx.doi.org/10.3934/Mine.2018.1.1.

[65] Geselowitz, D. B. and Miller Ill, W. T. "A bidomain model for anisotropic cardiac muscle". In: *Annals of Biomedical Engineering* 11 (1983), pp. 191–206. DOI: https://doi.org/10.1007/BF02363286.

[66] Göktepe, S. and Kuhl, E. "Electromechanics of the heart: a unified approach to the strongly coupled excitation–contraction problem". In: *Computational Mechanics* (45 2010), pp. 227–243. DOI: 10.1007/s00466-009-0434-z.

[67] Graves, L. M. "The Weierstrass condition for multiple integral variation problems". In: *Duke Mathematical Journal* 5.3 (1939), pp. 656–660. DOI: 10.1215/S0012-7094-39-00554-5.

[68] Gray, R. A. and Pathmanathan, P. "Patient-Specific Cardiovascular Computational Modeling: Diversity of Personalization and Challenges." In: *Journal of cardiovascular translational research* 11.2 (Apr. 2018), pp. 80–88. DOI: 10.1007/s12265-018-9792-2.

[69] Green, A. E. and Adkins, J. E. *Large elastic deformations and non-linear continuum mechanics*. Oxford: Clarendon Press, 1960.

[70] Griffith, B. E. and Peskin, C. S. "Electrophysiology". In: *Communications on Pure and Applied Mathematics* 66.12 (2013), pp. 1837–1913. DOI: 10.1002/cpa.21484. eprint: https://onlinelibrary.wiley.com/doi/pdf/10.1002/cpa.21484.

[71] Guccione, J. M., Costa, K. D., and McCulloch, A. D. "Finite element stress analysis of left ventricular mechanics in the beating dog heart". In: *Journal of Biomechanics* 28.10 (1995), pp. 1167–1177. ISSN: 0021-9290. DOI: 10.1016/0021-9290(94)00174-3.

[72] Guharay, F. and Sachs, F. "Stretch-activated single ion channel currents in tissue-cultured embryonic chick skeletal muscle." In: *The Journal of Physiology* 352.1 (1984), pp. 685–701. DOI: 10.1113/jphysiol.1984.sp015317.

[73] Gültekin, O., Sommer, G., and Holzapfel, G. A. "An orthotropic viscoelastic model for the passive myocardium: continuum basis and numerical treatment". In: *Computer Methods in Biomechanics and Biomedical Engineering* 19.15 (2016), pp. 1647–1664. DOI: 10.1080/10255842.2016.1176155.

[74] Gurev, V. et al. "Models of cardiac electromechanics based on individual hearts imaging data: image-based electromechanical models of the heart". In: *Biomechanics and Modeling in Mechanobiology* 10.3 (Jan. 2011), pp. 295–306. DOI: 10.1007/s10237-010-0235-5.

[75] Gurev, V. et al. “A high-resolution computational model of the deforming human heart.” In: *Biomechanics and modeling in mechanobiology* 14.4 (Aug. 2015), pp. 829–49. DOI: 10.1007/s10237-014-0639-8.

[76] Hackl, K. “Generalized standard media and variational principles in classical and finite strain elastoplasticity”. In: *Journal of the Mechanics and Physics of Solids* 45.5 (1997), pp. 667–688. ISSN: 0022-5096. DOI: 10.1016/S0022-5096(96)00110-X.

[77] Hai, C. M. and Murphy, R. A. “Cross-bridge phosphorylation and regulation of latch state in smooth muscle”. In: *American Journal of Physiology-Cell Physiology* 254.1 (1988). PMID: 3337223, pp. C99–C106. DOI: 10.1152/ajpcell.1988.254.1.C99.

[78] Hairer, E., Nørset, S. P., and Wanner, G. *Solving ordinary differential equations*. 2. rev. ed. Vol. 1: Nonstiff problems. Springer series in computational mathematics ; 8. Berlin: Springer, 1993. ISBN: 3540566708; 0387566708; 9783540566700.

[79] Hairer, E. and Wanner, G. *Solving ordinary differential equations*. Vol. 2: Stiff and differential algebraic problems. Springer series in computational mathematics ; 14. Berlin: Springer, 1991.

[80] Hansbo, P. and Larson, M. G. “Discontinuous Galerkin methods for incompressible and nearly incompressible elasticity by Nitsche’s method”. In: *Computer Methods in Applied Mechanics and Engineering* 191.17 (2002), pp. 1895–1908. ISSN: 0045-7825. DOI: 10.1016/S0045-7825(01)00358-9.

[81] Hanslien, M., Karlsen, K. H., and Tveito, A. “On a Finite Difference Scheme for a Beeler-Reuter Based Model of Cardiac Electrical Activity”. In: *International Journal of Numerical Analysis and Modeling* 3.4 (2006), pp. 395–412. ISSN: 2617-8710. URL: http://global-sci.org/intro/article_detail/ijnam/910.html.

[82] Hirschvogel, M. et al. “A monolithic 3D-0D coupled closed-loop model of the heart and the vascular system: Experiment-based parameter estimation for patient-specific cardiac mechanics”. In: *International Journal for Numerical Methods in Biomedical Engineering* 33.8 (2017), e2842. DOI: 10.1002/cnm.2842.

[83] Hirschvogel, M. et al. “A monolithic 3D-0D coupled closed-loop model of the heart and the vascular system: Experiment-based parameter estimation for patient-specific cardiac mechanics.” In: *International journal for numerical methods in biomedical engineering* 33.8 (Aug. 2017), e2842. DOI: 10.1002/cnm.2842.

[84] Hodgkin, A. L. and Huxley, A. F. “A quantitative description of membrane current and its application to conduction and excitation in nerve”. In: *The Journal of physiology* 117 (4 1952), pp. 500–44. ISSN: 0022-3751. DOI: 10.1113/jphysiol.1952.sp004764.

[85] Holzapfel, G. A. and Ogden, R. W. "Constitutive modelling of passive myocardium: a structurally based framework for material characterization". In: *Phil. Trans. R. Soc. A* 367.1902 (2009), pp. 3445–3475. DOI: 10.1098/rsta.2009.0091.

[86] Holzapfel, G. A., Gasser, T. C., and Ogden, R. W. "Comparison of a Multi-Layer Structural Model for Arterial Walls With a Fung-Type Model, and Issues of Material Stability". In: *Journal of Biomechanical Engineering* 126.2 (May 2004), pp. 264–275. ISSN: 0148-0731. DOI: 10.1115/1.1695572.

[87] Hsu, M.-C. and Bazilevs, Y. "Blood vessel tissue prestress modeling for vascular fluid–structure interaction simulation". In: *Finite Elements in Analysis and Design* 47.6 (2011). The Twenty-Second Annual Robert J. Melosh Competition, pp. 593–599. ISSN: 0168-874X. DOI: 10.1016/j.finel.2010.12.015.

[88] Hughes, T. J., Pister, K. S., and Taylor, R. L. "Implicit-explicit finite elements in nonlinear transient analysis". In: *Computer Methods in Applied Mechanics and Engineering* 17-18 (1979), pp. 159–182. ISSN: 0045-7825. DOI: 10.1016/0045-7825(79)90086-0.

[89] Huxley, A. "Muscle Structure and Theories of Contraction". In: *Progress in Biophysics and Biophysical Chemistry* 7 (1957), pp. 255–318. ISSN: 0096-4174. DOI: 10.1016/S0096-4174(18)30128-8.

[90] Jafari, A., Pszczolkowski, E., and Krishnamurthy, A. "A framework for biomechanics simulations using four-chamber cardiac models." In: *Journal of biomechanics* 91 (June 2019), pp. 92–101. DOI: 10.1016/j.jbiomech.2019.05.019.

[91] Jost, J. *Partial Differential Equations*. 3rd ed. 2013. Graduate Texts in Mathematics 214; SpringerLink. New York, NY: Springer, 2013. ISBN: 9781461448099.

[92] Keener, J. and Sneyd, J., eds. *Mathematical Physology; I: Cellular Physiology*. Interdisciplinary Applied Mathematics ; V. 8, 1. New York: Springer, 2009. ISBN: 978-0-387-75846-6.

[93] Keener, J. and Sneyd, J., eds. *Mathematical Physology; II: Systems Physiology*. Interdisciplinary Applied Mathematics ; V. 8, 2. New York: Springer, 2009. ISBN: 978-0-387-79387-0.

[94] Kerckhoffs, R. C. P. et al. "Coupling of a 3D Finite Element Model of Cardiac Ventricular Mechanics to Lumped Systems Models of the Systemic and Pulmonic Circulation". In: *Annals of Biomedical Engineering* 35.1 (Jan. 2007), pp. 1–18. DOI: 10.1007/s10439-006-9212-7.

[95] Kondaurov, V. and Nikitin, L. "Finite strains of viscoelastic muscle tissue". In: *Journal of Applied Mathematics and Mechanics* 51.3 (1987), pp. 346–353. ISSN: 0021-8928. DOI: 10.1016/0021-8928(87)90111-0.

[96] Kovacheva, E. "Model Based Estimation of the Elastomechanical Properties of the Human Heart". PhD thesis. Karlsruher Institut für Technologie (KIT), 2021. 192 pp. DOI: 10.5445/IR/1000135416.

[97] Kružík, M. *Mathematical methods in continuum mechanics of solids.* Ed. by Roubíček, T. Interaction of mechanics and mathematics. Cham: Springer, 2019. ISBN: 3030020649; 9783030020644.

[98] Ladyženskaja, O. A. *The boundary value problems of mathematical physics.* Ed. by Lohwater, J. Applied mathematical sciences ; 49. New York: Springer, 1985. ISBN: 0387909893; 3540909893.

[99] Land, S. et al. "Verification of cardiac mechanics software: benchmark problems and solutions for testing active and passive material behaviour". English. In: *Proc. R. Soc. Lond. A* 471.2184 (2015), p. 2015.0641. ISSN: 1364-5021. DOI: 10.1098/rspa.2015.0641.

[100] Land, S. et al. "A model of cardiac contraction based on novel measurements of tension development in human cardiomyocytes". In: *Journal of Molecular and Cellular Cardiology* 106 (2017), pp. 68–83. ISSN: 0022-2828. DOI: 10.1016/j.yjmcc.2017.03.008.

[101] Lee, A. W. C., Costa, C. M., Strocchi, M., et al. "Computational Modeling for Cardiac Resynchronization Therapy." In: *Journal of cardiovascular translational research* 11.2 (Apr. 2018), pp. 92–108. DOI: 10.1007/s12265-017-9779-4.

[102] Lee, J. M. *Introduction to Smooth Manifolds.* 2nd ed. 2012. Graduate Texts in Mathematics ; 218SpringerLink. New York, NY: Springer, 2012. ISBN: 9781441999825.

[103] Lehrmann, H. et al. "Novel Electrocardiographic Criteria for Real-Time Assessment of Anterior Mitral Line Block". In: *JACC: Clinical Electrophysiology* 4.7 (Jan. 2018), pp. 920–932. DOI: 10.1016/j.jacep.2018.03.007.

[104] Leone, M. *Theoretische Elektrotechnik.* 2nd ed. Wiesbaden: Springer Vieweg, 2020. ISBN: 978-3-658-29207-2. DOI: 10.1007/978-3-658-29208-9.

[105] Loewe, A., Poremba, E., Oesterlein, T., et al. "Patient-Specific Identification of Atrial Flutter Vulnerability - A Computational Approach to Reveal Latent Reentry Paths". In: *Front. Phys.* 9 (2018), p. 1910. DOI: 10.3389/fphys.2018.01910.

[106] Marsden, J. E. and Hughes, T. J. R. *Mathematical foundations of elasticity*. Unabr., corr. repub. of the ed. publ by. Prentice-Hall, Englewood Cliffs, 1983. New York, NY: Dover, 1994. ISBN: 978-04-866-7865-8.

[107] Martini, F. H., Timmons, M. J., and Tallitsch, R. B. *Human Anatomy*. 7th ed. Boston, Munich: Benjamin Cummings, 2023.

[108] Mitchell, J. R. and Wang, J.-J. "Expanding application of the Wiggers diagram to teach cardiovascular physiology". In: *Advances in Physiology Education* 38.2 (2014), pp. 170–175. DOI: 10.1152/advan.00123.2013.

[109] Morrey, C. B. "Quasi-convexity and the lower semicontinuity of multiple integrals". In: *Pacific Journal of Mathematics* 2.1 (1952), pp. 25–53. DOI: pjm/1103051941.

[110] Mourad, A. "Description topologique de l'architecture fibreuse et modélisation mécanique du myocarde". Theses. Institut National Polytechnique de Grenoble - INPG, Dec. 2003. URL: https://tel.archives-ouvertes.fr/tel-00004003.

[111] Mroue, F. "Cardiac electromechanical coupling: modeling, mathematical analysis and numerical simulation". Theses. Ecole Centrale de Nantes (ECN) ; Université Libanaise, Oct. 2019. URL: https://tel.archives-ouvertes.fr/tel-02395361.

[112] Murtada, S.-I., Kroon, M., and Holzapfel, G. A. "A calcium-driven mechanochemical model for prediction of force generation in smooth muscle". In: *Biomechanics and Modeling in Mechanobiology* 9 (2010), pp. 749–762. DOI: DOI10.1007/s10237-010-0211-0.

[113] Nash, M. P. and Panfilov, A. V. "Electromechanical model of excitable tissue to study reentrant cardiac arrhythmias". In: *Progress in Biophysics and Molecular Biology* 85.2 (2004). Modelling Cellular and Tissue Function, pp. 501–522. ISSN: 0079-6107. DOI: 10.1016/j.pbiomolbio.2004.01.016.

[114] Niederer, S. A., Kerfoot, E., Benson, A. P., et al. "Verification of cardiac tissue electrophysiology simulators using an N-version benchmark". In: *Phil. Trans. R. Soc. A* 369.1954 (2011), pp. 4331–4351. DOI: 10.1098/rsta.2011.0139.

[115] Niederer, S. A., Lumens, J., and Trayanova, N. A. "Computational models in cardiology." In: *Nature reviews. Cardiology* (Oct. 2018). DOI: 10.1038/s41569-018-0104-y.

[116] Noll, W. *The Foundations of Mechanics and Thermodynamics*. Berlin, Heidelberg: Springer, 1974. ISBN: 3-540-06646-2.

[117] Nordsletten, D. et al. "Fluid–solid coupling for the investigation of diastolic and systolic human left ventricular function". In: *International Journal for Numerical Methods in Biomedical Engineering* 27.7 (2011), pp. 1017–1039. DOI: https://doi.org/10.1002/cnm.1405.

[118] Ogden, R. W. and Hill, R. *Large deformation isotropic elasticity: on the correlation of theory and experiment for incompressible rubberlike solids.* 1972. DOI: 10.1098/rspa.1972.0026.

[119] Pathmanathan, P. et al. "Cardiac Electromechanics: The Effect of Contraction Model on the Mathematical Problem and Accuracy of the Numerical Scheme". In: *The Quarterly Journal of Mechanics and Applied Mathematics* 63.3 (July 2010), pp. 375–399. ISSN: 0033-5614. DOI: 10.1093/qjmam/hbq014.

[120] Pavliotis, G. A. and Stuart, A. M., eds. *Multiscale Methods : Averaging and Homogenization.* Texts Applied in Mathematics ; 53SpringerLink. New York, NY: Springer New York, 2008. ISBN: 9780387738291.

[121] Pfaller, M. R., Hörmann, J. M., Weigl, M., et al. "The importance of the pericardium for cardiac biomechanics: from physiology to computational modeling". In: *Biomechanics and modeling in mechanobiology* 18.2 (2019), pp. 503–529.

[122] Pfaller, M., Cruz Varona, M., Lang, J., et al. "Using parametric model order reduction for inverse analysis of large nonlinear cardiac simulations". In: *International Journal for Numerical Methods in Biomedical Engineering* 36.4 (2020), e3320.

[123] Pipkin, A. C. and Wineman, A. S. "Material Symmetry Restrictions on Non-Polynomial Constitutive Equations". In: *Archive for Rational Mechanics and Analysis* 12 (1963), pp. 420–426. DOI: 10.1007/BF00281238.

[124] Podio-Guidugli, P. and Caffarelli, G. V. "Extreme elastic deformations". In: *Arch. Rational Mech. Anal.* 155 (1991), pp. 311–328. DOI: 10.1007/BF00375278.

[125] Potse, M. et al. "A Comparison of Monodomain and Bidomain Reaction-Diffusion Models for Action Potential Propagation in the Human Heart". In: *IEEE Transactions on Biomedical Engineering* 53.12 (2006), pp. 2425–2435. DOI: 10.1109/TBME.2006.880875.

[126] Prakosa, A., Arevalo, H. J., Deng, D., et al. "Personalized virtual-heart technology for guiding the ablation of infarct-related ventricular tachycardia". In: *Nature Biomedical Engineering* (Jan. 2018). DOI: 10.1038/s41551-018-0282-2.

[127] Qu, Z. and Garfinkel, A. "An advanced algorithm for solving partial differential equation in cardiac conduction". In: *IEEE Transactions on Biomedical Engineering* 46.9 (1999), pp. 1166–1168. DOI: 10.1109/10.784149.

[128] Quarteroni, A. et al. “Integrated Heart - Coupling multiscale and multiphysics models for the simulation of the cardiac function”. In: *Computer Methods in Applied Mechanics and Engineering* 314 (1 2017), pp. 345–407. DOI: 10.1016/j.cma.2016.05.031.

[129] Quarteroni, A. et al. *Mathematical modelling of the human cardiovascular system: data, numerical approximation, clinical applications.* Vol. 33. Cambridge University Press, 2019.

[130] Rademakers, F. et al. “Relation of regional cross-fiber shortening to wall thickening in the intact heart: Three-dimensional strain analysis by NMR tagging”. In: *Circulation* 89.3 (1994), pp. 1174–1182. DOI: 10.1161/01.CIR.89.3.1174.

[131] Regazzoni, F. and Quarteroni, A. “An oscillation-free fully staggered algorithm for velocity-dependent active models of cardiac mechanics”. In: *Computer Methods in Applied Mechanics and Engineering* 373 (Jan. 2021), p. 113506. DOI: 10.1016/j.cma.2020.113506.

[132] Regazzoni, F. et al. “A cardiac electromechanics model coupled with a lumped parameters model for closed-loop blood circulation. Part I: model derivation”. In: *arXiv e-prints*, arXiv:2011.15040 (Nov. 2020), arXiv:2011.15040. arXiv: 2011.15040 [math.NA].

[133] Richter, T. *Fluid-structure Interactions : Models, Analysis and Finite Elements.* Lecture Notes in Computational Science and Engineering ; 118SpringerLink. Cham: Springer, 2017. ISBN: 9783319639703.

[134] Rogers, J. and McCulloch, A. “A collocation-Galerkin finite element model of cardiac action potential propagation”. In: *IEEE Transactions on Biomedical Engineering* 41.8 (1994), pp. 743–757. DOI: 10.1109/10.310090.

[135] Rossi, S., Lassila, T., Ruiz-Baier, R., et al. “Thermodynamically consistent orthotropic activation model capturing ventricular systolic wall thickening in cardiac electromechanics”. In: *European Journal of Mechanics - A/Solids* 48 (2014). Frontiers in Finite-Deformation Electromechanics, pp. 129–142. ISSN: 0997-7538. DOI: 10.1016/j.euromechsol.2013.10.009.

[136] Rossi, S. et al. “Orthotropic active strain models for the numerical simulation of cardiac biomechanics”. In: *International Journal for Numerical Methods in Biomedical Engineering* 28.6-7 (2012), pp. 761–788. DOI: 10.1002/cnm.2473.

[137] Ruiz-Baier, R. et al. “Mathematical modelling of active contraction in isolated cardiomyocytes”. In: *Mathematical Medicine and Biology: A Journal of the IMA* 31.3 (June 2013), pp. 259–283. ISSN: 1477-8599. DOI: 10.1093/imammb/dqt009.

[138] Sainte-Marie, J. et al. “Modeling and estimation of the cardiac electromechanical activity”. In: *Computers & Structures* 84.28 (Jan. 2006), pp. 1743–1759. DOI: 10.1016/j.compstruc.2006.05.003.

[139] Sainte-Marie, J. et al. “Modeling and estimation of the cardiac electromechanical activity”. In: *Computers & Structures* 84.28 (2006), pp. 1743–1759. ISSN: 0045-7949. DOI: 10.1016/j.compstruc.2006.05.003.

[140] Sansour, C. “On the physical assumptions underlying the volumetric-isochoric split and the case of anisotropy”. In: *European Journal of Mechanics - A/Solids* 27.1 (2008), pp. 28–39. ISSN: 0997-7538. DOI: 10.1016/j.euromechsol.2007.04.001.

[141] Santiago, A. et al. “Fully coupled fluid-electro-mechanical model of the human heart for supercomputers”. In: *International Journal for Numerical Methods in Biomedical Engineering* 34.12 (2018), e3140. DOI: https://doi.org/10.1002/cnm.3140.

[142] Schröder, J., Neff, P., and Balzani, D. “A variational approach for materially stable anisotropic hyperelasticity”. In: *International Journal of Solids and Structures* 42.15 (2005), pp. 4352–4371. ISSN: 0020-7683. DOI: 10.1016/j.ijsolstr.2004.11.021.

[143] Schröder, J. and Neff, P. “Invariant formulation of hyperelastic transverse isotropy based on polyconvex free energy functions”. In: *International Journal of Solids and Structures* 40.2 (2003), pp. 401–445. ISSN: 0020-7683. DOI: 10.1016/S0020-7683(02)00458-4.

[144] Schuler, S. et al. “Developing and coupling a lumped element model of the closed loop human vascular system to a model of cardiac mechanics”. In: *BMTMedPhys 2017*. Vol. 62. Dresden: de Gruyter, Jan. 2017, S69.

[145] Simo, J. C. and Hughes, T. J. R. *Computational inelasticity*. Corr. 2. print. Interdisciplinary applied mathematics ; 7. New York: Springer, 2000. ISBN: 9780387975207; 9781475771695; 0387975209. URL: http://www.gbv.de/dms/weimar/toc/487083776_toc.pdf.

[146] Simpson, H. C. and Spector, S. J. “On barrelling instabilities in finite elasticity”. In: *Journal of Elasticity* 14 (1984), pp. 103–125. DOI: 10.1007/BF00041660.

[147] Sivaloganathan, J. and Spector, S. J. “On the Uniqueness of Energy Minimizers in Finite Elasticity”. In: *Journal of Elasticity* 133 (2016), pp. 73–103. DOI: 10.1007/s10659-018-9671-8.

[148] Smith, G. F. “On Isotropic Integrity Bases”. In: *Archive for Rational Mechanics and Analysis* 18 (1965), pp. 282–292. DOI: https://doi.org/10.1007/BF00251667.

[149] Spencer, A. J. M., ed. *Continuum Theory of the Mechanics of Fibre-Reinforced Composites*. Wien, New York: Springer, 1984. ISBN: 3-211-81842-1.

[150] Spencer, A. J. M. "Isotropic Integrity Bases for Vectors and Second-Order Tensors". In: *Archive for Rational Mechanics and Analysis* 18 (1965), pp. 51–82. DOI: http://dx.doi.org/10.1007/BF00253982.

[151] Spencer, A. J. M. and Rivlin, R. S. "Isotropic Integrity Bases for Vectors and Second-Order Tensors". In: *Archive for Rational Mechanics and Analysis* 9 (1962), pp. 45–63. DOI: http://dx.doi.org/10.1007/BF00253332.

[152] Stålhand, J., Klarbring, A., and Holzapfel, G. "Smooth muscle contraction: Mechanochemical formulation for homogeneous finite strains". In: *Progress in Biophysics and Molecular Biology* 96.1 (2008). Cardiovascular Physiome, pp. 465–481. ISSN: 0079-6107. DOI: 10.1016/j.pbiomolbio.2007.07.025.

[153] Strobeck, J. E. and Sonnenblick, E. H. "Myocardial contractile properties and ventricular performance". In: *The heart and cardiovascular system* (1986), pp. 31–49.

[154] Sugiura, S. et al. "Multi-scale simulations of cardiac electrophysiology and mechanics using the University of Tokyo heart simulator". In: *Progress in Biophysics and Molecular Biology* 110.2-3 (Jan. 2012), pp. 380–389. DOI: 10.1016/j.pbiomolbio.2012.07.001.

[155] Sugiura, S. et al. "Multi-scale simulations of cardiac electrophysiology and mechanics using the University of Tokyo heart simulator". In: *Progress in Biophysics and Molecular Biology* 110.2 (2012). SI: Beating Heart, pp. 380–389. ISSN: 0079-6107. DOI: https://doi.org/10.1016/j.pbiomolbio.2012.07.001.

[156] Sundnes, J., ed. *Computing the electrical activity in the heart : with 23 tables*. Monographs in computational science and engineering ; 1. Berlin: Springer, 2006. ISBN: 9783540334323.

[157] Takizawa, K., Bazilevs, Y., and Tezduyar, T. E. "Blood vessel tissue prestress modeling for vascular fluid–structure interaction simulation". In: *Archives of Computational Methods in Engineering* 19 (2012), pp. 171–225. DOI: 10.1007/s11831-012-9071-3.

[158] Timmis, A. et al. "European Society of Cardiology: Cardiovascular Disease Statistics 2019". In: *European Heart Journal* 41.1 (Dec. 2019), pp. 12–85. DOI: 10.1093/eurheartj/ehz859.

[159] Truesdell, C. and Noll, W. "The Non-Linear Field Theories of Mechanics". In: *Encyclopedia of Physics*. Ed. by S.Flügge. Berlin, Heidelberg: Springer, 1965.

[160] Tung, L. "A bi-domain model for describing ischemic myocardial d-c potentials". PhD thesis. Massachusetts Institute of Technology, 1978.

[161] Tusscher, K. H. W. J. ten and Panfilov, A. V. "Alternans and spiral breakup in a human ventricular tissue model". In: *American Journal of Physiology. Heart and Circulatory Physiology* 291.3 (Jan. 2006), H1088–100. DOI: 10.1152/ajpheart.00109.2006.

[162] Tusscher, K. H. W. J. ten et al. "A model for human ventricular tissue". In: *American Journal of Physiology-Heart and Circulatory Physiology* 286.4 (2004). PMID: 14656705, H1573–H1589. DOI: 10.1152/ajpheart.00794.2003.

[163] Usyk, T. et al. "Computational model of three-dimensional cardiac electromechanics". In: *Computing and Visualization in Science* 4 (2002), pp. 249–257. DOI: 10.1007/s00791-002-0081-9.

[164] Milišić, V. and Quarteroni, A. "Analysis of lumped parameter models for blood flow simulations and their relation with 1D models". In: *ESAIM: Mathematical Modelling and Numerical Analysis* 38.4 (2004), pp. 613–632. DOI: 10.1051/m2an:2004036.

[165] Veneroni, M. "Reaction–diffusion systems for the macroscopic bidomain model of the cardiac electric field". In: *Nonlinear Analysis: Real World Applications* 10.2 (2009), pp. 849–868. ISSN: 1468-1218. DOI: 10.1016/j.nonrwa.2007.11.008.

[166] Wachter, A., Loewe, A., Krueger, M. W., et al. "Mesh structure-independent modeling of patient-specific atrial fiber orientation". In: vol. 1. 1. Jan. 2015, pp. 409–412. DOI: 10.1515/cdbme-2015-0099.

[167] Washio, T. et al. "Approximation for Cooperative Interactions of a Spatially-Detailed Cardiac Sarcomere Model". In: *Cellular and Molecular Bioengineering* 5 (2012), pp. 113–126. DOI: 10.1007/s12195-011-0219-2.

[168] Westerhof, N., Elzinga, G., and Sipkema, P. "An artificial arterial system for pumping hearts." In: *Journal of Applied Physiology* 31.5 (1971). PMID: 5117196, pp. 776–781. DOI: 10.1152/jappl.1971.31.5.776.

[169] Westerhof, N., Lankhaar, J.-W., and Westerhof, B. E. "The arterial Windkessel". In: *Medical & Biological Engineering & Computing* 47 (2009), pp. 131–141. DOI: 10.1007/s11517-008-0359-2.

[170] Wiggers, C. "Circulation in Health and Disease". In: *Lea & Febiger* (1915).

[171] Wikimedia. *Wiggers Diagram.* 14.09.2021. URL: https://commons.wikimedia.org/wiki/File:Wiggers_Diagram.svg.

[172] Wilber, J. P. and Walton, J. R. “The Convexity Properties of a Class of Constitutive Models for Biological Soft Issues”. In: *Mathematics and Mechanics of Solids* 7.3 (2002), pp. 217–235. DOI: 10.1177/108128602027726.

[173] Wriggers, P., ed. *Nonlinear Finite Element Methods*. Berlin, Heidelberg: Springer, 2008. ISBN: 978-3-642-09002-8.

[174] Yi, S.-Y., Lee, S., and Zikatanov, L. “Locking-Free Enriched Galerkin Method for Linear Elasticity”. In: *SIAM Journal on Numerical Analysis* 60.1 (2022), pp. 52–75. DOI: 10.1137/21M1391353.

[175] Zeidler, E. *Nonlinear functional analysis and its applications*. Vol. 3: Variational methods and optimization. New York: Springer, 1985. ISBN: 9781461295297.

[176] Zhang, C. and Chen, T. “Efficient feature extraction for 2D/3D objects in mesh representation”. In: *Proceedings 2001 International Conference on Image Processing (Cat. No.01CH37205)*. Vol. 3. 2001, 935–938 vol.3. DOI: 10.1109/ICIP.2001.958278.